

2017

# Silylation-Based Kinetic Resolution of 2-Arylcyclohexanols and Understanding Internal Chirality Transmission via Circular Dichroism

Li Wang  
*University of South Carolina*

Follow this and additional works at: <https://scholarcommons.sc.edu/etd>

 Part of the [Chemistry Commons](#)

---

## Recommended Citation

Wang, L. (2017). *Silylation-Based Kinetic Resolution of 2-Arylcyclohexanols and Understanding Internal Chirality Transmission via Circular Dichroism*. (Doctoral dissertation). Retrieved from <https://scholarcommons.sc.edu/etd/4246>

This Open Access Dissertation is brought to you by Scholar Commons. It has been accepted for inclusion in Theses and Dissertations by an authorized administrator of Scholar Commons. For more information, please contact [dillarda@mailbox.sc.edu](mailto:dillarda@mailbox.sc.edu).

SILYLATION-BASED KINETIC RESOLUTION OF 2-ARYLCYCLOHEXANOLS AND  
UNDERSTANDING INTERNAL CHIRALITY TRANSMISSION VIA CIRCULAR  
DICHROISM

by

Li Wang

Bachelor of Science  
China University of Petroleum, 2012

---

Submitted in Partial Fulfillment of the Requirements

For the Degree of Doctor of Philosophy in

Chemistry

College of Arts and Sciences

University of South Carolina

2017

Accepted by:

Sheryl L. Wiskur, Major Professor

John J. Lavigne, Committee Member

Dmitry V. Peryshkov, Committee Member

Campbell McInnes, Committee Member

Cheryl L. Addy, Vice Provost and Dean of the Graduate School

© Copyright by Li Wang, 2017  
All Rights Reserved.

## DEDICATION

This is dedicated to my beloved mother Yongping Zhong and father Daoyang Wang.

## ACKNOWLEDGEMENTS

First and foremost, I would like to express my sincere gratitude to my advisor Dr. Sheryl Wiskur for her five years continuous support of my Ph.D. career, for her patience, consideration, motivation, and guidance of my time at USC. She inspires me not only to pursue further success in the future, but also to balance the time between work and family. I always enjoy the time of spending hours sitting in her office to discuss research and life outside chemistry. I would also like to thank the rest of my committee member: Dr. Ken Shimizu, Dr. John Lavigne, Dr. Dimitry Peryshkov, Dr. James Chapman and Dr. Campbell McInnes, for their insightful comments and encouragement of my plan, proposal and dissertation.

My sincere thanks also go to the former and current members in Wiskur group. To Dr. Ravish Akhani, thank you for mentoring me both in and outside the lab, I have learned a lot from you and I really appreciate the time working with you. To Dr. Robert Clark, you are one of the most talented chemists I have ever met, thank you for teaching me all the lab techniques. To Tian Zhang and Brandon Redden, our discussion of chemistry as well as games will be remembered. To Shelby Dickson, Grace Hollenbeck, Julia Fountain, Naomi Plummer and those in the Wiskur group, thank you for bringing joy to the lab and wish you all success.

There are no words to express my gratitude to my parents for their unlimited love and support in my life. I am proud to be your son. Last but not the least, to my love Yu Pei,

it is such a blessing to meet you in my Ph.D. time. I want to put you in “Chapter 5” of this dissertation and I would like to spend the rest of life with you to write it.

## ABSTRACT

This work described herein focuses on the silylation-based kinetic resolution methodology developed by the Wiskur group in 2011. It is a powerful method for the separation of a single enantiomer from a mixture of racemic secondary alcohols. Chapter one is a summary of the background and related works of this methodology.

In chapter two, the silylation-based kinetic resolution of various *trans* 2-arylcyclohexanols will be discussed by employing a *p*-isopropyl triphenylsilyl chloride as the derivatizing reagent with (-)-benzotetramisole as the catalyst. The diastereoselective and enantioselective of *trans* alcohols over the *cis* will be investigated and a facial one-pot reaction sequence will be introduced.

In an effort to understand the mechanism, Chapter 3 will focus on our interest of chirality transmission from point chirality to helical chirality in our silylation-based kinetic resolution system. Circular dichroism spectroscopy, crystal structure studies and computational modelling were applied with various synthesized triarylsilyl ether to show that point chirality can induce helical chirality in triarylsilyl groups. The understanding of chirality transmission between the alcohol and the triarylsilyl group can be extrapolated to explain the importance of the phenyl groups in silylation-based kinetic resolutions.

Further endeavors to understand the mechanism of silylation-based kinetic resolution will be addressed in Chapter 4. The efforts will be focused on the investigations of directionality of nucleophilic displacement of silicon (retention or inversion) in the mechanism. This can be achieved by studying the stereogenic center at silicon of

enantiopure chiral silane. The ultimate goal of the work is to depict a complete mechanistic picture of silylation-based kinetic resolution, along with other approaches.



## TABLE OF CONTENTS

DEDICATION .....	iii
ACKNOWLEDGEMENTS.....	iv
ABSTRACT .....	vi
LIST OF TABLES .....	xi
LIST OF FIGURES .....	xii
LIST OF SCHEMES.....	xiv
CHAPTER 1: BACKGROUND AND INTRODUCTION OF ASYMMETRIC SILYLATION .....	1
1.1 INTRODUCTION.....	1
1.2 NATURAL CHIRAL POOL.....	4
1.3 ASYMMETRIC CATALYSIS .....	5
1.4 CLASSICAL RESOLUTION.....	7
1.5 CHIRAL CHROMATOGRAPHY RESOLUTION .....	8
1.6 KINETIC RESOLUTION .....	8
1.7 ACYLATION .....	11
1.8 SILYLATION .....	16
1.9 CONCLUSIONS .....	24
1.10 REFERENCES.....	25

CHAPTER 2: DIASTEREOSELECTIVE AND ENANTIOSELECTIVE Silylation of 2-ARYLCYCLOHEXANOLS .....	33
2.1 INTRODUCTION .....	33
2.2 INITIAL INVESTIGATION AND OPTIMIZATIONS .....	38
2.3 Silylation-based kinetic resolution of various 2-ARYLCYCLOHEXANOLS .....	40
2.4 INVESTIGATIONS OF <i>cis</i> -2-ARYLCYCLOHEXANOLS .....	43
2.5 ONE-POT REDUCTION-Silylation SEQUENCE .....	45
2.6 CONCLUSIONS AND OUTLOOK.....	47
2.7 EXPERIMENTAL .....	49
2.8 REFERENCES.....	89
CHAPTER 3: UNDERSTANDING INTERNAL CHIRALITY INDUCTION OF TRIARYLSilyl ETHERS FORMED FROM ENANTIOPURE ALCOHOLS .....	94
3.1 INTRODUCTION .....	94
3.2 SYNTHESIS OF ENANTIOPURE TRIARYLSilyl ETHERS.....	98
3.3 CIRCULAR DICHROISM ANALYSIS.....	100
3.4 CRYSTAL STRUCTURE ANALYSIS OF HELICAL TWIST FORMATION .....	106
3.5 MOLECULAR MODELING ANALYSIS.....	109
3.6 CONCLUSIONS AND OUTLOOK.....	111
3.7 EXPERIMENTAL .....	113
3.8 REFERENCES.....	162
CHAPTER 4: MECHANISTIC INVESTIGATION OF Silylation-based kinetic resolutions: STEREOCHEMISTRY STUDIES OF SILICON AS THE STEREOGENIC CENTER .....	168
4.1 INTRODUCTION .....	168
4.2 OUR FOCUS ON STEREOGENIC AT SILICON .....	172

4.3 PREVIOUS INVESTIGATIONS OF NUCLEOPHILIC DISPLACEMENT AT SILICON.....	174
4.4 SYNTHESIS OF ENANTIOENRICHED CHIRAL SILANES AND Silyl CHLORIDES .....	176
4.5 RESULTS AND DISCUSSIONS.....	178
4.6 CONCLUSIONS AND OUTLOOK .....	186
4.7 EXPERIMENTAL .....	187
4.8 REFERENCES .....	198

## LIST OF TABLES

Table 2.1 Initial Optimizations of 2-Phenylcyclohexanols.....	39
Table 2.2 Substrate Scope of the Silylation-Based Kinetic Resolution of trans-2-Arylcyclohexanols .....	41
Table 2.3 Further Demonstration of the Importance of Isopropyl-Substituted Silyl Chloride.....	42
Table 3.1 Selected CD Data ( $\Delta\epsilon$ (nm)) for Chiral Triphenylsilyl Ethers.....	105
Table 3.2 Selected CD Data ( $\Delta\epsilon$ (nm)) for Chiral Trinaphthylsilyl Ethers.....	106
Table 3.3 Dihedral Angles and Helicity Types of ( <b>R</b> )- <b>3.2</b> , ( <b>S</b> )- <b>3.2</b> and <b>3.4</b> .....	108
Table 3.4 Population of Helicity Types and Calculated Dihedral Angles of ( <b>S</b> )- <b>3.2</b> and <b>3.4</b> .....	110
Table 3.5 Crystal Data and Structure Refinement for ( <b>S</b> )- <b>3.2</b> .....	139
Table 3.6 Crystal Data and Structure Refinement for ( <b>R</b> )- <b>3.2</b> .....	141
Table 3.7 Crystal Data and Structure Refinement for <b>3.4</b> .....	142
Table 3.8 Absolute Energies of the Conformers of ( <b>S</b> )- <b>3.2</b> .....	145
Table 3.9 Cartesian Coordinates of the Conformers of ( <b>S</b> )- <b>3.2</b> .....	145
Table 3.10 Absolute Energies of the Conformers of <b>3.4</b> .....	155
Table 3.11 Cartesian Coordinates of the Conformers of <b>3.4</b> .....	156
Table 4.1 Investigation of Fast Rate of Cyclohexanol Attacking Intermediate .....	180
Table 4.2 Investigation of Stereochemistry at Silicon .....	183

## LIST OF FIGURES

Figure 1.1 A Pair of Enantiomers of Lactic Acid .....	2
Figure 1.2 Biological Differences of Ethambutol and Propoxyphene .....	2
Figure 1.3 The Structure of Morphine .....	4
Figure 1.4 Asymmetric Catalysis .....	5
Figure 1.5 Amidine- and Isothiourea-Based Catalysts .....	16
Figure 2.1 Ideal Substrate Class of Silylation-Based Kinetic Resolution.....	34
Figure 3.1 Helical Formation of Triarylmethyl and Triarylsilyl System .....	96
Figure 3.2 CD Spectrum and UV/VIS Spectrum (Absorbance) of ( <i>L</i> )- <b>3.1</b> .....	102
Figure 3.3 CD Spectrum and UV/VIS Spectrum (Absorbance) of ( <i>D</i> )- <b>3.1</b> .....	103
Figure 3.4 Model of The Correlation Between the Position of The Large Substituent ( <i>L</i> ) or $\Pi$ System to The Resultant Cotton Effect and Helical Twist .....	104
Figure 3.5 The independent molecular structures of ( <i>S</i> )- <b>3.2</b> and ( <i>R</i> )- <b>3.2</b> as viewed down the oxygen-silicon bond. The alcohol portion of the molecule is drawn in wireframe and the hydrogens are removed for clarity. The crystals of ( <i>S</i> )- <b>3.2</b> and ( <i>R</i> )- <b>3.2</b> were grown independently and are enantiomerically pure; all molecules in the crystals are identical. C1 determined by the X-ray data to have the “S” configuration for ( <i>S</i> )- <b>3.2</b> and the “R” configuration for ( <i>R</i> )- <b>3.2</b> .....	107
Figure 3.6 Model to Assign <i>M</i> or <i>P</i> to Each Phenyl Group .....	107
Figure 3.7 The structure of two independent, chemically identical but conformationally distinct molecules of <b>3.4</b> as viewed down the oxygen-silicon bond. The alcohol portion of the molecule is drawn in wireframe and the hydrogens are removed for clarity. ....	109
Figure 3.8 Molecular structure. Displacement ellipsoids drawn at the 30% probability level. The crystal is enantiomerically pure; all molecules in the crystal are identical. C1 determined by the X-ray data to have the “S” conformation.....	136

Figure 3.9 Molecular structure. Displacement ellipsoids drawn at the 30% probability level. The crystal is enantiomerically pure; all molecules in the crystal are identical. C1 determined by the X-ray data to have the “R” conformation .....	137
Figure 3.10 Asymmetric unit of the crystal. Two independent, chemically identical but conformationally distinct molecules, labeled “A” and “B”. .....	139
Figure 3.11 Calculated conformers of ( <i>S</i> )- <b>3.2</b> with the lowest energy .....	144
Figure 3.12 Calculated conformers of <b>3.4</b> in a <i>MMM</i> and <i>PPP</i> helicity.....	155
Figure 4.1 Proposed Mechanistic Cycle of Silylation-Based Kinetic Resolution .....	172
Figure 4.2 Tendency of Si-X to Be Displaced with Inversion.....	175

## LIST OF SCHEMES

Scheme 1.1 Sharpless Asymmetric Epoxidation .....	6
Scheme 1.2 Noyori's Asymmetric Hydrogenation of Ketone .....	6
Scheme 1.3 Classic Resolution of <i>N</i> -Formyl-Phenylalanine .....	8
Scheme 1.4 General Scheme of Kinetic Resolution of Alcohols Reacting with Resolving Agent.....	9
Scheme 1.5 Kinetic Resolution of Secondary Alcohols Using a Chiral Phosphine .....	12
Scheme 1.6 Modified Bicyclic Phosphine Catalyzed Kinetic Resolution of Secondary Alcohols .....	12
Scheme 1.7 Chiral DMAP Catalyzed Kinetic Resolution by Vedejs .....	13
Scheme 1.8 Kinetic Resolution using Fu's chiral DMAP catalyst .....	14
Scheme 1.9 Kinetic Resolution of Secondary Alcohols Using Amidine-Based Catalysts by Birman.....	15
Scheme 1.10 First Silylation-Based Kinetic Resolution of Secondary Alcohols Using Modified Guanidine .....	17
Scheme 1.11 Desymmetrization of <i>Meso</i> Diols with Amino-Acid-Based Catalyst .....	18
Scheme 1.12 Desymmetrization of <i>Meso</i> Diols with Brønsted Acid Catalyst .....	19
Scheme 1.13 Kinetic Resolution of Secondary Alcohols Using Chiral Silanes .....	20
Scheme 1.14 Silylation-Based Resolution of Monofunctional Secondary Alcohols by Wiskur .....	21
Scheme 1.15 One-Pot Reduction/Kinetic Resolution Sequence to Achieve Enantioenriched Alcohol.....	22
Scheme 1.16 Silylation-Based Kinetic Resolution of $\alpha$ -Hydroxy Lactones and -Lactams .....	23

Scheme 1.17 Polymer Supported Silylation-Based Kinetic Resolution .....	23
Scheme 2.1 Silylation-Based Kinetic Resolutions of Wiskur Group .....	34
Scheme 2.2 Methods to Obtain <i>Cis</i> and <i>Trans</i> 2-Arylcyclohexanols .....	35
Scheme 2.3 Acyl-Transfer Kinetic Resolution of 2-Arylcyclohexanols .....	36
Scheme 2.4 Organocatalytic Oxidative Kinetic Resolution of Secondary Alcohols .....	36
Scheme 2.5 Kinetic Resolution of Secondary Alcohols Catalyzed by Chiral Phosphoric Acids .....	37
Scheme 2.6 Substrate Reactivity toward Silylation Based on the OH Conformation (Axial vs Equatorial) and the Population of That Conformation at -78 °C.....	44
Scheme 2.7 One-pot, Chromatography-Free Reduction Followed by a Kinetic Resolution to Selectively Silylate One Stereoisomer out of a Mixture of Four .....	47
Scheme 2.8 Silylation-Based Kinetic Resolution of <i>Trans</i> -2-Carboethoxycyclohexanol ...	48
Scheme 2.9 One-pot Reduction/Kinetic Resolution to Isolate (1R,2S)-2-(3-methoxyphenyl)cyclohexan-1-ol Enantiomerically Enriched .....	87
Scheme 3.1 Investigation of Silyl Chlorides in Silylation-Based Kinetic Resolution.....	95
Scheme 3.2 Proposed Mechanism of Silylation-Based Kinetic Resolution .....	97
Scheme 3.3 Synthesis of Enantiopure Triphenylsilyl Ethers .....	99
Scheme 3.4 Synthesis the Enantiopure Trinaphthylsilyl Ethers .....	99
Scheme 4.1 Linear-Free Energy Relationship Studies of Triarylsilyl Chlorides.....	170
Scheme 4.2 General Scheme of Kinetic Runs .....	171
Scheme 4.3 Step-Wise Investigations of Nucleophilic Displacement.....	174
Scheme 4.4 Synthesis of Racemic Methoxymethylnaphthylphenyl Silane .....	176
Scheme 4.5 Synthesis of Enantioenriched L-Menthoxymethylnaphthylphenyl Silane ...	177
Scheme 4.6 Synthesis of Enantioenriched Methylnaphthylphenyl Silane .....	177
Scheme 4.7 Synthesis of Enantioenriched Chiral Silyl Chloride.....	178
Scheme 4.8 Silylation of Cyclohexanol Using Enantioenriched Chiral Silyl Chloride...	179



Scheme 4.9 Proposed Mechanistic Paths of Silylation for Cyclohexanol .....	182
Scheme 4.10 Stepwise Investigation of Stereochemistry at Silicon .....	184
Scheme 4.11 Proposed Mechanism of Alcohol Approaches from Catalyst Side .....	186

## CHAPTER 1

### BACKGROUND AND INTRODUCTION OF ASYMMETRIC SILYLATION

#### 1.1 Introduction

A molecule which is non-superimposable to its mirror image is called a chiral molecule:<sup>1</sup> it resembles the difference of our left hand and right hands. The left hand and right hand are mirror images to each other, however, due to the lack of symmetry, they are not superimposable to each other. In other words, a molecule is chiral if it is asymmetric. Among the many types of asymmetry, this research will be focused mainly on the asymmetry that results from tetrahedral geometry. A center atom, normally a carbon, that is bonded to four different substituents is called a stereogenic center or a chiral center and the whole molecule is chiral if there is a lack of symmetry.

The mirror image of a chiral compound is known as its enantiomer<sup>2</sup> (Figure 1.1). A pair of enantiomers will exhibit the same physical and chemical properties. However, in most cases they can have a vast difference in biological activities. Thus, it brings us the importance of isolating the racemic mixture (50:50 mixture of the two enantiomers) into a single pure enantiomer.<sup>2</sup> This is particularly crucial in the pharmaceutical industry. Normally, one enantiomer of a drug will have the desired biological effect, and the other will have less or no effect, and can sometimes exhibit a negative effect.<sup>3</sup>

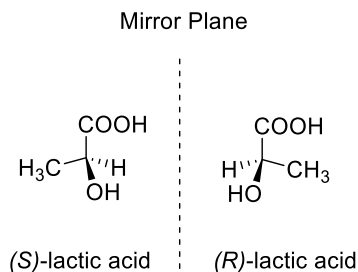


**Figure 1.1 A Pair of Enantiomers of Lactic Acid**

One example of enantiomers that have different biological activities is ethambutol<sup>4</sup> (Figure 1.2 (A)). In this case (*S,S*)-(+)-ethambutol is an antibacterial medication primarily used to treat tuberculosis, however its enantiomer (*R,R*)-(-)-ethambutol will cause blindness. Another example is dextropropoxyphene, an analgesic in the opioid category under the tradename “Darvon” by Eli Lilly and Company since 1955. However, its enantiomer levopropoxyphene, with a tradename “Novrad” can only be used as an antitussive (Figure 1.2 (B)).<sup>5</sup>

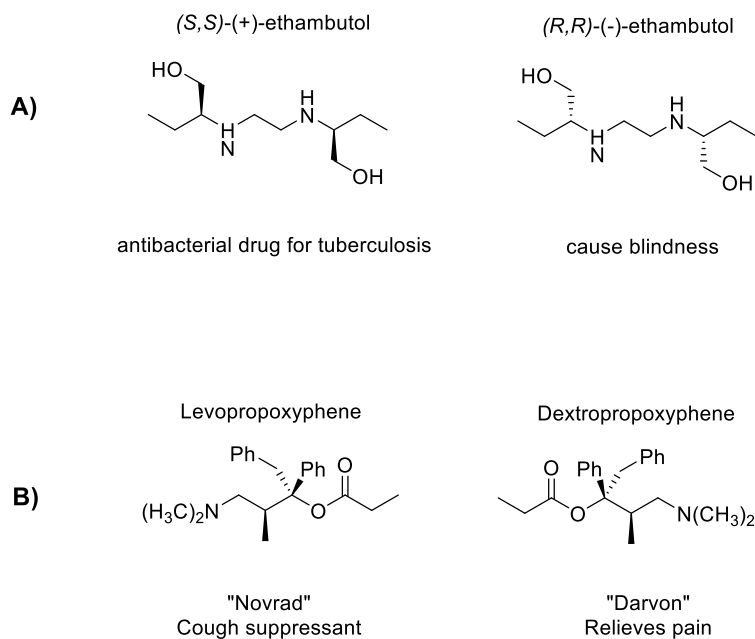


**Figure 1.2 Biological Differences of Ethambutol and Propoxyphene**

Because of this potential difference in biological activities, the US Food and Drug Administration (FDA) requires all pharmaceutical companies to test the biological effects of both enantiomers of potential drugs before it comes to the market.<sup>6</sup> The level of enantiopurity must be maintained high (greater than 99%) and be consistent with samples used in vitro and clinical trials if the drug is sold in single enantiomer form. And if the drug is sold as a racemic mixture, the pharmaceutical companies must prove that the other version of the enantiomer of the active one to be inert and nontoxic. Apparently, there is a huge demand for enantiomerically pure compounds in the pharmaceutical industry, and pharmaceutical companies are craving for different methods to access and improve the enantiopurity of their drug candidates and starting materials/intermediates.<sup>7</sup>

Therefore, it is important for us to quantify the enantiopurity of a compound. The term enantiomeric excess (*ee*) is a measurement used to tell the level of enantiomeric enrichment (Equation 1.1). The *ee* reflects the degree of which a sample contains one enantiomer in a greater amount than the other. A racemic compound will have an *ee* equals to 0% and a single enantiomer will have an *ee* of 100%. Thus, the goal is to increase the *ee* in order to obtain enantiomerically pure products, and there are many ways to achieve this goal.

$$\text{enantiomeric excess} = \left[ \frac{|[R]-[S]|}{[R]+[S]} \right] \times 100\%$$

**Equation 1.1**

## 1.2 Natural Chiral Pool

No one will doubt that nature has impressive synthetic skills that produce complicated, enantiomerically pure compounds, which still has humans discovering their structures and how to synthesize them. Opium has been actively collected and used ever since 1500 BCE in the Mediterranean region, and it wasn't until 1804 that morphine (Figure 1.3) was extracted from opium as the first active alkaloid by Friedrich Sertürner.<sup>8</sup> People waited another 150 years for the first total synthesis of morphine by Marshall Gates.<sup>9</sup>

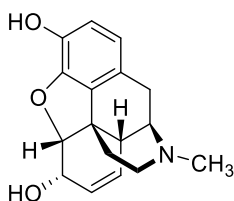


**Figure 1.3 The Structure of Morphine**

However, nature has its own limitations in terms of quantity and variety of bioactive enantiopure compounds. We cannot rely on luck to find a specific compound from a specific plant that coincidentally treats some lethal disease. Modern pharmaceutical companies normally need a variety of derivatized enantiopure compounds to be screened as possible candidates for a disease. Therefore, alternative synthetic routes to a single enantiomer are in huge demand and organic chemists are continually trying to fulfill that demand.

### 1.3 Asymmetric Catalysis

Asymmetric catalysis is widely used as a direct way to produce enantiopure compounds from a corresponding achiral starting material. In this way, a prochiral starting material will be treated with a chiral catalyst and the reaction could occur preferentially on either the *re* or *si* side of the prochiral molecule (Figure 1.4).

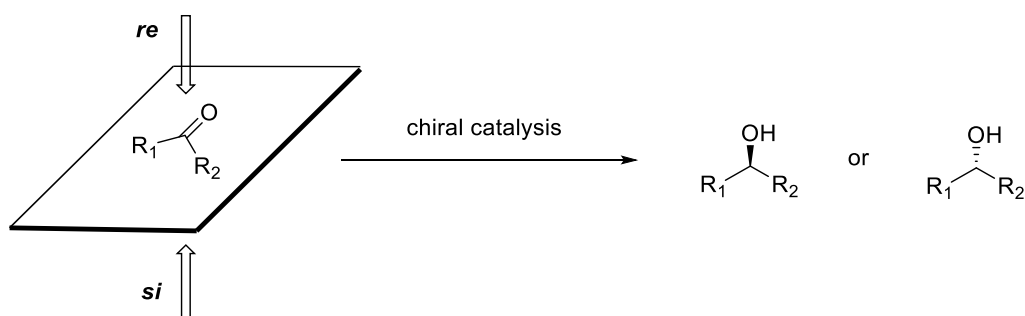
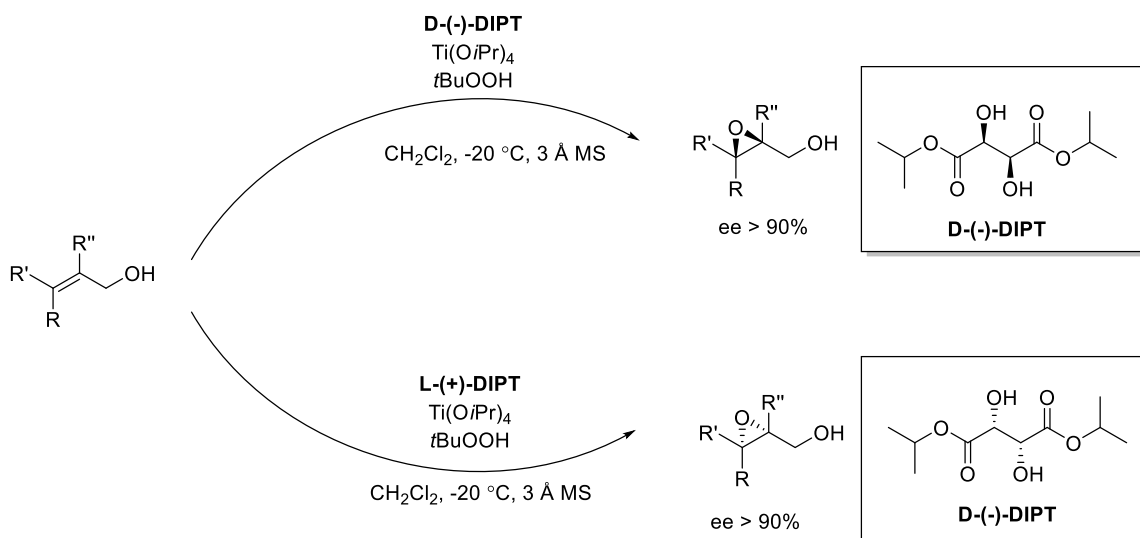


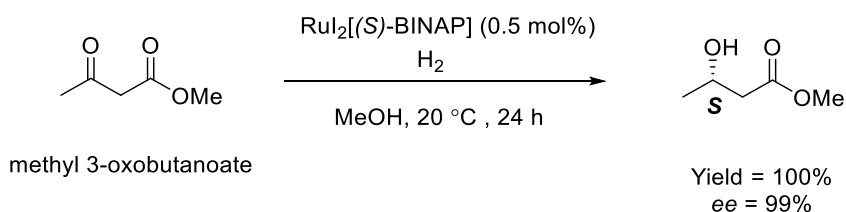
Figure 1.4 Asymmetric Catalysis

One of the most famous examples of asymmetric catalysis is the Sharpless enantioselective epoxidation (Scheme 1.1).<sup>10-11</sup> In this reaction, the diastereomer of chiral diisopropyl tartrate and titanium tetra(isopropoxide) were used to form the catalyst complex along with tert-butyl hydroperoxide as the oxidizing agent. This allows the enantioselective oxidation of the alkene of allylic alcohols to epoxides with a high level of control.



**Scheme 1.1 Sharpless Asymmetric Epoxidation**

Another important example of asymmetric catalysis is the Noyori asymmetric hydrogenation of ketones (Scheme 1.2). In 2001, Ryoji Noyori shared the Nobel Prize in Chemistry with William Knowles for the contribution of asymmetric hydrogenation.<sup>12</sup> The chiral BINAP-Ru(II) catalyst was used, and a variety of functionalized ketones and olefins could be hydrogenated with high *ee* and quantitative yield.<sup>12-15</sup>



**Scheme 1.2 Noyori's Asymmetric Hydrogenation of Ketone**

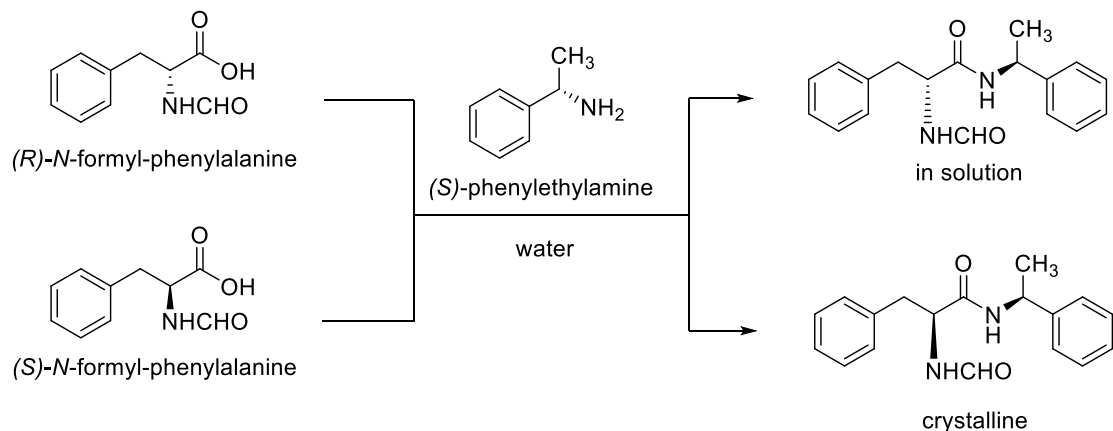
Despite the power of asymmetric catalysis and the numerous published reports in asymmetric catalysis, one of the significant disadvantages is the enantioenrichment will remain unchanged throughout the reaction and is independent of conversion. This means

the entire system has to be optimized for substrates with low *ee*'s in asymmetric catalysis, and this will result in an increase in cost to bring it to industrial production. Due to this drawback of asymmetric catalysis, it is important for us to look for alternative methods of enantioenrichment of compounds in industry.

#### 1.4 Classical Resolution

Classical resolution is one of the oldest approaches to obtain enantiomerically pure compounds, normally through a crystallization process.<sup>16-17</sup> During a classical resolution, a racemic mixture of starting material is treated with an enantiopure chiral resolving reagent and is converted into a pair of diastereomers. This method is dependent on a difference in physical properties of these two diastereomers, such as different solubility in a specific solvent. In the below example,<sup>18</sup> the racemic *N*-formyl-phenylalanine is reacted with enantiopure (*S*)-phenylethylamine (Scheme 1.3). The resulting amide diastereomers have different solubilities in water. One of the diastereomeric salts will precipitate out and the other one will remain in solution. However, the main limitation of this technique is the stoichiometric amount of chiral resolving agent being used and only a 50% theoretical yield can be achieved.





**Scheme 1.3 Classic Resolution of *N*-Formyl-Phenylalanine**

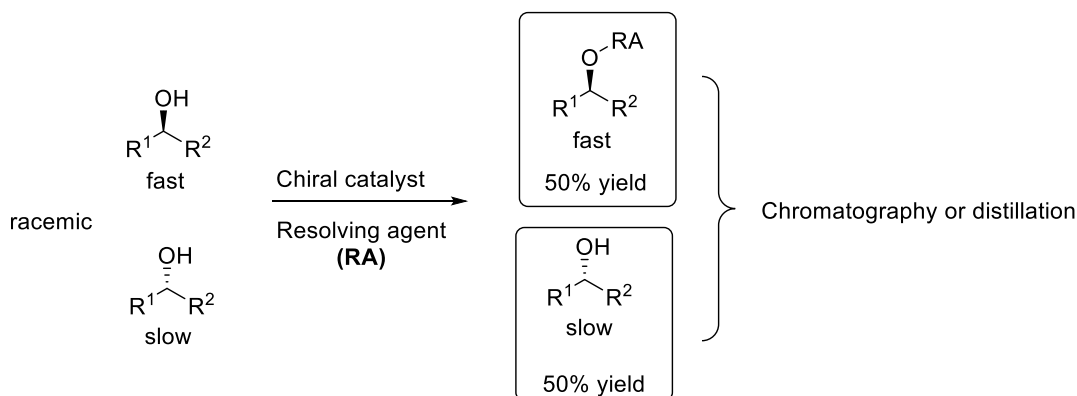
### 1.5 Chiral Chromatography Resolution

In the method, column chromatography with a chiral stationary phase is utilized for the isolation of racemic compounds.<sup>2</sup> The chiral stationary phase could be prepared by attaching a specific chiral compound to the surface of an achiral support such as silica gel. Because of this additional chiral environment on stationary phase, the two enantiomers will have different affinities to the stationary phase and thus exit the column at different times. The major drawback of this technique is the large use of solvent, high cost of the chiral column, and limitation of chiral stationary phase.

### 1.6 Kinetic Resolution

The last technique introduced here is the kinetic resolution,<sup>19</sup> which is also the major focus in this dissertation. In kinetic resolutions, the two enantiomers are competing kinetically in terms of reaction rate. The faster enantiomer will either selectively react with the resolving agent in the presence of a chiral catalyst or being oxidized, and the slow enantiomer will remain unreacted. In this case, the “reacted product” and the “unreacted

starting material” will have different physical properties and could be isolated either with column chromatography or by distillation (Scheme 1.4).



**Scheme 1.4 General Scheme of Kinetic Resolution of Alcohols Reacting with Resolving Agent**

Unlike asymmetric catalysis, the *ee* changes over the course of the reaction in kinetic resolutions. The *ee* of the unreacted starting materials will increase with increasing conversion, and the *ee* of the product will decrease if we push the reaction to go further. For highly efficient kinetic resolutions, it is ideal to stop the reaction at around 50% conversion to achieve the best yields of both enantiomerically enriched, unreacted starting materials and products. The beauty of this intrinsic characteristic of kinetic resolutions is that we can still achieve enantiomerically enriched targets with less efficient kinetic resolutions by pushing the reaction to a high conversion. This is especially important in the pharmaceutical industry with regard to the large expense associated with optimization of asymmetric catalysis. Due to the fact that *ee* changes based on the conversion, a selectivity factor (*s*) is used as a measurement of efficiency in a kinetic resolution.<sup>19</sup> The selectivity factor is a ratio of the rate of the fast enantiomer over the slow enantiomer (Equation 1.2).

It is directly related to the energy difference in the diastereomeric transition states of the two enantiomers. The bigger the energy difference in diastereomeric transition states, the larger the selectivity factor and the more efficient the kinetic resolution.

$$s = k_{\text{rel}} = k_{\text{fast}}/k_{\text{slow}} = e^{\Delta\Delta G^\ddagger/RT}$$

### Equation 1.2

The selectivity factor can be calculated using the enantiomeric excess of both the starting materials ( $ee_{\text{sm}}$ ) and the products ( $ee_{\text{pr}}$ ) obtained from HPLC by first calculating the conversion (Equation 1.3) then using that information with  $ee$  to obtain  $s$  (Equation 1.4). Generally, a selectivity factor  $s \geq 10$  for a kinetic resolution is considered to be efficient in practical use. Due to the fact that in a kinetic resolution, the  $ee$  changes relative to conversion and the selectivity remains constant a desired  $ee$  can be achieved by controlling the conversion. The needed conversion could be calculated (Equation 1.5) using the selectivity of the specific substrate ( $s$ ), the enantiomeric ratio of the starting material ( $S_{\text{min}}^0 : S_{\text{maj}}^0$ ; 50:50 for racemic mixtures), and the enantiomeric ratio of the desired unreacted starting material ( $S_{\text{min}}$  for minor enantiomer and  $S_{\text{maj}}$  for major enantiomer). For example, if a specific substrate has a selectivity factor of 10, we can obtain the enantiomerically enriched unreacted starting materials (e.r. : 99:1) by pushing the conversion to 70%.

$$\text{conv} = \frac{ee_{\text{sm}}}{ee_{\text{sm}} + ee_{\text{pr}}}$$

### Equation 1.3

$$s = \frac{\ln[(1-\text{conv})(1-ee_{sm})]}{\ln[(1-\text{conv})(1+ee_{pr})]}$$

**Equation 1.4**

$$\text{conv} = 1 - \left[ \left( \frac{S_{\min}}{S_{\min}^0} \right) \left( \frac{S_{\text{maj}}^0}{S_{\text{maj}}} \right)^s \right]^{1/(s-1)}$$

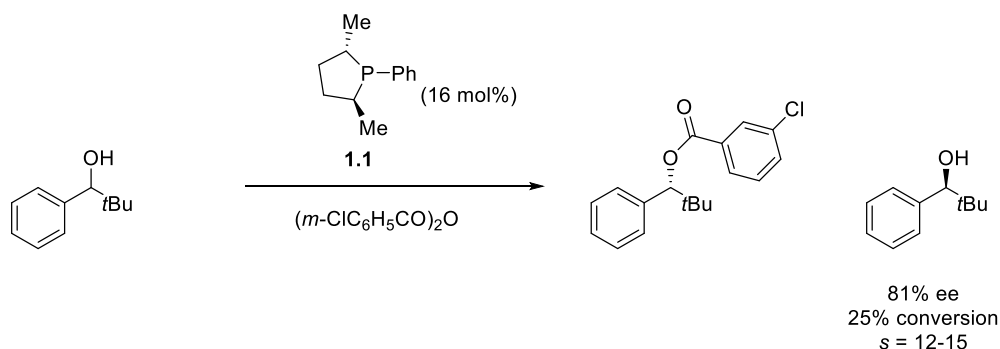
**Equation 1.5**

Kinetic resolutions can be achieved through enzymatic-catalyzed, transition-metal-catalyzed or organocatalyzed processes. Despite the great successes of enzymatic<sup>20-21</sup> and transition-metal-catalyzed<sup>22</sup> kinetic resolutions, kinetic resolutions that are organocatalyzed is evolving quickly and offers promising advantages, including low cost, low toxicity of the catalyst and the resistance to oxygen or water.<sup>23-24</sup> With regards to this, organocatalyzed kinetic resolutions will be discussed in detail here. The substrates of interest in this dissertation are secondary alcohols specifically due to the fact that enantiopure chiral secondary alcohols are important building blocks in pharmaceutical industries.<sup>25</sup>

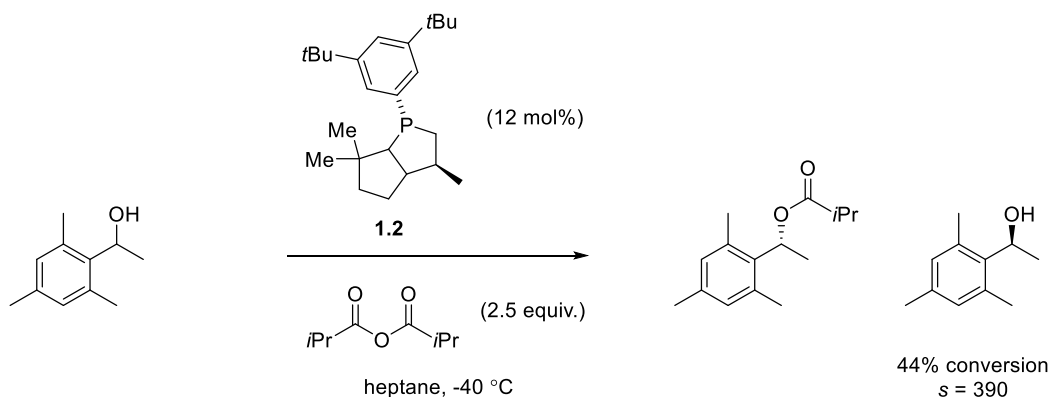
## 1.7 Acylation

The organocatalyzed acylation of alcohols is probably the most studied among organocatalyzed kinetic resolutions. Several important classes of catalysts have been studied including, but not limited to, chiral phosphines,<sup>26-28</sup> chiral DMAP (4-dimethylaminopyridine),<sup>29</sup> and amidine-based isothiourea catalysts.<sup>30-33</sup> One of the very

first examples of an efficient organocatalyzed acylation of secondary alcohols was conducted using a chiral phosphine catalyst by the Vedejs group.<sup>26</sup> In this reaction, a chiral phosphine catalyst **1.1** was combined with *m*-chlorobenzoic anhydride to selectively acylate one enantiomer from the racemic acyclic secondary alcohols (Scheme 1.5). The catalyst **1.1** was later modified to a more efficient bicyclic phosphine version **1.2** for the kinetic resolution of alkyl carbinols.<sup>28</sup> In this kinetic resolution, isobutyric anhydride was used as the acylating agent in a non-polar solvent like heptane, at a cold temperature (Scheme 1.6). This kinetic resolution showed a high degree of discrimination for benzylic alcohols with a selectivity factor of 390 for 1-mesitylethanol.

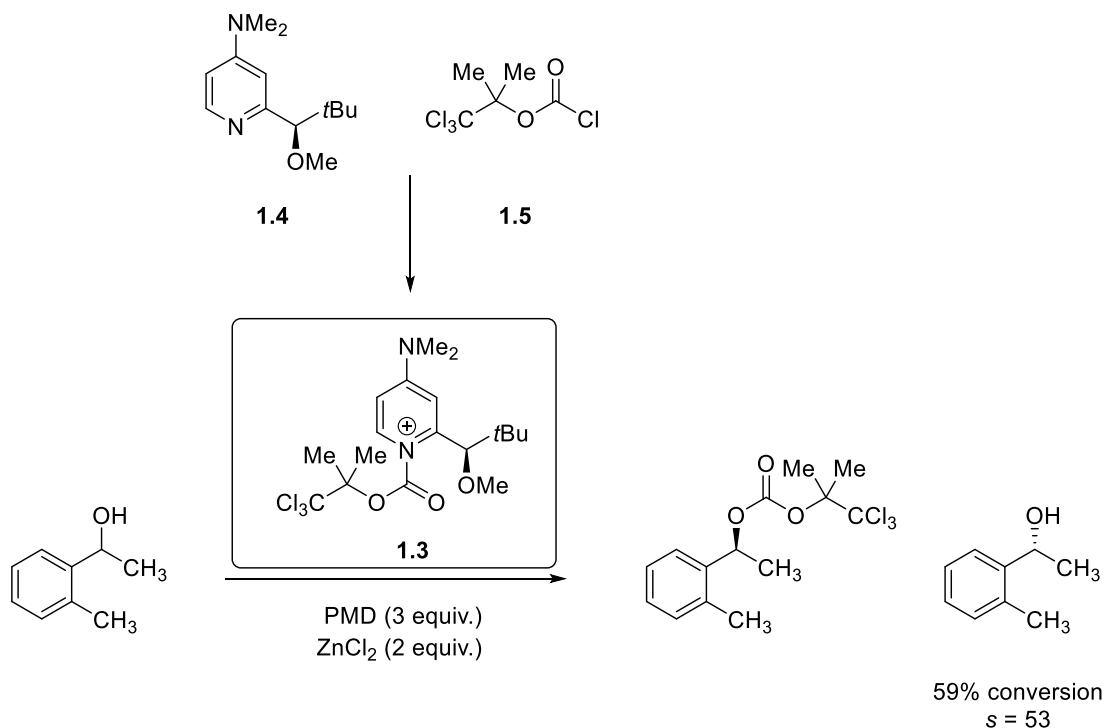


**Scheme 1.5 Kinetic Resolution of Secondary Alcohols Using a Chiral Phosphine**



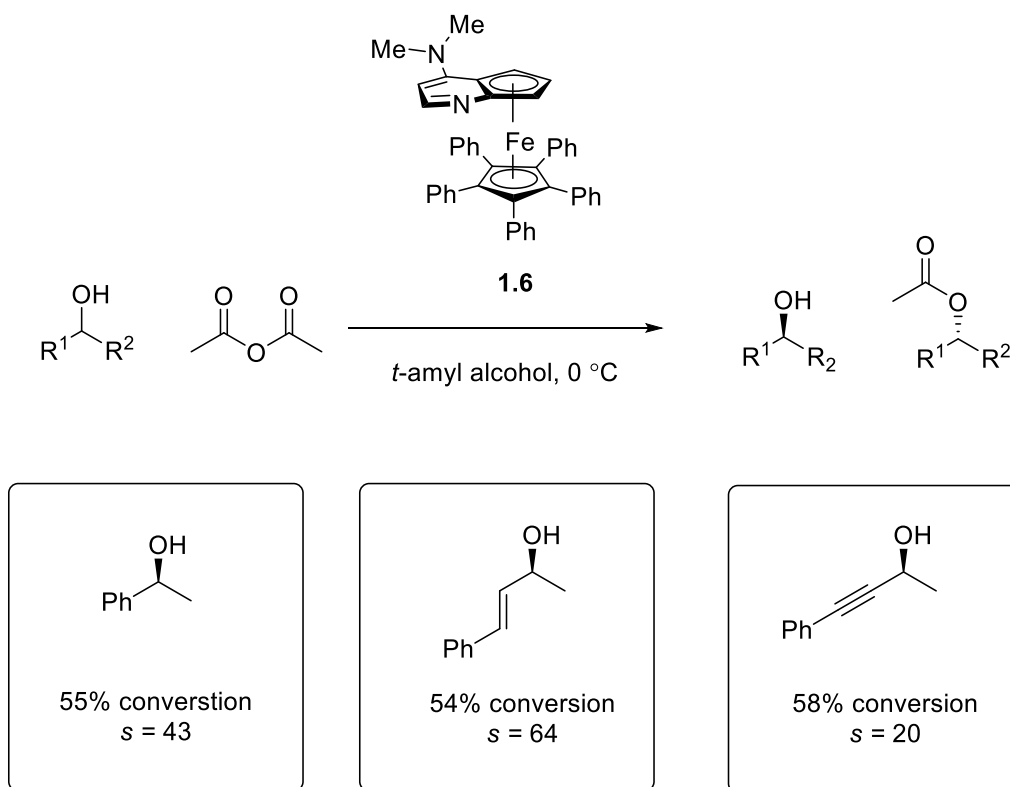
**Scheme 1.6 Modified Bicyclic Phosphine Catalyzed Kinetic Resolution of Secondary Alcohols**

Shortly after the phosphine-catalyzed kinetic resolution was introduced, another type of catalyst, a chiral 4-dimethylaminopyridine (DMAP), was investigated in the same group and proved to be an excellent acyl-transfer catalyst for secondary alcohols.<sup>29</sup> This was one of the very first examples of chiral DMAP catalyzed kinetic resolutions. In this reaction, an acyl pyridinium salt **1.3** was formed by reacting a chiral DMAP derivative **1.4** with the 2,2,2-trichloro-1,1-dimethylethyl chloroformate **1.5**. The reaction required ZnCl<sub>2</sub> as the Lewis acid and 1,2,2,6,6-pentamethylpiperidine (PMD) as the base to achieve a better conversion (Scheme 1.7). Decent selectivity factors up to 53 were achieved for a variety of secondary alcohols. Despite the high stoichiometric amount of chiral DMAP used in this reaction, these results encouraged other researchers to investigate chiral DMAP-based catalysts in kinetic resolutions because DMAP is known for its good nucleophilicity and the promising selectivity factors achieved by the Vedejs group.



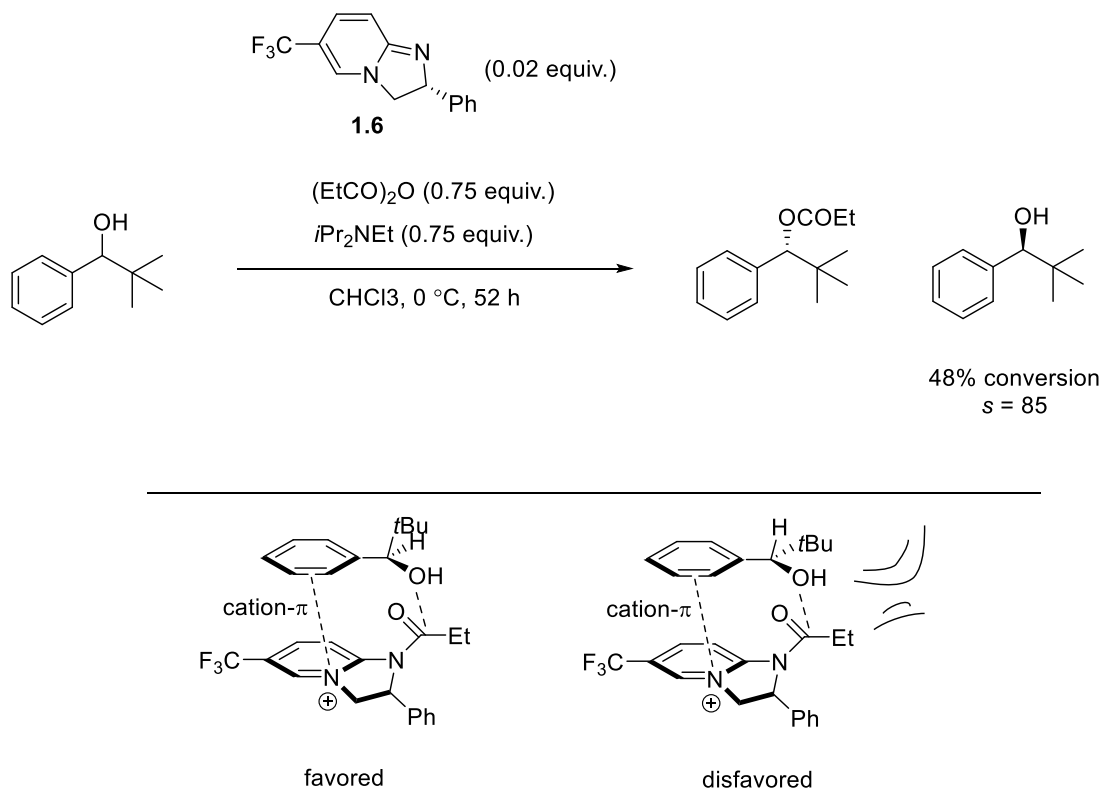
**Scheme 1.7. Chiral DMAP Catalyzed Kinetic Resolution by Vedejs**

At around the same time, Fu and coworkers designed a novel chiral DMAP catalyst by introducing a derivatized planar DMAP onto the FeCpCl or FeCp\*Cl (Cp = cyclopentadiene; CP\* = pentaphenyl cyclopentadiene ligand) through  $\pi$  bonding.<sup>34</sup> The catalyst itself is still considered as the organocatalyst considering the metal is not involved in the catalytic cycle of the reaction. The optimized Fu's planar-chiral DMAP catalyst **1.6** has proven to be very efficient in kinetic resolution for a variety of different classes of secondary alcohols, such as allylic<sup>35</sup>, propargylic<sup>36</sup>, and benzylic alcohols<sup>37</sup> (Scheme 1.8). Besides the great contributions from Vedejs and Fu to the chiral DMAP-based catalyst, there are some other important DMAP- or pyridine-based chiral catalysts in the kinetic resolution of secondary alcohols.<sup>38-42</sup>



**Scheme 1.8. Kinetic Resolution using Fu's chiral DMAP catalyst**

Other classes of acylation-based kinetic resolution discussed here are the amidine- and isothiurea-based catalysts developed by Birman in 2004.<sup>43</sup> The original catalyst (*R*)-CF<sub>3</sub>-PIP **1.7** showed great efficiency with a variety of secondary alcohols with a  $\pi$  system, and a selectivity factor up to 85 was achieved with only a 2 mol% catalyst loading (Scheme 1.9). The proposed mechanism explains why a  $\pi$  system is necessary for a decent selectivity. This is due to the formation of a favorable cation- $\pi$  or  $\pi$ - $\pi$  stacking interaction between the cationic acylated catalyst intermediate and the substrate. This allows one enantiomer of the alcohol to approach the reactive acyl part rather than the unreactive one (Scheme 1.9). Later versions of this catalyst included levamisole **1.7**, (+)-benzotetramisole (+)-**1.8** and homobenzotetramisole **1.9** (Figure 1.5) which were selective in resolving different classes of secondary alcohols.<sup>30-31</sup>



**Scheme 1.9. Kinetic Resolution of Secondary Alcohols Using Amidine-Based Catalysts by Birman**



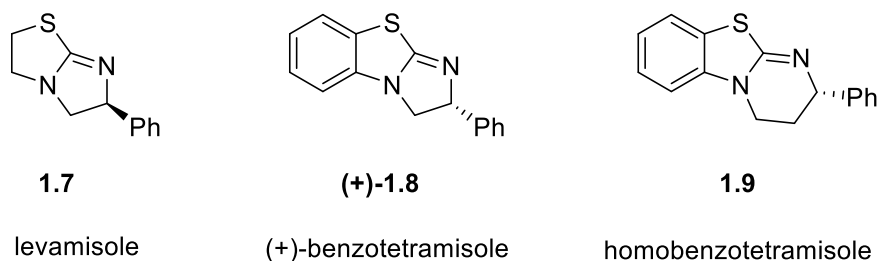
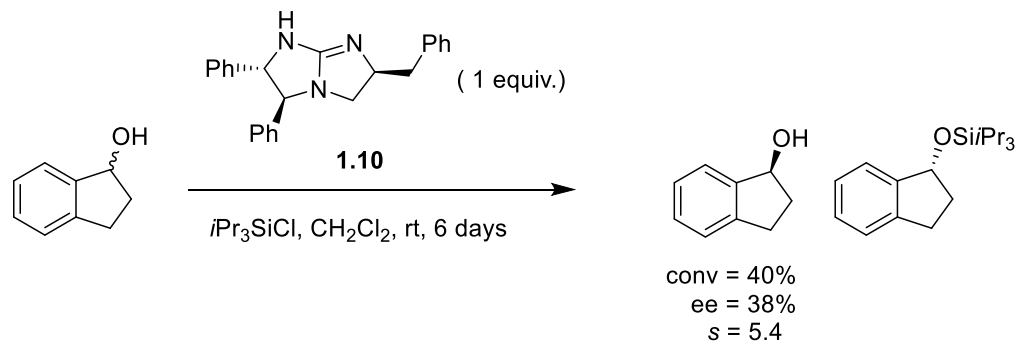


**Figure 1.5 Amidine- and Isothiourea-Based Catalysts**

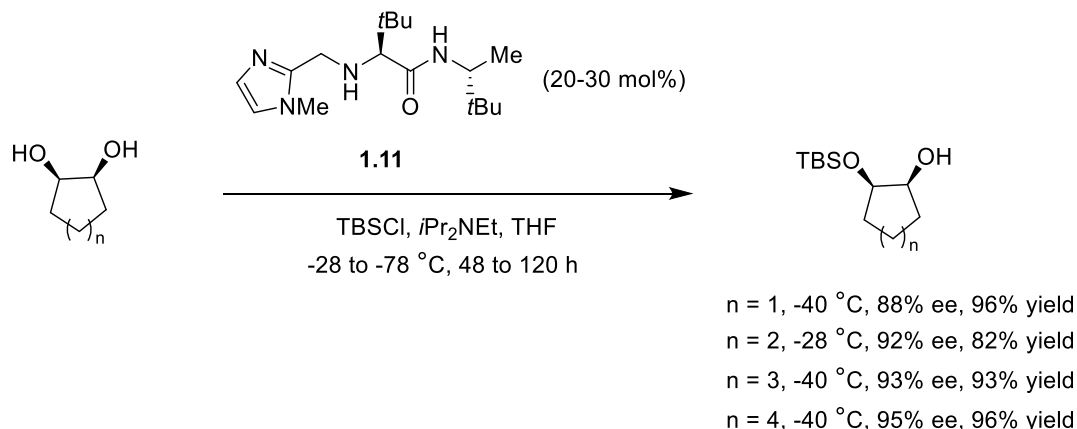
### 1.8 Silylation

Silyl ethers are arguably the most commonly used protecting groups for alcohols. This is because silyl ethers are easy to install and remove. Additionally, the orthogonality of silyl ether protecting groups is an extremely important factor in terms of organic synthesis. However, compared to the enormous investigations on the asymmetric acylation of alcohols, the idea of asymmetric silylation of alcohols was relatively unexplored. It was not until 2001 when Ishikawa and co-workers reported the first kinetic resolution of alcohols with asymmetric silylation.<sup>44</sup> In this kinetic resolution, a stoichiometric amount of chiral guanidine **1.10** was used as the catalyst and this reaction took several days to achieve poor to moderate selectivities for various bicyclic secondary alcohols (Scheme 1.10). Despite the drawbacks of this report, this is the first example of enantioselective silylation of secondary alcohols and it inspired many researchers in the field of asymmetric functionalization of secondary alcohols using silicon as the derivatizing agent. The author also suggested that the silyl guanidinium salt resulting from the reaction between guanidine catalyst and silyl chloride might be the actual silyl agent based on the NMR studies of an equimolar mixture of both.



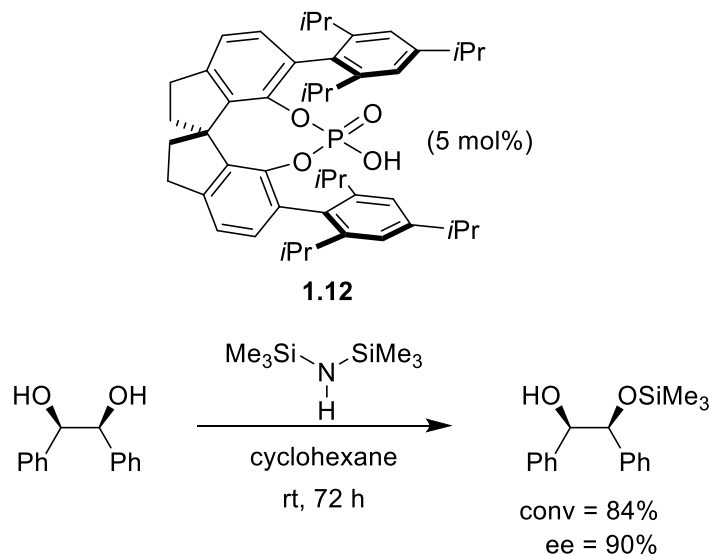
**Scheme 1.10. First Silylation-Based Kinetic Resolution of Secondary Alcohols Using Modified Guanidine**

Inspired by Ichikawa's work, Hoveyda, Snapper and co-workers reported an enantioselective silylation of *meso* diols using amino-acid-based small molecules as catalysts.<sup>45</sup> In this report, the amino-acid-based catalyst **1.11** was carefully designed to contain both the Lewis basic moiety and a potential hydrogen bonding site. The bifunctional catalyst could activate the silyl chloride as well as approach the alcohol asymmetrically using hydrogen bonding, allowing a variety of diols<sup>45</sup> and triols<sup>46</sup> to be enantioselectively silylated (Scheme 1.11). In the proposed mechanism, the imidazole moiety was believed to bind to silicon, leading to a polarization of the Si-Cl bond which activates the silyl chloride by increasing the electrophilicity at the silicon center.<sup>47</sup> The drawbacks of this initial report, high catalyst loading and long reaction time were solved by adding a more nucleophilic co-catalyst later.<sup>48</sup>



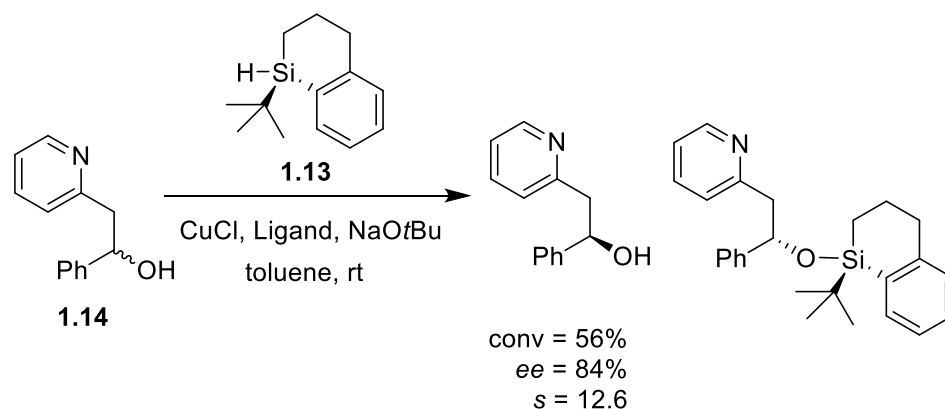
**Scheme 1.11. Desymmetrization of *Meso* Diols with Amino-Acid-Based Catalyst**

Another example of catalytic enantioselective desymmetrization of *meso* diols is reported by the List group.<sup>49</sup> They developed a Brønsted acid catalyst (**1.12**) with hexamethyldisilazane (HMDS) as the silyl source and moderate to good results were obtained with a number of aryl substituted *meso* diols (Scheme 1.12). In the proposed mechanism, protonation of the basic silicon source (HMDS) will generate an ion pair consisting of a cationic silylium source accompanied by the enantiopure counteranion. The reaction of this ion pair intermediate with the diol substrate could then potentially proceed enantioselectively via a desymmetrization reaction. Good enantioselectivity was achieved even with low catalyst loading of only 5 mol%.



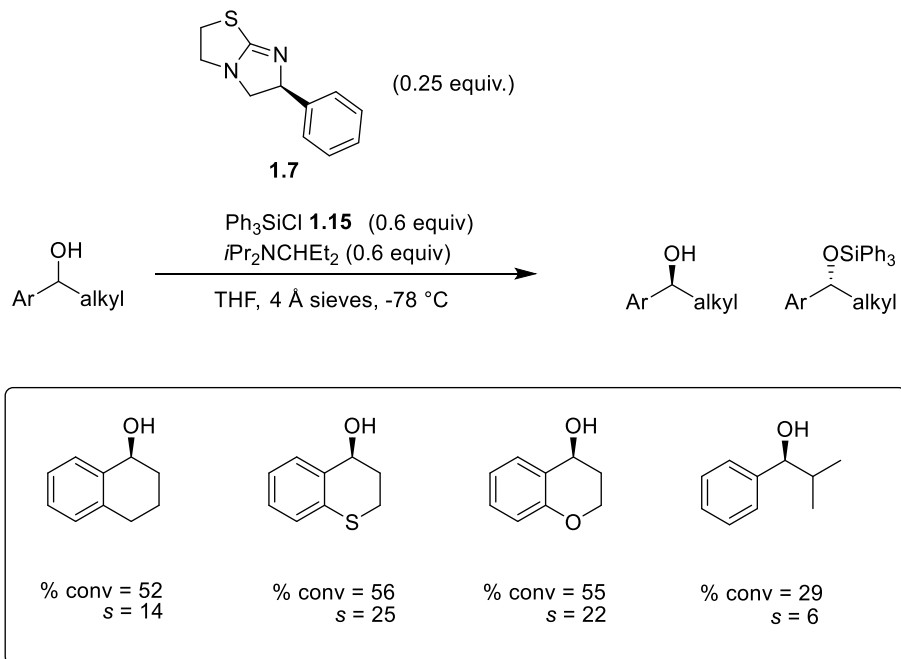
**Scheme 1.12. Desymmetrization of *Meso* Diols with Brønsted Acid Catalyst**

Another approach to achieve asymmetric silylation of secondary alcohols is through a transition metal-catalyzed dehydrogenative coupling reaction. In 2005, the Oestreich group reported their first example of the kinetic resolution of secondary alcohols with silicon-stereogenic silanes.<sup>50</sup> In this reaction, a copper(I) precatalyst was used to promote the dehydrogenative coupling between the alcohol and chiral silane **1.13**. It was found that a substrate that has two-point binding like the 2-pyridyl-substituted alcohol **1.14** was crucial to obtain good selectivity (Scheme 1.13). The chiral silane was recovered and recycled without racemization. Despite the drawbacks of the difficulty to prepare the chiral silane and the limited substrate scope, this methodology opens a new window of asymmetric silylation of alcohols. Later the same group investigated other potential donor groups other than the 2-pyridyl unit and found ways to do the kinetic resolution by just using chiral ligands on the metal instead of chiral silanes. The optimized methodology was applied to a variety of challenging alcohols.<sup>51-54</sup>



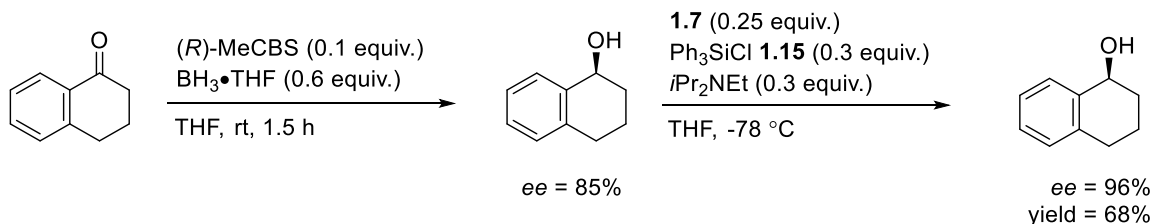
**Scheme 1.13. Kinetic Resolution of Secondary Alcohols Using Chiral Silanes**

In 2011, the Wiskur group reported a successful silylation-based kinetic resolution of a monofunctional secondary alcohol that employed an isothioureia catalyst.<sup>55</sup> This chiral isothioureia catalyst levamisole (**1.7**) was originally reported by Birman<sup>30</sup> for promoting the kinetic resolution of alcohols via acylation (Section 1.4); it also showed promising selectivity in Wiskur's silylation-based kinetic resolution. In this system, triphenylsilyl chloride **1.15** was used as the silyl source along with the nucleophilic catalyst **1.7**, a variety of monofunctional bicyclic alcohols were resolved with selectivity factors up to 25. However, it is ineffective with acyclic alcohols resulting in low conversion and poor selectivity factors (Scheme 1.14).



**Scheme 1.14 Silylation-Based Resolution of Monofunctional Secondary Alcohols by Wiskur**

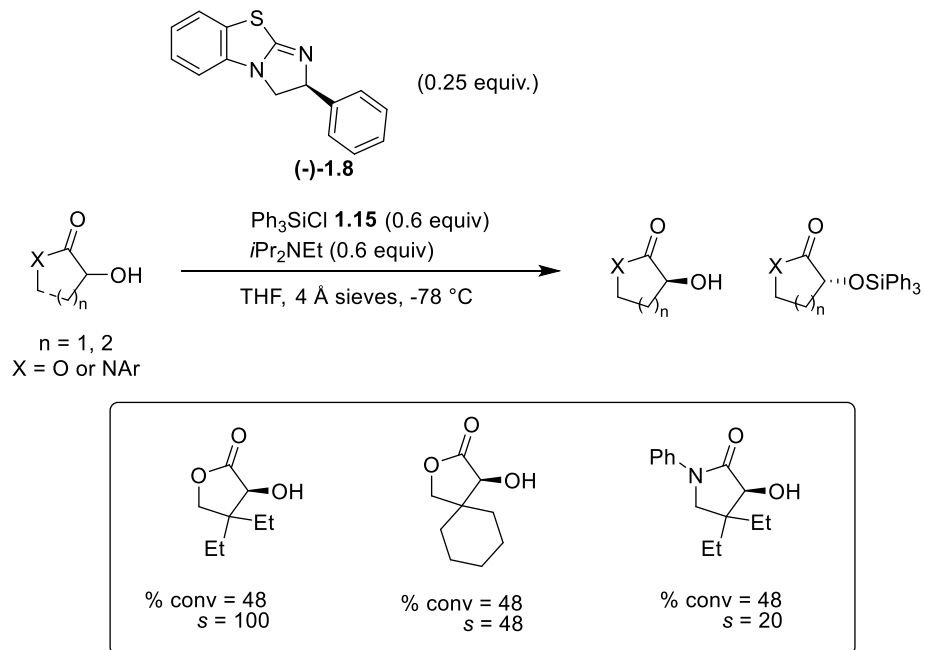
Inspired by this initial successful result of using levamisole and triphenylsilyl chloride to resolve secondary alcohols, the Wiskur group continued to apply this methodology into a one-pot *ee* polishing reaction sequence.<sup>56</sup> In this report, an enantioselective reduction and a silylation-based kinetic resolution were coupled to prepare highly enantioenriched alcohols (Scheme 1.15). The starting material tetralone was reduced asymmetrically using the CBS reduction to prepare the corresponding partially enriched (*ee* = 85%) tetralol, the crude was then subjected to a silylation-based kinetic resolution to achieve enantioenriched (*ee* = 96%) tetralol with an overall 68% yield. This one-pot reaction sequence overcame the drawbacks of a single kinetic resolution (the maximum yield cannot be larger than 50%) and the asymmetric catalysis (*ee* remains the same).



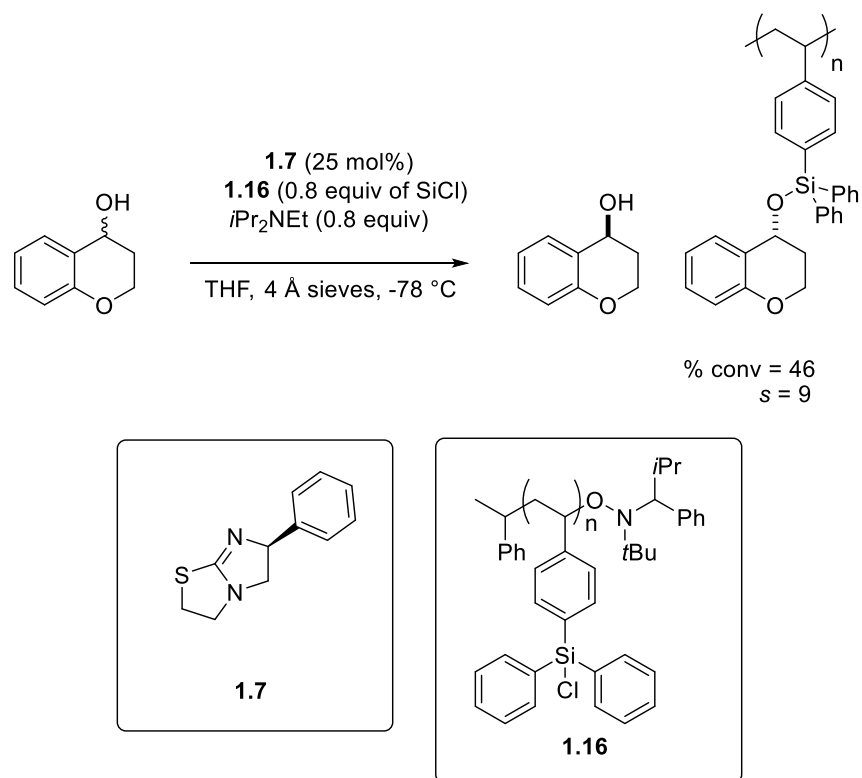
### Scheme 1.15 One-Pot Reduction/Kinetic Resolution Sequence to Achieve Enantioenriched Alcohol

Later Wiskur and co-workers successfully applied this methodology to  $\alpha$ -hydroxy lactones and lactams with the presence of (-)-benzotetramisole (-)-**1.8** as the nucleophilic catalyst (Scheme 1.16).<sup>57</sup> This commercially available catalyst (-)-**1.8** was first introduced by Birman in his asymmetric acylation system.<sup>30</sup> This is one of the few nonenzymatic kinetic resolutions of  $\alpha$ -hydroxy lactones and the first nonenzymatic kinetic resolutions of lactams. Moderate to decent selectivity factors were achieved with a selectivity factor of 100 when sterics were included on one side of the hydroxy group and a planar  $\pi$  system on the other side. This study showed the importance of having both sterics and  $\pi$  systems adjacent to the alcohol to achieve a decent selectivity.

Soon after this substrate expansion of silylation-based kinetic resolution, the Wiskur group performed mechanistic studies by studying the substituent effect of different *p*-substituted triarylsilyl chlorides in the system. A linear free-energy relationship was discovered proposing a pentavalent  $S_N2$ -like transition state with the catalyst as the leaving group and the alcohol as the incoming nucleophile.<sup>58</sup> Recently, they also employed a polystyrene-supported triphenylsilyl chloride in this methodology for the facile separation of the silylated products from the remaining enriched alcohol starting material (Scheme 1.17).<sup>59</sup>



**Scheme 1.16 Silylation-Based Kinetic Resolution of  $\alpha$ -Hydroxy Lactones and -Lactams**



**Scheme 1.17 Polymer Supported Silylation-Based Kinetic Resolution**



## 1.9 Conclusions

The isothiourea catalyzed silylation-based kinetic resolution developed by the Wiskur group has so far shown promising results to resolve monofunctional secondary alcohols. This methodology has been applied to bicyclic alcohols,<sup>55</sup>  $\alpha$ -hydroxy lactones and -lactams<sup>57</sup> with decent selectivity factors. The research has been focused on the expansion of this methodology to a different synthetically useful substrate class as well as on the understanding of the mechanism.

In chapter two, the silylation-based kinetic resolution of various *trans* 2-arylcyclohexanols will be discussed by employing a *p*-isopropyl triphenylsilyl chloride as the derivatizing reagent with (-)-benzotetramisole as the catalyst.<sup>60</sup> The diastereoselective and enantioselective of *trans* alcohols over the *cis* will be investigated and a facial one-pot reaction sequence will be introduced. In chapter three, our efforts towards the understanding of the mechanism will be addressed and the chirality transmission from point chirality to helical chirality was explored using circular dichroism.<sup>61</sup> These studies could help us understand the importance of helical formation in the mechanism and how the chirality is transmitting in this silylation system. The last chapter will discuss some initial studies of stereospecificity at silicon in our silylation-based kinetic resolution system. This study aims to provide us with a more vivid picture of the process of this silylation system.

## 1.10 References

1. Wade, L. G.; Simek, J. W., *Organic chemistry*. Ninth edition. ed.; Pearson: Glenview, IL, 2017.
2. Eliel, E. L.; Wilen, S. H.; Mander, L. N., *Stereochemistry of organic compounds*. Wiley: New York, 1994.
3. Shah, R. R.; Midgley, J. M.; Branch, S. K., Stereochemical origin of some clinically significant drug safety concerns: Lessons for future drug development. *Adverse. Drug. React. T.* **1998**, *17* (2-3), 145-190.
4. Yendapally, R.; Lee, R. E., Design, synthesis, and evaluation of novel ethambutol analogues. *Bioorg. Med. Chem. Lett.* **2008**, *18* (5), 1607-1611.
5. Wainer, I. W., Three-dimensional view of pharmacology. *Am. J. Hosp. Pharm.* **1992**, *49* (9 Suppl 1), S4-8.
6. USFDA  
<http://www.fda.gov/Drugs/GuidanceComplianceRegulatoryInformation/Guidances/ucml22883.htm>.
7. Breuer, M.; Ditrich, K.; Habicher, T.; Hauer, B.; Kessler, M.; Sturmer, R.; Zelinski, T., Industrial methods for the production of optically active intermediates. *Angew. Chem. Int. Ed.* **2004**, *43* (7), 788-824.
8. Luch, A., *Molecular, clinical, and environmental toxicology*. Birkhäuser: Boston, 2009.
9. Gates, M.; Tschudi, G., The Synthesis of Morphine. *J. Am. Chem. Soc.* **1952**, *74* (4), 1109-1110.

10. Katsuki, T.; Sharpless, K. B., The 1st Practical Method for Asymmetric Epoxidation. *J. Am. Chem. Soc.* **1980**, *102* (18), 5974-5976.
11. Finn, M. G.; Sharpless, K. B., Mechanism of Asymmetric Epoxidation .2. Catalyst Structure. *J. Am. Chem. Soc.* **1991**, *113* (1), 113-126.
12. Noyori, R.; Ohkuma, T.; Kitamura, M.; Takaya, H.; Sayo, N.; Kumobayashi, H.; Akutagawa, S., Asymmetric Hydrogenation of Beta-Keto Carboxylic Esters - a Practical, Purely Chemical Access to Beta-Hydroxy Esters in High Enantiomeric Purity. *J. Am. Chem. Soc.* **1987**, *109* (19), 5856-5858.
13. Noyori, R.; Ohta, M.; Hsiao, Y.; Kitamura, M.; Ohta, T.; Takaya, H., Asymmetric-Synthesis of Isoquinoline Alkaloids by Homogeneous Catalysis. *J. Am. Chem. Soc.* **1986**, *108* (22), 7117-7119.
14. Mashima, K.; Kusano, K. H.; Sato, N.; Matsumura, Y.; Nozaki, K.; Kumobayashi, H.; Sayo, N.; Hori, Y.; Ishizaki, T.; Akutagawa, S.; Takaya, H., Cationic Binap-Ru(II) Halide-Complexes - Highly Efficient Catalysts for Stereoselective Asymmetric Hydrogenation of Alpha-Functionalized and Beta-Functionalized Ketones. *J. Org. Chem.* **1994**, *59* (11), 3064-3076.
15. Noyori, R., Asymmetric catalysis: Science and opportunities (Nobel lecture). *Angew. Chem. Int. Ed.* **2002**, *41* (12), 2008-2022.
16. Porter, W. H., Resolution of Chiral Drugs. *Pure. Appl. Chem.* **1991**, *63* (8), 1119-1122.
17. Keith, J. M.; Larrow, J. F.; Jacobsen, E. N., Practical considerations in kinetic resolution reactions. *Adv. Synth. Catal.* **2001**, *343* (1), 5-26.

18. Palovics, E.; Schindler, J.; Faigl, F.; Fogassy, E., The influence of molecular structure and crystallization time on the efficiency of diastereoisomeric salt forming resolutions. *Tetrahedron-Asymmetry*. **2010**, *21* (19), 2429-2434.
19. Fiaud, J. C.; Kagan, H. B., *In Topics in Stereochemistry, L., E.; Wilen, S. H., .* John Wiley and Sons, Inc.: New York, 1988; Vol. 18.
20. Koeller, K. M.; Wong, C. H., Enzymes for chemical synthesis. *Nature*. **2001**, *409* (6817), 232-240.
21. Rachwalski, M.; Vermue, N.; Rutjes, F. P. J. T., Recent advances in enzymatic and chemical deracemisation of racemic compounds. *Chem. Soc. Rev.* **2013**, *42* (24), 9268-9282.
22. Hoveyda, A. H.; Didiuk, M. T., Metal-catalyzed kinetic resolution processes. *Curr. Org. Chem.* **1998**, *2* (5), 489-526.
23. Gaunt, M. J.; Johansson, C. C. C.; McNally, A.; Vo, N. T., Enantioselective organocatalysis. *Drug. Discov. Today*. **2007**, *12* (1-2), 8-27.
24. List, B., Introduction: Organocatalysis. *Chem. Rev.* **2007**, *107* (12), 5413-5415.
25. Patel, R. N., Biocatalytic synthesis of chiral alcohols and amino acids for development of pharmaceuticals. *Biomolecules*. **2013**, *3* (4), 741-77.
26. Vedejs, E.; Daugulis, O.; Diver, S. T., Enantioselective acylations catalyzed by chiral phosphines. *J. Org. Chem.* **1996**, *61* (2), 430-431.
27. Vedejs, E.; MacKay, J. A., Kinetic resolution of allylic alcohols using a chiral phosphine catalyst. *Org. Lett.* **2001**, *3* (4), 535-536.

28. Vedejs, E.; Daugulis, O., A highly enantioselective phosphabicyclooctane catalyst for the kinetic resolution of benzylic alcohols. *J. Am. Chem. Soc.* **2003**, *125* (14), 4166-4173.
29. Vedejs, E.; Chen, X. H., Kinetic resolution of secondary alcohols. Enantioselective acylation mediated by a chiral (dimethylamino)pyridine derivative. *J. Am. Chem. Soc.* **1996**, *118* (7), 1809-1810.
30. Birman, V. B.; Li, X. M., Benzotetramisole: A remarkably enantioselective acyl transfer catalyst. *Org. Lett.* **2006**, *8* (7), 1351-1354.
31. Birman, V. B.; Li, X. M., Homobenzotetramisole: An effective catalyst for kinetic resolution of aryl-cycloalkanols. *Org. Lett.* **2008**, *10* (6), 1115-1118.
32. Yang, X.; Lu, G. J.; Birman, V. B., Benzotetramisole-Catalyzed Dynamic Kinetic Resolution of Azlactones. *Org. Lett.* **2010**, *12* (4), 892-895.
33. Li, X. M.; Jiang, H.; Uffman, E. W.; Guo, L.; Zhang, Y. H.; Yang, X.; Birman, V. B., Kinetic Resolution of Secondary Alcohols Using Amidine-Based Catalysts. *J. Org. Chem.* **2012**, *77* (4), 1722-1737.
34. Ruble, J. C.; Fu, G. C., Chiral pi-complexes of heterocycles with transition metals: A versatile new family of nucleophilic catalysts. *J. Org. Chem.* **1996**, *61* (21), 7230-7231.
35. Bellemin-Lapponaz, S.; Tweddell, J.; Ruble, J. C.; Breitling, F. M.; Fu, G. C., The kinetic resolution of allylic alcohols by a non-enzymatic acylation catalyst; application to natural product synthesis. *Chem. Commun.* **2000**, (12), 1009-1010.
36. Tao, B.; Ruble, J. C.; Hoic, D. A.; Fu, G. C., Nonenzymatic kinetic resolution of propargylic alcohols by a planar-chiral DMAP derivative: Crystallographic

characterization of the acylated catalyst (vol 121, pg 5091, 1999). *J. Am. Chem. Soc.* **1999**, *121* (44), 10452-10452.

37. Ruble, J. C.; Latham, H. A.; Fu, G. C., Effective kinetic resolution of secondary alcohols with a planar-chiral analogue of 4-(dimethylamino)pyridine. Use of the Fe(C(5)Ph(5)) group in asymmetric catalysis. *J. Am. Chem. Soc.* **1997**, *119* (6), 1492-1493.

38. Kawabata, T.; Nagato, M.; Takasu, K.; Fuji, K., Nonenzymatic kinetic resolution of racemic alcohols through an "induced fit" process. *J. Am. Chem. Soc.* **1997**, *119* (13), 3169-3170.

39. Spivey, A. C.; Fekner, T.; Spey, S. E., Axially chiral analogues of 4-(dimethylamino)pyridine: Novel catalysts for nonenzymatic enantioselective acylations. *J. Org. Chem.* **2000**, *65* (10), 3154-3159.

40. Naraku, G.; Shimomoto, N.; Hanamoto, T.; Inanaga, J., Synthesis of enantiomerically pure C-2-symmetric 4-pyrrolidinopyridine derivative as a chiral acyl transfer catalyst for the kinetic resolution of secondary alcohols. *Enantiomer.* **2000**, *5* (1), 135-138.

41. Yamada, S.; Misono, T.; Iwai, Y., Kinetic resolution of sec-alcohols by a new class of pyridine catalysts having a conformation switch system. *Tetrahedron. Lett.* **2005**, *46* (13), 2239-2242.

42. O'Dalaigh, C.; Connon, S. J., Nonenzymatic acylative kinetic resolution of Baylis-Hillman adducts. *J. Org. Chem.* **2007**, *72* (18), 7066-7069.

43. Birman, V. B.; Uffman, E. W.; Hui, J.; Li, X. M.; Kilbane, C. J., 2,3-dihydroimidazo[1,2-a]pyridines: A new class of enantioselective acyl transfer catalysts and their use in kinetic resolution of alcohols. *J. Am. Chem. Soc.* **2004**, *126* (39), 12226-12227.

44. Isobe, T.; Fukuda, K.; Araki, Y.; Ishikawa, T., Modified guanidines as chiral superbases: the first example of asymmetric silylation of secondary alcohols. *Chem. Commun.* **2001**, (03), 243-244.
45. Zhao, Y.; Rodrigo, J.; Hoveyda, A. H.; Snapper, M. L., Enantioselective silyl protection of alcohols catalysed by an amino-acid-based small molecule. *Nature*. **2006**, 443 (7107), 67-70.
46. You, Z.; Hoveyda, A. H.; Snapper, M. L., Catalytic Enantioselective Silylation of Acyclic and Cyclic Triols: Application to Total Syntheses of Cleroindicins D, F, and C. *Angew. Chem. Int. Ed.* **2009**, 48 (3), 547-550.
47. Denmark, S. E.; Beutner, G. L., Lewis base catalysis in organic synthesis. *Angew. Chem. Int. Ed.* **2008**, 47 (9), 1560-1638.
48. Manville, N.; Alite, H.; Haeffner, F.; Hoveyda, A. H.; Snapper, M. L., Enantioselective silyl protection of alcohols promoted by a combination of chiral and achiral Lewis basic catalysts. *Nat. Chem.* **2013**, 5 (9), 768-774.
49. Hyodo, K.; Gandhi, S.; van Gemmeren, M.; List, B., Bronsted Acid Catalyzed Asymmetric Silylation of Alcohols. *Synlett*. **2015**, 26 (8), 1093-1095.
50. Rendler, S.; Auer, G.; Oestreich, M., Kinetic resolution of chiral secondary alcohols by dehydrogenative coupling with recyclable silicon-stereogenic silanes. *Angew. Chem. Int. Ed.* **2005**, 44 (46), 7620-7624.
51. Rendler, S.; Plefka, O.; Karatas, B.; Auer, G.; Frohlich, R.; Muck-Lichtenfeld, C.; Grimme, S.; Oestreich, M., Stereoselective Alcohol Silylation by Dehydrogenative Si-O Coupling: Scope, Limitations, and Mechanism of the Cu-H-Catalyzed Non-Enzymatic

Kinetic Resolution with Silicon-Stereogenic Silanes. *Chem. - Eur. J.* **2008**, *14* (36), 11512-11528.

52. Karatas, B.; Rendler, S.; Frohlich, R.; Oestreich, M., Kinetic resolution of donor-functionalised tertiary alcohols by Cu-H-catalysed stereoselective silylation using a strained silicon-stereogenic silane. *Org. Biomol. Chem.* **2008**, *6* (8), 1435-1440.

53. Steves, A.; Oestreich, M., Facile preparation of CF<sub>3</sub>-substituted carbinols with an azine donor and subsequent kinetic resolution through stereoselective Si-O coupling. *Org. Biomol. Chem.* **2009**, *7* (21), 4464-4469.

54. Weickgenannt, A.; Mohr, J.; Oestreich, M., Catalytic enantioselective dehydrogenative Si-O coupling of oxime ether-functionalized alcohols. *Tetrahedron.* **2012**, *68* (17), 3468-3479.

55. Sheppard, C. I.; Taylor, J. L.; Wiskur, S. L., Silylation-Based Kinetic Resolution of Monofunctional Secondary Alcohols. *Org. Lett.* **2011**, *13* (15), 3794-3797.

56. Klauck, M. I.; Patel, S. G.; Wiskur, S. L., Obtaining Enriched Compounds via a Tandem Enantioselective Reaction and Kinetic Resolution Polishing Sequence. *J. Org. Chem.* **2012**, *77* (7), 3570-3575.

57. Clark, R. W.; Deaton, T. M.; Zhang, Y.; Moore, M. I.; Wiskur, S. L., Silylation-Based Kinetic Resolution of alpha-Hydroxy Lactones and Lactams. *Org. Lett.* **2013**, *15* (24), 6132-6135.

58. Akhani, R. K.; Moore, M. I.; Pribyl, J. G.; Wiskur, S. L., Linear Free-Energy Relationship and Rate Study on a Silylation-Based Kinetic Resolution: Mechanistic Insights. *J. Org. Chem.* **2014**, *79* (6), 2384-2396.



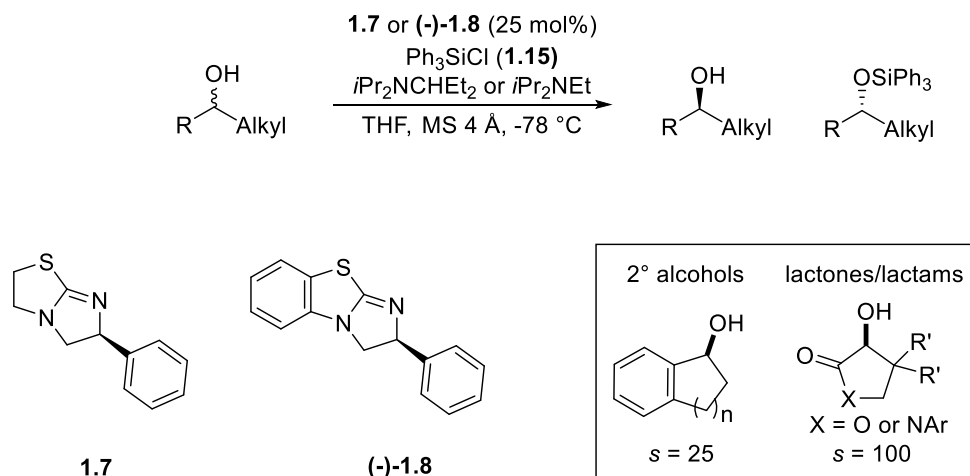
59. Akhani, R. K.; Clark, R. W.; Yuan, L.; Wang, L.; Tang, C. B.; Wiskur, S. L., Polystyrene-Supported Triphenylsilyl Chloride for the Silylation-Based Kinetic Resolution of Secondary Alcohols. *Chemcatchem*. **2015**, 7 (10), 1527-1530.
60. Wang, L.; Akhani, R. K.; Wiskur, S. L., Diastereoselective and Enantioselective Silylation of 2-Arylcyclohexanols. *Org. Lett.* **2015**, 17 (10), 2408-2411.
61. Wang, L.; Zhang, T.; Redden, B. K.; Sheppard, C. I.; Clark, R. W.; Smith, M. D.; Wiskur, S. L., Understanding Internal Chirality Induction of Triarylsilyl Ethers Formed from Enantiopure Alcohols. *J. Org. Chem.* **2016**, 81 (18), 8187-8193.

## CHAPTER 2

### DIASTEREOSELECTIVE AND ENANTIOSELECTIVE Silylation OF 2-ARYLCYCLOHEXANOLS

#### 2.1 Introduction

In chapter 1, we talked about the silylation-based kinetic resolution developed by the Wiskur group for the enrichment of monofunctional secondary alcohols<sup>1</sup> and  $\alpha$ -hydroxy lactones and lactams<sup>2</sup>. The silylation systems either employed the isothioureia catalyst levamisole (**1.7**) or (-)-benzotetramisole ((-)-**1.8**) as the nucleophilic catalyst and a triphenylsilyl chloride (**1.15**) as the silyl source (Scheme 2.1), where the selectivity factors were up to 100. In order to further apply our silylation-based kinetic resolution to other useful substrate classes, we tried to conclude and model the so far successful substrate class which consists of a relatively planar  $\pi$  system on one side of the alcohol and steric effects on the other side of the alcohol, leading us to the investigation of 2-arylcyclohexanol (Figure 2.1). This substrate class has a freely-rotating  $\pi$  system adjacent to the alcohol as well as a six-member ring for the steric effects.



**Scheme 2.1 Silylation-Based Kinetic Resolutions of Wiskur Group**

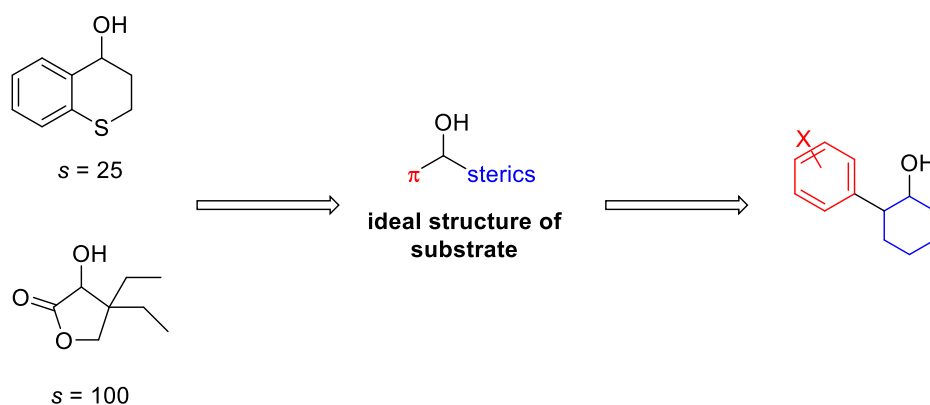
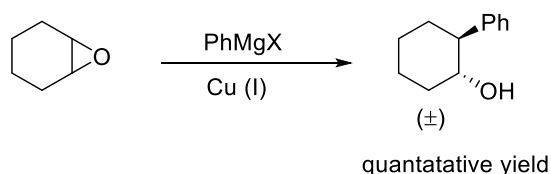


**Figure 2.1 Ideal Substrate Class of Silylation-Based Kinetic Resolution**

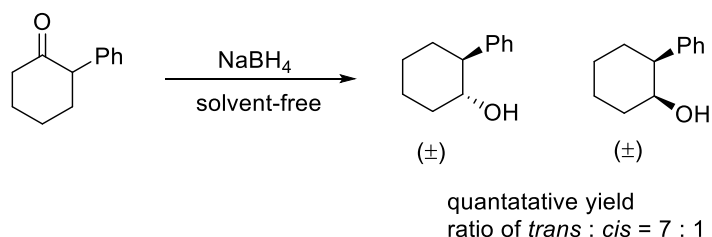
Specifically, enantiomerically pure 2-arylcylohexanols are widely used as chiral auxiliaries and building blocks in a variety of asymmetric syntheses.<sup>3-4</sup> While these alcohols could be obtained through asymmetric catalysis,<sup>5-9</sup> an alternative approach is to enrich them through kinetic resolution, enzymatically<sup>10-13</sup> and nonenzymatically.<sup>14-26</sup> Nonenzymatic kinetic resolution offers the advantage of facile access to both enantiomers of the catalyst. A number of these reactions are very effective in resolving 2-arylcylohexanols, for both *cis* and *trans* stereoisomers. The common ways to obtain these

alcohols are through nucleophilic opening of epoxides<sup>27</sup> and the reduction of corresponding ketones (Scheme 2.2).<sup>28</sup> Since *trans* substituted 2-arylcyclohexanols are preferably formed through ring opening of epoxides and a mixture of *cis* and *trans* alcohols are formed via ketone reduction, additional purification steps are required to separate the diastereomers before the kinetic resolution.

1) Nucleophilic opening of epoxide

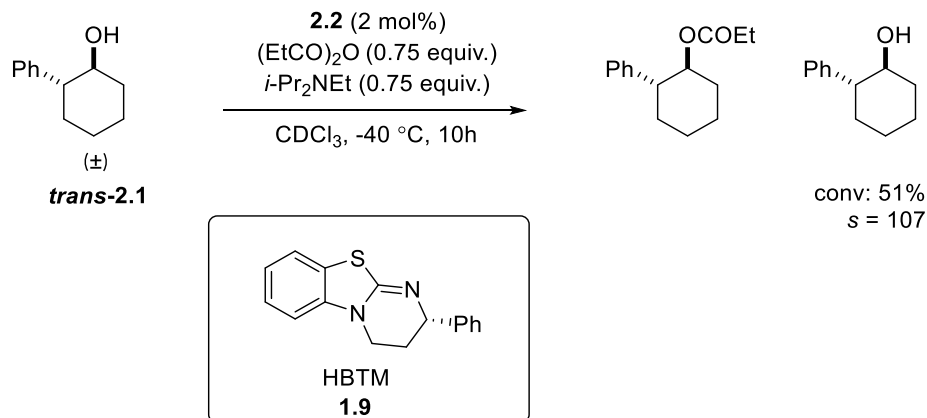


2) Reduction of ketones



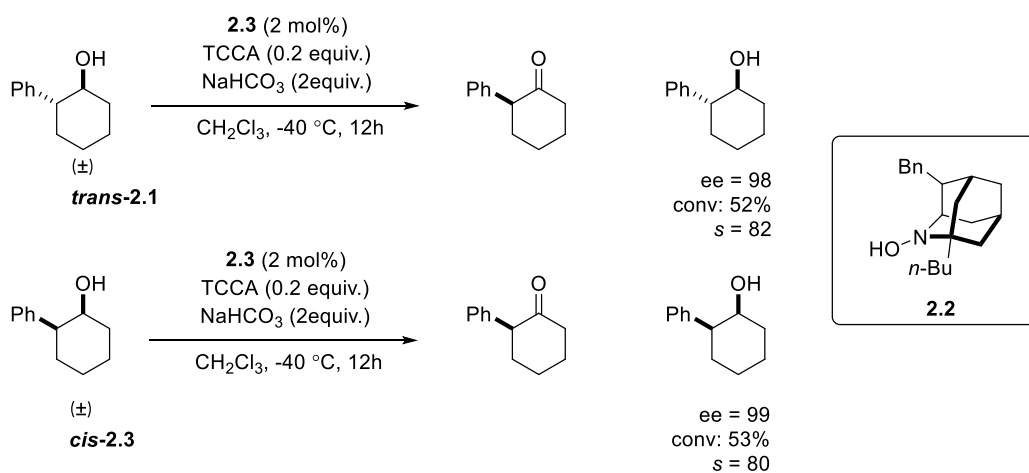
**Scheme 2.2 Methods to Obtain *Cis* and *Trans* 2-Arylcyclohexanols**

There are a number of current examples of non-enzymatic kinetic resolutions of 2-arylcyclohexanols. Birman and coworkers utilized acyl-transfer kinetic resolutions to resolve racemic *trans*-2-phenyl cyclohexanols (***trans*-2.1**) by employing homobenzotetramisole (HBTM) (**1.9**), which is a ring-expanded analogue of the previously reported catalyst benzotetramisole ((-)-**1.8**).<sup>23</sup> This catalyst is particularly effective in the kinetic resolution of 2-arylcyclohexanols with selectivity factors up to 107 for 2-phenyl cyclohexanol (Scheme 2.3). The *cis*-isomer of the 2-phenylcyclohexanol reacts rather slowly and reaches a comparatively lower selectivity factor of 28.



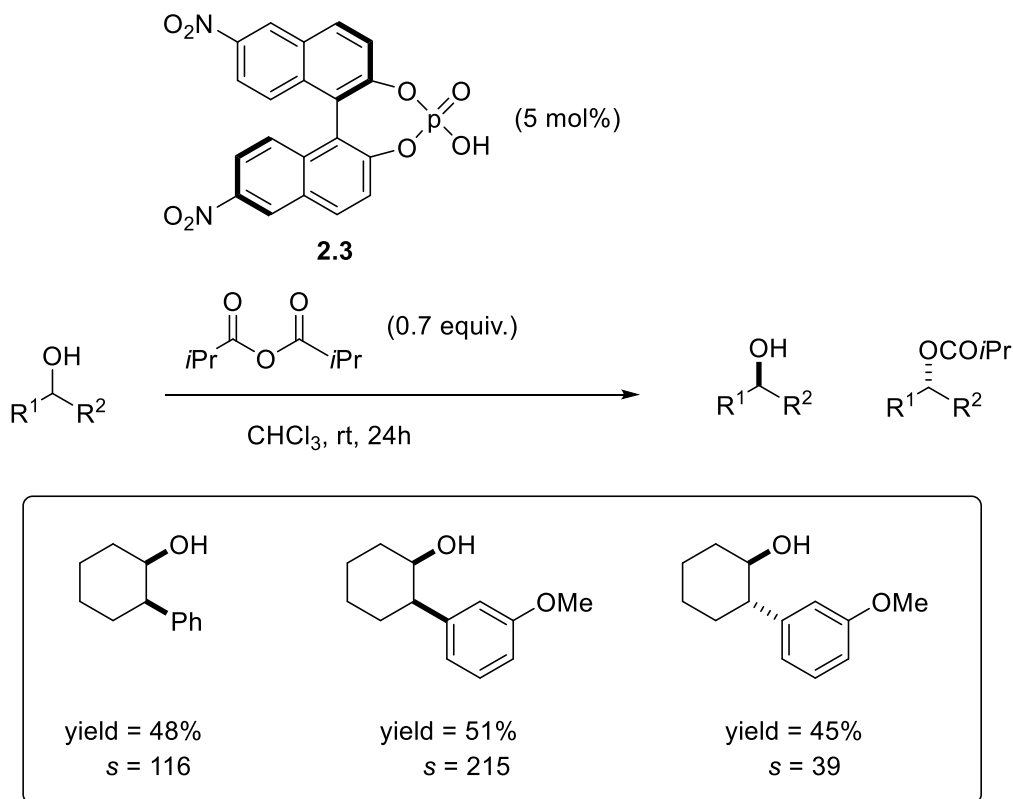
### Scheme 2.3 Acyl-Transfer Kinetic Resolution of 2-Arylcyclohexanols

In another approach, Iwabuchi's group developed a highly enantioselective organocatalytic oxidative kinetic resolution (OKR) of these 2-arylcyclohexanols, which one of the enantiomers will be oxidized to ketones with the other one being unreacted.<sup>24</sup> In this system, a number of modified 2-azaadamantane *N*-oxyls (AZADOs) were investigated as the chiral catalyst, and the highly sterically hindered *n*-butyl version of the catalyst **2.2** showed excellent selectivities up to 83 for both **trans-2.1** and **cis-2.1** of the 2-phenylcyclohexanol (Scheme 2.3).



### Scheme 2.4 Organocatalytic Oxidative Kinetic Resolution of Secondary Alcohols

Yamada and Takasu also introduced a new approach through chiral phosphoric acid-catalyzed acylation for the resolution of various *cis*-2-arylcyclohexanols.<sup>25</sup> The new, electronically-tuned binaphthyl-based phosphoric acid catalyst **2.3** was developed to efficiently resolve *cis*-2-arylcyclohexanols with a high selectivity even at room temperature (Scheme 2.5). In their system, the chiral phosphoric acid **2.4** would catalyze acylation not only as a Brønsted acid to activate acid anhydride as an electrophile by protonation, but also as a general base to enhance the nucleophilicity of alcohol. Contrary to the previous two examples, this method is more selective for *cis* isomers than the *trans* with a selectivity factor drop from 215 to 39 comparing *cis* with *trans*.



**Scheme 2.5 Kinetic Resolution of Secondary Alcohols Catalyzed by Chiral Phosphoric Acids.**

To the best of our knowledge, the method of separating one stereoisomer from a mixture of four *cis* and *trans* stereoisomers of 2-arylcyclohexanols is absent. In this chapter, the silylation-based kinetic resolution of *trans* 2-arylcyclohexanols will be discussed. This methodology is selective for the *trans* diastereomers over the *cis*, which provides an opportunity to selectively derivatize one stereoisomer from the mixture of four. The hypothesis of why *trans* is more selective than the *cis* will be discussed and a facile reduction-silylation reaction sequence will also be introduced to obtain enantiomerically enriched 2-arylcyclohexanols.

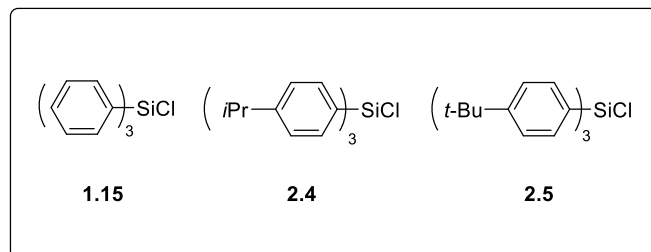
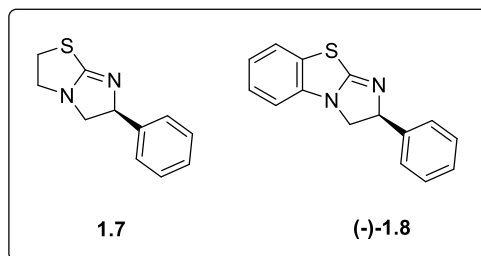
## 2.2 Initial Investigations and Optimizations

The commercially available *trans* 2-phenylcyclohexanol was initially investigated with reaction conditions similar to previous work. When catalyst **1.7** was employed, very little selectivity was achieved (Table 2.1, entry 1), changing the catalyst to (-)-**1.8** increased the selectivity three folds (Table 2.1, entry 2). It was interesting to note that the extension of aromaticity on the catalyst increased the selectivity and we speculated it involving the similar  $\pi$ - $\pi$  and/or cation- $\pi$  interactions Birman reported in their acylation kinetic resolutions using the same catalyst (Scheme 1.9).<sup>23</sup> Our next optimization was the choice of silyl chloride. Our previous research revealed the importance of having three phenyl groups on the silicon for good selectivity.<sup>1</sup> Almost at the same time, Dr. Akhiani in our group discovered that electron-donating alkyl groups in the para position of the phenyl groups on triphenylsilyl chloride improved selectivity.<sup>29</sup> Inspired by these previous reports, an electron donating tris(4-isopropylphenyl)silyl chloride (**2.4**) was investigated in the

kinetic resolution of 2-phenylcyclohexanols, and an improvement in selectivity was again observed as expected (Table 2.1, entry 3).

**Table 2.1 Initial Optimizations of 2-Phenylcyclohexanols**

Entry <sup>a</sup>	catalyst	R <sub>3</sub> SiCl	R <sub>3</sub> SiCl (equiv)	t (h)	conv (%) <sup>b</sup>	s <sup>b</sup>
1	<b>1.7</b>	<b>1.15</b>	0.6	24	52 <sup>c</sup>	2
2	<b>(-)-1.8</b>	<b>1.15</b>	0.6	24	59	6
3	<b>(-)-1.8</b>	<b>2.6</b>	0.65	48	51	10
4 <sup>d</sup>	<b>(-)-1.8</b>	<b>2.7</b>	0.65	72	<5 <sup>c</sup>	-
5	<b>none</b>	<b>1.15</b>	0.6	24	0	-



<sup>a</sup>Reactions were run at a concentration of 0.42 M with respect to alcohol. <sup>b</sup>See ref<sup>30</sup>. <sup>c</sup>Conversion was determined by <sup>1</sup>H NMR. <sup>d</sup>Reactions were run at a concentration of 0.28 M with respect to alcohol.

However, due to the steric effect on the para position, the loading of the silyl chloride and reaction time have to be increased to improve the conversion. Interestingly, the previously more selective, sterically hindered tris(4-*tert*-butylphenyl)silyl chloride

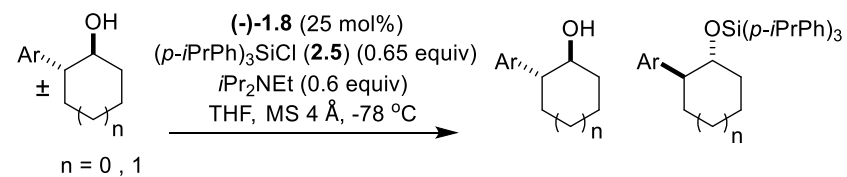


(**2.5**) was unreactive under the same conditions even with an increased reaction time up to 3 days (Table 2.1, entry 4). Moreover, there was no background reaction with the absence of catalyst when the less sterically hindered silyl chloride **1.15** was employed (Table 2.1, entry 5).

### 2.3 Silylation-Based Kinetic Resolution of Various 2-Arylcyclohexanols.

With this information in hand, a variety of *trans*-2-arylcyclohexanol substrates were then tested in the silylation-based kinetic resolution employing the more selective catalyst (-)-**1.8** and the isopropyl-substituted silyl chloride **2.4** (Table 2.2). When the aryl group of the alcohol was substituted with a methoxy, the selectivity generally improved compared to just a phenyl (Table 2.2, entry 2-4 vs entry 1), but the selectivity was dependent on the position of the methoxy on the aryl group (ortho, meta, or para). When the methoxy was placed in the ortho position, the conversion was lower compared with methoxy in the meta and para positions due to the increased steric effect (Table 2.2, entry 2 vs entry 3-4). The *m*- and *p*-methoxy-substituted compounds had excellent selectivity factors of 53 and 28, respectively (Table 2.2, entries 3 and 4). With the assumption that substituents on the meta position had a larger influence on selectivity, electronic effects on the meta position were then investigated. The electron-withdrawing *m*-fluoro-substituted aryl compound had significantly higher selectivity over just a phenyl group (Table 2.2, entry 5 vs entry 1), but when an electron-donating *m*-methyl-substituted aryl group was employed, it was only modestly more selective than a phenyl group (Table 2.2, entry 6, *s* = 14). The aryl  $\pi$  system proved to be important for selectivity, as shown by the very small selectivity factor of the saturated cyclohexyl-substituted substrate (Table 2.2, entry 7).

**Table 2.2 Substrate Scope of the Silylation-Based Kinetic Resolution of *trans*-2-Arylcyclohexanols**



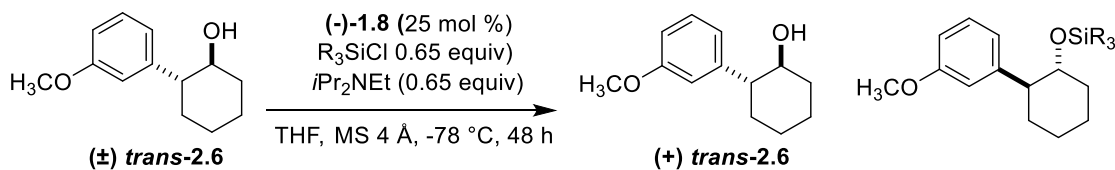
entry <sup>a</sup>	recovered alcohol	er of recovered alcohol	% conv <sup>b</sup>	s <sup>b</sup>
1		83:17	51	10
2		66:34	28	13
3		95:5	50	53
4		95:5	52	28
5		85:15	45	27
6		64:36	26	14
7		60:40	40	2
8		54:46	11	5
9		51:49	54	1.1

<sup>a</sup>Reactions were run for 48 hours at a concentration of 0.42 M with respect to alcohol on a 0.4 mmol scale. <sup>b</sup>See Ref<sup>30</sup>

However, when the increased  $\pi$  surface area of 2-naphthylaryl group was tested, little to modest conversion (11%) and selectivity (5) were achieved possibly due to the bulkiness of the naphthyl group in the system (Table 2.2, entry 8). Cyclohexanol rings are needed for selectivity, as shown by the inability of the method to resolve 2-phenylcyclopentanol (Table 2.2, entry 9).

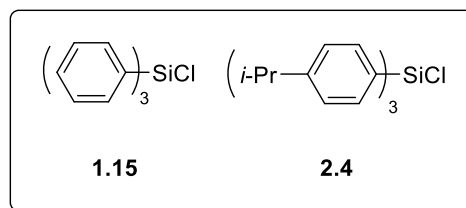
We further demonstrated the importance of isopropyl-substituted silyl chloride for maintaining high selectivity when the so far most selective substrate *m*-methoxy-substituted compound **trans-2.6** was resolved with triphenylsilyl chloride **1.15**, resulting in a much lower selectivity factor (Table 2.3 entry 1 vs 2). This methodology can also be scaled up to grams in a good yield and without any loss in selectivity (1 g scale of 2-phenylcyclohexanol with  $s = 10$  and 52% conversion. The er of the recovered alcohol was 85:15. The silyl ether product was efficiently desilylated with fluoride to obtain the alcohol in 86% yield.).

**Table 2.3 Further Demonstration of the Importance of Isopropyl-Substituted Silyl Chloride**



Entry <sup>a</sup>	$R_3SiCl$	conv (%) <sup>b</sup>	$s^b$
1	<b>1.15</b>	45	13
2	<b>2.4</b>	50	53

<sup>a</sup>Reactions were run for 48 hours at a concentration of 0.42 M with respect to alcohol on a 0.4 mmol scale. <sup>b</sup>See Ref<sup>30</sup>



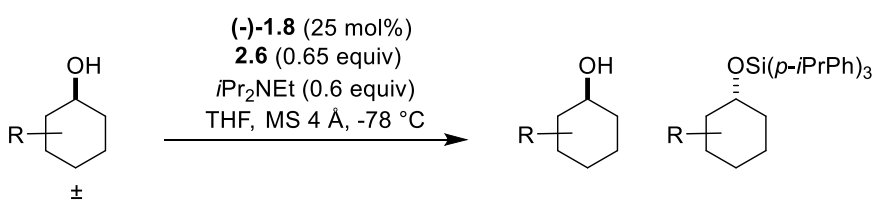
## 2.4 Investigations of *cis*-2-Arylcyclohexanols

As for the corresponding *cis* compounds, those substrates failed to even silylate under our silylation-based kinetic resolution conditions. Both the phenyl and *m*-methoxyphenyl *cis*-substituted compounds (*cis*-**2.1** and *cis*-**2.6** respectively) were employed under the same reaction conditions but no conversion was observed (Scheme 2.6). This specific selectivity of only silylating *trans* alcohols over the *cis* attracted us to dig deeper into this by investigating the unique six-member ring system. The difference in conversion is likely due to the position of the alcohol in the cyclohexane chair conformation, axial versus equatorial, affecting the reactivity of the substrate. By employing the empirical A values and Equation 2.1, the lowest energy conformation and the percentage of the compound found at that conformation could be determined for both the *cis*- and *trans*-2-phenylcyclohexanol (*cis*-**2.1** and *trans*-**2.1** respectively). Due to the large A value difference of a phenyl substituent over the alcohol group (2.8 and 0.95 kcal/mol, respectively),<sup>31</sup> the phenyl group dominates the overall conformation of *trans*-**2.1** and *cis*-**2.1** by placing the phenyl group in the lower energy equatorial position (Scheme 2.6). This results in >99% of *trans*-**2.1** in the conformation where the alcohol is equatorial and 99% of *cis*-**2.1** in the conformation where the alcohol is axial at -78 °C. Based on these calculations, the reactivity of the alcohol towards silylation in this methodology seems to be controlled by the position of the alcohol, axial versus equatorial. It is believed that when the alcohol is predominantly placed in the axial position, the silylation is unlikely to proceed. In order to further validate this idea, *cis*- and *trans*-4-*tert*-butylcyclohexanols (*cis*-**2.8** and *trans*-**2.8**, respectively) were employed. These compounds lack any substituents in the 2-position, eliminating any steric or electronic effect the phenyl group of *cis*-2-

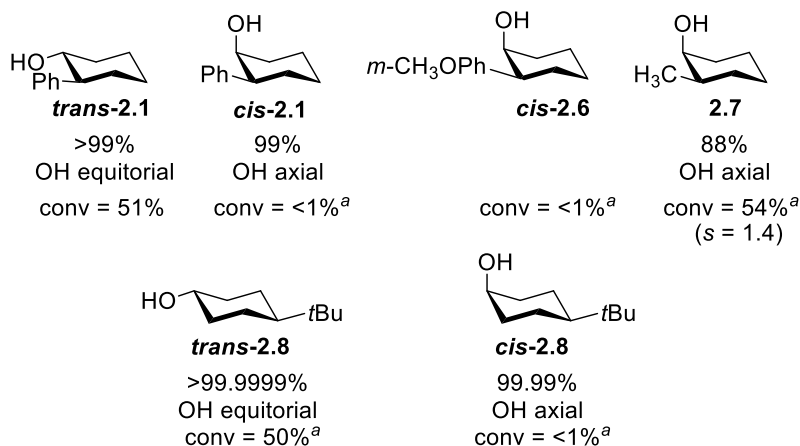
phenylcyclohexanol (*cis*-**2.1**) may have played. Since the A value of a *tert*-butyl group is 4.7 kcal/mol,<sup>31</sup> at low temperatures these compounds have a nearly quantitative bias toward one conformation over the other (>99.99%) with the alcohol group in either the axial (*cis*) or equatorial (*trans*) position. This reduces the possibility of the Curtin-Hammett principle<sup>32</sup> playing a role by eliminating the presence of one conformation. When the compound was subjected to the same reaction conditions as above, the alcohol group in the equatorial position becomes silylated and the alcohol group in the axial position is unreactive as we expected (Scheme 2.6).

$$K_{\text{eq}} = e^{-\Delta G/RT}$$

**Equation 2.3**



**Population of Low Energy Conformation at -78 °C vs. Conversion**



<sup>a</sup>Conversion determined via <sup>1</sup>H NMR

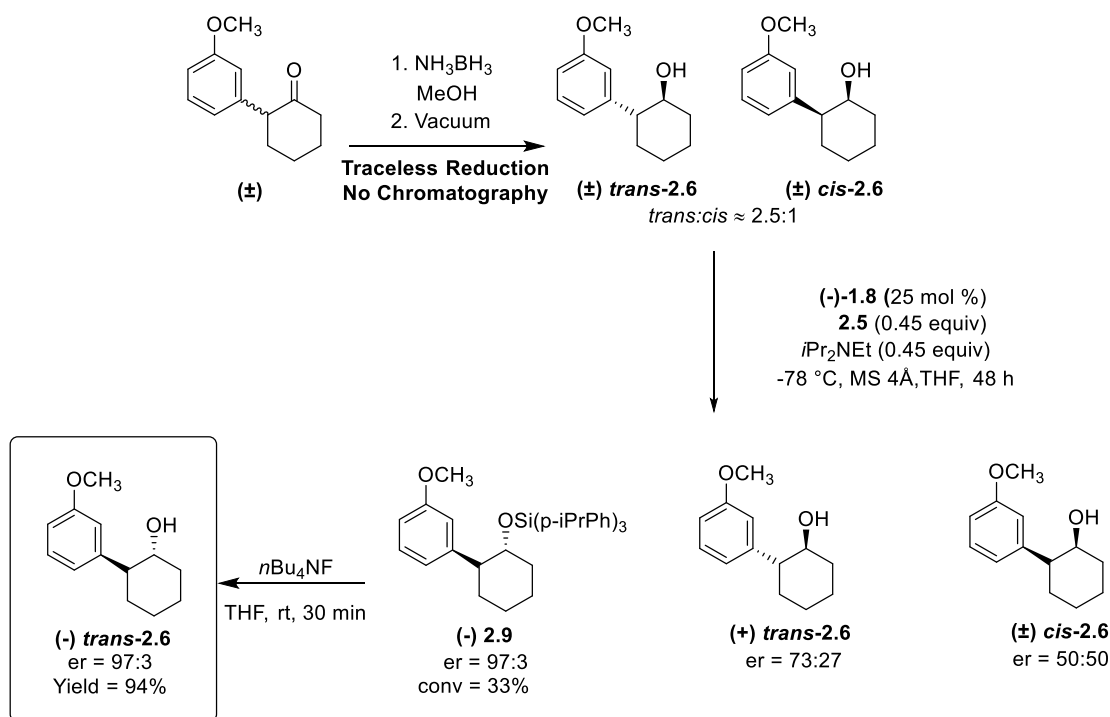
**Scheme 2.6 Substrate Reactivity toward Silylation Based on the OH Conformation (Axial vs Equatorial) and the Population of That Conformation at -78 °C**

With all the information in hand, the reactivity of other *cis*-2-substituted cyclohexanols toward silylation could be determined by again employing the A values to calculate the population of the two chair conformations. When a substituent with a small A value was employed, it resulted in the presence of both conformations, with the alcohol in both the axial (not reactive) and the equatorial (reactive) position. With the A value of methyl group equals to 1.74, the investigation of *cis*-2-methylcyclohexanol (**2.7**) gave us approximately a 12% population of the conformation with the alcohol equatorial and 88% of the conformation where the alcohol is in the axial position at -78 °C (Scheme 2.6). As expected, there was significant conversion of **2.7** to the silylated product with the increased concentration of the more reactive conformation. This substrate has a very low selectivity factor due to the lack of a  $\pi$  system adjacent to the alcohol as was discussed earlier in this chapter.

## 2.5 One-Pot Reduction-Silylation Sequence

With the unique reactivity of the alcohol being reactive when it is in the equatorial position and unreactive when it is in the axial position, this idea could be simply translated to the selectivity of *trans* compounds being reactive and *cis* compound being completely unreactive by carefully performing the calculations using A values (Equation 2.1). This provides the opportunity to selectively resolve *trans* enantiomers in the presence of *cis* enantiomers and ultimately silylate only one stereoisomer over the other three stereoisomers (Scheme 2.7). Additionally, we wanted to start with a ketone to show a one-pot reduction-silylation sequence procedure. The reduction part can be achieved through an ammonia-borane ketone reduction in methanol.<sup>33</sup> The reduction is essentially traceless

after the removal of solvents, due to the volatility of the  $B(OMe)_3$  as the only byproduct. Therefore, the beauty of this reduction is that there is no additional chromatography once the solvent is removed. The crude product after the reduction of 2-(3-methoxyphenyl)cyclohexanone was the mixture of *trans* and *cis* alcohols ( $\pm$ ) ***trans*-2.6** and ( $\pm$ ) ***cis*-2.6** (d.r. = 2.5:1) and the mixture was subjected to the kinetic resolution directly (Scheme 2.7). In order to obtain the product with a high enantiomeric ratio, the reaction needed to be stopped at some point before full conversion, which was achieved by limiting the silyl chloride to 0.45 equivalent. The selectivity factor of this resulting one-pot reduction, silylation sequence was the same compared to the previous kinetic resolution runs ( $s = 53$ ), and the resulting silylated product (-)-**2.9** was obtained with a high enantiomeric ratio of 97:3. The silylated product could be easily deprotected by tetra-*n*-butylammonium fluoride to obtain the alcohol (-) ***trans*-2.6**, maintaining the same enantiomeric ratio with high yield (Scheme 2.7). This provides a valuable tool for the facile formation and separation of 2-substituted cyclohexanol diastereomers from the starting ketone by eliminating the need for a workup or chromatography between reactions.



**Scheme 2.7 One-pot, Chromatography-Free Reduction Followed by a Kinetic Resolution to Selectively Silylate One Stereoisomer out of a Mixture of Four**

## 2.6 Conclusions and Outlook

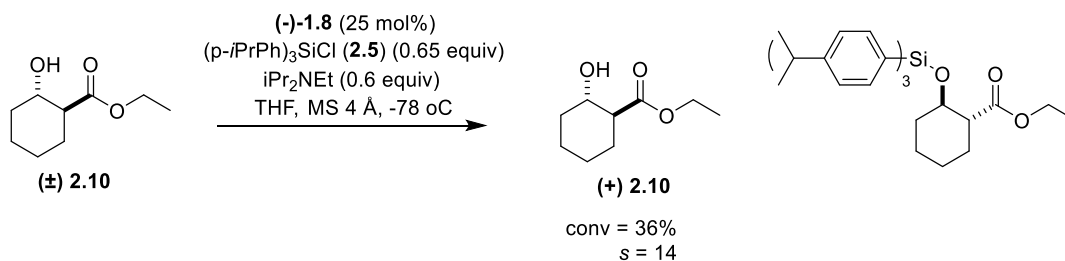
In conclusion, silylation-based kinetic resolutions have been expanded to a synthetically useful *trans*-2-arylcyclohexanol substrate class. This methodology employs a commercially available isothioureia catalyst and an isopropyl-substituted silyl chloride as the derivatizing reagent. The system obtains high selectivity when the aryl group is derivatized with a fluoro or a methoxy substituent. A selectivity factor up to 53 was achieved for 2-(3-methoxyphenyl)cyclohexanol.

Compared to other methods, our silylation-based kinetic resolution has the advantage of selectively resolving the *trans* enantiomer from a mixture of the *cis* and *trans* diastereomers due to its preference for only silylating alcohols in the equatorial position. This affords the opportunity to selectively remove one stereoisomer from a mixture of four



stereoisomers. Because of this unique selectivity of silylating *trans* over the *cis*, we hypothesize that the alcohol needs to be in the equatorial position to be reactive, and alcohols locked in the axial position are completely unreactive. If there is a small amount of equatorial is present in the equilibrium, the Curtin Hammett principle takes over and we will lose the selectivity.

There are additional substrate scope expansion studies being conducted by Tian Zhang in our group. Since the importance of having a  $\pi$  system adjacent to the alcohol has been shown in this chapter as well as in our previous reports,<sup>1-2, 26</sup> this substrate expansion project investigates the ester- $\pi$  system. The initial studies of these substrates have shown promising results of successfully resolving *trans*-2-carbethoxycyclohexanol ( $\pm$ ) **2.10** under the similar reaction conditions of silylation-based kinetic resolution (Scheme 2.8).



### Scheme 2.8 Silylation-Based Kinetic Resolution of *Trans*-2-Carbethoxycyclohexanol

Due to the significance of having a  $\pi$  system in the alcohol to achieve decent selectivity, we proposed a possible cation- $\pi/\pi-\pi$  interaction in the transition state which enhance the selectivity of enantiomers. This hypothesis is similar to Birman's acylation system utilizing imidazole-based catalysts (-)-**1.8**, and it is supported by computational analysis.<sup>23</sup> Future investigation to support this hypothesis in our silylation-based kinetic resolution could be focused on using computation modelling to study the transition state.

And we could also apply linear free energy relationship (LFER) to study the electronic effects on the  $\pi$  system by modifying the substituents on the *meta* position of 2-arylcylohexanols.

Understanding the mechanism, especially how the chirality is transferring from the isothiourea catalyst to the alcohol is essential for us to further apply this methodology. Multiple studies have been done or are being conducted to elucidate the mechanism, including a linear free energy relationship (LFER) finished by Ravish Akhani<sup>29</sup> and a kinetic study conducted by Robert Clark and Brandon Redden. Another approach towards the understanding of the mechanism is through the studies of propeller or helical twist formation of triphenyl silyl chloride in the transition state. This study helped us to understand the chirality transmission in the methodology and the results will be discussed in Chapter 3.

## 2.7 Experimental

### General information

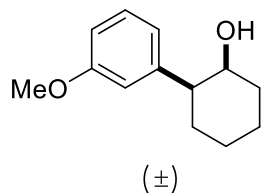
All the reactions were carried out under a nitrogen atmosphere using oven-dried glassware. Molecular sieves were activated in an oven at 170 °C before use. Tetrahydrofuran (THF), diethyl ether and dichloromethane ( $\text{CH}_2\text{Cl}_2$ ) were dried by passing through a column of activated alumina before use and stored over molecular sieves. Carbon tetrachloride ( $\text{CCl}_4$ ) was distilled and degassed prior to use. Sulfuryl chloride ( $\text{SO}_2\text{Cl}_2$ ) and tetramethylethylenediamine (TMDEA) were distilled before use. *n*-Butyl lithium was titrated prior to use. Unless otherwise stated, all the other chemicals were obtained from major commercial sources and used without further purification. High resolution mass

spectrometry (HRMS) was submitted to and conducted by the Department of Chemistry and Biochemistry's mass spectrometry facility at the University of South Carolina. Infrared spectroscopy (IR) was conducted using a Perkin Elmer Spectrum 100 FT-IR ATR spectrophotometer,  $\nu_{\text{max}}$  in  $\text{cm}^{-1}$ .  $^1\text{H}$  NMR was taken on a Bruker Avance (300 or 400 MHz). Chemical shifts were reported in ppm with TMS or Chloroform as an internal standard (TMS 0.00 ppm for  $^1\text{H}$  and  $^{13}\text{C}$  or  $\text{CHCl}_3$  7.26 ppm and 77.16 for  $^1\text{H}$  and  $^{13}\text{C}$  respectively).  $^{13}\text{C}$  NMR spectra were taken on a Bruker Avance (101 or 75 MHz) with complete proton decoupling. Enantiomeric ratios were determined via HPLC using an Agilent 1200 series. The chiral stationary phases were Daicel Chiralcel OD-H, OJ-H, AD, AD-H or Daicel Chiralpak IC columns, and the enantiomers were measured by a diode array detector in comparison with the racemic materials. Optical Rotations were obtained utilizing a JASCO P-1010 polarimeter. Uncorrected melting points (mp) were taken with a Laboratory Devices Mel-Temp.

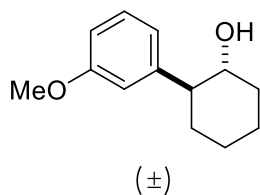
## **Preparation of racemic substituted 2-aryl cyclohexanols and general procedures**

### **General Information**

The following compounds *trans*-2-phenylcyclohexan-1-ol, 2-(3-methoxyphenyl)cyclohexan-1-ol, *trans*-2-(4-methoxyphenyl)cyclohexan-1-ol, *trans*-2-(3-fluorophenyl)cyclohexan-1-ol, *trans*-2-(3-methylphenyl)cyclohexan-1-ol, [1,1'-bi(cyclohexan)]-2-ol, *trans*-2-(naphthalen-1-yl)cyclohexan-1-ol, *trans*-2-phenylcyclopentan-1-ol and *cis*-2-methylcyclohexan-1-ol were purchased. The compounds 2-(3-methoxyphenyl)cyclohexan-1-ol and *trans*-[1,1'-bi(cyclohexan)]-2-ol were purified via silica gel chromatography prior to use.



***cis-2-(3-methoxyphenyl)cyclohexan-1-ol***



***trans-2-(3-methoxyphenyl)cyclohexan-1-ol***

Compounds *trans-2-(3-methoxyphenyl)cyclohexan-1-ol* ((±) ***trans-2.6***), and *cis-2-(3-methoxyphenyl)cyclohexan-1-ol* ((±) ***cis-2.6***) were prepared from known literature procedures.<sup>25</sup> To a solution of commercially available 2-(3-methoxyphenyl)cyclohexanone (0.90 g, 4.4 mmol) in MeOH (20 mL) was added NaBH<sub>4</sub> (0.47 g, 12 mmol) at room temperature. The reaction was allowed to stir for 1 hour. Water (10 mL) and toluene (30 mL) was added to the reaction mixture, and the organic layer was washed with 1M HCl, water and saturated NaHCO<sub>3</sub> solution. It was then dried over Na<sub>2</sub>SO<sub>4</sub> and concentrated via Rotary Evaporator. The *cis* and *trans* alcohols were purified through silica gel chromatography (5% EtOAc to 25% EtOAc in hexanes). The pure product was colorless oil for (±) ***trans-2.6***, 0.39 g, 43%; and colorless oil for (±) ***cis-2.6***, 0.3 g, 37%.

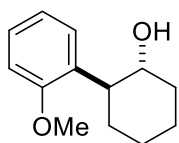
**(±) *trans-2-(3-methoxyphenyl)cyclohexan-1-ol***

<sup>1</sup>H NMR (400 MHz, CDCl<sub>3</sub>): δ ppm 7.30 – 7.22 (m, 1H), 6.88 – 6.76 (m, 3H), 3.81 (s, 3H), 3.70 – 3.60 (m, 1H), 2.48 – 2.35 (m, 1H), 2.18 – 2.07 (m, 1H), 1.94 – 1.19 (m, 7H).

$^{13}\text{C}$  NMR (101 MHz,  $\text{CDCl}_3$ )  $\delta$  ppm 159.6, 144.8, 129.5, 120.0, 113.5, 111.8, 74.2, 55.1, 53.2, 34.3, 33.2, 26.0, 25.0.

**( $\pm$ ) *cis*-2-(3-methoxyphenyl)cyclohexan-1-ol**

$^1\text{H}$  NMR (400 MHz,  $\text{CDCl}_3$ ):  $\delta$  ppm 7.24 (1H, *dad*,  $J = 7.5, 8.0$ ), 6.85 (1H, *d*,  $J = 7.5$ ), 6.81 (1H, *s*), 4.01 (1H, *m*), 3.80 (3H, *s*), 2.72 (1H, *m*), 1.97–2.07 (2H, *m*), 1.89 (1H, *m*), 1.33–1.71 (5H, *m*).  $^{13}\text{C}$  NMR (101 MHz,  $\text{CDCl}_3$ )  $\delta$  ppm 159.7, 145.6, 129.5, 120.0, 113.6, 116.0, 70.5, 55.1, 48.0, 32.8, 26.1, 24.3, 19.5.

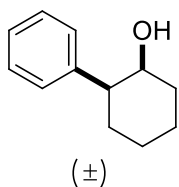


( $\pm$ )

***Trans*-2-(2-methoxyphenyl)cyclohexan-1-ol.**

Compound *trans*-2-(2-methoxyphenyl)cyclohexan-1-ol was prepared according to the reported literature.<sup>34</sup> An oven-dried 50 ml three-neck flask equipped with a magnetic stirring bar and rubber stopper was added anisole (324 mg, 3 mmol) and TMEDA (70 mg, 0.6 mmol) via syringe. The mixture was then dissolved in THF (8 mL) and cooled in an ice-bath for 10 minutes. Then 1.875 ml of the 1.6 M solution of *n*BuLi in hexanes (3 mmol) was added to the mixture dropwise. The mixture was allowed to stir for 3 hours while the temperature was allowed to rise to room temperature. Then the mixture was allowed to cool to  $-78\text{ }^\circ\text{C}$  in a dry-ice bath. Then cyclohexene oxide (98 mg, 1 mmol) and  $\text{BF}_3\cdot\text{OEt}_2$  (355 mg, 2.5 mmol) were successively added to the reaction mixture. After stirring the reaction for 2 hours at  $-78\text{ }^\circ\text{C}$ , the mixture was quenched with saturated  $\text{NaHCO}_3$  (8mL). The organic layer was extracted with diethyl ether three times and was concentrated via

Rotary Evaporator. The product was isolated via silica gel chromatography (10% EtOAc in hexanes) to yield a colorless oil, 100 mg, 50%).  $^1\text{H NMR}$  (400 MHz,  $\text{CDCl}_3$ ):  $\delta$  ppm 7.30 – 7.21 (m, 2H), 6.99 (td,  $J = 7.5, 0.9$  Hz, 1H), 6.92 (d,  $J = 8.2$  Hz, 1H), 3.86 (s, 3H), 3.81 – 3.72 (m, 1H), 3.10 – 2.98 (m, 1H), 2.21 – 2.11 (m, 1H), 1.93 – 1.70 (m, 4H), 1.59 – 1.29 (m, 3H).  $^{13}\text{C NMR}$  (101 MHz,  $\text{CDCl}_3$ )  $\delta$  ppm 157.7, 131.5, 127.4, 127.3, 121.05, 110.8, 74.1, 55.5, 45.1, 35.2, 32.6, 26.2, 25.2.



### ***Cis-2-phenylcyclohexan-1-ol***

To a 50-mL round bottom flask fitted with Teflon coated stir-bar was added the commercially available 2-phenylcyclohexan-1-one (1.05 g, 6 mmol) and ethanol (30 mL) to a concentration of 0.2 M. The solution was treated with  $\text{NaBH}_4$  (0.62 g, 16.38 mmol) and stirred at room temperature for 2 hours. The reaction was then quenched with saturated  $\text{NH}_4\text{Cl}$ , and the aqueous layer was extracted with diethyl ether (3 x 10 mL). The organic layers were then combined, dried over anhydrous  $\text{Na}_2\text{SO}_4$ , filtered and concentrated. The crude mixture (mixture of diastereomers) was purified on silica gel chromatography (gradient of 5% to 10% to 25% EtOAc in hexanes) giving a white solid (438 mg, 2.49 mmol, yield 42%).  $^1\text{H NMR}$ : (300 MHz,  $\text{CDCl}_3$ )  $\delta$  ppm 7.38-7.20 (m, 5H), 4.03 (d,  $J = 2.0$  Hz, 1H), 2.16 – 1.29 (m, 9H)  $^{13}\text{C NMR}$ : (75 MHz,  $\text{CDCl}_3$ )  $\delta$  ppm 144.4, 128.9, 128.2, 126.9, 71.0, 48.4, 33.3, 26.6, 24.7, 20.0.

## General procedure for the tandem ammonia-borane ketone reduction and silylation-based kinetic resolution (GP1)

The synthesis of a mixture of *cis* and *trans* alcohols employed a procedure similar to the published literature.<sup>33</sup> To a 4-dram vial fitted with a Teflon coated stir-bar was charged with the ketone (1 mmol), ammonia borane ( $\text{NH}_3\text{BH}_3$ , 0.51 mmol) and methanol to a concentration of 0.3 M. The reaction was allowed to stir at room temperature for 4 hours, which was monitored by TLC for full conversion. The solvent and all the volatile compounds (trimethyl borate and ammonia) were removed under vacuum after the reaction. The ratio of *cis* alcohol versus *trans* alcohol could be determined by  $^1\text{H}$  NMR. Catalyst (25 mol% in relationship to *trans* alcohol) and activated 4Å molecular sieves were added to the mixture of *cis* and *trans* alcohols. The vial was then purged with argon and sealed with a septum. *N,N*-Diisopropylethylamine (0.45 equiv in relationship to *trans* alcohol) was added via syringe and the mixture was dissolved in 1.25 mL of THF. The vial was then cooled to  $-78\text{ }^\circ\text{C}$  for 30 min. The cooled mixture was then treated with a 0.71 M solution of silyl chloride in THF (0.45 equiv of  $\text{SiCl}_4$  in relationship to *trans* alcohol) and was left to react for 48 hours at  $-78\text{ }^\circ\text{C}$ , then quenched with 0.5 mL of methanol. The solution was left to warm to room temperature and then the crude contents were extracted with diethyl ether and the organic layer was transferred to a 4-dram vial. The solvent was removed under vacuum and the residue was purified via silica gel chromatography (gradient of 5% to 10% to 25% EtOAc in hexanes). The silylated alcohols and unreacted alcohols were collected and concentrated under vacuum for further HPLC analysis.

### **General procedures for sodium borohydride ketone reduction (GP2)**

To a 4-dram vial with a stir bar was added the ketone and absolute methanol to a concentration of 0.5 M. The solution was treated with NaBH<sub>4</sub> and stirred at room temperature. Full conversion was monitored by TLC after 2 hours. The reaction mixture was then quenched with 3 mL brine and then extracted with diethyl ether (3 \* 4 mL). The organic layers were combined and then dried over anhydrous Na<sub>2</sub>SO<sub>4</sub> and evaporated to dryness. The residue was then purified through silica gel chromatography (10% EtOAc in hexanes to 25% EtOAc in hexanes).

### **General procedure for the kinetic resolution of the alcohols (GP3)**

To a 1-dram vial with an oven dried Teflon coated stir bar and activated 4Å molecular sieves, the racemic substrate (0.4 mmol) and catalyst (0.1 mmol) were added. The vial was then purged with argon and sealed with a septum. The *N,N*-diisopropylethylamine (0.26 mmol) was added via syringe and the starting materials were dissolved in 0.55 mL of THF to make a 0.42 M concentration solution. The vial was then cooled to -78 °C for 30 min. The cooled mixture was then treated with a 0.65 M solution of silyl chloride in THF (0.4 mL, 0.26 mmol) and was left to react for a set amount of time at -78 °C, then quenched with 0.3 mL of methanol. The solution was left to warm to room temperature and then the crude contents were extracted with diethyl ether and the organic layer was transferred to a 4-dram vial. The solvent was removed under vacuum and the residue was purified via silica gel chromatography (gradient of 5% to 10% to 25% EtOAc in hexanes). The silylated alcohol was concentrated under vacuum and saved for analysis



and the unreacted alcohol could either be analyzed by HPLC or be converted to a benzoate ester for HPLC analysis.

#### **General procedure for deprotection of silylated alcohols (GP4)**

To a 4-dram vial with stir bar and a septum was added the silyl protected alcohol. The solid was then dissolved in 2 ml of THF with stirring. To this solution of tetra-*n*-butylammonium fluoride (TBAF) (1 ml) was added and stir for 2 h for full deprotection. The reaction was then quenched with brine, and extracted with diethyl ether three times. The crude organic layers were combined, then concentrated under vacuum, and purified by silica gel chromatography (gradient of 10 to 25% EtOAc in hexanes). The isolated, deprotected alcohol was then analyzed by HPLC or converted to a benzoate ester.

#### **General procedure for benzylation of alcohols for HPLC analysis (GP5)**

A 4-dram vial containing the alcohols was fitted with a stir bar and a septum. DMAP (4-dimethylaminopyridine, 0.1 equiv) and triethyl amine (2.0 equiv) was added, and the mixture was then dissolved in 2 mL of dichloromethane with stirring. The vial was cooled to 0 °C in an ice bath and 3,5-dinitrobenzoyl chloride (1.4 equiv) was added to the mixture. The reaction was allowed to stir for 2 h and quenched with sat. sodium bicarbonate and extracted three time with dichloromethane. The crude organic layers were combined, then concentrated under vacuum, and purified by silica gel chromatography (5% EtOAc in hexanes) to obtain the desired benzylation alcohols. The benzoate esters could then be analyzed by HPLC.

### **General Procedure Making a *p*-Substituted Triphenylsilane. (GP6)**

In an oven-dried 250 mL three-neck round-bottom flask, *p*-substituted bromo/iodobenzene (1 equiv) was dissolved using diethyl ether (28 mL) under nitrogen at room temperature. To the stirred solution was slowly added *n*BuLi (1.025 equiv) at room temperature. After addition of *n*BuLi, the resulting mixture formed a precipitate which was then allowed to stir for 1–1.5 h. After 1–1.5 h, a solution of HSiCl<sub>3</sub> (0.4 M in diethyl ether, 0.3 equiv) was added dropwise to the three-neck flask at -40 °C using dry ice/acetonitrile bath. The reaction mixture was then allowed to stir for another 2 h. After 2 h, the resulting suspension was then quenched with water and extracted with diethyl ether. Organic layer was dried with anhydrous Na<sub>2</sub>SO<sub>4</sub> and concentrated under vacuum to yield the crude product. In most cases, purification of silane was done by recrystallization or silica gel chromatography using hexane.

### **General Procedure Making a *p*-Substituted Triphenylsilyl chloride. (GP7)**

An oven-dried 50 mL three-neck round-bottom flask was charged with *p*-substituted triphenylsilane and the mixture dissolved using dry degassed carbon tetrachloride (CCl<sub>4</sub>) under a nitrogen atmosphere. The mixture was allowed to stir for 10–15 min. Sulfuryl chloride (SO<sub>2</sub>Cl<sub>2</sub>) (2–6 equiv) was then added to the flask. The resulting mixture was then allowed to reflux for 2–10 h (conversion was monitored by disappearance of the silane peak using <sup>1</sup>H NMR). After full conversion, the mixture was concentrated using vacuum. The final product was then recrystallized using pentane at -78 °C.

## Analytical data and HPLC traces for kinetic resolutions

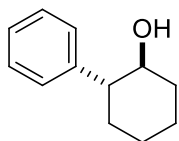
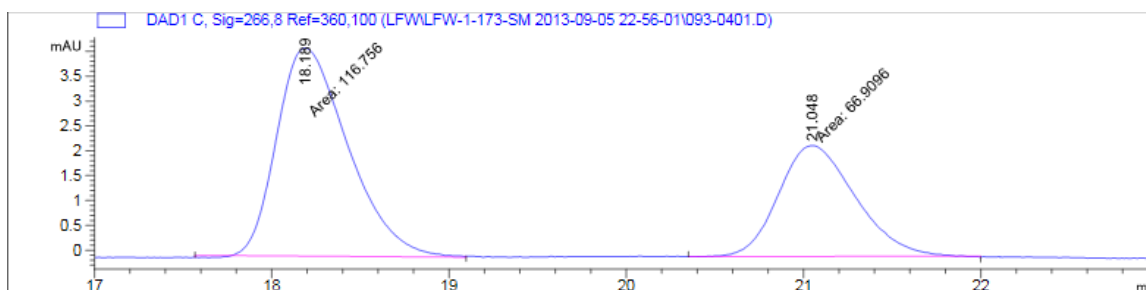


**Table 2.1, Entry 1:** GP3. Recovered starting material: 34 mg, 39%.  $^1\text{H NMR}$  (400 MHz,  $\text{CDCl}_3$ ):  $\delta$  ppm 7.38 – 7.29 (m, 2H), 7.29 – 7.21 (m, 3H), 3.67 (ddd,  $J = 10.1, 6.3, 2.5$  Hz, 1H), 2.43 (ddd,  $J = 13.2, 10.0, 3.5$  Hz, 1H), 2.16 – 2.06 (m, 1H), 1.85 (dt,  $J = 12.5, 6.6$  Hz, 2H), 1.80 – 1.71 (m, 1H), 1.62 – 1.28 (m, 4H).  $^{13}\text{C NMR}$  (101 MHz,  $\text{CDCl}_3$ )  $\delta$  ppm 143.2, 128.8, 127.9, 126.8, 74.4, 53.2, 34.4, 33.3, 26.1, 25.1. **Optical Rotation**  $[\alpha]_D^{25}$ : +3.5 ( $c = 0.031$ )  $\text{CHCl}_3$

**HPLC** separation conditions and stereochemical assignment<sup>23</sup>: Chiralpak OD-H Column 2% isopropyl alcohol in hexane, flow rate: 1 mL/min, 25 °C;  $t_R$  18.2 min for (*S*)-enantiomer (major) and 21.0 min for (*R*)-enantiomer (minor). (e.r. = 64:36)



Peak #	RetTime [min]	Type	Width [min]	Area [mAU*s]	Height [mAU]	Area %
1	18.189	MM	0.4652	116.75569	4.18267	63.5698
2	21.048	MM	0.5005	66.90955	2.22821	36.4302

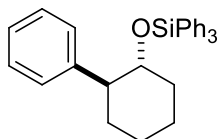


**Table 2.1, Entry 1:** GP3. Recovered product: 108 mg, 48%, white solid, **mp range** = 118-120 °C. **<sup>1</sup>H NMR** (400 MHz, CDCl<sub>3</sub>): δ ppm 7.49 – 7.19 (m, 18H), 7.11 – 7.03 (m, 2H), 3.82 (td, *J* = 10.3, 4.0 Hz, 1H), 2.73 – 2.64 (m, 1H), 2.03 – 1.94 (m, 1H), 1.88 – 1.51 (m, 4H), 1.45 – 1.11 (m, 3H). **<sup>13</sup>C NMR** (101 MHz, CDCl<sub>3</sub>) δ ppm 135.5, 135.4, 134.7, 129.6, 128.3, 128.1, 127.5, 126.0, 76.4, 53.1, 36.5, 34.1, 25.9, 25.1. **HRMS (ESI)** Calculated for (C<sub>30</sub>H<sub>30</sub>OSi +) (M +): 434.2066 Observed: 434.2069. **IR** (neat, cm<sup>-1</sup>) 3060, 2929, 1600, 1447, 1250, 1114, 1029, 982, 840, 794, 709. Conversion was calculated based on <sup>1</sup>H NMR.

#### Kinetic Resolution Data for Table 2.1, Entry 1

	er <sup>SM</sup>	% conv	<i>s</i>	<i>S</i> AVERAGE
1	64:36	51.6	2.2	2
2	59:41	49.0	1.7	

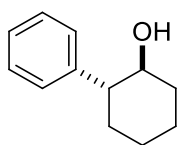
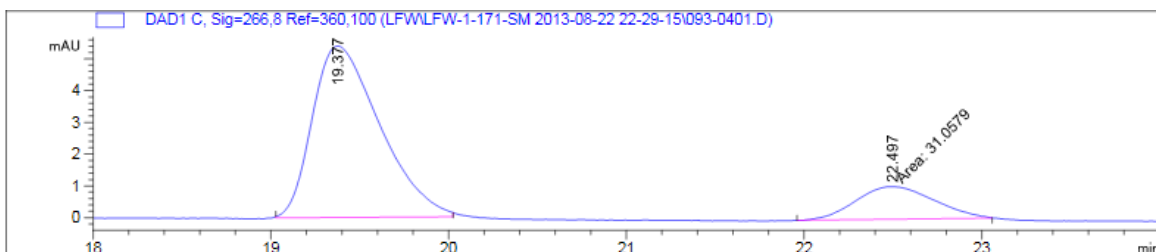


**Table 2.1, Entry 2:** GP3. Recovered starting material: 36 mg, 41%. **<sup>1</sup>H NMR** (400 MHz, CDCl<sub>3</sub>): δ ppm 7.38 – 7.29 (m, 2H), 7.29 – 7.21 (m, 3H), 3.67 (ddd, *J* = 10.1, 6.3, 2.5 Hz, 1H), 2.43 (ddd, *J* = 13.2, 10.0, 3.5 Hz, 1H), 2.16 – 2.06 (m, 1H), 1.85 (dt, *J* = 12.5, 6.6 Hz, 2H), 1.80 – 1.71 (m, 1H), 1.62 – 1.28 (m, 4H). **<sup>13</sup>C NMR** (101 MHz, CDCl<sub>3</sub>) δ ppm 143.2, 128.8, 127.9, 126.8, 74.4, 53.2, 34.4, 33.3, 26.1, 25.1 **Optical Rotation** [α]<sup>25</sup><sub>D</sub>: +11.0 (c = 0.04) CHCl<sub>3</sub>

**HPLC** separation conditions and stereochemical assignment<sup>23</sup>: Chiralpak OD-H Column  
2% isopropyl alcohol in hexane, flow rate: 1 mL/min, 25 °C;  $t_R$  19.4 min for (*S*)-enantiomer  
(major) and 22.5 min for (*R*)-enantiomer (minor). (e.r. = 82:18)



Peak #	RetTime [min]	Type	Width [min]	Area [mAU*s]	Height [mAU]	Area %
1	19.375	BB	0.3902	195.52405	7.37843	81.7723
2	22.497	MM	0.5145	43.58389	1.41175	18.2277

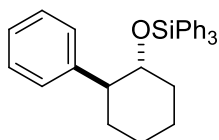
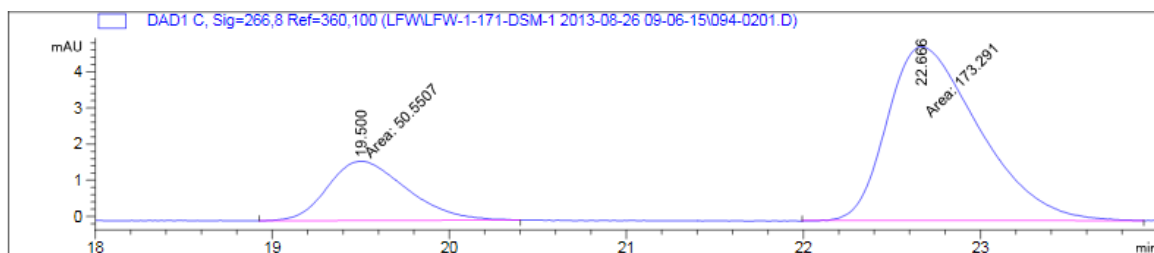


**Table 2.1, Entry 2:** GP3. Recovered product: 86 mg, 40%, white solid, **mp range** = 118-120°C. **<sup>1</sup>H NMR** (400 MHz, CDCl<sub>3</sub>): δ ppm 7.49 – 7.19 (m, 18H), 7.11 – 7.03 (m, 2H), 3.82 (td, *J* = 10.3, 4.0 Hz, 1H), 2.73 – 2.64 (m, 1H), 2.03 – 1.94 (m, 1H), 1.88 – 1.51 (m, 4H), 1.45 – 1.11 (m, 3H). **<sup>13</sup>C NMR** (101 MHz, CDCl<sub>3</sub>) δ ppm 135.5, 135.4, 134.7, 129.6, 128.3, 128.1, 127.5, 126.0, 76.4, 53.1, 36.5, 34.1, 25.9, 25.1. **HRMS (ESI)** Calculated for (C<sub>30</sub>H<sub>30</sub>OSi +) (M +): 434.2066 Observed: 434.2069. **IR** (neat, cm<sup>-1</sup>) 2929, 2856, 1447, 1428, 1114, 1106, 1091, 1029, 998, 982, 878, 840, 794, 709. **Optical Rotation** [ $\alpha$ ]<sub>D</sub><sup>25</sup>: -17.8 (c = 0.023) CHCl<sub>3</sub>

HPLC data is of the desilylated product formed by following GP4. The same HPLC separation conditions as the recovered starting materials were utilized. (e.r. = 77:23)



Peak #	RetTime [min]	Type	Width [min]	Area [mAU*s]	Height [mAU]	Area %
1	19.500	MM	0.5137	50.55070	1.64016	22.5832
2	22.666	MM	0.6018	173.29129	4.79962	77.4168

#### Kinetic Resolution Data for Table 2.1, Entry 2

	er <sup>SM</sup>	er <sup>PR</sup>	% conv	s	S AVERAGE
1	82:18	77:23	56.5	6	6
2	81:19	75:25	58.5	5	

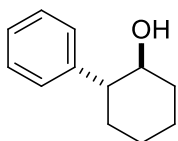


**Table 2.1, Entry 3/ Table 2.2, Entry 1:** GP3. Recovered starting material: 32 mg, 45%.

<sup>1</sup>H NMR (400 MHz, CDCl<sub>3</sub>): δ ppm 7.38 – 7.29 (m, 2H), 7.29 – 7.21 (m, 3H), 3.67 (ddd, *J* = 10.1, 6.3, 2.5 Hz, 1H), 2.43 (ddd, *J* = 13.2, 10.0, 3.5 Hz, 1H), 2.16 – 2.06 (m, 1H), 1.85 (dt, *J* = 12.5, 6.6 Hz, 2H), 1.80 – 1.71 (m, 1H), 1.62 – 1.28 (m, 4H). <sup>13</sup>C NMR (101 MHz, CDCl<sub>3</sub>) δ ppm 143.2, 128.8, 127.9, 126.8, 74.4, 53.2, 34.4, 33.3, 26.1, 25.1 **Optical Rotation** [α]<sub>D</sub><sup>25</sup>: +11.3 (c = 0.039) CHCl<sub>3</sub>.

**HPLC** separation conditions and stereochemical assignment<sup>23</sup>: Chiralpak OD-H Column  
2% isopropyl alcohol in hexanes, flow rate: 1 mL/min, 25 °C;  $t_R$  10.3 min for (*S*)-  
enantiomer (major) and 11.8 min for (*R*)-enantiomer (minor). (e.r. = 83:17)

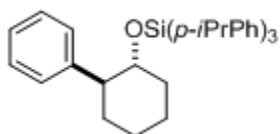
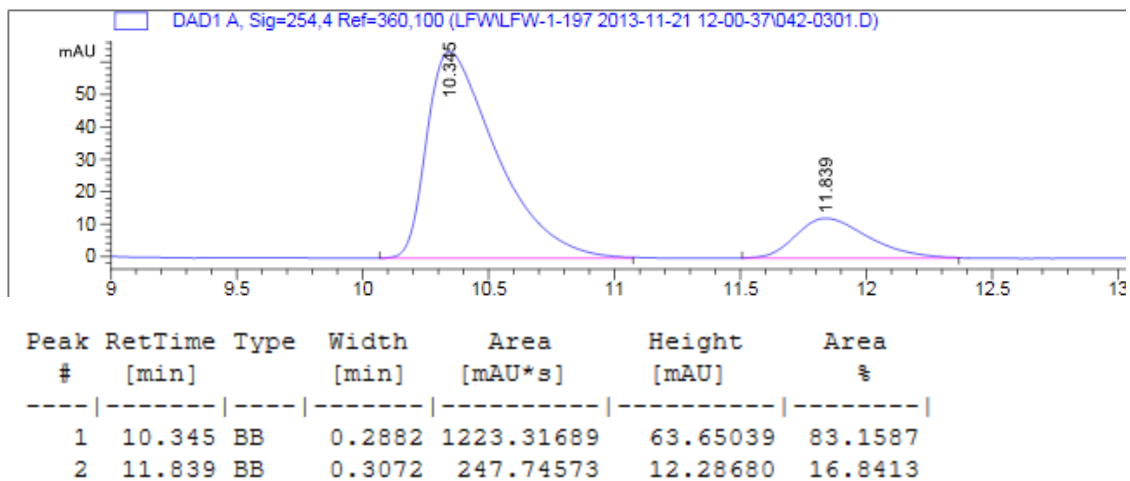
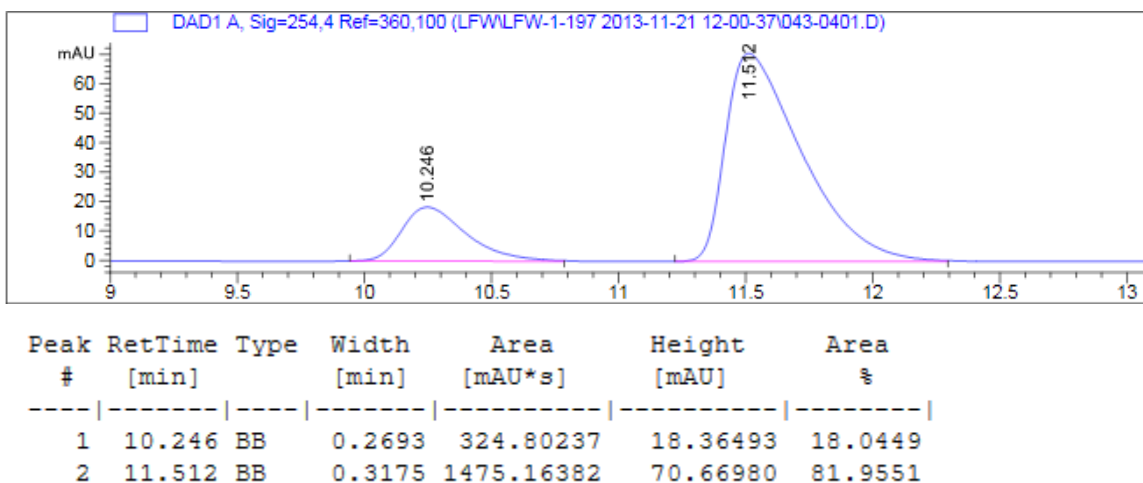


**Table 2.1, Entry 3/ Table 2.2, Entry 1:** GP3. Recovered product: 110 mg, 49%, white solid, **mp range** = 120-122°C.  $^1\text{H NMR}$  (400 MHz,  $\text{CDCl}_3$ ):  $\delta$  ppm 7.23 – 7.17 (m, 9H), 7.10 (d,  $J = 7.9$  Hz, 6H), 7.06 – 7.02 (m, 2H), 3.82 (td,  $J = 10.3, 4.3$  Hz, 1H), 2.87 (hept,  $J = 6.9$  Hz, 3H), 2.70 – 2.62 (m, 1H), 2.02 – 1.93 (m, 1H), 1.87 – 1.77 (m, 1H), 1.74 – 1.29 (m, 6H), 1.24 (d,  $J = 6.9$  Hz, 18H).  $^{13}\text{C NMR}$  (101 MHz,  $\text{CDCl}_3$ )  $\delta$  ppm 150.0, 145.0, 135.7, 132.1, 128.2, 128.2, 125.9, 125.6, 76.0, 53.2, 36.5, 34.2, 34.1, 26.0, 25.1, 23.9. **HRMS (ESI)** Calculated for ( $\text{C}_{39}\text{H}_{48}\text{OSi}^+$ ) ( $\text{M}^+$ ): 560.3474 Observed: 560.3466. **IR** (neat,  $\text{cm}^{-1}$ ) 3065, 2959, 1600, 1460, 1298, 1118, 981, 878, 840, 796, 698 **Optical Rotation**  $[\alpha]_{\text{D}}^{25}$ : -5.6 ( $c = 0.015$ )  $\text{CHCl}_3$

HPLC data is of the desilylated product formed by following GP4. The same HPLC separation conditions as the recovered starting materials were utilized. (e.r. = 82:18)



**Kinetic Resolution Data for Table 2.1, Entry 3/Table 2.2, Entry 1**

	er <sup>SM</sup>	er <sup>PR</sup>	% conv	s	S AVERAGE
1	83:17	82:18	50.8	9	10
2	78:22	87:13	43.0	11	

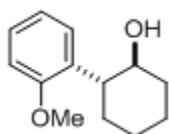
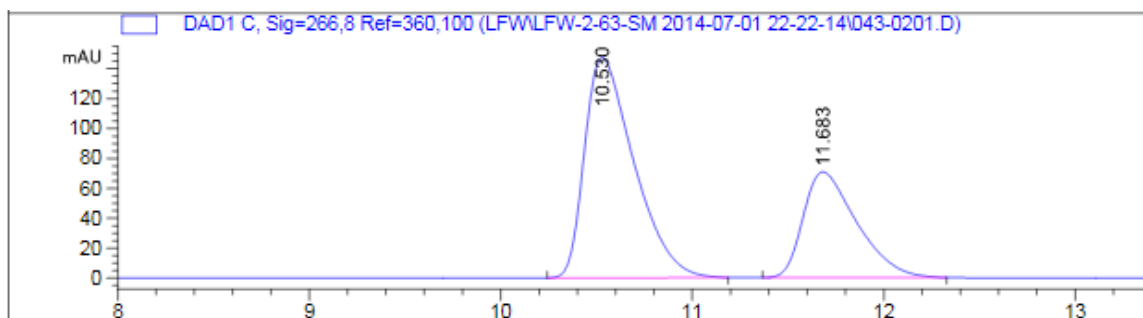


**Table 2.2, Entry 2:** GP3. Recovered starting material: 54 mg, 65 %. <sup>1</sup>H NMR (400 MHz, CDCl<sub>3</sub>): δ ppm 7.30 – 7.21 (m, 2H), 6.99 (td, *J* = 7.5, 0.9 Hz, 1H), 6.92 (d, *J* = 8.2 Hz, 1H), 3.86 (s, 3H), 3.81 – 3.72 (m, 1H), 3.10 – 2.98 (m, 1H), 2.21 – 2.11 (m, 1H), 1.93 – 1.70 (m, 4H), 1.59 – 1.29 (m, 3H). <sup>13</sup>C NMR (101 MHz, CDCl<sub>3</sub>) δ ppm 157.7, 131.5, 127.4, 127.3, 121.05, 110.8, 74.1, 55.5, 45.1, 35.2, 32.6, 26.2, 25.2. **Optical Rotation** [α]<sup>25</sup><sub>D</sub>: +12.3 (c = 0.04) CHCl<sub>3</sub>



**HPLC** separation conditions and stereochemical assignment<sup>8</sup>: Chiralpak OJ-H Column 2% isopropyl alcohol in hexane, flow rate: 1 mL/min, 25 °C;  $t_R$  10.5 min for (*S*)-enantiomer (major) and 11.7 min for (*R*)-enantiomer (minor). (e.r. = 66:34)



Peak #	RetTime [min]	Type	Width [min]	Area [mAU*s]	Height [mAU]	Area %
1	10.530	BB	0.2688	2638.36279	147.45033	65.7533
2	11.683	BB	0.2938	1374.15417	70.67300	34.2467

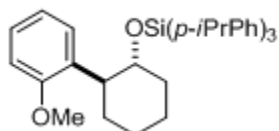
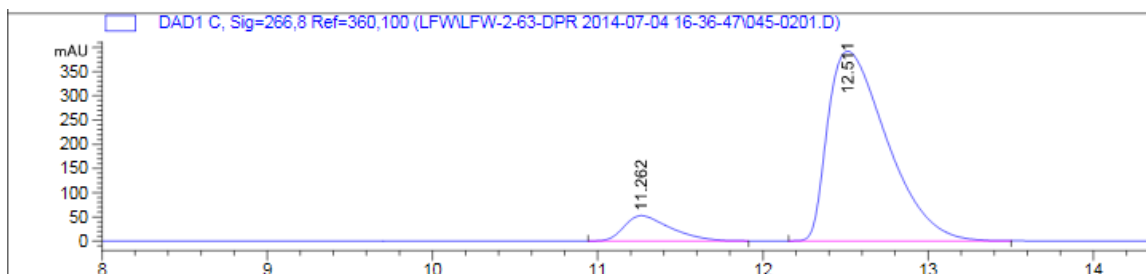


**Table 2.2, Entry 2:** GP3. Recovered product: 56 mg, 24%, white solid. **mp range** = 145-149 °C. <sup>1</sup>H NMR (400 MHz, CDCl<sub>3</sub>): δ ppm 7.21 (d, *J* = 7.9 Hz, 6H), 7.18 – 7.13 (m, 1H), 7.10 (d, *J* = 7.9 Hz, 6H), 6.88 – 6.72 (m, 3H), 4.00 (s, 1H), 3.68 (s, 3H), 3.19 (s, 1H), 2.87 (hept, *J* = 6.9 Hz, 3H), 2.06 – 1.94 (m, 1H), 1.80 – 1.48 (m, 5H), 1.44 – 1.28 (m, 2H), 1.24 (d, *J* = 6.9 Hz, 18H). <sup>13</sup>C NMR (101 MHz, CDCl<sub>3</sub>) δ ppm 157.7, 149.9, 138.7, 135.7, 133.3, 132.4, 126.5, 125.5, 120.6, 110.6, 75.0, 55.4, 36.7, 34.1, 32.8, 26.1, 25.2, 23.9. **IR** (neat, cm<sup>-1</sup>) 3406, 3069, 2959, 1600, 1586, 1463, 1263, 1156, 926, 823, **HRMS (ESI)** Calculated for (C<sub>40</sub>H<sub>50</sub>O<sub>2</sub>Si +) (M +): 590.3580 Observed: 590.3553. **Optical Rotation** [α]<sub>D</sub><sup>25</sup>: -7.9 (c = 0.017) CHCl<sub>3</sub>

HPLC data is of the desilylated product formed by following GP4. The same HPLC separation conditions as the recovered starting materials were utilized. (e.r. = 90:10)



Peak #	RetTime [min]	Type	Width [min]	Area [mAU*s]	Height [mAU]	Area %
1	11.262	BB	0.2936	1024.49329	52.27458	9.5022
2	12.511	BB	0.3875	9757.10254	391.85245	90.4978

#### Kinetic Resolution Data for Table 2.2, Entry 2

	er <sup>SM</sup>	er <sup>PR</sup>	% conv	s	S AVERAGE
1	66:34	90:10	28.6	13	13
2	65:35	90:10	27.3	13	

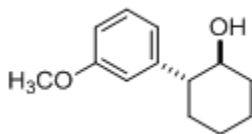
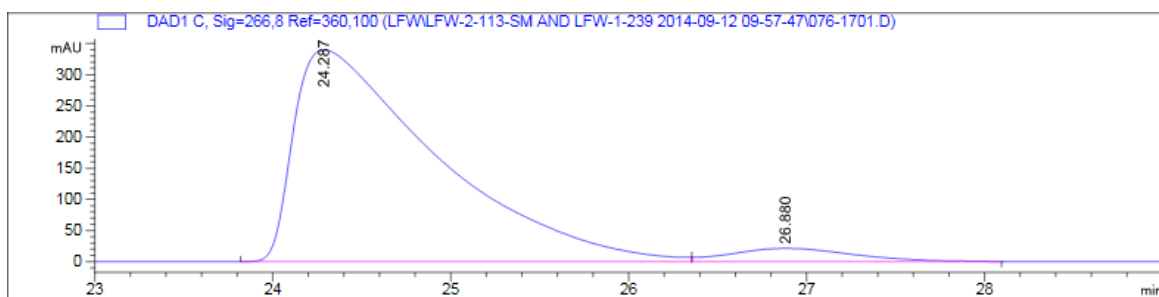


**Table 2.2, Entry 3:** GP3. Recovered starting material: 35 mg, 43%. <sup>1</sup>H NMR (400 MHz, CDCl<sub>3</sub>): δ ppm 7.30 – 7.22 (m, 1H), 6.88 – 6.76 (m, 3H), 3.81 (s, 3H), 3.70 – 3.60 (m, 1H), 2.48 – 2.35 (m, 1H), 2.18 – 2.07 (m, 1H), 1.94 – 1.19 (m, 7H). <sup>13</sup>C NMR (101 MHz, CDCl<sub>3</sub>) δ ppm 159.6, 144.8, 129.5, 120.0, 113.5, 111.8, 74.2, 55.1, 53.2, 34.3, 33.2, 26.0,

25.0. **Optical Rotation**  $[\alpha]_D^{25}$ : +23.2 ( $c = 0.044$ )  $\text{CHCl}_3$ . Stereochemical assignment was matched with reported literature.<sup>25</sup>

**HPLC** separation conditions: Chiralpak OD-H Column 2% isopropyl alcohol in hexane, flow rate: 1 mL/min, 25 °C;  $t_R$  24.3 min for (*S*)-enantiomer (major) and 26.9 min for (*R*)-enantiomer (minor). (e.r. = 95:5)



Peak #	RetTime [min]	Type	Width [min]	Area [mAU*s]	Height [mAU]	Area %
1	24.287	BB	0.8061	1.88863e4	339.98151	94.8859
2	26.880	BB	0.7178	1017.91699	21.32901	5.1141

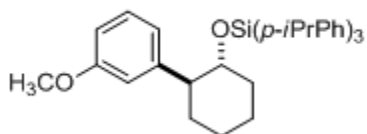
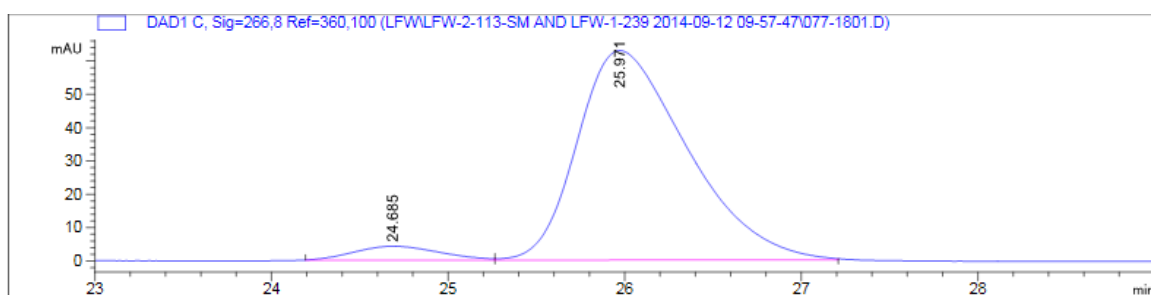


**Table 2, Entry 3:** GP3. Recovered product: 115 mg, 49%, white solid. **mp range** = 137-140 °C.  $^1\text{H NMR}$  (400 MHz,  $\text{CDCl}_3$ ):  $\delta$  ppm 7.21 (d,  $J = 8.0$  Hz, 6H), 7.14 (d,  $J = 7.9$  Hz, 1H), 7.10 (d,  $J = 7.9$  Hz, 6H), 6.76 (dd,  $J = 8.1, 1.9$  Hz, 1H), 6.69 – 6.62 (m, 2H), 3.80 (td,  $J = 10.2, 4.2$  Hz, 1H), 3.68 (s, 3H), 2.93 – 2.81 (m, 3H), 2.69 – 2.60 (m, 1H), 2.03 – 1.92 (m, 1H), 1.82 (d,  $J = 12.4$  Hz, 1H), 1.74 – 1.31 (m, 6H), 1.24 (d,  $J = 6.9$  Hz, 18H).  $^{13}\text{C}$

**NMR** (101 MHz, CDCl<sub>3</sub>)  $\delta$  ppm 159.5, 150.0, 146.7, 135.6, 132.1, 129.1, 125.6, 120.6, 113.3, 112.0, 76.1, 55.0, 53.2, 36.5, 34.1, 30.3, 25.9, 25.0, 23.8. **HRMS (ESI)** Calculated for (C<sub>40</sub>H<sub>50</sub>O<sub>2</sub>Si +) (M +): 590.3582 Observed: 590.3580. **IR** (neat, cm<sup>-1</sup>) 3066, 2959, 2868, 1600, 1461, 1261, 1156, 1089, 990, 875, 785, 698. **Optical Rotation** [ $\alpha$ ]<sub>D</sub><sup>25</sup>: -10.8 (c = 0.017) CHCl<sub>3</sub>.

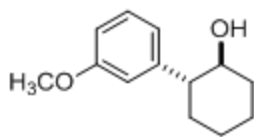
**HPLC** data is of the desilylated product formed by following GP4. The same HPLC separation conditions as the recovered starting materials were utilized. (e.r. = 95:5)



Peak #	RetTime [min]	Type	Width [min]	Area [mAU*s]	Height [mAU]	Area %
1	24.685	BV	0.4042	142.59865	4.20928	4.9757
2	25.971	VB	0.6385	2723.31787	62.84921	95.0243

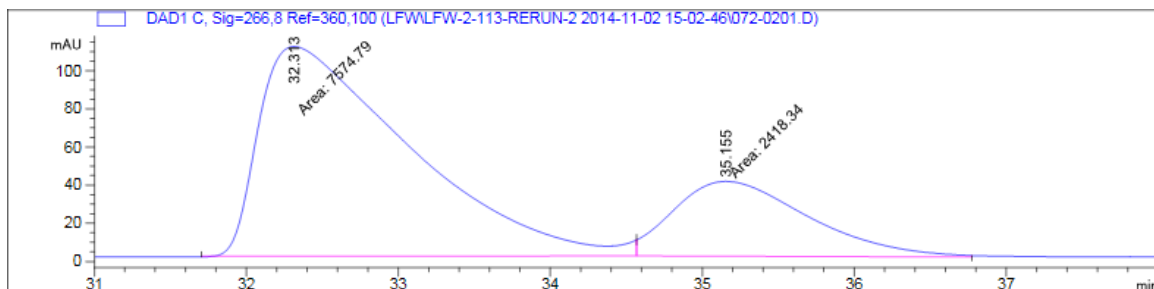
### Kinetic Resolution Data for Table 2.2, Entry 3

	er <sup>SM</sup>	er <sup>PR</sup>	% conv	s	S AVERAGE
1	89:11	96:4	45.8	50	53
2	95:5	95:5	50.0	56	

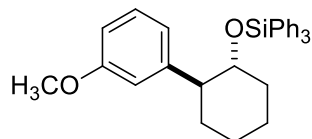


**Kinetic resolution with triphenylsilyl chloride (1.15):** GP3. Recovered starting material: 32 mg, 39%.  $^1\text{H NMR}$  (400 MHz,  $\text{CDCl}_3$ ):  $\delta$  ppm 7.30 – 7.22 (m, 1H), 6.88 – 6.76 (m, 3H), 3.81 (s, 3H), 3.70 – 3.60 (m, 1H), 2.48 – 2.35 (m, 1H), 2.18 – 2.07 (m, 1H), 1.94 – 1.19 (m, 7H).  $^{13}\text{C NMR}$  (101 MHz,  $\text{CDCl}_3$ )  $\delta$  ppm 159.6, 144.8, 129.5, 120.0, 113.5, 111.8, 74.2, 55.1, 53.2, 34.3, 33.2, 26.0, 25.0. **Optical Rotation**  $[\alpha]_D^{25}$ : +15.8 (c = 0.037)  $\text{CHCl}_3$ . Stereochemical assignment was matched with reported literature.<sup>25</sup>

**HPLC** separation conditions: Chiralpak OD-H Column 2% isopropyl alcohol in hexane, flow rate: 1 mL/min, 25 °C;  $t_R$  32.3 min for (S)-enantiomer (major) and 35.2 min for (R)-enantiomer (minor). (e.r. = 76:24)

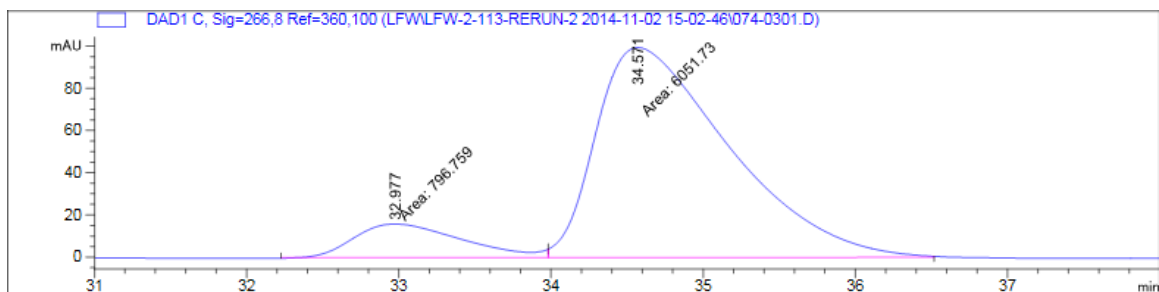


Peak #	RetTime [min]	Type	Width [min]	Area [mAU*s]	Height [mAU]	Area %
1	32.313	MM	1.1483	7574.79004	109.93856	75.8000
2	35.155	MM	1.0302	2418.33789	39.12281	24.2000



**Kinetic resolution with triphenylsilyl chloride (1.15):** GP3. Recovered product: 76 mg, 41%, white solid. **mp range** = 118-120 °C. **<sup>1</sup>H NMR** (400 MHz, CDCl<sub>3</sub>): δ ppm 7.33 – 7.26 (m, 3H), 7.24 – 7.16 (m, 12H), 7.07 (t, *J* = 7.8 Hz, 1H), 6.69 (dd, *J* = 8.2, 1.8 Hz, 1H), 6.71 – 6.67 (m, 2H), 3.73 (td, *J* = 10.4, 4.4 Hz, 1H), 3.63 (s, 3H), 2.64 – 2.55 (m, 1H), 1.95 – 1.85 (m, 1H), 1.80 – 1.72 (m, 1H), 1.67 – 1.42 (m, 3H), 1.38 – 1.06 (m, 3H). **<sup>13</sup>C NMR** (101 MHz, CDCl<sub>3</sub>) δ ppm 159.6, 146.6, 135.6, 134.8, 129.6, 129.2, 127.5, 120.6, 113.6, 111.9, 76.5, 55.1, 53.3, 36.5, 34.0, 25.9, 25.1. **HRMS (ESI)** Calculated for (C<sub>31</sub>H<sub>32</sub>O<sub>2</sub>Si +) (M<sup>+</sup>): 464.2172 Observed: 464.2175. **IR** (neat, cm<sup>-1</sup>) 2931, 2856, 1601, 1429, 1262, 1115, 998, 980, 816, 787, 699. **Optical Rotation** [α]<sup>25</sup><sub>D</sub>: -9.8 (c = 0.020) CHCl<sub>3</sub>

**HPLC** data is of the desilylated product formed by following GP4. The same HPLC separation conditions as the recovered starting materials were utilized. (e.r. = 88:12)



Peak #	RetTime [min]	Type	Width [min]	Area [mAU*s]	Height [mAU]	Area %
1	32.977	MM	0.8284	796.75946	16.03003	11.6341
2	34.571	MM	1.0129	6051.73486	99.58092	88.3659

### Kinetic Resolution Data with triphenylsilyl chloride (1.15)

	er <sup>SM</sup>	er <sup>PR</sup>	% conv	<i>s</i>	<i>S</i> AVERAGE
1	76:24	88:12	40.0	12	13
2	82:18	87:13	45.0	13	

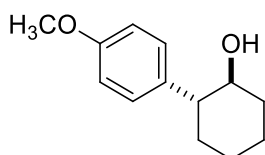
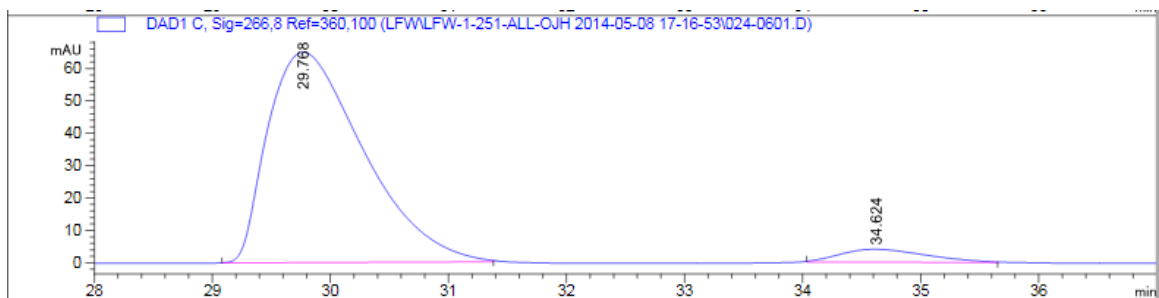


**Table 2, Entry 4:** GP3. Recovered starting material: 35 mg, 43%. <sup>1</sup>H NMR (400 MHz, CDCl<sub>3</sub>): δ ppm 6.88 (d, *J* = 8.7 Hz, 2H), 6.88 (d, *J* = 8.7 Hz, 2H), 3.80 (s, 3H), 3.60 (td, *J* = 10.1, 4.4 Hz, 1H), 2.42 – 2.33 (m, 1H), 1.90 – 1.71 (m, 3H), 1.64 – 1.24 (m, 5H), <sup>13</sup>C NMR (101 MHz, CDCl<sub>3</sub>) δ ppm 158.4, 135.2, 128.8, 114.2, 74.6, 55.3, 52.4, 34.4, 33.5, 26.1, 25.1. **Optical Rotation** [α]<sub>D</sub><sup>25</sup>: +19.8 (c = 0.045) CHCl<sub>3</sub>. Stereochemical assignment was matched with reported literature.<sup>8</sup>

**HPLC** separation conditions: Chiralpak OJ-H Column 3% isopropyl alcohol in hexane, flow rate: 1 mL/min, 25 °C; t<sub>R</sub> 29.8 min for (*S*)-enantiomer (major) and 34.6 min for (*R*)-enantiomer (minor). (e.r. = 95:5)



Peak #	RetTime [min]	Type	Width [min]	Area [mAU*s]	Height [mAU]	Area %
1	29.768	BB	0.8671	3660.67969	64.99129	94.8284
2	34.624	BB	0.6186	199.64166	3.97076	5.1716

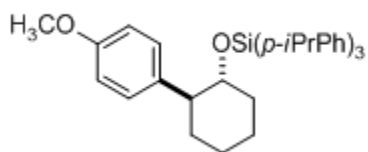
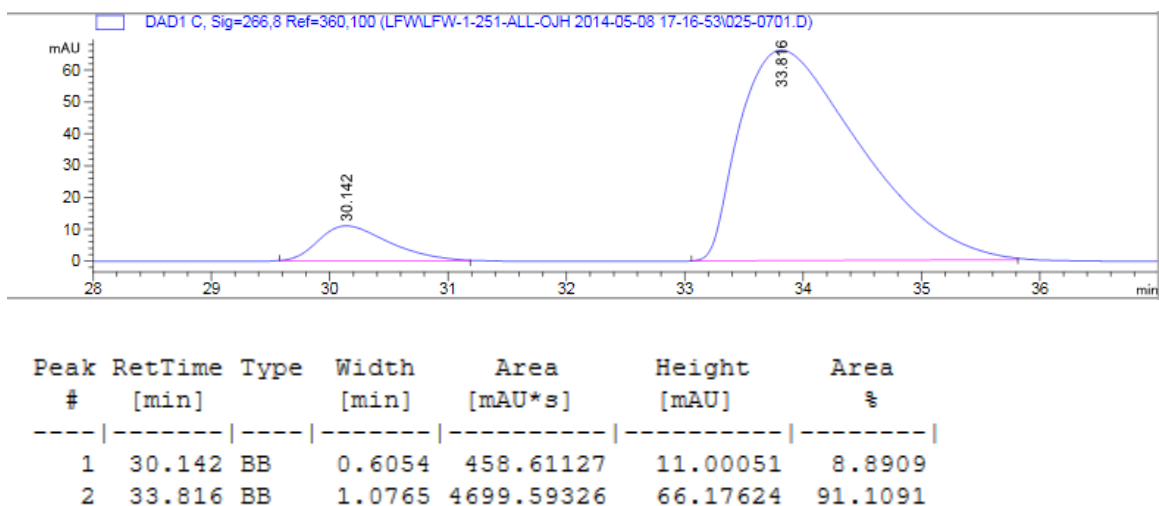


**Table 2, Entry 4:** GP3. Recovered product: 122 mg, 52%, white solid. **mp range** = 130-135 °C  $^1\text{H NMR}$  (400 MHz,  $\text{CDCl}_3$ ):  $\delta$  ppm 7.14 (d,  $J = 7.9$  Hz, 6H), 7.04 (d,  $J = 7.9$  Hz, 6H), 6.90 (d,  $J = 8.6$  Hz, 2H), 6.69 (d,  $J = 8.6$  Hz, 2H), 3.75 (s, 3H), 3.68 (td,  $J = 10.3, 4.3$  Hz, 1H), 2.80 (hept,  $J = 6.9$  Hz, 3H), 2.59 – 2.49 (m, 1H), 1.92 – 1.83 (m, 1H), 1.77 – 1.22 (m, 7H). 1.17 (d,  $J = 6.9$  Hz, 18H).  $^{13}\text{C NMR}$  (101 MHz,  $\text{CDCl}_3$ )  $\delta$  ppm 158.0, 150.0, 137.3, 135.7, 132.2, 129.0, 125.6, 113.6, 76.3, 55.3, 52.2, 36.5, 34.2, 34.1, 26.0, 25.1, 23.9. **IR** (neat,  $\text{cm}^{-1}$ ) 3060, 2955, 2868, 1600, 1490, 1394, 1261, 1150, 1089, 990, 862, 785, 699. **HRMS (ESI)** Calculated for ( $\text{C}_{40}\text{H}_{50}\text{O}_2\text{Si}^+$ ) ( $\text{M}^+$ ): 590.3580 Observed: 590.3582. **Optical Rotation**  $[\alpha]_D^{25}$ : -9.6 (c = 0.016)  $\text{CHCl}_3$



HPLC data is of the desilylated product formed by following GP4. The same HPLC separation conditions as the recovered starting materials were utilized. (e.r. = 91:9)



#### Kinetic Resolution Data for Table 2.2, Entry 4

	er <sup>SM</sup>	er <sup>PR</sup>	% conv	s	S AVERAGE
1	82:18	93:7	42.5	25	28
2	95:5	91:9	52.3	30	

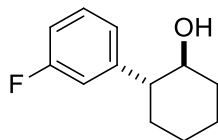
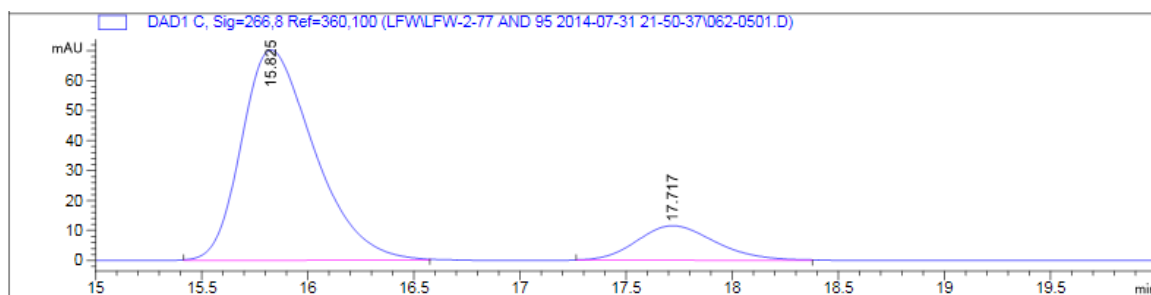


**Table 2.2, Entry 5:** GP3. Recovered starting material: 38 mg, 49%. <sup>1</sup>H NMR (400 MHz, CDCl<sub>3</sub>): δ ppm 7.33 – 7.27 (m, 1H), 7.03 (d, *J* = 7.7 Hz, 1H), 6.99 – 6.90 (m, 2H), 3.68 – 3.59 (m, 1H), 2.50 – 2.38 (m, 1H), 2.15 – 2.06 (m, 1H), 1.92 – 1.72 (m, 3H), 1.55 – 1.26 (m, 4H), <sup>13</sup>C NMR (101 MHz, CDCl<sub>3</sub>) δ ppm 164.4, 161.9, 146.2, 146.2, 130.2, 130.1,

123.7, 123.6, 114.7, 114.5, 113.8, 113.6. 74.3, 53.0, 34.6, 33.2, 25.9, 25.0. (Peaks splitting due to the fluorine) Optical **Rotation**  $[\alpha]_D^{25}$ : +12.3 (c = 0.046) CHCl<sub>3</sub>. Stereochemical assignment was made by analogy to similar compounds in Table 2 as well as (1R,2S)-*trans*-2-(4-fluorophenyl)-1-cyclohexanol as reported in the literature.<sup>8</sup>

**HPLC** separation conditions: Chiralpak OD-H column 2% isopropyl alcohol in hexane, flow rate: mL/min, 25 °C;  $t_R$  15.8 min for (*S*)-enantiomer (major) and 17.7 min for (*R*)-enantiomer (minor). (e.r. = 85:15)



Peak #	RetTime [min]	Type	Width [min]	Area [mAU*s]	Height [mAU]	Area %
1	15.826	BB	0.3645	1207.61597	50.77181	85.0669
2	17.718	BB	0.3757	211.99130	8.28030	14.9331

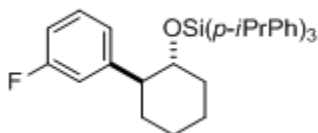
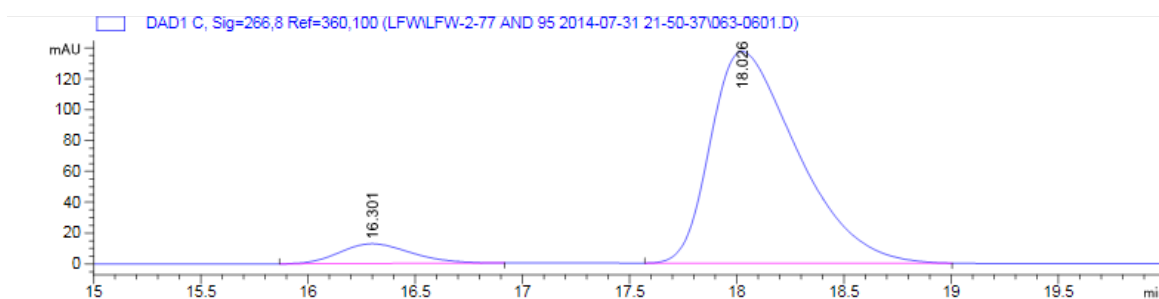


**Table 2.2, Entry 5:** GP3. Recovered product: 101 mg, 44%, colorless liquid. <sup>1</sup>H NMR (400 MHz, CDCl<sub>3</sub>): δ ppm 7.22 (d, *J* = 8.0 Hz, 6H), 7.18 – 7.10 (m, 7H), 6.90 – 6.83 (m, 2H), 6.70 – 6.65 (m, 1H), 3.76 (td, *J* = 10.3, 4.3 Hz, 1H), 2.94 – 2.81 (m, 3H), 2.71 – 2.62 (m, 1H), 2.04 – 1.94 (m, 1H), 1.86 – 1.27 (m, 7H), 1.24 (d, *J* = 6.9 Hz, 18H). <sup>13</sup>C NMR

(101 MHz, CDCl<sub>3</sub>)  $\delta$  ppm 164.1, 161.7, 150.2, 147.8, 135.6, 131.9, 129.4, 126.0, 125.7, 124.1, 114.9, 114.7, 112.9, 112.6, 75.9 53.0, 36.4, 34.1, 33.9, 25.8, 25.0, 23.9. (Peaks splitting due to the fluorine) **IR** (neat, cm<sup>-1</sup>) 3067, 2960, 1600, 1460, 1446, 1394, 1255, 1119, 1087, 994, 862, 770, 695. **HRMS (ESI)** Calculated for (C<sub>39</sub>H<sub>47</sub>FOSi +) (M +): 578.3380 Observed: 578.3378. **Optical Rotation** [ $\alpha$ ]<sub>D</sub><sup>25</sup>: -11.3 (c = 0.017) CHCl<sub>3</sub>

**HPLC** data is of the desilylated product formed by following GP4. The same HPLC separation conditions as the recovered starting materials were utilized. (e.r. = 93:7)



Peak #	RetTime [min]	Type	Width [min]	Area [mAU*s]	Height [mAU]	Area %
1	16.301	BB	0.3554	296.59589	12.74962	7.1039
2	18.026	BB	0.4297	3878.53809	137.24733	92.8961

#### Kinetic Resolution Data for Table 2.2, Entry 5

	er <sup>SM</sup>	er <sup>PR</sup>	% conv	s	S AVERAGE
1	85:15	93:7	45.0	27	27
2	82:18	93:7	42.6	26	

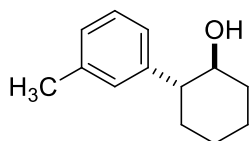
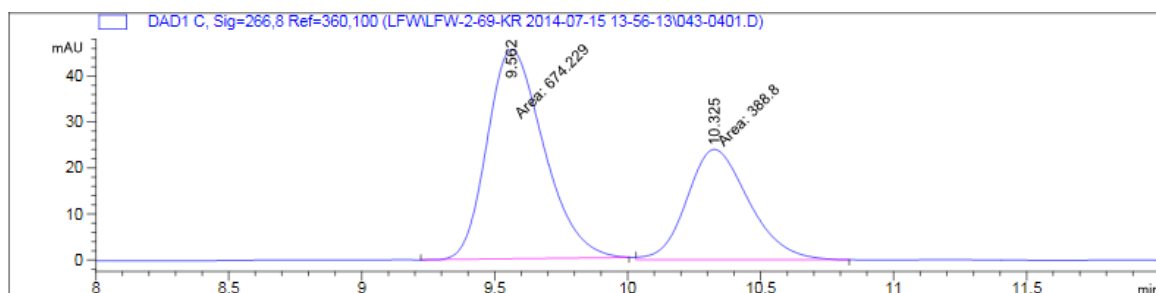


**Table 2.2, Entry 6:** GP3. Recovered starting material: 53 mg, 70%.  $^1\text{H NMR}$  (400 MHz,  $\text{CDCl}_3$ ):  $\delta$  ppm 7.22 (t,  $J = 7.5$  Hz, 1H), 7.06 (d,  $J = 7.9$  Hz, 3H), 3.70 – 3.61 (m, 1H), 2.44 – 2.36 (m, 1H), 2.35 (s, 3H), 2.15 – 2.07 (m, 1H), 1.89 – 1.71 (m, 3H), 1.60 – 1.27 (m, 4H),  $^{13}\text{C NMR}$  (101 MHz,  $\text{CDCl}_3$ )  $\delta$  ppm 143.2, 138.8, 128.7, 128.6, 127.6, 124.9, 74.4, 53.2, 34.4, 33.3, 26.1, 25.1, 21.5. **Optical Rotation**  $[\alpha]_D^{25}$ : +8.7 (c = 0.044)  $\text{CHCl}_3$ . Stereochemical assignment was matched with reported literature.<sup>8</sup>

**HPLC** separation conditions: Chiralpak OJ-H Column 2% isopropyl alcohol in hexane, flow rate: 1 mL/min, 25 °C;  $t_R$  9.6 min for (*S*)-enantiomer (major) and 10.3 min for (*R*)-enantiomer (minor). (e.r. = 63:37)



Peak #	RetTime [min]	Type	Width [min]	Area [mAU*s]	Height [mAU]	Area %
1	9.562	MM	0.2469	674.22943	45.51537	63.4253
2	10.325	MM	0.2703	388.79980	23.97302	36.5747

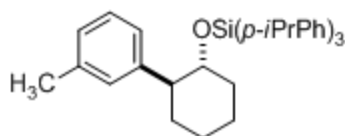
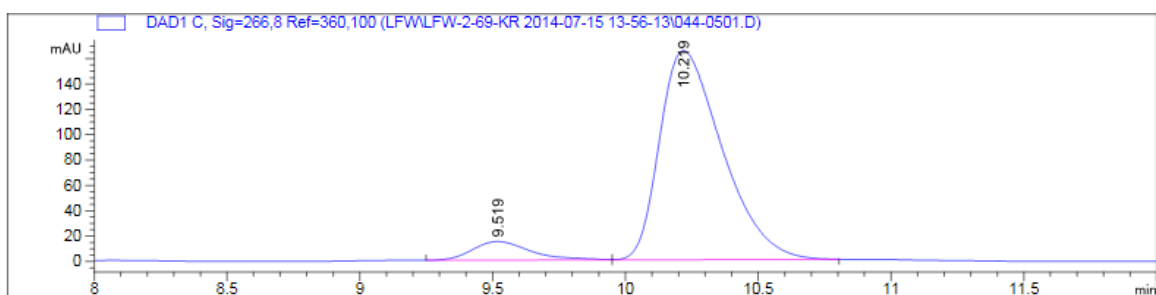


**Table 2.2, Entry 6:** GP3. Recovered product: 58 mg, 25%, white solid. **mp range** = 128-133 °C. **<sup>1</sup>H NMR** (400 MHz, CDCl<sub>3</sub>): 7.19 (d, *J* = 8.0 Hz, 6H), 7.15 – 7.07 (m, 7H), 7.02 (d, *J* = 7.4 Hz, 1H), 6.85 (d, *J* = 10.9 Hz, 2H), 3.80 (td, *J* = 10.3, 4.2 Hz, 1H), 2.94 – 2.82 (m, 3H), 2.68 – 2.57 (m, 1H), 2.25 (s, 3H), 2.04 – 1.93 (m, 1H), 2.02 – 1.29 (m, 7H), 1.24 (d, *J* = 6.9 Hz, 18H). **<sup>13</sup>C NMR** (101 MHz, CDCl<sub>3</sub>) δ ppm 150.0, 145.0, 137.5, 135.7, 132.1, 129.0, 128.2, 126.7, 125.6, 125.3, 76.1, 53.1, 36.5, 34.1, 30.3, 26.0, 25.1, 23.9, 21.5. **IR** (neat, cm<sup>-1</sup>) 3102, 2933, 1623, 1450, 1282, 1173, 1071, 919, 838, 724, 715. **HRMS (ESI)** Calculated for (C<sub>40</sub>H<sub>50</sub>OSi +) (M +): 574.3631 Observed: 574.3630. **Optical Rotation** [α]<sup>25</sup><sub>D</sub>: -11.3 (c = 0.017) CHCl<sub>3</sub>

**HPLC** data is of the desilylated product formed by following GP4. The same HPLC separation conditions as the recovered starting materials were utilized. (e.r. = 92:8)



Peak #	RetTime [min]	Type	Width [min]	Area [mAU*s]	Height [mAU]	Area %
1	9.519	BV	0.2328	223.05510	14.72028	7.6130
2	10.219	VB	0.2524	2706.88354	165.03851	92.3870

### Kinetic Resolution Data for Table 2.2, Entry 6

	er <sup>SM</sup>	er <sup>PR</sup>	% conv	<i>s</i>	<i>S</i> AVERAGE
1	64:36	92:8	25.0	15	14
2	63:37	92:8	24.0	13	

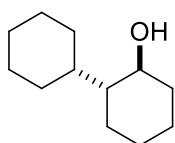


**Table 2.2, Entry 7:** GP3. Recovered starting material: 42 mg, 58%. <sup>1</sup>H NMR (400 MHz, CDCl<sub>3</sub>): 3.48 – 3.39 (m, 1H), 2.03 – 1.94 (m, 1H), 1.81 – 1.59 (m, 7H), 1.47 – 0.92 (m, 12H). δ ppm <sup>13</sup>C NMR (101 MHz, CDCl<sub>3</sub>) δ ppm 71.2, 50.7, 37.1, 36.4, 31.6, 27.3, 27.2, 26.9, 26.9, 26.0, 25.3, 25.0. **Optical Rotation** [α]<sup>25</sup><sub>D</sub>: +5.4 (c = 0.027) CHCl<sub>3</sub>. Stereochemical assignment was made by analogy to similar compounds in Table 2.

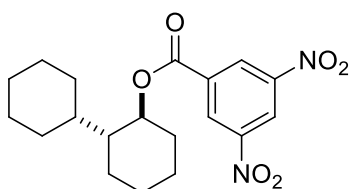
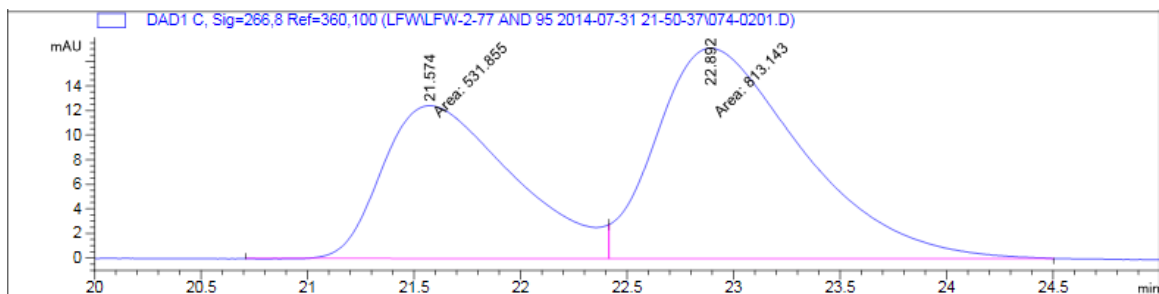


**Table 2.2, Entry 7:** Benzyl ester of recovered starting material formed through GP5: <sup>1</sup>H NMR (400 MHz, CDCl<sub>3</sub>): 9.24 (t, *J* = 2.1 Hz, 1H), 9.16 (d, *J* = 2.1 Hz, 2H), 5.10 (td, *J* = 10.3, 4.3 Hz, 1H), 9.25 – 9.22 (m, 1H), 1.86 – 0.92 (m, 19H), <sup>13</sup>C NMR (101 MHz, CDCl<sub>3</sub>) δ ppm 162.0, 148.7, 134.6, 129.4, 122.2, 47.4, 37.9, 32.2, 31.2, 29.7, 27.6, 27.0, 26.9, 26.7,

25.6, 25.3, 24.6. **Optical Rotation**  $[\alpha]_D^{25}$ : +6.7 ( $c = 0.022$ )  $\text{CHCl}_3$ . Stereochemical assignment was made by analogy to similar compounds in Table 2.

**HPLC** separation conditions: Chiralpak OD-H Column 2% isopropyl alcohol in hexane, flow rate: 0.75 mL/min, 25 °C;  $t_R$  21.6 min for (*R*)-enantiomer (minor) and 22.9 min for (*S*)-enantiomer (major). (e.r. = 61:39)



Peak #	RetTime [min]	Type	Width [min]	Area [mAU*s]	Height [mAU]	Area %
1	21.574	MM	0.7083	528.87708	12.44531	38.9903
2	22.892	MM	0.8039	827.55371	17.15611	61.0097

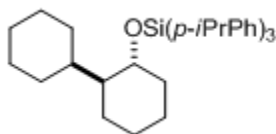


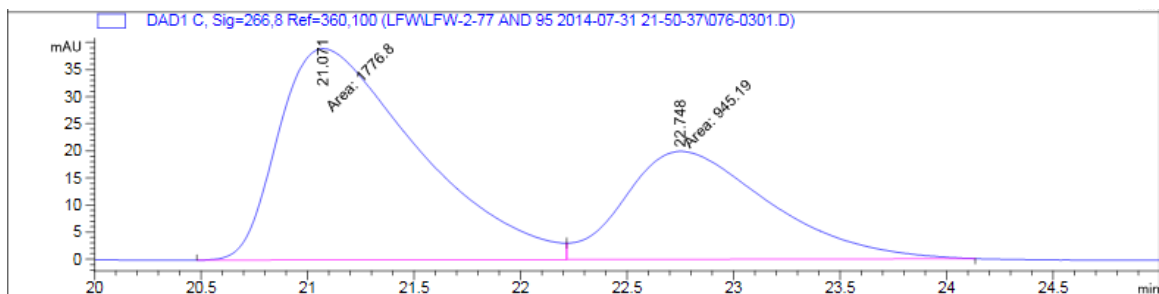
**Table 2.2, Entry 7:** GP3. Recovered product: 86 mg, 38%, white solid. **mp range** = 128-133 °C.  **$^1\text{H NMR}$**  (400 MHz,  $\text{CDCl}_3$ ): 7.55 (d,  $J = 8.0$  Hz, 6H), 7.21 (d,  $J = 7.9$  Hz, 6H), 3.58 (td,  $J = 9.8, 4.2$  Hz, 1H), 2.90 (hept,  $J = 6.9$  Hz, 3H), 2.01 – 1.30 (m, 12H), 1.21 – 0.81 (m, 8H).  **$^{13}\text{C NMR}$**  (101 MHz,  $\text{CDCl}_3$ )  $\delta$  ppm 150.3, 135.8, 132.5, 125.8, 72.9, 50.5, 36.2, 36.1, 34.2, 31.9, 27.3, 27.0, 26.8, 25.7, 24.9, 24.8, 23.9, 23.9. **IR** (neat,  $\text{cm}^{-1}$ ) 3011, 2959, 2853, 1600, 1460, 1363, 1298, 1118, 1080, 938, 868, 813, 770. **HRMS (ESI)**

Calculated for (C<sub>39</sub>H<sub>54</sub>OSi +) (M +): 566.3944 Observed: 566.3946. **Optical Rotation**

[ $\alpha$ ]<sub>D</sub><sup>25</sup>: -2.9 (c = 0.019) CHCl<sub>3</sub>

HPLC data is of the desilylated, benzoylated product following GP4 and GP5. The same HPLC separation conditions as the benzoylated, recovered starting materials were utilized.

(e.r. = 65:35)



Peak #	RetTime [min]	Type	Width [min]	Area [mAU*s]	Height [mAU]	Area %
1	21.071	MM	0.7593	1776.80334	39.00140	65.2758
2	22.748	MM	0.7903	945.19012	19.93430	34.7242

#### Kinetic Resolution Data for Table 2.2, Entry 7

	er <sup>SM</sup>	er <sup>PR</sup>	% conv	s	S AVERAGE
1	61:39	65:35	42.3	2	2
2	60:40	65:35	40.0	2	



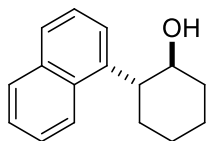
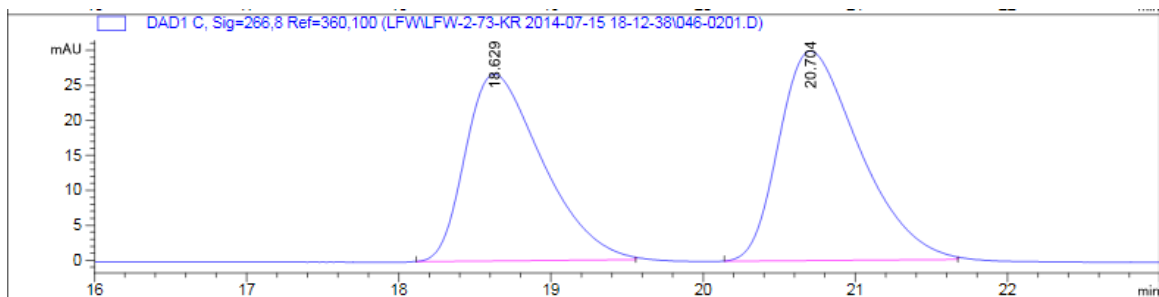


**Table 2.2, Entry 8:** GP3. Recovered starting material: 77 mg, 85%.  $^1\text{H NMR}$  (400 MHz,  $\text{CDCl}_3$ ):  $\delta$  ppm 8.20 (d,  $J = 8.4$  Hz, 1H), 7.90 – 7.84 (m, 1H), 7.78 – 7.72 (m, 1H), 7.57 – 7.45 (m, 4H), 4.05 – 3.95 (m, 1H), 3.44 – 3.35 (m, 1H), 2.28 – 2.18 (m, 1H), 2.04 – 1.75 (m, 3H), 1.65 – 1.41 (m, 4H).  $^{13}\text{C NMR}$  (101 MHz,  $\text{CDCl}_3$ )  $\delta$  ppm 139.5, 134.2, 132.7, 129.0, 127.1, 126.1, 125.7, 125.7, 123.2, 122.7, 74.3, 46.7, 34.8, 33.9, 26.4, 25.2. **Optical Rotation**  $[\alpha]_D^{25}$ : +1.8 ( $c = 0.017$ )  $\text{CHCl}_3$ . Stereochemical assignment was matched with reported literature.<sup>8</sup>

**HPLC** separation conditions: Chiralpak OJ-H Column 3% isopropyl alcohol in hexane, flow rate: 1 mL/min, 25 °C;  $t_R$  18.6 min for (*R*)-enantiomer (minor) and 20.7 min for (*S*)-enantiomer (major). (e.r. = 54:46)



Peak #	RetTime [min]	Type	Width [min]	Area [mAU*s]	Height [mAU]	Area %
1	18.629	BB	0.5221	938.14044	26.68749	46.0087
2	20.704	BB	0.5549	1100.91089	29.94416	53.9913

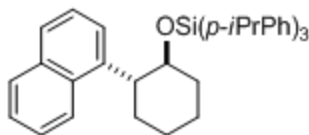
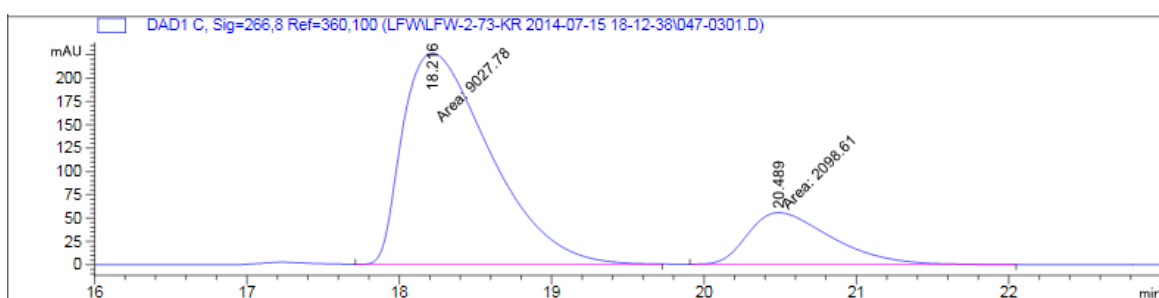


**Table 2.2, Entry 8:** GP3. Recovered product: 23 mg, 10%, white solid. **mp range** = 140-142 °C. **<sup>1</sup>H NMR** (400 MHz, CDCl<sub>3</sub>): δ ppm 8.29 (d, *J* = 8.1 Hz, 1H), 7.91 – 7.84 (m, 1H), 7.65 (d, *J* = 8.1 Hz, 1H), 7.54 – 7.44 (m, 2H), 7.19 (t, *J* = 7.7 Hz, 1H), 7.07 (d, *J* = 7.9 Hz, 6H), 7.03 – 6.96 (m, 7H). 4.11 – 4.00 (m, 1H), 3.68 – 3.55 (m, 1H), 2.84 (hept, *J* = 6.9 Hz, 3H), 2.15 – 2.06 (m, 1H), 1.99 – 1.88 (m, 1H), 1.82 – 1.64 (m, 3H), 1.49 – 1.34 (m, 3H), 1.22 (dd, *J* = 6.9, 1.1 Hz, 18H). **<sup>13</sup>C NMR** (101 MHz, CDCl<sub>3</sub>) δ ppm 149.9, 141.2, 135.6, 134.0, 132.7, 132.0, 128.7, 126.0, 125.6, 125.5, 125.1, 123.8, 104.0, 103.0, 76.2, 36.9, 34.1, 26.3, 25.2, 23.8, 23.8, 18.0. **IR** (neat, cm<sup>-1</sup>) 3011, 2960, 2930, 2868, 1600, 1460, 1362, 1119, 1094, 972, 823, 811, 776. **HRMS (ESI)** Calculated for (C<sub>43</sub>H<sub>50</sub>OSi +) (M +): 610.3631 Observed: 610.3630. **Optical Rotation** [α]<sub>D</sub><sup>25</sup>: -12.5 (c = 0.017) CHCl<sub>3</sub>

**HPLC** data is of the desilylated product formed by following GP4. The same HPLC separation conditions as the recovered starting materials were utilized. (e.r. = 81:19)



Peak #	RetTime [min]	Type	Width [min]	Area [mAU*s]	Height [mAU]	Area %
1	18.216	MM	0.6646	9027.78027	226.39357	81.1385
2	20.489	MM	0.6319	2098.60742	55.35519	18.8615

### Kinetic Resolution Data for Table 2.2, Entry 8

	er <sup>SM</sup>	er <sup>PR</sup>	% conv	<i>s</i>	<i>S</i> AVERAGE
1	54:46	81:19	11.0	5	5
2	53:47	80:20	9.0	4	

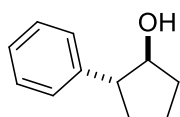
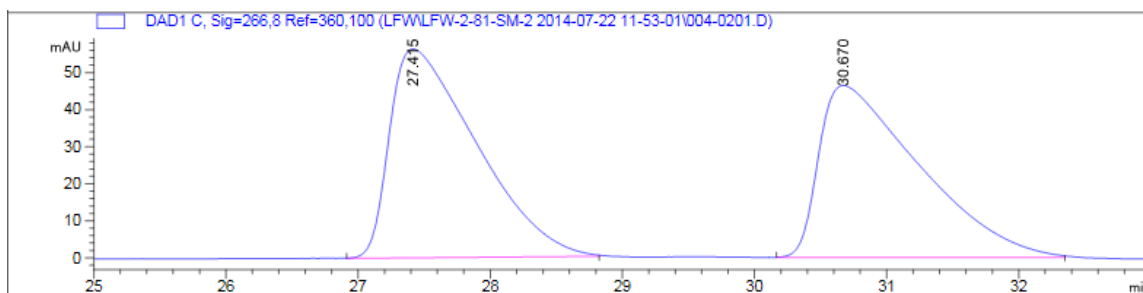


**Table 2.2, Entry 9:** GP3. Recovered starting material: 27 mg, 42%. <sup>1</sup>H NMR (400 MHz, CDCl<sub>3</sub>): δ ppm 7.34 – 7.18 (m, 5H), 4.14 (q, *J* = 7.2 Hz, 1H), 2.92 – 2.80 (m, 1H), 2.21 – 2.03 (m, 2H), 1.93 – 1.60 (m, 5H). <sup>13</sup>C NMR (101 MHz, CDCl<sub>3</sub>) δ ppm 143.3, 128.6, 127.4, 126.4, 80.5, 54.5, 34.0, 31.9, 21.8. **Optical Rotation** [ $\alpha$ ]<sub>D</sub><sup>25</sup>: +1.8 (c = 0.017) CHCl<sub>3</sub>, Stereochemical assignment was matched with reported literature.<sup>8</sup>

**HPLC** separation conditions: Chiralpak OD-H Column 2% isopropyl alcohol in hexane, flow rate: 1 mL/min, 25 °C; *t*<sub>R</sub> 27.4 min for (*S*)-enantiomer (major) and 30.7 min for (*R*)-enantiomer (minor). (e.r. = 51:49)



Peak #	RetTime [min]	Type	Width [min]	Area [mAU*s]	Height [mAU]	Area %
1	27.415	BB	0.6439	2569.69312	56.36797	51.2580
2	30.670	BB	0.7226	2443.55957	46.38841	48.7420

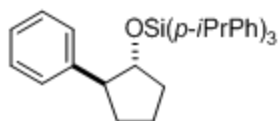
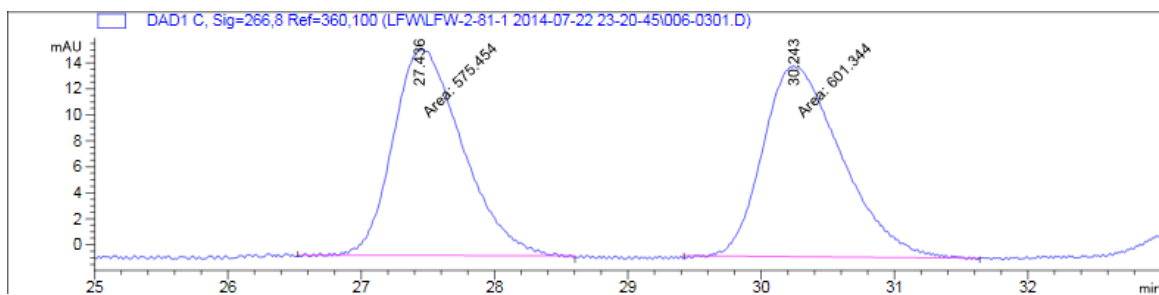


**Table 2.2, Entry 9:** GP3. Recovered product: 114 mg, 52%, white solid. **mp range** = 115-118 °C. **<sup>1</sup>H NMR** (400 MHz, CDCl<sub>3</sub>): δ ppm 7.40 (d, *J* = 8.0 Hz, 6H), 7.20 – 7.11 (m, 9H), 7.02 – 6.98 (m, 2H), 4.28 (q, *J* = 6.0 Hz, 1H), 3.09 (dd, *J* = 14.5, 8.2 Hz, 1H), 2.87 (hept, *J* = 6.9 Hz, 3H), 2.22 – 2.10 (m, 1H), 1.94 – 1.34 (m, 5H), 1.24 (d, *J* = 6.9 Hz, 18H) **<sup>13</sup>C NMR** (101 MHz, CDCl<sub>3</sub>) δ ppm 150.3, 144.0, 135.6, 132.0, 128.2, 127.8, 125.9, 125.8, 81.9, 54.6, 34.6, 34.2, 31.3, 23.9, 22.4. **IR** (neat, cm<sup>-1</sup>) 3012, 2959, 1600, 1459, 1298, 1118, 1093, 952, 888, 769, 699. **HRMS (ESI)** Calculated for (C<sub>38</sub>H<sub>46</sub>OSi +) (M +): 546.3318 Observed: 546.3320. **Optical Rotation** [α]<sub>D</sub><sup>25</sup>: -1.1 (c = 0.017) CHCl<sub>3</sub>

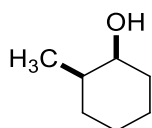
**HPLC** data is of the desilylated product formed by following GP4. The same HPLC separation conditions as the recovered starting materials were utilized. (e.r. = 51:49)



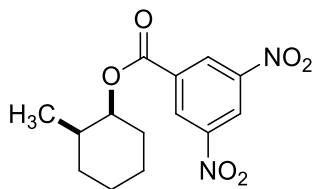
Peak #	RetTime [min]	Type	Width [min]	Area [mAU*s]	Height [mAU]	Area %
1	27.436	MM	0.6026	575.45380	15.91496	48.9000
2	30.243	MM	0.6812	601.34424	14.71205	51.1000

### Kinetic Resolution Data for Table 2.2, Entry 9

	er <sup>SM</sup>	er <sup>PR</sup>	% conv	<i>s</i>	<i>S</i> AVERAGE
1	51:49	51:49	54.0	1.1	1.1
2	51:49	51:49	54.0	1.1	

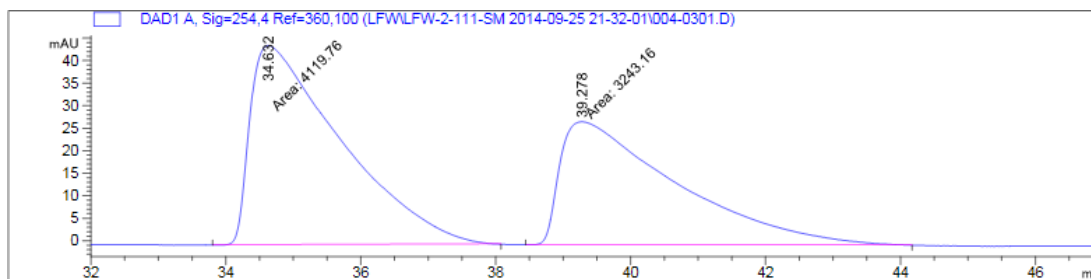


**Scheme 2.5, R = CH<sub>3</sub>:** GP3. Recovered starting material: 11 mg, 24%. **<sup>1</sup>H NMR** (400 MHz, CDCl<sub>3</sub>): δ ppm 3.80 – 3.74 (m, 1H), 1.78 – 1.19 (m, 9H), 0.93 (d, *J* = 7.0 Hz, 3H). **<sup>13</sup>C NMR** (101 MHz, CDCl<sub>3</sub>) δ ppm 71.1, 35.8, 32.5, 28.8, 24.5, 20.7, 17.0. **Optical Rotation** [ $\alpha$ ]<sub>D</sub><sup>25</sup>: +2.1 (*c* = 0.077) CHCl<sub>3</sub>. Stereochemical assignment was matched with reported literature.<sup>35</sup>

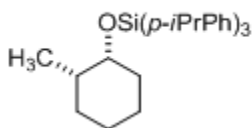


**Scheme 2.5, R = CH<sub>3</sub>:** Benzyl ester of recovered starting material formed through GP5: **<sup>1</sup>H NMR** (400 MHz, CDCl<sub>3</sub>): δ ppm 9.24 (t, *J* = 2.1 Hz, 1H), 9.16 (d, *J* = 2.2 Hz, 2H), 5.33 – 5.29 (m, 1H), 2.09 – 1.10 (m, 9H), 0.98 (d, *J* = 6.9 Hz, 3H). **<sup>13</sup>C NMR** (101 MHz, CDCl<sub>3</sub>) δ ppm 162.1, 148.7, 134.7, 129.3, 122.2, 34.7, 29.7, 29.7, 24.3, 21.2, 27.4, 25.3. **Optical Rotation** [ $\alpha$ ]<sub>D</sub><sup>25</sup>: +3.2 (*c* = 0.027) CHCl<sub>3</sub>.

**HPLC** separation conditions: Chiralpak OD-H Column 2% isopropyl alcohol in hexane, flow rate: 1 mL/min, 25 °C;  $t_R$  34.6 min for (*S*)-enantiomer (major) and 39.3 min for (*R*)-enantiomer (minor). (e.r. = 56:44)



Peak #	RetTime [min]	Type	Width [min]	Area [mAU*s]	Height [mAU]	Area %
1	34.632	MM	1.5549	4119.76367	44.15929	55.9528
2	39.278	MM	1.9803	3243.16284	27.29562	44.0472

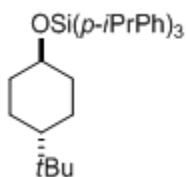


**Scheme 2.5, R = CH<sub>3</sub>:** GP3. Recovered product: 97 mg, 49%, white solid. **mp range** = 120-125 °C. **<sup>1</sup>H NMR** (400 MHz, CDCl<sub>3</sub>): δ ppm 7.57 (d, *J* = 8.0 Hz, 6H), 7.21 (d, *J* = 7.9 Hz, 6H), 3.92 (dt, *J* = 5.2, 2.6 Hz, 1H), 2.96 – 2.85 (m, 3H), 1.81 – 1.30 (m, 9H), 1.25 (d, *J* = 6.9 Hz, 18H), 0.85 (d, *J* = 6.6 Hz, 3H). **<sup>13</sup>C NMR** (101 MHz, CDCl<sub>3</sub>) δ ppm 150.2, 135.7, 131.7, 125.8, 72.9, 36.7, 34.1, 32.6, 29.4, 24.4, 23.9, 21.3, 17.3 **IR** (neat, cm<sup>-1</sup>) 3012, 2960, 2930, 1667, 1600, 1553, 1460, 1394, 1363, 1298, 1263, 1119, 1091, 1050, 1018, 961, 878, 822, 770, 746, 733. **HRMS (ESI)** Calculated for (C<sub>38</sub>H<sub>46</sub>OSi +) (M<sup>+</sup>): 498.3318 Observed: 546.3320. **Optical Rotation** [ $\alpha$ ]<sub>D</sub><sup>25</sup>: -2.3 (c = 0.018) CHCl<sub>3</sub>

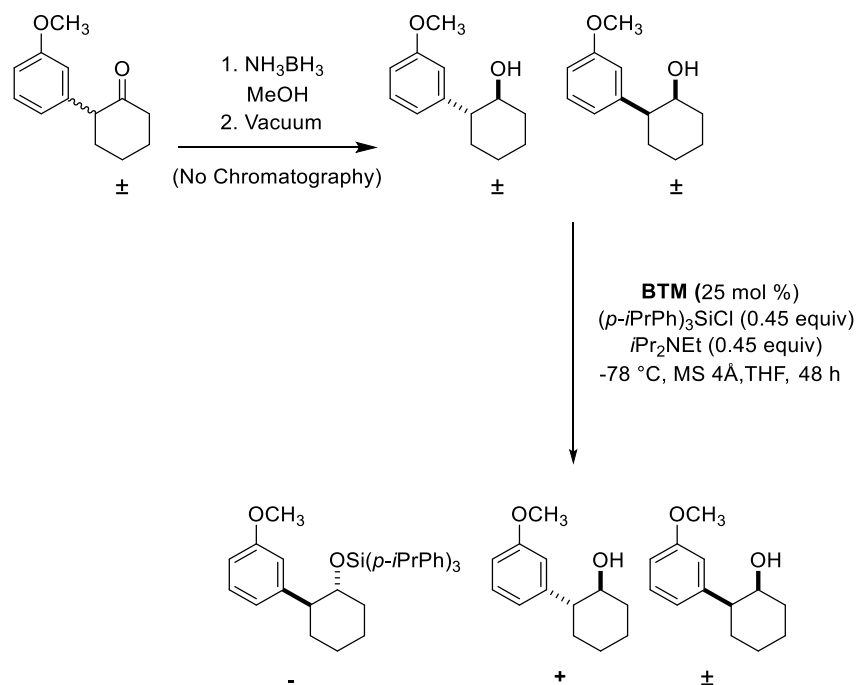
Due to the volatility of the desilylated product, only trace amounts of the desilylated product were collected after removal of the solvent under vacuum. Thus, NMR conversion was used for the calculation of the selectivity factor.

**Kinetic Resolution Data for Scheme 2, R = CH<sub>3</sub>**

	er <sup>SM</sup>	% conv	s	S AVERAGE
1	51:49	54.0	1.4	1.4
2	51:49	54.0	1.4	



**Scheme 2.5, *trans* substituted:** GP1. Recovered product: 104 mg, 48%, white solid. **mp range** = 140-143 °C. **<sup>1</sup>H NMR** (400 MHz, CDCl<sub>3</sub>): δ ppm 7.55 (d, *J* = 8.0 Hz, 6H), 7.22 (d, *J* = 7.9 Hz, 6H), 3.73 – 3.64 (m, 1H), 2.90 (hept, *J* = 6.9 Hz, 3H), 1.96 – 1.85 (m, 2H), 1.70 – 1.61 (m, 2H), 1.45 – 1.31 (m, 2H), 1.25 (d, *J* = 6.9 Hz, 18H), 0.99 – 0.82 (m, 3H), 0.78 (s, 9H). **<sup>13</sup>C NMR** (101 MHz, CDCl<sub>3</sub>) δ ppm 150.3, 135.6, 132.5, 125.9, 72.7, 47.2, 36.3, 34.2, 32.3, 27.7, 25.7, 23.9. **IR** (neat, cm<sup>-1</sup>) 3012, 1600, 1496, 1460, 1364, 1298, 1117, 1050, 999, 843, 769 **HRMS (ESI)** Calculated for (C<sub>37</sub>H<sub>52</sub>OSi +) (M +): 540.3787 Observed: 540.3790.

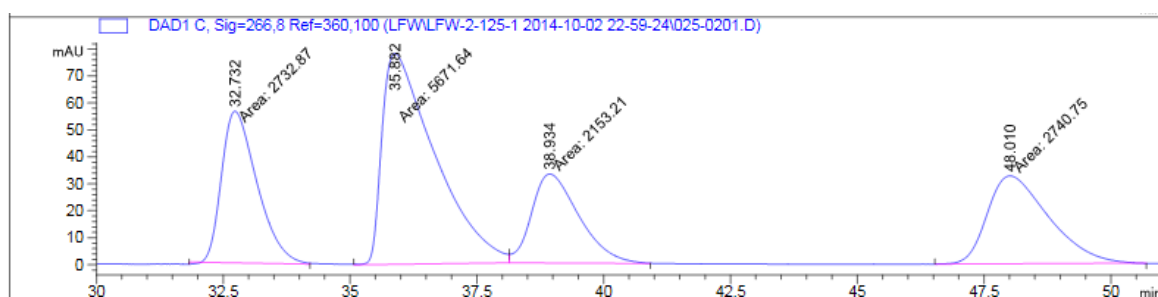


**Scheme 2.9: One-pot Reduction/Kinetic Resolution to Isolate (1R,2S)-2-(3-methoxyphenyl)cyclohexan-1-ol Enantiomerically Enriched,**

Procedure: See GP1.

**HPLC** of recovered starting materials:

Separation conditions: Chiralpak OD-H Column 2% isopropyl alcohol in hexane, flow rate: 1 mL/min, 25 °C;  $t_R$  32.7 min and 48.0 min for two enantiomers of *cis*-2-(3-methoxyphenyl)cyclohexan-1-ol.  $t_R$  35.9 min for (1*S*,2*R*)-2-(3-methoxyphenyl)cyclohexan-1-ol (major) and 38.9 min for (1*R*,2*S*)-2-(3-methoxyphenyl)cyclohexan-1-ol.



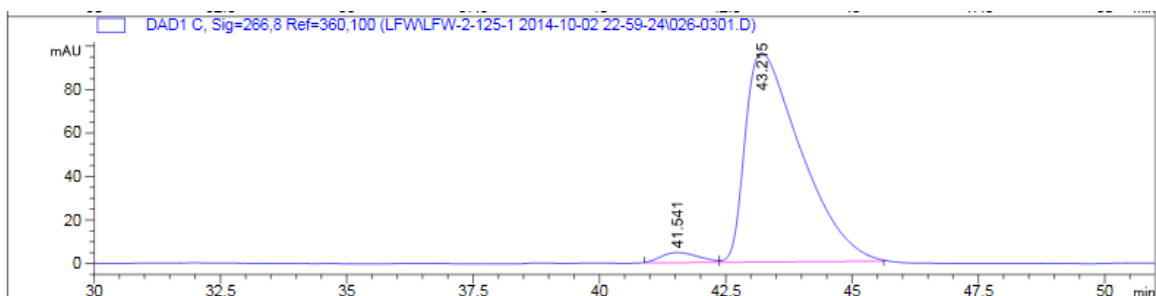


Peak #	RetTime [min]	Type	Width [min]	Area [mAU*s]	Height [mAU]	Area %
1	32.732	MM	0.8103	2732.86597	56.21363	49.9280
2	48.010	MM	1.4018	2740.74951	32.58558	50.0720

Peak #	RetTime [min]	Type	Width [min]	Area [mAU*s]	Height [mAU]	Area %
1	35.882	MM	1.2089	5671.64160	78.19499	72.4824
2	38.934	MM	1.0863	2153.20874	33.03622	27.5176

**HPLC** of recovered product:

Separation conditions: Data is of the desilylated product formed by following GP4. The same HPLC separation conditions as the recovered starting materials were utilized.



Peak #	RetTime [min]	Type	Width [min]	Area [mAU*s]	Height [mAU]	Area %
1	41.541	BV	0.6017	235.11639	4.60508	3.0838
2	43.215	VB	1.0782	7389.15771	96.08588	96.9162

### Kinetic Resolution Data for Scheme 2.9

	er <sup>SM</sup>	er <sup>PR</sup>	% conv	s	S AVERAGE
1	78:22	96:4	37.3	49	50
2	72:28	97:3	32.7	50	

## 2.7 References

1. Sheppard, C. I.; Taylor, J. L.; Wiskur, S. L., Silylation-Based Kinetic Resolution of Monofunctional Secondary Alcohols. *Org. Lett.* **2011**, *13* (15), 3794-3797.
2. Clark, R. W.; Deaton, T. M.; Zhang, Y.; Moore, M. I.; Wiskur, S. L., Silylation-Based Kinetic Resolution of alpha-Hydroxy Lactones and Lactams. *Org. Lett.* **2013**, *15* (24), 6132-6135.
3. Brown, H. C.; Cho, B. T.; Park, W. S., Chiral Synthesis Via Organoboranes .15. Selective Reductions .42. Asymmetric Reduction of Representative Prochiral Ketones with Potassium 9-O-(1,2-5,6-Di-O-Isopropylidene-Alpha-D-Glucofuranosyl)-9-Boratabicyclo[3.3.1]-Nonane. *J. Org. Chem.* **1988**, *53* (6), 1231-1238.
4. Whitesell, J. K., Cyclohexyl-Based Chiral Auxiliaries. *Chem. Rev.* **1992**, *92* (5), 953-964.
5. Brown, H. C.; Prasad, J. V. N. V.; Gupta, A. K.; Bakshi, R. K., Hydroboration .80. Preparation of (Trans-2-Phenylcyclopentyl)Boronates and (Trans-2-Phenylcyclohexyl)Boronates of Very High Enantiomeric Purities. *J. Org. Chem.* **1987**, *52* (2), 310-311.
6. Ling, A.; Plewe, M.; Gonzalez, J.; Madsen, P.; Sams, C. K.; Lau, J.; Gregor, V.; Murphy, D.; Teston, K.; Kuki, A.; Shi, S.; Truesdale, L.; Kiel, D.; May, J.; Lakis, J.; Anderes, K.; Iatsimirskaia, E.; Sidelmann, U. G.; Knudsen, L. B.; Brand, C. L.; Polinsky, A., Human glucagon receptor antagonists based on alkylidene hydrazides. *Bioorg. Med. Chem. Lett.* **2002**, *12* (4), 663-666.
7. Alexakis, A.; Tomassini, A.; Leconte, S., Synthesis and applications of chiral bis-THF in asymmetric synthesis. *Tetrahedron.* **2004**, *60* (42), 9479-9484.

8. Vrancken, E.; Alexakis, A.; Mangeney, P., Organolithium/chiral Lewis base/BF<sub>3</sub>: a versatile combination for the enantioselective desymmetrization of meso-epoxides. *Eur. J. Org. Chem.* **2005**, (7), 1354-1366.
9. Cho, B. T.; Shin, S. H., Enantioselective ring opening of meso- and racemic epoxides with phenyl lithium catalyzed by chiral gamma-amino alcohols derived from alpha-D-xylose. *B. Kor. Chem. Soc.* **2006**, 27 (9), 1283-1284.
10. Whitesell, J. K.; Chen, H. H.; Lawrence, R. M., Trans-2-Phenylcyclohexanol - a Powerful and Readily Available Chiral Auxiliary. *J. Org. Chem.* **1985**, 50 (23), 4663-4664.
11. Schwartz, A.; Belica, P.; Coffen, D.; Madan, P.; Manchand, P., An Enantioselective Synthesis of Calcium-Antagonists of the Diltiazem Class. *Abstr. Pap. Am. Chem. S.* **1990**, 200, 192-Orgn.
12. Laumen, K.; Seemayer, R.; Schneider, M. P., Enzymic Preparation of Enantiomerically Pure Cyclohexanols - Ester Synthesis by Irreversible Acyl Transfer. *J. Chem. Soc. Chem. Comm.* **1990**, (1), 49-51.
13. Basavaiah, D.; Rao, P. D., Enzymatic Resolution of Trans-2-Arylcyclohexan-1-Ols Using Crude Chicken Liver Esterase (Ccle) as Biocatalyst. *Tetrahedron-Asymmetry.* **1994**, 5 (2), 223-234.
14. Oriyama, T.; Hori, Y.; Imai, K.; Sasaki, R., Nonenzymatic enantioselective acylation of racemic secondary alcohols catalyzed by a SnX(2)-chiral diamine complex. *Tetrahedron. Lett.* **1996**, 37 (47), 8543-8546.
15. Sano, T.; Imai, K.; Ohashi, K.; Oriyama, T., Catalytic asymmetric acylation of racemic secondary alcohols with benzoyl chloride in the presence of a chiral diamine. *Chem. Lett.* **1999**, (3), 265-266.

16. Miyake, Y.; Iwata, T.; Chung, K. G.; Nishibayashi, Y.; Uemura, S., Kinetic resolution of secondary alcohols via chiral Pd(II)-complex-catalysed enantioselective benzoylation using CO and organobismuth(v) compound. *Chem. Commun.* **2001**, (24), 2584-2585.
17. Copeland, G. T.; Miller, S. J., Selection of enantioselective acyl transfer catalysts from a pooled peptide library through a fluorescence-based activity assay: An approach to kinetic resolution of secondary alcohols of broad structural scope. *J. Am. Chem. Soc.* **2001**, *123* (27), 6496-6502.
18. Sekar, G.; Nishiyama, H., Nonenzymatic kinetic resolution of secondary alcohols: Enantioselective S(N)2 displacement of hydroxy groups by halogens in the presence of chiral BINAP. *J. Am. Chem. Soc.* **2001**, *123* (15), 3603-3604.
19. Spivey, A. C.; Zhu, F. J.; Mitchell, M. B.; Davey, S. G.; Jarvest, R. L., Concise synthesis, preparative resolution, absolute configuration determination, and applications of an atropisomeric biaryl catalyst for asymmetric acylation. *J. Org. Chem.* **2003**, *68* (19), 7379-7385.
20. Matsugi, M.; Hagimoto, Y.; Nojima, M.; Kita, Y., Effective nonenzymatic kinetic resolution of (+/-)-trans-2-arylcyclohexanols using 3 beta-acetoxyetienic acid, DCC, and DMAP. *Org. Process. Res. Dev.* **2003**, *7* (4), 583-584.
21. Dalaigh, C. O.; Hynes, S. J.; O'Brien, J. E.; McCabe, T.; Maher, D. J.; Watson, G. W.; Connon, S. J., Asymmetric acyl-transfer promoted by readily assembled chiral 4-N,N-dialkylaminopyridine derivatives. *Org. Biomol. Chem.* **2006**, *4* (14), 2785-2793.

22. Ebner, D. C.; Trend, R. M.; Genet, C.; McGrath, M. J.; O'Brien, P.; Stoltz, B. M., Palladium-catalyzed enantioselective oxidation of chiral secondary alcohols: Access to both enantiomeric series. *Angew. Chem. Int. Ed.* **2008**, *47* (34), 6367-6370.
23. Birman, V. B.; Li, X. M., Homobenzotetramisole: An effective catalyst for kinetic resolution of aryl-cycloalkanols. *Org. Lett.* **2008**, *10* (6), 1115-1118.
24. Tomizawa, M.; Shibuya, M.; Iwabuchi, Y., Highly Enantioselective Organocatalytic Oxidative Kinetic Resolution of Secondary Alcohols Using Chirally Modified AZADOs. *Org. Lett.* **2009**, *11* (8), 1829-1831.
25. Harada, S.; Kuwano, S.; Yamaoka, Y.; Yamada, K.; Takasu, K., Kinetic Resolution of Secondary Alcohols Catalyzed by Chiral Phosphoric Acids. *Angew. Chem. Int. Ed.* **2013**, *52* (39), 10227-10230.
26. Wang, L.; Akhani, R. K.; Wiskur, S. L., Diastereoselective and Enantioselective Silylation of 2-Arylcyclohexanols. *Org. Lett.* **2015**, *17* (10), 2408-2411.
27. Huynh, C.; Derguiniboumechal, F.; Linstrumelle, G., Copper-Catalysed Reactions of Grignard-Reagents with Epoxides and Oxetane. *Tetrahedron. Lett.* **1979**, (17), 1503-1506.
28. Cho, B. T.; Kang, S. K.; Kim, M. S.; Ryu, S. R.; An, D. K., Solvent-free reduction of aldehydes and ketones using solid acid-activated sodium borohydride. *Tetrahedron.* **2006**, *62* (34), 8164-8168.
29. Akhani, R. K.; Moore, M. I.; Pribyl, J. G.; Wiskur, S. L., Linear Free-Energy Relationship and Rate Study on a Silylation-Based Kinetic Resolution: Mechanistic Insights. *J. Org. Chem.* **2014**, *79* (6), 2384-2396.

30. a) Conversions and selectivity factors are based on the ee of the recovered starting materials and products. % Conversion =  $\frac{ees}{ees + eep} \times 100\%$  and  $s = \frac{\ln[(1 - C)(1 - ees)]}{\ln[(1 - C)(1 + ees)]}$ , where ees = ee of recovered starting material and eep = ee of product. b) Selectivity factors are an average of two runs. Conversions are from a single run.
31. Eliel, E. L.; Wilen, S. H.; Mander, L. N., *Stereochemistry of organic compounds*. Wiley: New York, 1994.
32. Carey, F. A. S., Richard J., *Advanced Organic Chemistry Part A Structure and Mechanisms*. Plenum Press: New York N.Y, 1984.
33. Yang, X. H.; Fox, T.; Berke, H., Ammonia borane as a metal free reductant for ketones and aldehydes: a mechanistic study. *Tetrahedron*. **2011**, 67 (37), 7121-7127.
34. Erturk, E.; Tezeren, M. A.; Atalar, T.; Tilki, T., Regioselective ring-opening of epoxides with ortho-lithioanisoles catalyzed by BF<sub>3</sub> center dot OEt<sub>2</sub>. *Tetrahedron*. **2012**, 68 (32), 6463-6471.
35. Bruni, R.; Fantin, G.; Maietti, S.; Medici, A.; Pedrini, P.; Sacchetti, G., Plants-mediated reduction in the synthesis of homochiral secondary alcohols. *Tetrahedron-Asymmetry*. **2006**, 17 (15), 2287-2291.

## CHAPTER 3

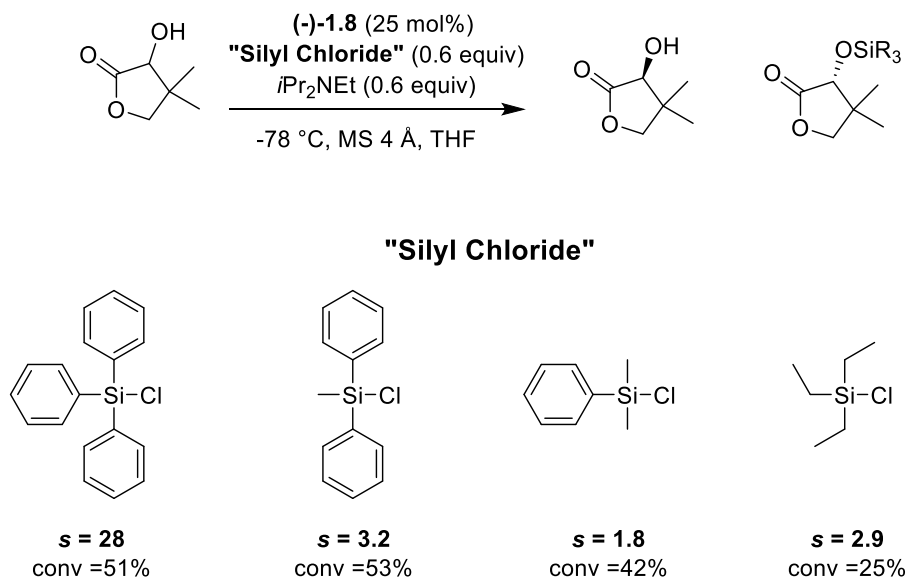
# UNDERSTANDING INTERNAL CHIRALITY INDUCTION OF TRIARYLSILYL ETHERS FORMED FROM ENANTIOPURE ALCOHOLS

### 3.1 Introduction

This chapter will focus on our interest of chirality transmission from point chirality to helical chirality in our silylation-based kinetic resolution system. The transmission of chirality, either intra- or intermolecularly, is important in areas ranging from asymmetric catalysis<sup>1-3</sup> to sensing<sup>4-5</sup>. And this is also one of the many approaches being taken towards understanding the mechanism of silylation-based kinetic resolution conducted in the Wiskur group.

As discussed earlier in Chapter 2, the phenyl groups on the silyl chloride have shown to be very important for selectivity. Replacing even one of the phenyl groups with an alkyl group will decrease the selectivity dramatically (Scheme 3.1). It is hypothesized that the phenyl groups form a propeller or helical twist in the intermediate that aids in chirality transmission. Thus, this brings us to a discussion on molecular propellers which are an interesting class of molecules that have been studied over the years, where a particular gearing in the propeller can be induced by transmission or communication of chiral information from a source of point chirality.<sup>6-12</sup> We are interested in propellers or

helical twists that are formed from the three phenyl groups around a central atom and ways to induce one propeller/helical twist over another.



### Scheme 3.1 Investigation of Silyl Chlorides in Silylation-Based Kinetic Resolution<sup>13</sup>

The study of stereochemistry of molecular propeller/helical twist was initiated by Mislow and coworkers almost 40 years ago and a lot of research has been done in this field since then.<sup>6, 8, 14-19</sup> It is generally agreed that in the triaryl methyl system, the aryl groups have restricted rotation and exist as a pair of enantiomeric propeller conformations. All three aryl rings have the same sense of twist if the molecule has true  $C_3$  symmetry ( $X = Cl, H, \text{etc.}$ ), resulting in a helical chirality, either P or M (Figure 3.1 A).

More recently, Gawroński and co-workers synthesized trityl ethers of chiral secondary alcohols, which act as molecular bevel gears to transmit chirality from the point chirality of the alcohol to the trityl group.<sup>6</sup> The addition of enantiopure point chirality results in the gearing of the trityl phenyl groups into predominately one conformational isomer. With the lack of true  $C_3$  symmetry ( $X = OR$ ), they discovered one of the aryl groups



has a different twist than the other two, but the trityl group still had stereoisomerism (either in a *PMP* or *MPM* helicity). This could be detected via circular dichroism (CD) spectroscopy showing a strong Cotton effect<sup>20</sup> patterns from the helicity of the trityl group.

The success of helicity formation in the trityl group<sup>6, 8, 21</sup> encourages us to explore the potential propeller/helical twist in our triarylsilyl system, and more specifically, we wanted to know if a molecule with point chirality could induce helical chirality in a triphenylsilyl group if the two components were covalently bonded (Figure 3.1 B). While the triphenylsilyl group is widely reported throughout the literature due to its use as a protecting group,<sup>22</sup> to our knowledge induction of point chirality to helical chirality of a triarylsilane has not been studied. Because of the longer bonds silicon has compared to carbon (C-Si bond  $\sim 1.9 \text{ \AA}$  versus C-C bond  $\sim 1.5 \text{ \AA}$ ) and silicon has a larger van der Waals radius than carbon, there was a question of whether the components of a triarylsilyl group were too far apart to induce one helical conformation over another via point chirality.

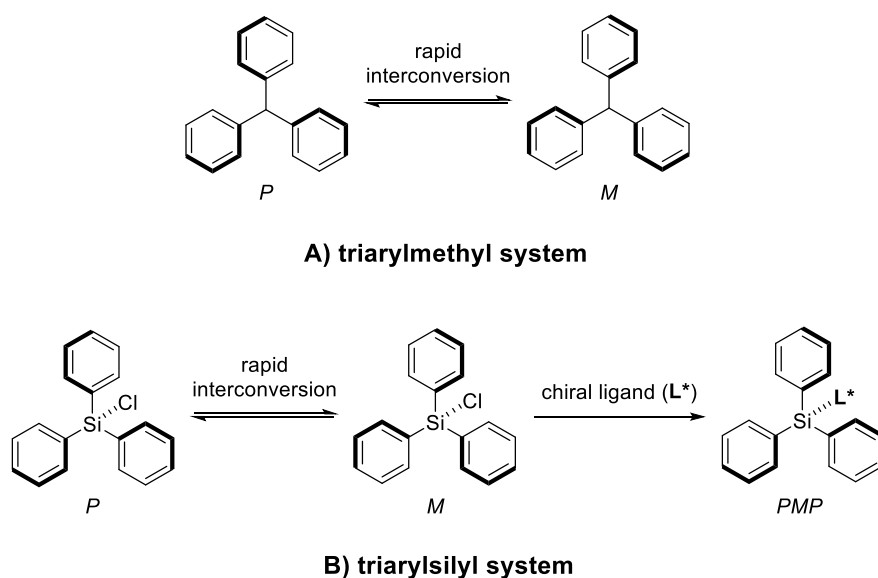
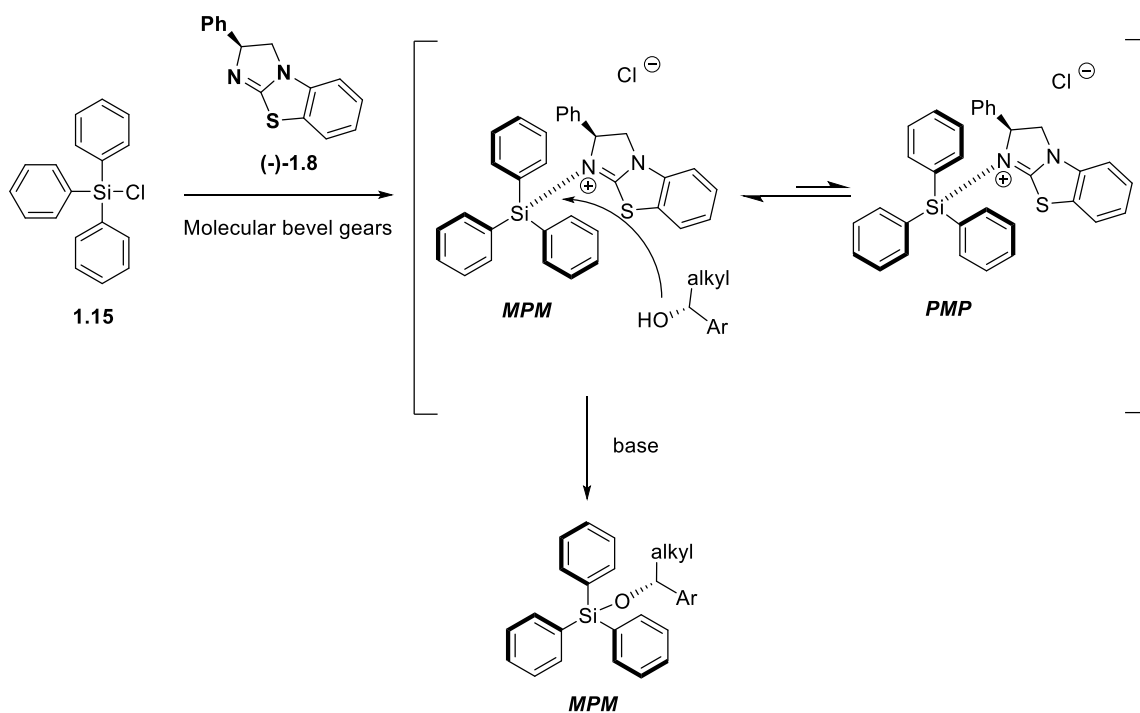


**Figure 3.1 Helical Formation of Triarylmethyl and Triarylsilyl System**

In our hypothesized mechanism, the nucleophilic catalyst (-)-**1.8** reacts with the silyl chloride **1.15** to form a reactive intermediate, and a specific helical twist of the triphenylsilyl group is induced by the chiral catalyst attached to the silicon (Scheme 3.2). Since the alcohol breaks the true  $C_3$  symmetry, it will be either *MPM* or *PMP* helical twist formation of the reactive intermediate. This helical twist formation will enhance the chiral space since the alcohol will have to pass through the chiral arrangement of the aryl groups. Our original idea was to investigate this helical formation in the silyl chloride catalyst intermediate through chirality transmission of the point chirality of the catalyst to the triarylsilyl group. However, since the catalyst complex is highly reactive and thus far undetectable, we moved to investigate enantiopure silyl ethers (Si-O bond), an analogue that can be easily handled and characterized to see if attaching a compound with point chirality would induce helical chirality in the triphenylsilyl group.

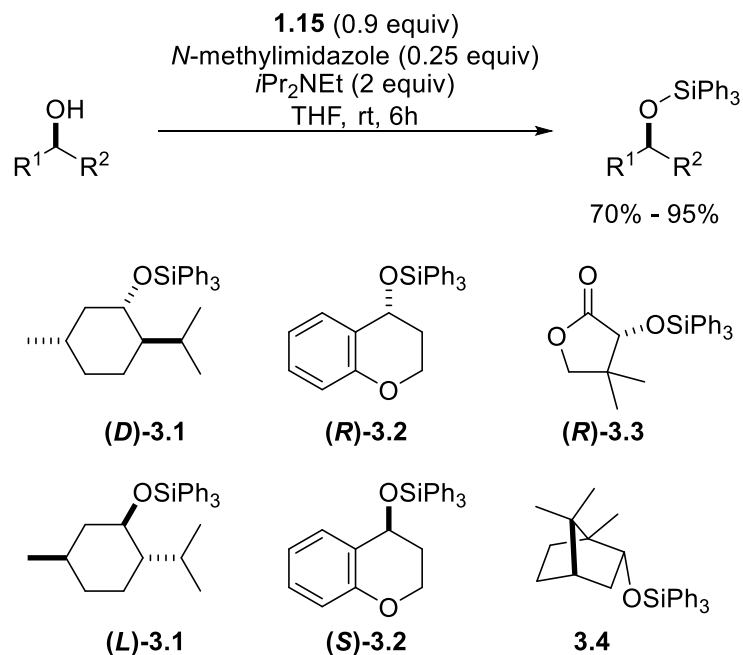


**Scheme 3.2 Proposed Mechanism of Silylation-Based Kinetic Resolution**

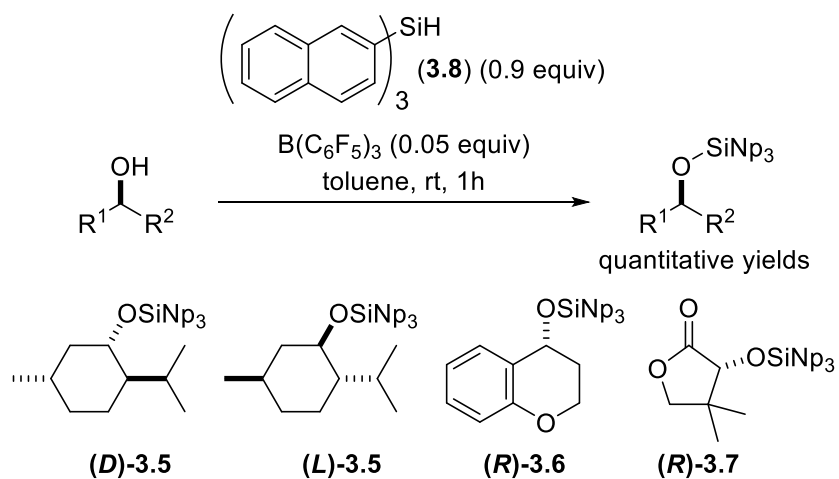
Therefore, the following chapter will discuss our detailed studies of helical twist formation of triarylsilyl ethers formed from enantiopure alcohols. Circular dichroism (CD) spectroscopy will be used as the indicator of propeller/helical twist formation through a characteristic Cotton effect. The helicity of the propeller is also explored through crystal structures and molecular modeling.

### 3.2 Synthesis of Enantiopure Triarylsilyl Ethers

A series of enantiopure secondary alcohols (*D/L*-menthol, (*R/S*) chromanol, (*R*)-pantolactone, and (-)-borneol) were silylated with triphenyl- and trinaphthylsilyl groups to be tested. The triphenylsilyl ether compound (**3.1-3.4**) were synthesized by protecting the alcohols with **1.15**, catalyzed by *N*-methylimidazole (Scheme 3.3). However, the initial attempts to synthesize the 2-substituted trinaphthylsilyl ethers (**3.5-3.7**) using the similar method in Scheme 3.3 was unsuccessful. Therefore, a tris(pentafluorophenyl)borane catalyzed<sup>23</sup> dehydrogenative silylation employing trinaphthylsilane **3.8** was used to obtain those trinaphthylsilyl ethers (Scheme 3.4).



**Scheme 3.3 Synthesis of Enantiopure Triphenylsilyl Ethers**



**Scheme 3.4 Synthesis the Enantiopure Trinaphthylsilyl Ethers**

### 3.3 Circular Dichroism Analysis

Circular dichroism (CD) spectroscopy is a powerful tool for investigating the three-dimensional space of compounds.<sup>20, 24-25</sup> It has a wide range of applications in many different fields, including the investigation of protein structures<sup>26-28</sup> as well as the study of small organic molecule configurations.<sup>29-30</sup> CD spectroscopy relies on the principle that nonracemic chiral molecules absorb left and right circularly polarized light differently. In particular, if the chiral compound is arranged in a propeller/helical twist conformation, a characteristic Cotton effect<sup>24</sup> will be observed (the absolute magnitude of the optical rotation crosses zero near the compound's  $\lambda_{\text{max}}$  and goes to the opposite direction), which allows for easy confirmation of helical chirality.

Thus, we wanted to explore the conformational properties of a triarylsilyl group covalently bonded to enantiopure alcohols by this method. If the alcohol transmits chirality to the aryl groups, a characteristic Cotton effect should be present in the 180-210 nm range of the spectrum, indicating the three aryl groups formed a higher percentage of one helical twist conformation.<sup>6</sup> If there is no Cotton effect signal in that region, this is an indication that there is no preference for one helical twist over the other. This is because equal ratio of two opposite helical twists would not be CD active.

The silyl ethers **3.1-3.7** synthesized in Section 3.2 were investigated by CD spectroscopy, and a Cotton effect, characteristic for the helical twist of triaryl groups, was observed for all the compounds. The compounds were dissolved in solutions of pentane in cyclohexane (1-10% v/v) or 2-propanol in cyclohexane (3.5% v/v). These specific solvents were chosen to avoid a background absorbance of the solvent in the same region of the spectrum where the phenyl groups on the silicon absorb. The concentration was set to

approximately 80  $\mu\text{M}$  to give the maximum absorbance without reaching a high tension (HT) voltage  $> 600$  V. Once the high-tension voltage reaches  $> 600$  V, the detector becomes saturated and false signals can occur.<sup>31</sup> The samples were analyzed in a 1 mm path length, strain free, quartz cell, and the reported spectra were processed by using 15-point Savitzky-Golay smoothing.<sup>32</sup>

Triphenylsilyl ether (**L**)-**3.1** was employed to provide a direct comparison to the CD spectra of the trityl ether version of this compound from the literature.<sup>6</sup> The CD spectrum of (**L**)-**3.1** gave a positive Cotton effect curve<sup>33</sup> (recognizable by a positive peak at the longer wavelengths which then crosses the zero-rotation axis at around the  $\lambda_{\text{max}}$ , and gives a negative peak at a shorter wavelength) (Figure 3.2). This pattern is similar to the trityl version of this compound, which the Cotton effect appears at around 193 nm with a same positive Cotton effect curve.<sup>6</sup> This indicates an induction of chirality is indeed taking place from the enantiopure alcohols to the triphenylsilyl groups despite the longer C-Si/O-Si bonds, resulting in a higher population of one helical twist conformation. Its enantiomer (**D**)-**3.1** shows a symmetrically opposite pattern as the negative Cotton effect curve, where the negative peak appears at the higher wavelength and crosses zero to reach the positive peak at a shorter wavelength (Figure 3.3).

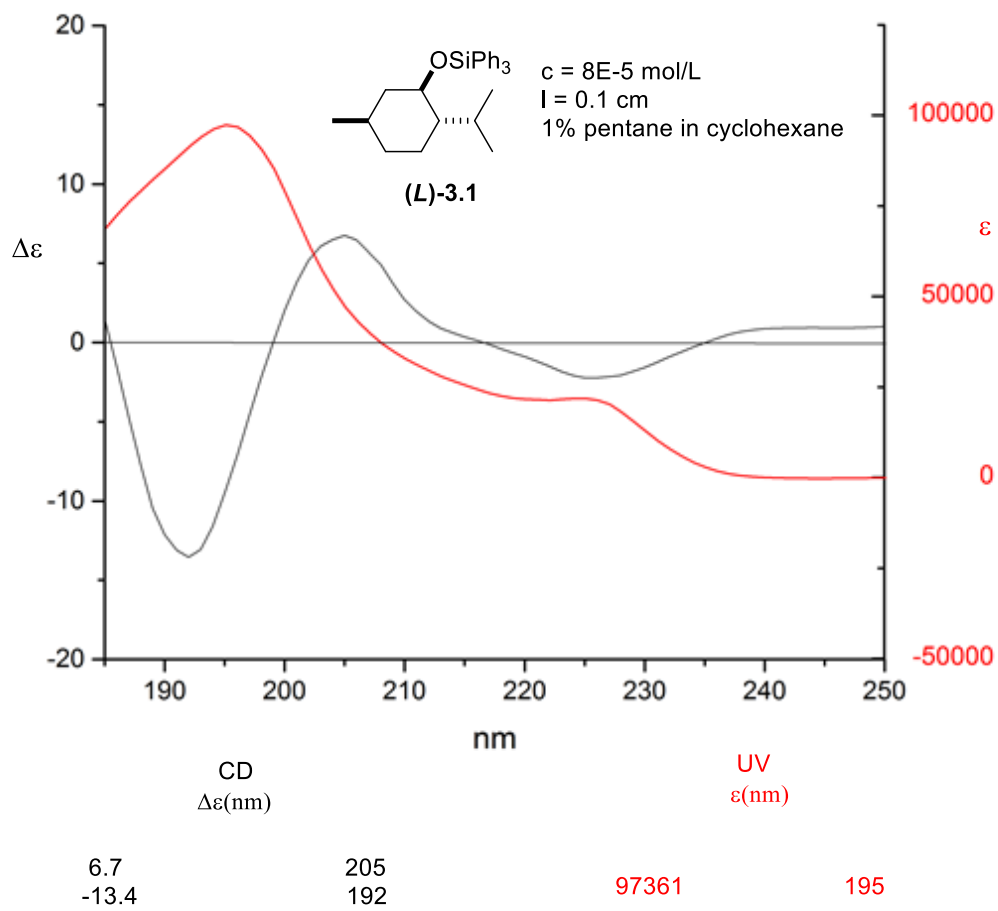
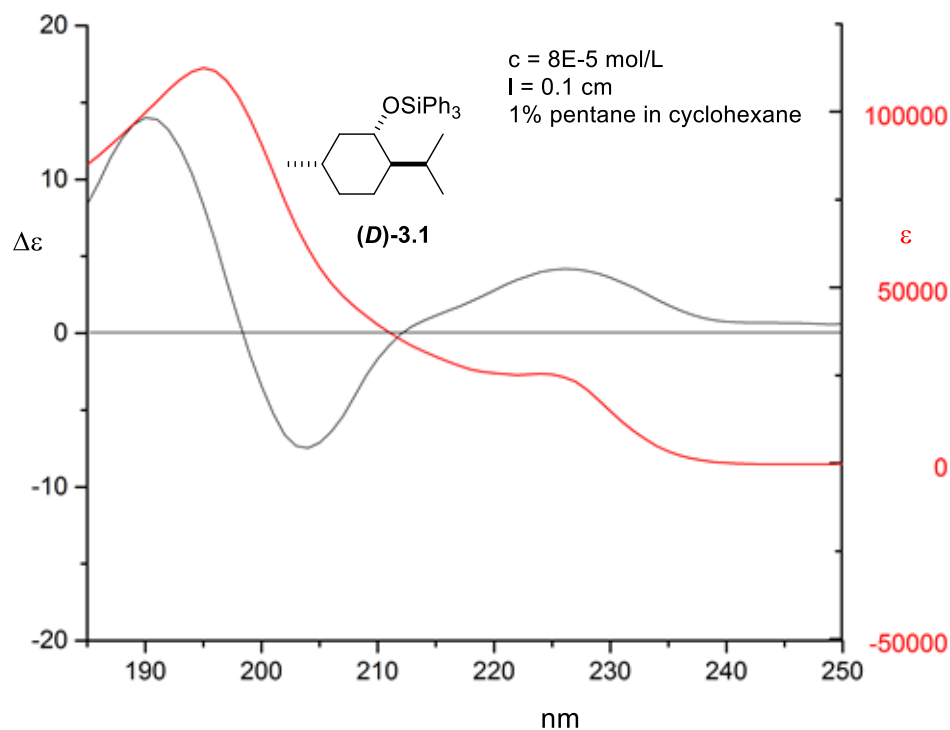


Figure 3.2 CD Spectrum and UV/VIS Spectrum (Absorbance) of (L)-3.1



CD $\Delta\epsilon(\text{nm})$		UV $\epsilon(\text{nm})$	
-7.5	204	112490	195
14	190		

**Figure 3.3 CD Spectrum and UV/VIS Spectrum (Absorbance) of (D)-3.1**

The helicity resulting from a positive Cotton effect curve of (*L*)-3.1 (Table 3.1, entry 1) could be tentatively assigned as *PMP*, and the opposite CD spectra pattern of (*D*)-3.1 (Table 3.1, entry 2) could be assigned as *MPM*, based on the model developed by Gawroński (Figure 3.4).<sup>6</sup> The model depends on the size of the substituents as well as  $\pi$  system around the stereocenter, not the absolute configuration of the chiral center of the alcohol. This model builds up the connection between the point chirality of the alcohol, the



Cotton effect pattern from the CD spectra, to understand the helical twist formation of the triaryl groups.

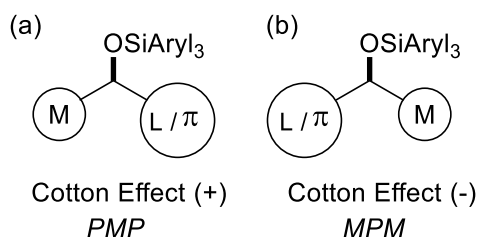


**Figure 3.4 Model of The Correlation Between the Position of The Large Substituent (L) or  $\pi$  System to The Resultant Cotton Effect and Helical Twist**

Silyl ether **3.4** displayed a negative Cotton effect curve, which is also similar to the trityl ether version of the corresponding alcohol,<sup>6</sup> predicting as a *MPM* helical twist (Table 3.1, entry 3). Silyl ethers **3.2** (*R* and *S*) and **3.3** were a little more complicated. The alcohols used to synthesize **3.2** and **3.3** are also CD active at low wavelength, causing an overlap of signals.<sup>33</sup> In order to clearly demonstrate the Cotton effect directly resulting from the helical twist of the triphenyl group, the CD spectra of the free alcohols were subtracted from the CD spectra of the silyl ethers. These results are given in Table 1, entry 4-6. A positive Cotton effect curve is obtained for compound (*R*)-**3.2** and (*R*)-**3.3**, indicating a *PMP* helicity (Table 1, entry 4 and 6). This is also consistent with the model that the  $\pi$  system adjacent to the stereocenter now plays a more dominate role in directing the helical twist of the triphenylsilyl group (Figure 3.4). The *S* enantiomer of **3.2** again generates the opposite result, with a predicted *MPM* helicity for the negative Cotton effect (Table 3.1, entry 5). These results again show that even with the longer silicon bond lengths, one

helical twist is predominately formed over another due to the point chirality of the alcohols but now the pi system has an effect on the preferred helical conformation.

**Table 3.1 Selected CD Data ( $\Delta\epsilon$  (nm)) for Chiral Triphenylsilyl Ethers**

Entry <sup>a</sup>	triphenyl silyl ether	CD $\Delta\epsilon$ (nm)	CD $\Delta\epsilon$ (nm)	predicted helicity
1	<b>(L)-3.1</b>	6.7 (205)	-13.4 (192)	<i>PMP</i>
2	<b>(D)-3.1</b>	-7.5 (204)	14 (190)	<i>MPM</i>
3	<b>3.4</b>	-17 (196)	29 (186)	<i>MPM</i>
4 <sup>b</sup>	<b>(R)-3.2</b>	23 (202)	-10 (190)	<i>PMP</i>
5 <sup>b</sup>	<b>(S)-3.2</b>	-23 (202)	15 (191)	<i>MPM</i>
6 <sup>c</sup>	<b>(R)-3.3</b>	1.9 (210)	-7.2 (199)	<i>PMP</i>

<sup>a</sup>Data was collected at 80  $\mu\text{M}$  (1% pentane in cyclohexane (v/v)) with a 0.1 cm path length quartz cell. <sup>b</sup>The solvent condition was 10% pentane in cyclohexane (v/v) due to solubility issues. <sup>c</sup>The solvent condition was 3.5% isopropanol in cyclohexane (v/v) due to solubility issues.

One of the factors that could affect the accuracy of CD spectra is the solvent interference at low wavelengths. One approach to eliminate this impact is to extend the conjugation of the aromatic rings on silicon by changing the phenyls to naphthyls. The CD spectra associated with the helical twist is shifted to longer wavelengths, therefore moving away from potential solvent interference. Synthesized trinaphthylsilyl ethers **3.5-3.7** were employed as direct comparisons to the triphenylsilyl ethers **3.1-3.3**. The trinaphthylsilyl ethers all exhibited red shifts in the CD spectra of 20-30 nm (Table 3.2 verses Table 3.1) as would be expected with a change from phenyl to naphthyl groups.<sup>34</sup> All the compounds exhibited the same Cotton effects as their phenyl counterparts. Trinaphthylsilyl ether (*L*)-**3.5** (Table 3.2, entry 1) has the same positive Cotton effect curve as (*L*)-**3.1** (Table 3.1, entry 1), predicting a *PMP* helical twist on the triaryl group. Their enantiomers (*D*)-**3.5**

(Table 3.2, entry 2) and **(D)-3.1** (Table 3.1, entry 2), also displayed opposite Cotton effects indicating a *MPM* helical twist on the triaryl group. Again, the CD spectra for silyl ethers **3.6** and **3.7** overlapped with the spectra of the basic core structure of the alcohol. Thus, the CD spectra of the free alcohols were subtracted from the CD spectra of the trinaphthylsilyl ether compounds to get the data in entries 3 and 4, Table 3.2. All of these results show that point chirality can still induce a helical twist in the trinaphthylsilyl group, and the orientation of these aryl groups matches the results from the phenylsilyl ether equivalents.

**Table 3.2 Selected CD Data ( $\Delta\epsilon$  (nm)) for Chiral Trinaphthylsilyl Ethers**

Entry <sup>a</sup>	trinaphthyl silyl ether	CD $\Delta\epsilon$ (nm)	CD $\Delta\epsilon$ (nm)	predicted helicity
1	<b>(L)-3.5</b>	4.9 (236)	-5.3 (220)	PMP
2	<b>(D)-3.5</b>	-4.6 (236)	4.8 (220)	MPM
3 <sup>b</sup>	<b>(R)-3.6</b>	27 (229)	-23 (213)	PMP
4 <sup>c</sup>	<b>3.7</b>	5.3 (232)	-4.1 (214)	PMP

<sup>a</sup>Data was collected at 80  $\mu$ M (1% pentane in cyclohexane (v/v)) with a 0.1 cm path length quartz cell. <sup>b</sup>The solvent condition was 10% pentane in cyclohexane (v/v) due to solubility issues. <sup>c</sup>The solvent condition was 3.5% isopropanol in cyclohexane (v/v) due to solubility issues.

### 3.4 Crystal Structure Analysis of Helical Twist Formation

To gain further evidence of helical twist formation in the triarylsilyl group, crystal structures of the triphenylsilyl ethers **(R)-3.2**, **(S)-3.2**, and **3.4** were prepared and analyzed by single crystal x-ray analysis. Both enantiomers of **3.2** were crystallized independently, and the resulting structures showed the phenyl groups on the silicon are in the same but opposite pattern for the two enantiomers (Figure 3.5). To quantitatively assign each phenyl group as *M* or *P*, a dihedral angle ( $\omega$ ) was measured between the O-Si bond and the closest

$C_{\text{ipso}}-C_{\text{ortho}}$  bond for each phenyl group. Then looking down the  $C_{\text{ipso}}-\text{Si}$  bond, if the turn from the  $C_{\text{ipso}}-C_{\text{ortho}}$  to the  $\text{Si}-\text{O}$  bond is clockwise,  $\omega$  is positive and the phenyl is assigned *M*; if the turn is counterclockwise,  $\omega$  is negative and the phenyl is assigned *P* (Figure 3.6).

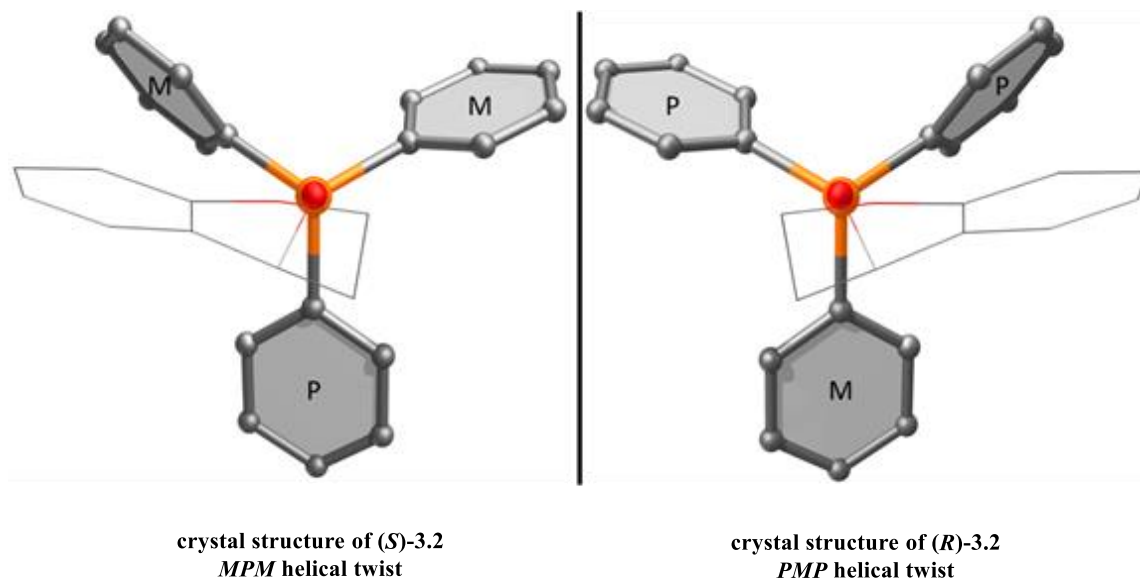


**Figure 3.5.** The independent molecular structures of (*S*)-3.2 and (*R*)-3.2 as viewed down the oxygen-silicon bond. The alcohol portion of the molecule is drawn in wireframe and the hydrogens are removed for clarity. The crystals of (*S*)-3.2 and (*R*)-3.2 were grown independently and are enantiomerically pure; all molecules in the crystals are identical. C1 determined by the X-ray data to have the “*S*” configuration for (*S*)-3.2 and the “*R*” configuration for (*R*)-3.2.

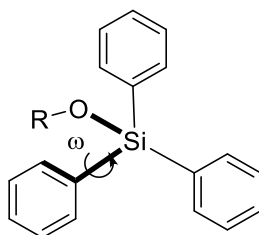


**Figure 3.6 Model to Assign *M* or *P* to Each Phenyl Group**

With this information in hand, the dihedral angles were measured, and the resulting phenyl group helicity assignments were assigned for (*R*)-3.2, (*S*)-3.2, and 3.4 in Table 3.3.

Enantiomers **(R)-3.2** and **(S)-3.2** have opposite helical twists of the triphenylsilyl groups as expected, with very similar angles but different signs (Table 3.3, entry 1 and 2 respectively). The helicity of the solid-phase structure showed **(R)-3.2** as *PMP* and **(S)-3.2** as *MPM*, which matched the predicted helical conformations from the CD spectra (Table 3.1, entry 4-5 versus Table 3.3, entry 1-2). The pattern of one phenyl group being geared opposite the other two comes from the lack of  $C_3$  symmetry discussed previously, which will not affect the overall helicity.<sup>6</sup> These structures also show that the silicon-oxygen bond lengths (1.64 Å) and silicon-carbon bond lengths (1.86-1.87 Å) in the crystal structures are similar to literature values,<sup>35</sup> again signifying that helical twist formations are possible even with these extended bond lengths versus a trityl group.

**Table 3.3** Dihedral Angles and Helicity Types of **(R)-3.2**, **(S)-3.2** and **3.4**.

Entry	Alcohol	$\omega_1$	$\omega_2$	$\omega_3$	Helicity type
1	<b>(R)-3.2</b>	-34	75	-16	<i>PMP</i>
2	<b>(S)-3.2</b>	32	-76	17	<i>MPM</i>
3a	<b>3.4</b>	-45	-50	-37	<i>PPP</i>
b	<b>3.4</b>	31	61	40	<i>MMM</i>

However, when the bicyclic triphenylsilyl ether of (-)-borneol **3.4** was crystallized, two independent conformational stereoisomers were crystallized in solution, and they were in the opposite helical twist pattern (Table, 3.3, entry 3a/b). These two conformational diastereomers resulted in helical twists of *MMM* and *PPP*, which are true propeller formations (Figure 3.7). Because the CD spectra of **3.4** showed a preferable helicity formed from the triphenyl group on silicon, it is argued that the presence of these two stereoisomers

in the crystal structure does not necessarily suggest that the two conformational diastereomers are present in equal amounts, but that these two conformations successfully pack well in the solid state. Molecular modeling in the next subchapter provided additional support toward our CD findings that there is a preference for one specific helicity in solution over the two structures observed in the solid-state.

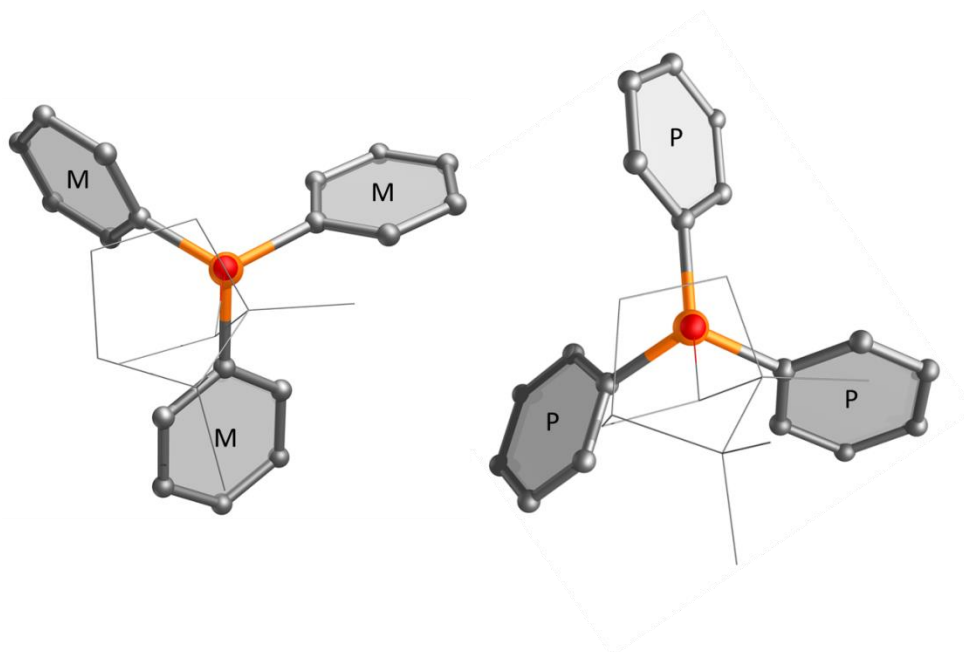


**Figure 3.7.** The structure of two independent, chemically identical but conformationally distinct molecules of **3.4** as viewed down the oxygen-silicon bond. The alcohol portion of the molecule is drawn in wireframe and the hydrogens are removed for clarity.

### 3.5 Molecular Modeling Analysis

To further investigate the structure of the low energy conformations in triphenylsilyl ethers, molecular modeling using a Monte Carlo search<sup>36</sup> was employed for (*S*)-**3.2** and **3.4**. All of the conformers within 2 kcal/mol of the lowest energy conformation were selected, and geometry optimization was performed using density functional theory (DFT), specifically B3LYP<sup>37-38</sup> and 6-311++G\*\* basis set.<sup>39</sup> Three types of triphenylsilyl

conformers resulted from the modeling of (*S*)-**3.2**, with the two predominant ones having an *MPM* helical twist (92%) with minor differences in the dihedral angles and only small percentages of the less thermodynamically stable conformers *MMM* (6%) and *PMP* (2%) (Table 3.4, entry 1-4). This result (*MPM* preference) is consistent with the predicted helicity from the CD experiments (Table 3.1, entry 5) as well as the helicity in the crystal structure of (*S*)-**3.2** (Table 3.3, entry 2).

**Table 3.4.** Population of Helicity Types and Calculated Dihedral Angles of (*S*)-**3.2** and **3.4**.

Entry	Silyl ether	Conformer distribution (%)	$\omega_1$	$\omega_2$	$\omega_3$	Helicity type
1	<b>(S)-3.2</b>	23	24	-7	87	<i>MPM</i>
2		69	1	-88	15	<i>MPM</i>
3		6	83	28	28	<i>MMM</i>
4		2	-69	9	-18	<i>PMP</i>
<i>MPM : MMM : PMP = 92 : 6 : 2</i>						
5	<b>3.4</b>	85	79	31	32	<i>MMM</i>
6		15	-35	-29	-78	<i>PPP</i>
<i>MMM : PPP = 85 : 15</i>						

As discussed in the previous subchapter, the solid-state structure of **3.4** indicated the presence of two opposite helicities (*MMM* and *PPP*) while the CD spectroscopy indicated a higher population of *MPM* configuration. A Monte Carlo search resulted in two low energy triphenylsilyl conformations, the *MMM* and *PPP* stereoisomers (Table 3.4, entry 5-6), being consistent with the crystal structure studies (Table 3.3, entry 3). However, after DFT optimization, these two structures were shown to have an energy difference of

1.1 kcal/mol with a preference for the *MMM* helical twist. The ratio of the population of *MMM* versus *PPP* is 85% to 15%. This preference of *MMM* helical twist would result in a negative Cotton effect curve in the CD spectra, which is consistent with our observed experimental outcome (Table 3.1, entry 3). The nature of bicyclic **3.4** offers less steric hindrance compared to the other substrates studied, resulting in a smaller energy difference between the two conformations, leading to an increased presence of the higher energy conformation. This also offers an explanation as to why two different conformations were observed in solid-state study, because they both seem to be present in solution. Finally, the tied-back bicyclic structure limiting the steric affect from the alcohol ultimately affects the resulting helical twist, allowing for a true propeller formation.

### 3.6 Conclusions and Outlook

We successfully showed that point chirality can induce helical chirality in triarylsilyl groups by derivatizing enantiopure alcohols with triphenylsilyl and trinaphthylsilyl groups. These findings have been supported by CD spectroscopy, solid-state structures, and molecular modeling. CD spectroscopy of the compounds all displayed a Cotton effect that was characteristic for a helical twist formation. The alcohols with *R* configuration generally exhibited a positive Cotton effect curve, indicating a *PMP* helical twist, while the alcohols in *S* configuration presented a negative Cotton effect curve, with a *MPM* helical twist.

The crystal structure for (*R*)-**3.2**, (*S*)-**3.2** each crystalized as one conformation, with the gearing of the helicity being consistent with the assignment predicted by CD spectroscopy. The molecular modeling of (*S*)-**3.2**, using a Monte Carlo search and DFT



optimization, also provided strong support to the CD spectroscopy and crystal structure studies. The solid-state study of **3.4** showed the presence of two conformers with opposite helical twists. This was further explained by molecular modeling that one of the stereoisomers with a *MMM* helical twist had a lower energy and was present in a higher population out of the two. This would result in a negative Cotton effect curve which was consistent with the CD spectroscopy.

Ultimately, the understanding of chirality transmission between the alcohol and the triarylsilyl group can be extrapolated to explain the importance of the phenyl groups in silylation-based kinetic resolutions. It is hypothesized that the nucleophilic catalyst attacks the triphenylsilyl chloride and forms the reactive catalyst-triphenylsilyl intermediate. The nitrogen on the catalyst is covalently bonded to silicon and the covalent attachment of a chiral entity serves as a molecular bevel gear, transmitting point chirality from the catalyst to helical chirality of the triphenyl group. This will result in a preferable helical twist (either *MPM* or *PMP*) and aids in selectively derivatizing one alcohol enantiomer from a racemic mixture through this enhanced chiral environment.

Future studies will be focused on using CD spectroscopy to analyze point chirality attached to the helical chirality and quantify the enantiomeric ratio of the point chirality. Further efforts to elucidate the mechanism of asymmetric silylation and initial studies of stereospecificity at silicon will be discussed in the next chapter.

## 3.7 Experimental

### General information

Trinaphthylsilane and all the triarylsilyl ethers were obtained through the general procedures below. Reactions were carried out under a nitrogen atmosphere using oven-dried glassware. Tetrahydrofuran (THF), toluene and diethyl ether were degassed and passed through a column of activated alumina prior to use. Unless otherwise stated, all the other chemicals, including the enantiopure starting alcohols, were obtained from major commercial sources and used without further purification. High resolution mass spectrometry (HRMS) was obtained either using an orthogonal quadrupole time-of-flight instrument or an orbitrap instrument. Infrared spectroscopy (IR) was conducted using an FT-IR ATR spectrophotometer,  $\nu_{\max}$  in  $\text{cm}^{-1}$ . NMR spectra were recorded with a 400 MHz instrument for  $^1\text{H}$  and a 101 MHz instrument for  $^{13}\text{C}$  with complete proton decoupling. Chemical shifts were reported in ppm with TMS or chloroform as an internal standard (TMS 0.00 ppm or  $\text{CHCl}_3$  7.26 ppm for  $^1\text{H}$  and 77.16 for  $^{13}\text{C}$ ). Optical rotations were obtained utilizing a polarimeter. Circular dichroism (CD) spectra were taken on a CD spectrometer. The concentrations were kept at approximately  $8 \times 10^{-5}$  M, aiming to reach a maximum absorbance without oversaturating the detector.<sup>31</sup> The samples were analyzed in a 1 mm path length, strain free, quartz cell in order to have a better observed Cotton effect while minimizing noise. All reported spectra were processed by using 15-point Savitzky-Golay smoothing.<sup>32</sup> Structure determinations were performed using standard single crystal X-ray diffraction techniques. See supporting information for full experimental and structure refinement details.

### General procedure for the preparation of triphenylsilyl ether derivatives (GP1)

To a 4-dram vial with a stir bar was added the enantiopure alcohol (1 equiv), *N,N*-diisopropylethylamine (0.9 equiv.) and *N*-methylimidazole (0.25 equiv.). Dry THF was then added to obtain a concentration of 0.3 M with respect to alcohol. The solution was allowed to stir at room temperature for 5 minutes followed by the addition of triphenylsilyl chloride in a THF solution (0.6 M, 0.9 equiv.). The reaction was allowed to react for 24 hours at room temperature and the crude reaction was concentrated under vacuum. The residue was then purified via silica gel chromatography (2% EtOAc to 5% EtOAc in hexane).

### Preparation of tri(naphthalen-2-yl)silane (3.8).<sup>40</sup>

A 250-mL round bottom flask was fitted with a stir bar and septa and purged with argon. The flask was charged with 20 mL of ether and the solution was allowed to cool to 0 °C in an ice bath. *N*-Butyllithium (10.25 mmol, 8.1 mL of 1.26 M in hexane) was added via syringe with stirring. A solution of 1-iodonaphthalene (10 mmol, 1.46 mL in 20 mL ether) was prepared and added to the reaction vessel slowly via syringe. The mixture was then allowed to warm to room temperature for 1 hour. The mixture was then cooled to -40 °C in a dry ice/MeCN bath. A solution of trichlorosilane Cl<sub>3</sub>SiH (3.0 mmol, 303 μL in 7.5 mL ether) was prepared and added to the reaction slowly via syringe. The reaction was left to stir at -40 °C for 2 hours and then quenched with water. A significant quantity of solid formed. The solid was filtered and washed with cold acetone to reveal a white solid, 0.99 g, 80% yield.

**<sup>1</sup>H NMR** (400 MHz, CDCl<sub>3</sub>): δ ppm 8.16 (s, 3H), 7.89 – 7.83 (m, 6H), 7.80 (d, *J* = 7.9 Hz, 3H), 7.71 (d, *J* = 8.2 Hz, 3H), 7.56 – 7.44 (m, 6H), 5.85 (s, 1H). **<sup>13</sup>C NMR** (101 MHz, CDCl<sub>3</sub>) δ ppm 137.3, 134.2, 133.1, 131.5, 130.8, 128.3, 127.8, 127.5, 126.9, 126.1

### General procedures for the preparation of trinaphthylsilyl ether derivatives (GP2)

Synthesis of trinaphthylsilyl ether derivatives followed a similar procedure reported in the literature.<sup>23</sup> To a 4-dram vial that was oven dried with a stir bar, enantiopure alcohol (1 equiv) and trinaphthylsilane (0.9 equiv.) was added under N<sub>2</sub>. Commercially available tris(pentafluorophenyl)borane (B(C<sub>6</sub>F<sub>5</sub>)<sub>3</sub>) (0.02 equiv.) was added to the mixture in a glove box. Enough toluene was then added to make a concentration of 0.5 M with respect to alcohol. The reaction was then allowed to stir at room temperature and was monitored through <sup>1</sup>H NMR. Full conversion was achieved after 1 hour. The crude mixture was concentrated under vacuum and the residue was purified via silica gel chromatography (2% EtOAc to 5% EtOAc in hexane).

### Characterization of Triarylsilyl Ether Derivatives.

*(((1R,2S,5R)-2-Isopropyl-5-methylcyclohexyl)oxy)triphenylsilane ((L)-3.1)*:<sup>41</sup> Synthesized according to GP1 with 48 mg *L*-menthol and 76 mg triphenylsilyl chloride which yielded a white solid 120 mg, 90%; **<sup>1</sup>H NMR** (400 MHz, CDCl<sub>3</sub>): δ ppm 7.62 (dd, *J* = 7.9, 1.5 Hz, 6H), 7.46 – 7.32 (m, 9H), 3.54 (td, *J* = 10.1, 4.3 Hz, 1H), 2.38 (dtd, *J* = 13.9, 6.9, 2.4 Hz, 1H), 1.93 – 1.82 (m, 1H), 1.62 – 1.47 (m, 2H), 1.39 – 1.07 (m, 3H), 0.88 (d, *J* = 7.1 Hz, 3H), 0.84 – 0.80 (m, 2H), 0.79 (d, *J* = 6.0 Hz, 3H), 0.39 (d, *J* = 6.9 Hz, 3H). **<sup>13</sup>C NMR** (101

MHz, CDCl<sub>3</sub>) δ ppm 135.6, 135.2, 129.8, 127.7, 73.9, 50.2, 45.3, 34.5, 31.6, 25.3, 22.6, 22.3, 21.4, 15.3. **Optical Rotation** [α]<sup>25</sup><sub>D</sub>: -40.0 (c = 0.022) CHCl<sub>3</sub>

*(((1S,2R,5S)-2-Isopropyl-5-methylcyclohexyl)oxy)triphenylsilane ((D)-3.2)*:<sup>41</sup> Synthesized according to GP1 with 48 mg *D*-menthol and 76 mg triphenylsilyl chloride which yielded a white solid 120 mg, 90%; <sup>1</sup>H NMR (400 MHz, CDCl<sub>3</sub>): δ ppm 7.62 (dd, *J* = 7.9, 1.5 Hz, 6H), 7.49 – 7.31 (m, 9H), 3.54 (td, *J* = 10.1, 4.3 Hz, 1H), 2.38 (dtd, *J* = 13.9, 6.9, 2.4 Hz, 1H), 1.94 – 1.83 (m, 1H), 1.63 – 1.50 (m, 2H), 1.39 – 1.09 (m, 3H), 0.88 (d, *J* = 7.1 Hz, 3H), 0.85 – 0.80 (m, 2H), 0.79 (d, *J* = 6.0 Hz, 3H), 0.38 (d, *J* = 6.9 Hz, 3H). <sup>13</sup>C NMR (101 MHz, CDCl<sub>3</sub>) δ ppm 135.6, 135.2, 129.8, 127.7, 73.9, 50.2, 45.3, 34.5, 31.6, 25.3, 22.6, 22.3, 21.4, 15.3. **Optical Rotation** [α]<sup>25</sup><sub>D</sub>: +39.0 (c = 0.02) CHCl<sub>3</sub>

*Triphenyl(((1S,2R,4S)-1,7,7-trimethylbicyclo[2.2.1]heptan-2-yl)oxy)silane (3.4)*:<sup>42</sup> Synthesized according to GP1 with 18 mg (-)-borneol and 24 mg triphenylsilyl chloride which yielded a white solid 40 mg, 95%; <sup>1</sup>H NMR (400 MHz, CDCl<sub>3</sub>): δ ppm 7.66 – 7.57 (m, 6H), 7.46 – 7.33 (m, 9H), 4.18 (d, *J* = 9.4 Hz, 1H), 2.39 – 2.27 (m, 1H), 1.98 – 1.87 (m, 1H), 1.77 – 1.64 (m, 1H), 1.34 – 1.18 (m, 3H), 1.01 (dd, *J* = 13.2, 3.2 Hz, 1H), 0.81 (s, 3H), 0.70 (d, *J* = 6.6 Hz, 6H). <sup>13</sup>C NMR (101 MHz, CDCl<sub>3</sub>) δ ppm 135.6, 135.2, 129.8, 127.7, 78.6, 50.2, 47.3, 45.2, 39.4, 28.4, 26.5, 20.2, 18.8, 13.6. **Optical Rotation** [α]<sup>25</sup><sub>D</sub>: +24.1 (c = 0.02) CHCl<sub>3</sub>

*(R)-(Chroman-4-yloxy)triphenylsilane ((R)-3.2)*:<sup>43</sup> Synthesized according to GP1 with 23 mg (*R*)-chromanol and 36 mg triphenylsilyl chloride which yielded a white solid 50 mg,

81%; <sup>1</sup>H NMR (400 MHz, CDCl<sub>3</sub>): δ ppm 7.66 (d, J = 6.5 Hz, 6H), 7.48–7.37 (m, 9H), 7.18–7.14 (m, 1H), 6.99 (d, J = 7.2 Hz, 1H), 6.83–6.76 (m, 2H), 4.97 (t, J = 4.0 Hz, 1H), 4.51–4.45 (m, 1H), 4.24–4.19 (m, 1H), 2.02–1.96 (m, 2H); <sup>13</sup>C NMR (101 MHz, CDCl<sub>3</sub>) δ ppm 154.5, 135.5, 134.3, 130.1, 130.0, 129.2, 127.8, 124.2, 120.0, 116.7, 65.0, 62.2, 31.4.  
**Optical Rotation** [α]<sub>D</sub><sup>25</sup>: +53.4 (c = 0.031) CHCl<sub>3</sub>

*(S)*-(Chroman-4-yloxy)triphenylsilane ((**S**)-**3.2**):<sup>43</sup> Synthesized according to GP1 with 23 mg (*S*)-chromanol and 36 mg triphenylsilyl chloride which yielded a white solid 43 mg, 70%; <sup>1</sup>H NMR (400 MHz, CDCl<sub>3</sub>): δ ppm 7.62 (t, J = 12.8 Hz, 6H), 7.41 (dt, J = 24.3, 7.2 Hz, 9H), 7.14 (t, J = 7.7 Hz, 1H), 6.97 (d, J = 7.5 Hz, 1H), 6.78 (dd, J = 17.2, 8.0 Hz, 2H), 4.96 (t, J = 4.0 Hz, 1H), 4.46 (td, J = 10.4, 3.1 Hz, 1H), 4.24 – 4.15 (m, 2H); <sup>13</sup>C NMR (101 MHz, CDCl<sub>3</sub>) δ ppm 154.6, 135.6, 134.5, 130.2, 130.1, 129.3, 128.0, 124.3, 120.1, 116.8, 65.1, 62.2, 31.5. **Optical Rotation** [α]<sub>D</sub><sup>25</sup>: -49.0 (c = 0.031) CHCl<sub>3</sub>

*(R)*-4,4-Dimethyl-3-((triphenylsilyl)oxy)dihydrofuran-2(3H)-one ((**R**)-**3.3**):<sup>13</sup> Synthesized according to GP1 with 6 mg (*R*)-pantolactone and 10 mg triphenylsilyl chloride which yielded a white solid 12 mg, 70%; <sup>1</sup>H NMR (400 MHz, CDCl<sub>3</sub>): δ 7.72 (d, J = 6.6 Hz, 6H), 7.48–7.37 (m, 9H), 4.15 (s, 1H), 3.94 (d, J = 8.9 Hz, 1H), 3.76 (d, J = 8.9 Hz, 1H), 1.18 (s, 3H), 0.86 (s, 3H) <sup>13</sup>C NMR (101 MHz, CDCl<sub>3</sub>) δ ppm 175.2, 135.7, 133.4, 130.4, 127.9, 75.5, 41.1, 22.6, 19.7. **Optical Rotation** [α]<sub>D</sub><sup>25</sup>: +8.2 (c = 0.84) CHCl<sub>3</sub>

*(1R,2S,5R)*-2-Isopropyl-5-methylcyclohexyl)oxy)tri(naphthalen-2-yl)silane ((**L**)-**3.5**):  
Synthesized according to GP2 with 51 mg *L*-menthol and 125 mg trinaphthyl silane which

yielded a white solid 180 mg, 97%. **mp range** = 102-105 °C **<sup>1</sup>H NMR** (400 MHz, CDCl<sub>3</sub>): δ 8.22 (s, 3H), 7.80 (ddd, *J* = 14.8, 9.2, 4.5 Hz, 12H), 7.50 (dtd, *J* = 14.7, 6.9, 1.3 Hz, 6H), 3.68 (td, *J* = 10.3, 4.3 Hz, 1H), 2.56 (dtd, *J* = 13.9, 6.9, 2.4 Hz, 1H), 2.03 (d, *J* = 11.9 Hz, 1H), 1.60 – 1.54 (m, 2H), 1.51 – 1.12 (m, 3H), 0.93 (d, *J* = 7.1 Hz, 3H), 0.85 (dd, *J* = 19.6, 10.9 Hz, 2H), 0.78 (d, *J* = 6.4 Hz, 3H), 0.41 (d, *J* = 6.9 Hz, 3H). **<sup>13</sup>C NMR** (101 MHz, CDCl<sub>3</sub>) δ ppm 137.1, 134.2, 132.9, 132.7, 131.4, 128.5, 127.8, 127.1, 126.9, 126.0, 74.3, 50.3, 45.5, 34.5, 31.6, 25.5, 22.6, 22.3, 21.4, 15.6. **Optical Rotation** [ $\alpha$ ]<sub>D</sub><sup>25</sup>: -24.9 (c = 0.03) CHCl<sub>3</sub> **HRMS**: (ESI) calculated for (C<sub>40</sub>H<sub>40</sub>OSi<sup>+</sup>) (M<sup>+</sup>): 564.2848, Observed: 564.2850. **IR** (neat, cm<sup>-1</sup>) 3049, 2953, 2921, 1589, 1250, 1456, 1272, 1083, 853, 816, 740.

*(((1S,2R,5S)-2-Isopropyl-5-methylcyclohexyl)oxy)tri(naphthalen-2-yl)silane ((D)-3.5)*:

Synthesized according to GP2 with 51 mg *D*-menthol and 125 mg trinaphthyl silane which yielded a white solid 183 mg, 97%; **mp range** = 102-105 °C **<sup>1</sup>H NMR** (400 MHz, CDCl<sub>3</sub>): δ 8.22 (s, 3H), 7.80 (ddd, *J* = 14.8, 9.2, 4.5 Hz, 12H), 7.50 (dtd, *J* = 14.7, 6.9, 1.3 Hz, 6H), 3.68 (td, *J* = 10.3, 4.3 Hz, 1H), 2.56 (dtd, *J* = 13.9, 6.9, 2.4 Hz, 1H), 2.03 (d, *J* = 11.9 Hz, 1H), 1.60 – 1.54 (m, 2H), 1.51 – 1.12 (m, 3H), 0.93 (d, *J* = 7.1 Hz, 3H), 0.85 (dd, *J* = 19.6, 10.9 Hz, 2H), 0.78 (d, *J* = 6.4 Hz, 3H), 0.41 (d, *J* = 6.9 Hz, 3H). **<sup>13</sup>C NMR** (101 MHz, CDCl<sub>3</sub>) δ ppm 137.1, 134.2, 132.9, 132.7, 131.4, 128.5, 127.8, 127.1, 126.9, 126.0, 74.3, 50.3, 45.5, 34.5, 31.6, 25.5, 22.6, 22.3, 21.4, 15.6. **Optical Rotation** [ $\alpha$ ]<sub>D</sub><sup>25</sup>: +24.0 (c = 0.03) CHCl<sub>3</sub> **HRMS**: (ESI) calculated for (C<sub>40</sub>H<sub>40</sub>OSi<sup>+</sup>) (M<sup>+</sup>): 564.2848, Observed: 564.2851. **IR** (neat, cm<sup>-1</sup>) 3050, 2952, 2918, 1589, 1456, 1272, 1082, 852, 815, 739.

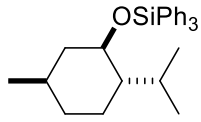
*(R)-(Chroman-4-yloxy)tri(naphthalen-2-yl)silane ((R)-3.6)*: Synthesized according to GP2 with 36 mg (*R*)-chromanol and 85 mg trinaphthyl silane which yielded a white solid 125

mg, 96%. **mp range** = 110-112 °C **<sup>1</sup>H NMR** (400 MHz, CDCl<sub>3</sub>): δ ppm 8.22 (s, 3H), 8.22 (s, 6H), 7.79 (dd, *J* = 7.5, 4.8 Hz, 6H), 7.51 (ddd, *J* = 14.9, 13.6, 6.8 Hz, 6H), 7.21 – 7.14 (m, 1H), 7.11 (d, *J* = 7.6 Hz, 1H), 6.84 (d, *J* = 8.1 Hz, 1H), 6.77 (t, *J* = 7.4 Hz, 1H), 5.11 (t, *J* = 4.0 Hz, 1H), 4.58 (td, *J* = 10.7, 2.7 Hz, 1H), 4.25 (dt, *J* = 8.5, 4.1 Hz, 1H), 2.16 – 1.94 (m, 2H); **<sup>13</sup>C NMR** (101 MHz, CDCl<sub>3</sub>) δ ppm 154.7, 137.2, 134.3, 132.9, 131.9, 131.1, 130.2, 129.4, 128.5, 127.8, 127.4, 127.1, 126.1, 124.2, 120.1, 116.8, 65.4, 62.3, 31.6. **Optical Rotation** [ $\alpha$ ]<sub>D</sub><sup>25</sup>: +22.0 (c = 0.26) CHCl<sub>3</sub> **HRMS**: (ESI) calculated for (C<sub>39</sub>H<sub>30</sub>O<sub>2</sub>Si<sup>+</sup>) (M<sup>+</sup>): 558.2015, Observed: 558.2050. **IR** (neat, cm<sup>-1</sup>) 2974, 2928, 1736, 1590, 1458, 1387, 1263, 1142, 1092, 962, 858, 818, 742

*(R)*-4,4-Dimethyl-3-((tri(naphthalen-2-yl)silyl)oxy)dihydrofuran-2(3H)-one ((**R**)-**3.7**): Synthesized according to GP2 with 29 mg (*R*)-pantolactone and 82 mg trinaphthyl silane which yielded a white solid 110 mg, 95%; **mp range** = 70-71 °C **<sup>1</sup>H NMR** (400 MHz, CDCl<sub>3</sub>): δ 8.24 (s, 3H), 7.91 (t, *J* = 7.3 Hz, 6H), 7.85 (d, *J* = 8.0 Hz, 3H), 7.78 (dd, *J* = 8.2, 1.0 Hz, 3H), 7.60 – 7.49 (m, 6H), 4.25 (dd, *J* = 5.1, 3.3 Hz, 1H), 3.86 – 3.80 (m, 2H), 1.23 (s, 3H), 0.94 (s, 3H). **<sup>13</sup>C NMR** (101 MHz, CDCl<sub>3</sub>) δ ppm 137.1, 134.3, 132.9, 131.7, 131.0, 128.5, 127.8, 127.4, 127.1, 126.2, 80.5, 78.7, 75.0, 43.3, 24.8, 19.6. **Optical Rotation** [ $\alpha$ ]<sub>D</sub><sup>25</sup>: +17.6 (c = 0.031) CHCl<sub>3</sub> **HRMS**: (ESI) calculated for (C<sub>36</sub>H<sub>30</sub>O<sub>3</sub>Si<sup>+</sup>) (M<sup>+</sup>): 538.1964, Observed: 538.1965. **IR** (neat, cm<sup>-1</sup>) 3051, 2959, 2928, 1733, 1590, 1464, 1272, 1087, 1021, 951, 853, 818, 741



## CD Spectra of Triarylsilyl Ether Derivatives

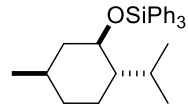


(L)-3.1

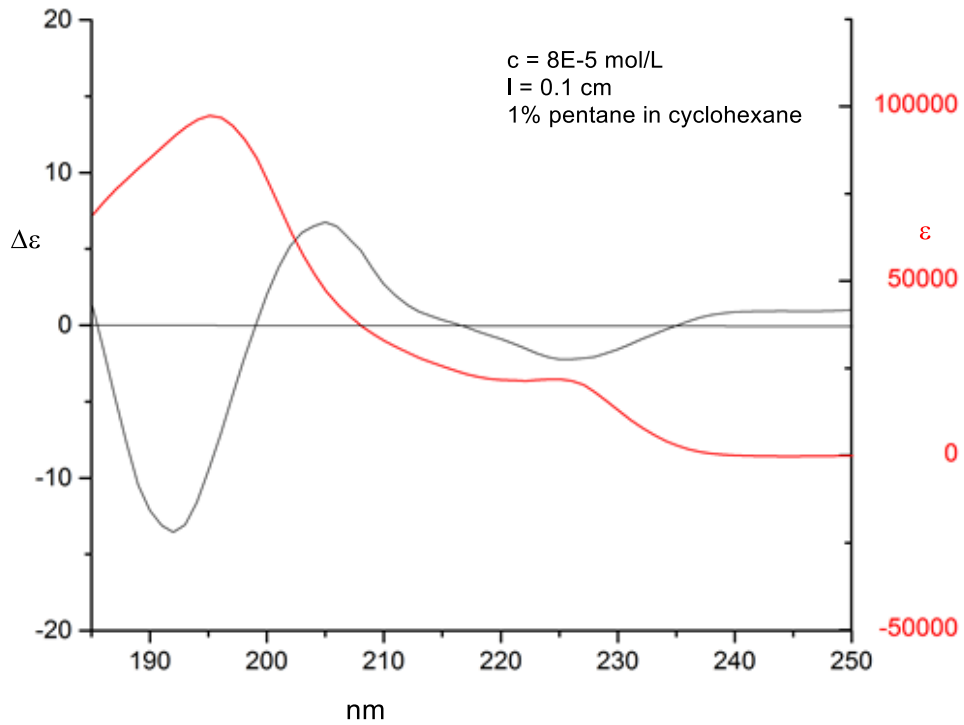
*(((1R,2S,5R)-2-Isopropyl-5-methylcyclohexyl)oxy)triphenylsilane ((L)-3.1)*

### Circular Dichroism Spectra:

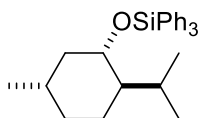
Table 3.1, Entry 1:



(L)-3.1



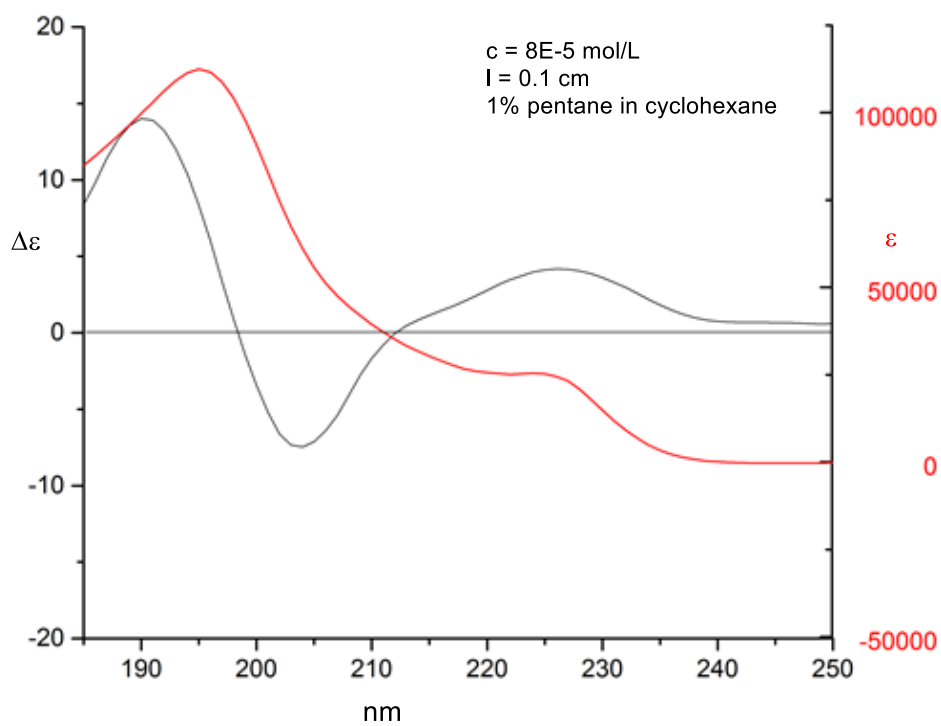
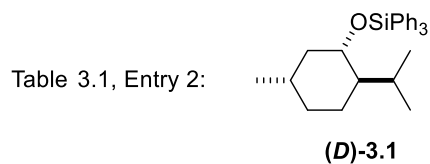
CD $\Delta\epsilon(\text{nm})$		UV $\epsilon(\text{nm})$	
6.7	205	97361	195
-13.4	192		



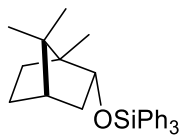
**(D)-3.1**

*(((1S,2R,5S)-2-Isopropyl-5-methylcyclohexyl)oxy)triphenylsilane ((D)-3.1*

**Circular Dichroism Spectra:**



$\Delta\epsilon(\text{nm})$	$\epsilon(\text{nm})$
-7.5	112490
14	195
204	
190	

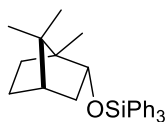


3.4

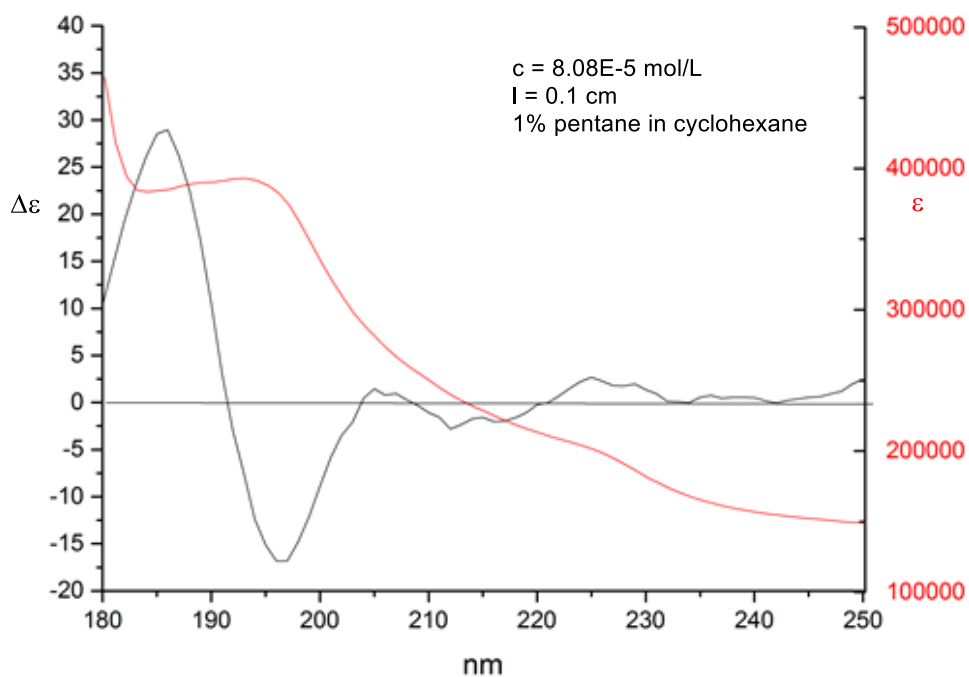
Triphenyl(((1S,2R,4S)-1,7,7-trimethylbicyclo[2.2.1]heptan-2-yl)oxy)silane (7):

Circular Dichroism Spectra:

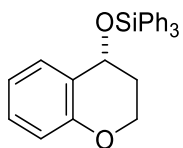
Table 3.1, Entry 3:



3.4



CD $\Delta\epsilon(\text{nm})$		UV $\epsilon(\text{nm})$	
-17	196	393104	193
29	186		

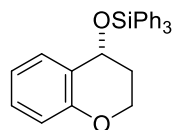


**(R)-3.2**

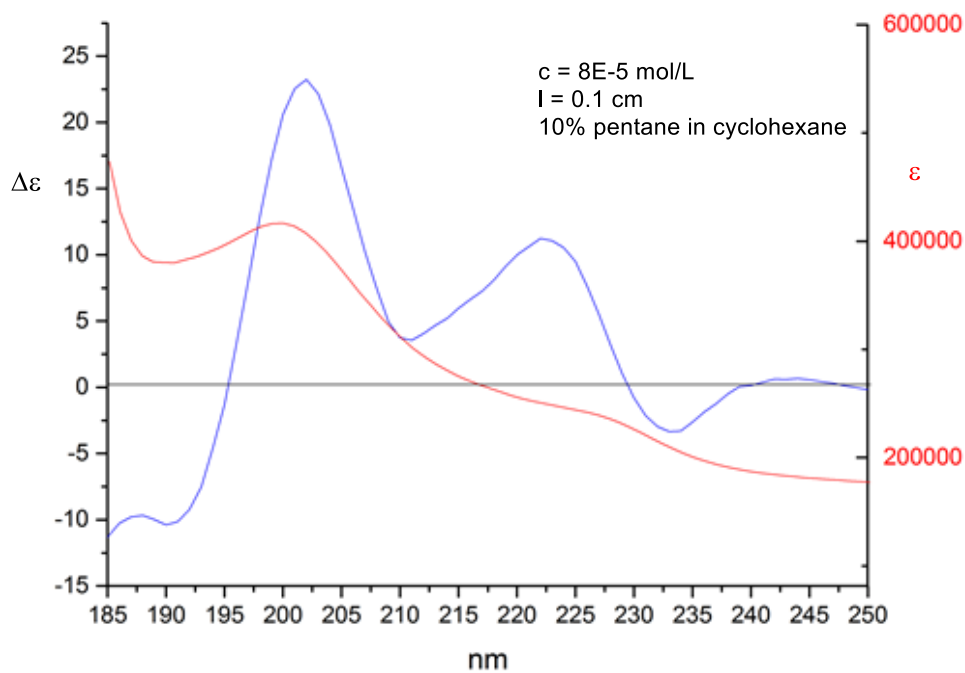
*(R)*-(Chroman-4-yloxy)triphenylsilane **((R)-3.2)**

**Circular Dichroism Spectra:**

Table 3.1, Entry 4:



**(R)-3.2**



CD  
 $\Delta\epsilon(\text{nm})$

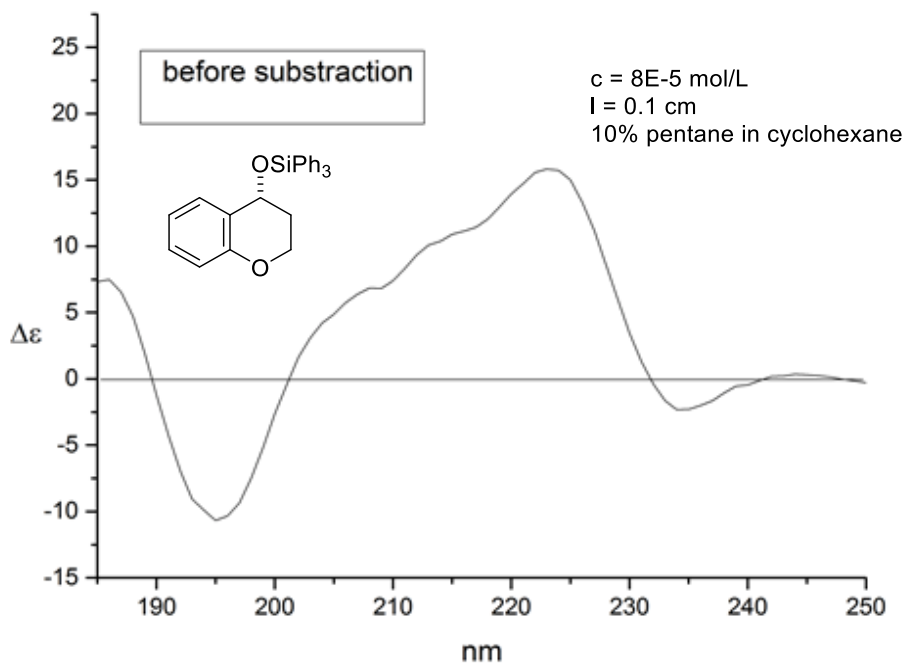
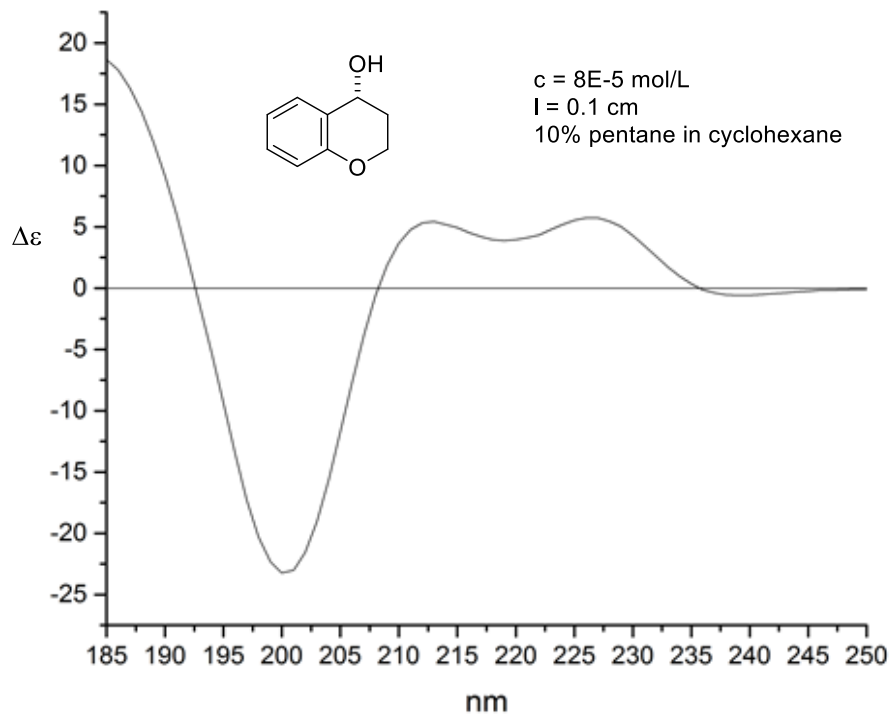
UV  
 $\epsilon(\text{nm})$

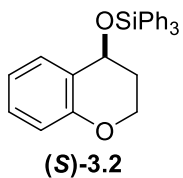
23  
-10

202  
190

414958

196

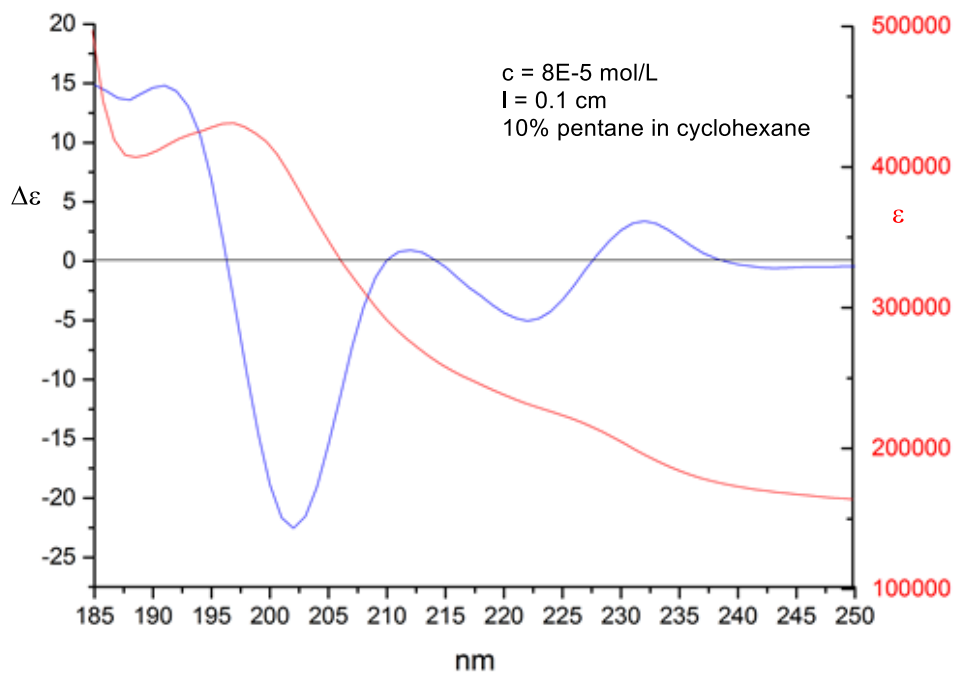
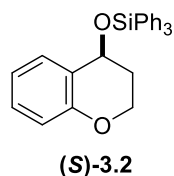




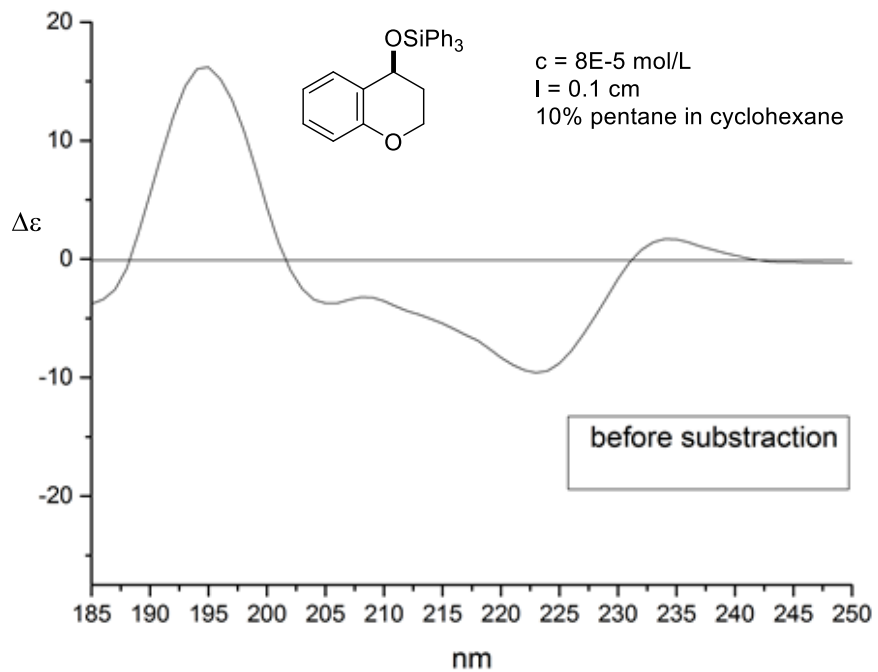
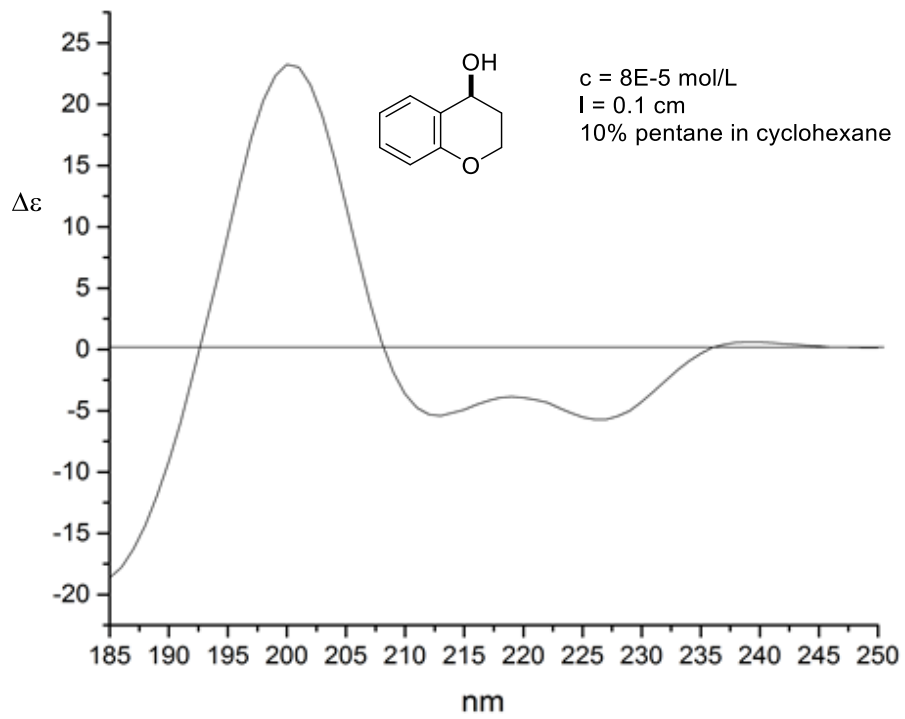
*(S)*-(Chroman-4-yloxy)triphenylsilane ((S)-3.2):

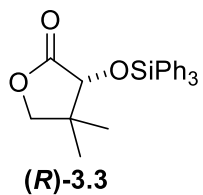
**Circular Dichroism Spectra:**

Table 3.1, Entry 5:



CD $\Delta\epsilon(\text{nm})$		UV $\epsilon(\text{nm})$	
-23	202	431104	193
15	191		

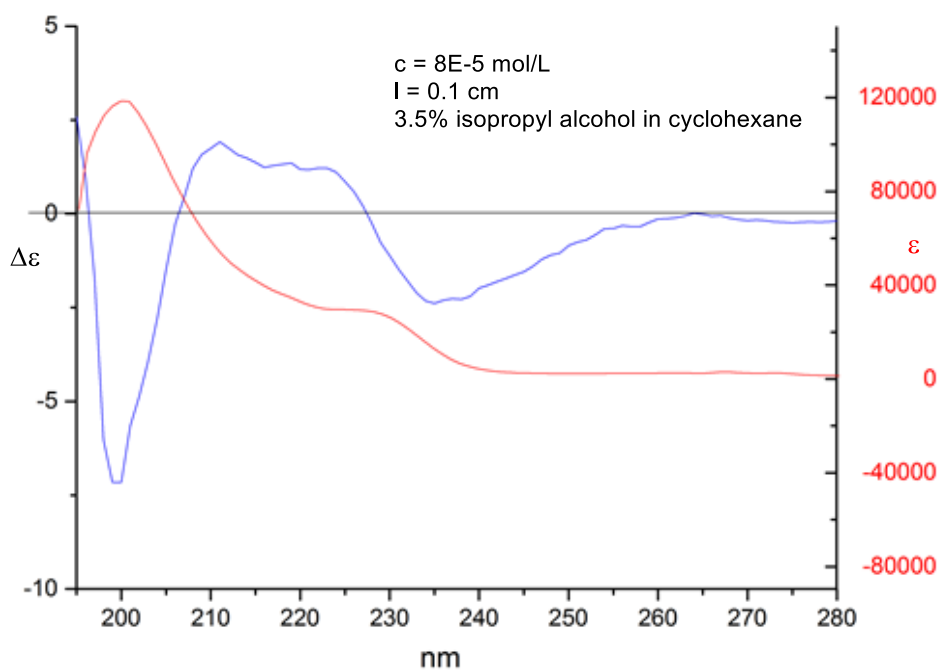
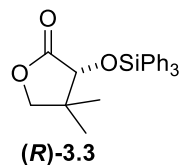




*(R)*-4,4-Dimethyl-3-((triphenylsilyl)oxy)dihydrofuran-2(3H)-one **((R)-3.3)**

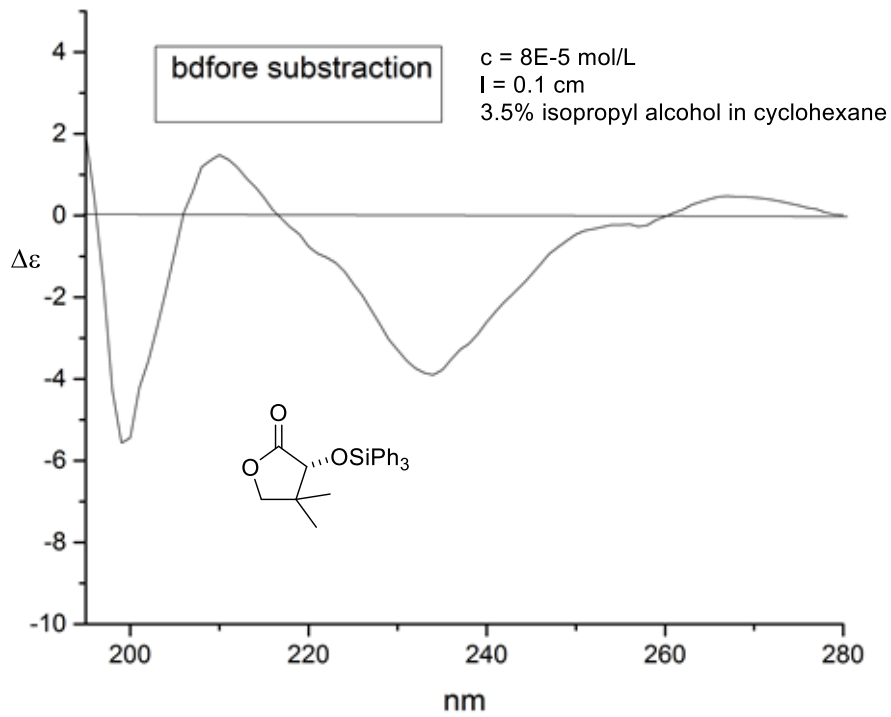
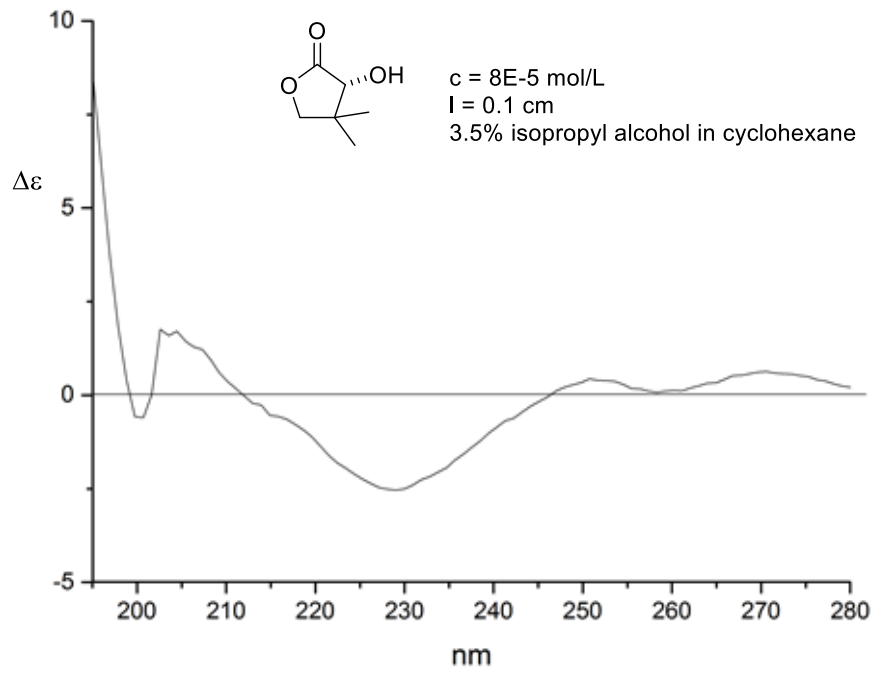
**Circular Dichroism Spectra:**

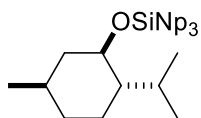
Table 3.1, Entry 6:



CD $\Delta\epsilon(\text{nm})$		UV $\epsilon(\text{nm})$	
1.9	210	118443	195
-7.2	199		



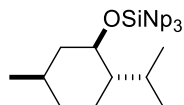




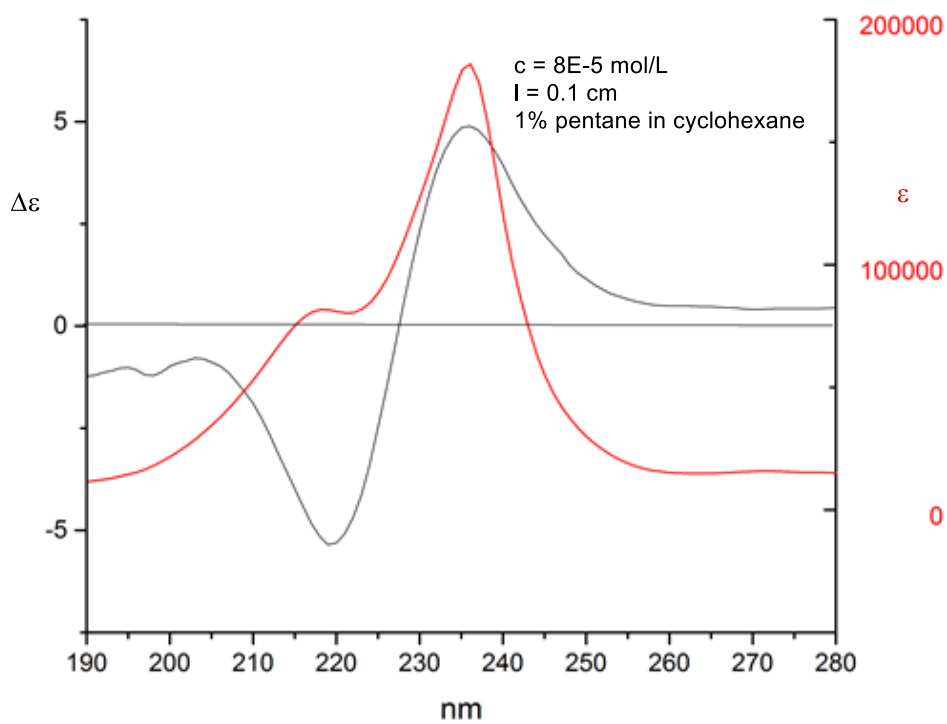
**(L)-3.5**

*(((1R,2S,5R)-2-Isopropyl-5-methylcyclohexyl)oxy)tri(naphthalen-2-yl)silane ((L)-3.5)*

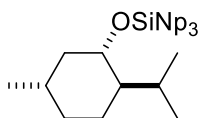
Table 3.2, Entry 1:



**(L)-3.5**



CD $\Delta\epsilon(\text{nm})$		UV $\epsilon(\text{nm})$	
4.9	236	181772	236
-5.3	220		



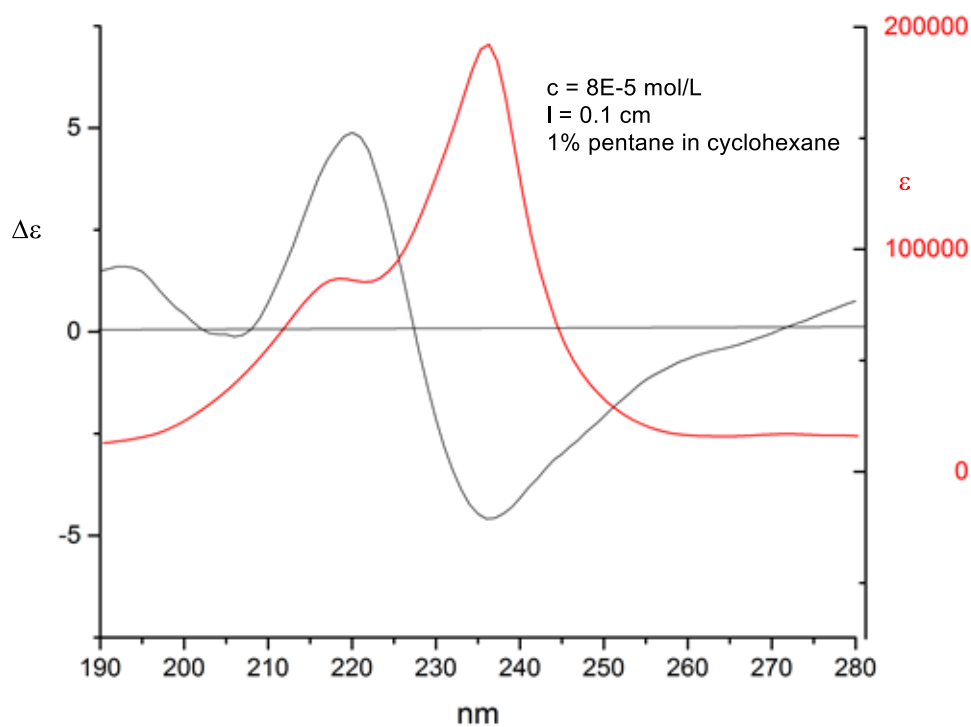
**(D)-3.5**

*(((1S,2R,5S)-2-Isopropyl-5-methylcyclohexyl)oxy)tri(naphthalen-2-yl)silane ((D)-3.5)*

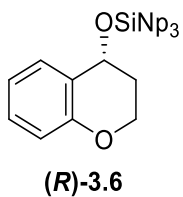
**Circular Dichroism Spectra:**



**(D)-3.5**

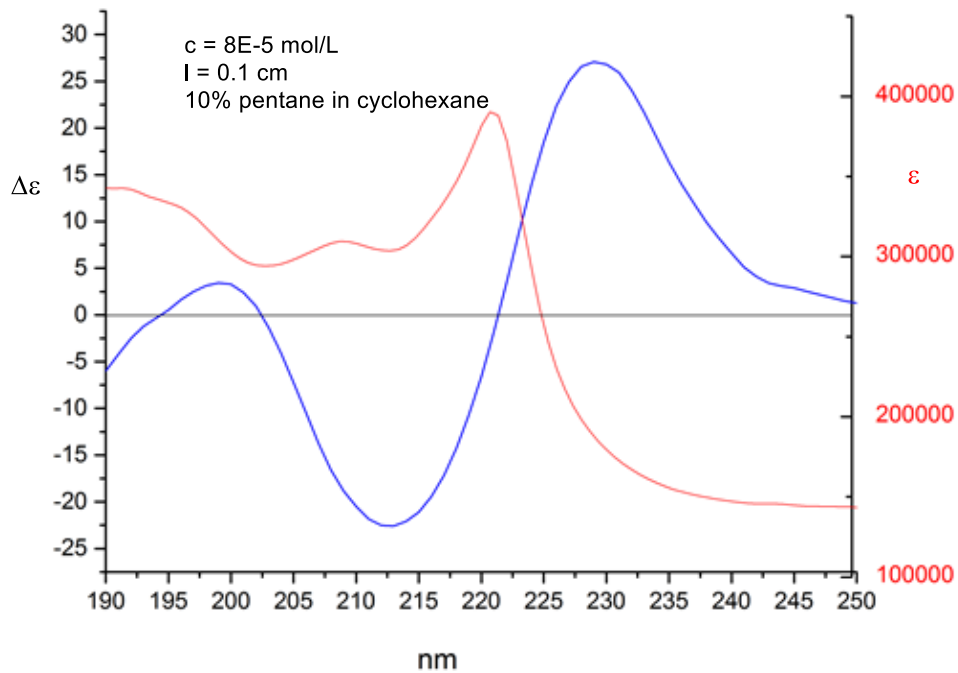
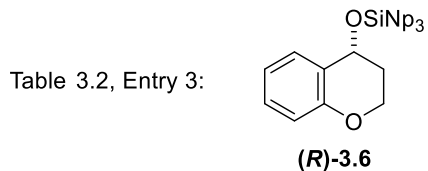


CD $\Delta\epsilon(\text{nm})$		UV $\epsilon(\text{nm})$	
-4.6	236	192216	236
4.8	220		

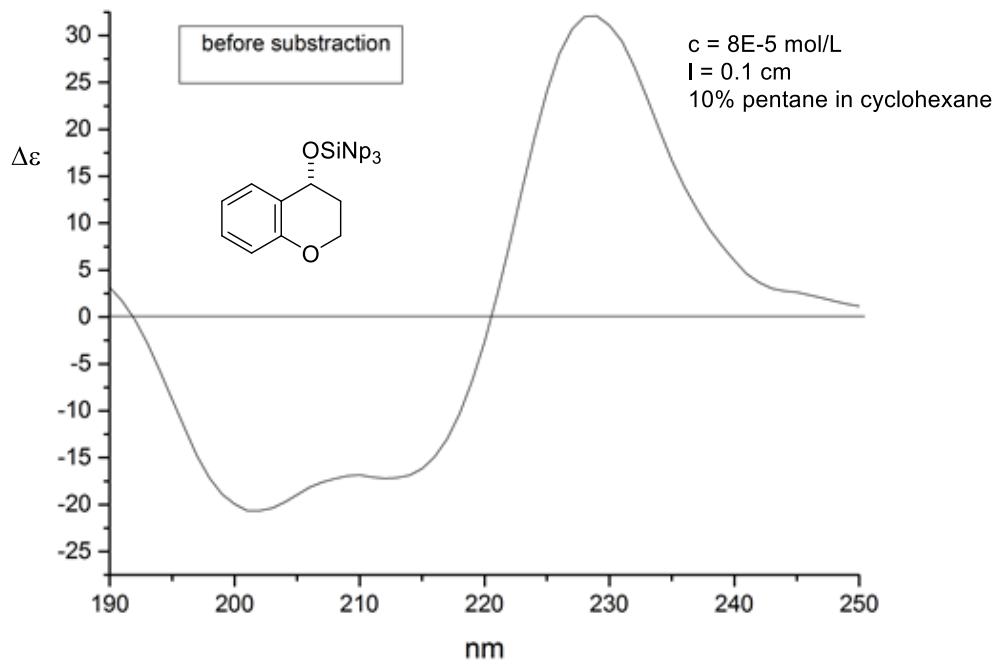
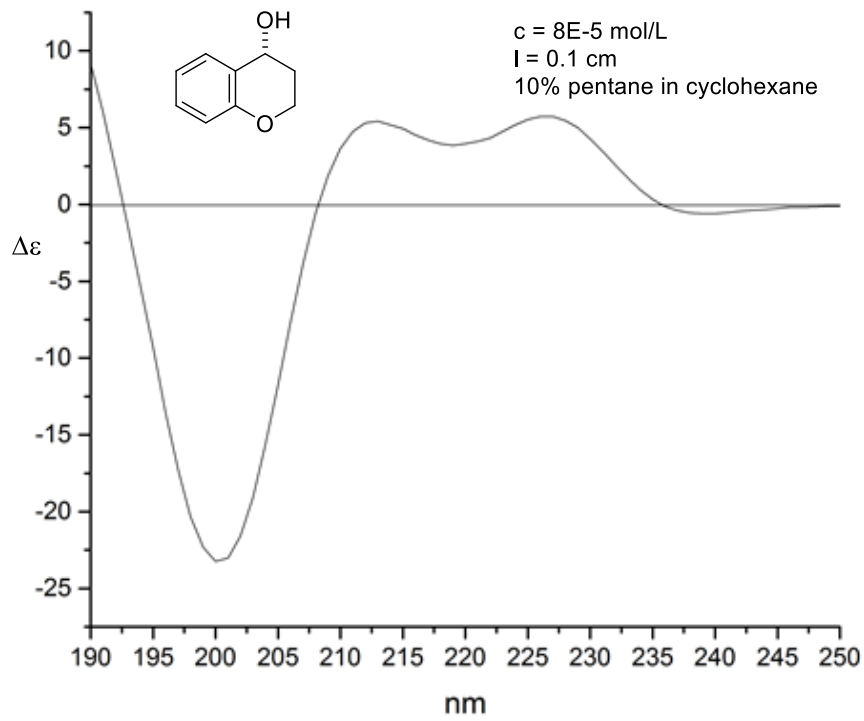


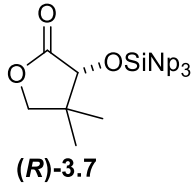
*(R)*-(Chroman-4-yloxy)tri(naphthalen-2-yl)silane **((R)-3.6**

**Circular Dichroism Spectra:**



CD $\Delta\epsilon(\text{nm})$		UV $\epsilon(\text{nm})$	
27	229	390295	221
-23	213		

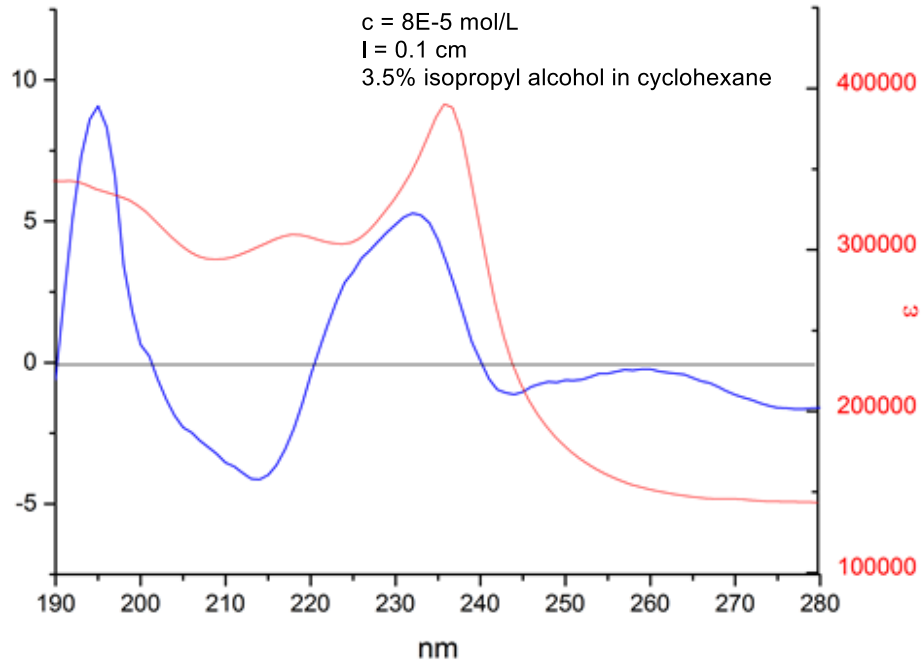
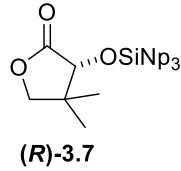




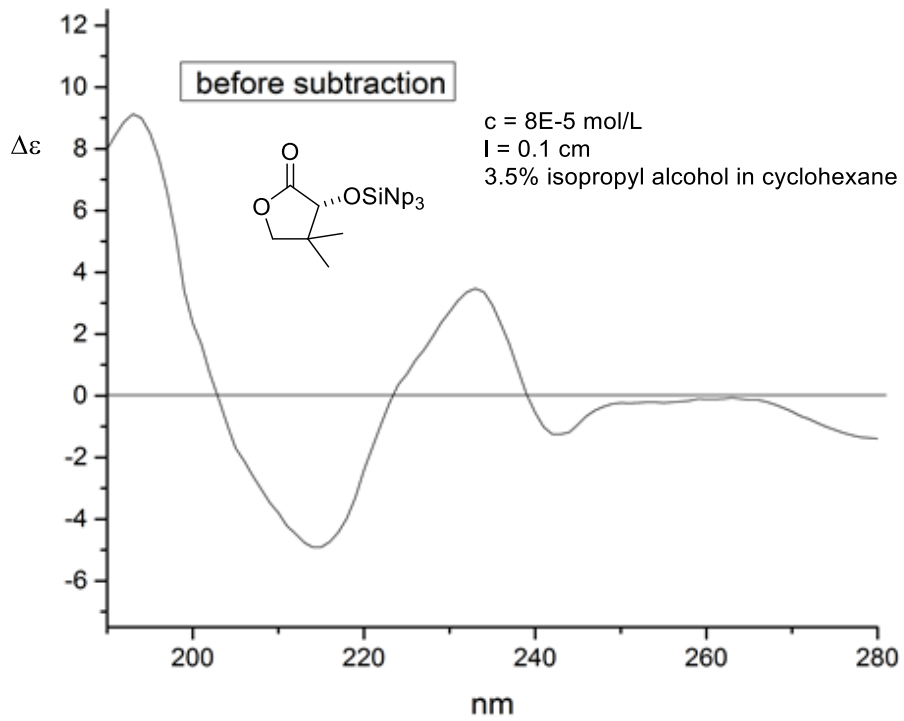
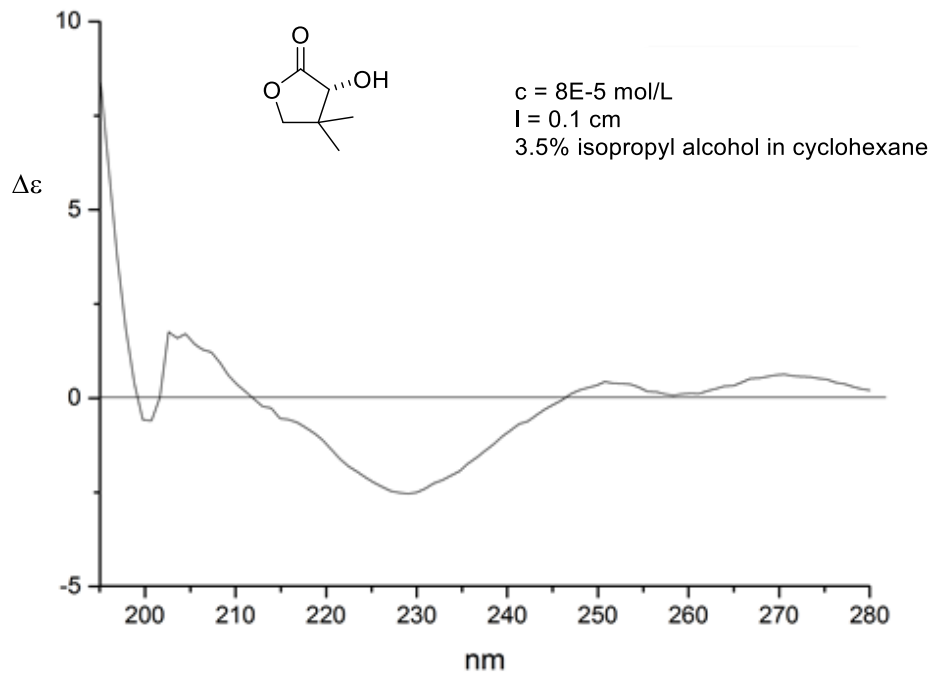
*(R)*-4,4-Dimethyl-3-((tri(naphthalen-2-yl)silyl)oxy)dihydrofuran-2(3H)-one **((R)-3.7)**

**Circular Dichroism Spectra:**

Table 3.2, Entry 4:



CD $\Delta\epsilon(\text{nm})$		UV $\epsilon(\text{nm})$	
5.3	232	390295	236
-4.1	214		



## Crystal structure data

**X-Ray Structure Determination of (S)-3.2.** X-ray intensity data from a colorless plate crystal were collected at 296(2) K using a Bruker SMART APEX diffractometer (Mo K $\alpha$  radiation,  $\lambda = 0.71073$  Å).<sup>44</sup> The raw area detector data frames were reduced with the Bruker SAINT+ program.<sup>44</sup> Final unit cell parameters were determined by least-squares refinement of 2025 reflections from the data set. Direct methods structure solution, difference Fourier calculations and full-matrix least-squares refinement against  $F^2$  were performed with SHELXS/L<sup>45</sup> as implemented in OLEX2<sup>46</sup>.

The compound crystallizes in the monoclinic system. Intensity statistics indicated an acentric structure (mean  $|E^*E-1| = 0.722$ ). The space group  $P2_1$  and  $P2_1/m$  were consistent with the pattern of systematic absences in the intensity data.  $P2_1$  was confirmed by obtaining a physically sensible and stable solution and refinement of the structure. The structure solution was checked for missed symmetry elements with the ADDSYM program run from PLATON<sup>47-50</sup>, which found none. The absolute structure (Flack) parameter after the final refinement cycle was 0.04(11). The asymmetric unit consists of one molecule. Non-hydrogen atoms were refined with anisotropic displacement parameters. Hydrogen atoms were placed in geometrically idealized positions and included as riding atoms.



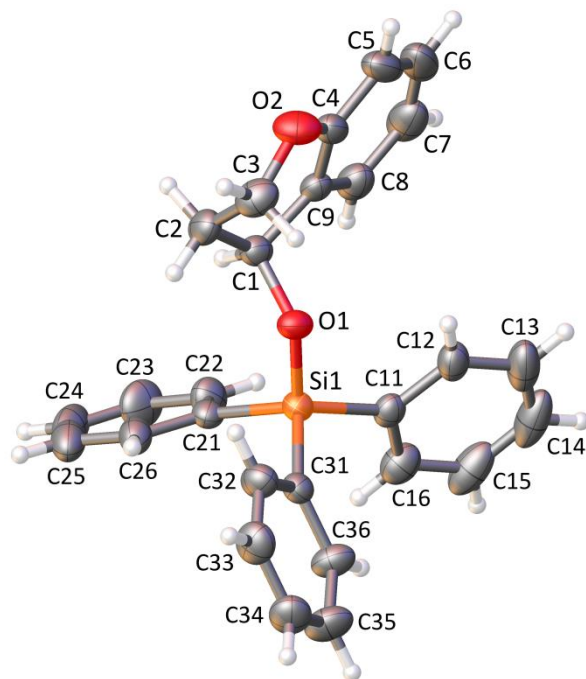


**Figure 3.8** Molecular structure. Displacement ellipsoids drawn at the 30% probability level. The crystal is enantiomerically pure; all molecules in the crystal are identical. C1 determined by the X-ray data to have the “S” conformation.

**X-Ray Structure Determination of (*R*)-5.** X-ray intensity data from a colorless plate crystal were collected at 200(2) K using a Bruker SMART APEX diffractometer (Mo K $\alpha$  radiation,  $\lambda = 0.71073 \text{ \AA}$ )<sup>44</sup>. The raw area detector data frames were reduced with the Bruker SAINT+ program.<sup>44</sup> Final unit cell parameters were determined by least-squares refinement of 4370 reflections from the data set. Direct methods structure solution, difference Fourier calculations and full-matrix least-squares refinement against  $F^2$  were performed with SHELXS/L<sup>45</sup> as implemented in OLEX2.<sup>46</sup>

The compound crystallizes in the monoclinic system. Intensity statistics indicated an acentric structure (mean  $|E^*E-1| = 0.752$ ). The space group  $P2_1$  and  $P2_1/m$  were consistent with the pattern of systematic absences in the intensity data.  $P2_1$  was confirmed

by obtaining a physically sensible and stable solution and refinement of the structure. The structure solution was checked for missed symmetry elements with the ADDSYM program run from PLATON<sup>47-50</sup>, which found none. The absolute structure (Flack) parameter after the final refinement cycle was 0.03(9). The asymmetric unit consists of one molecule. Non-hydrogen atoms were refined with anisotropic displacement parameters. Hydrogen atoms were placed in geometrically idealized positions and included as riding atoms.

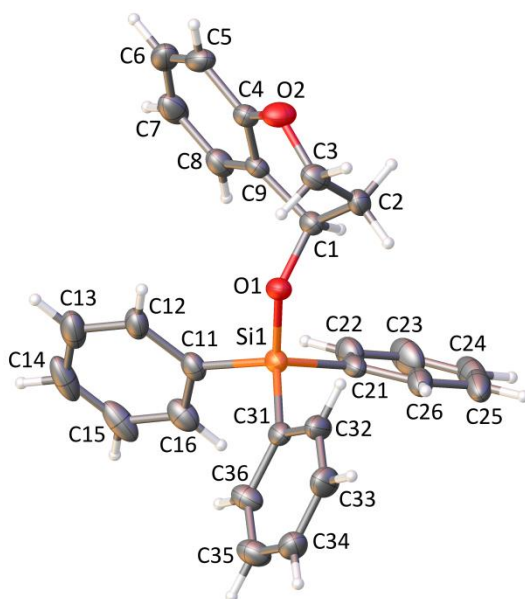


**Figure 3.9** Molecular structure. Displacement ellipsoids drawn at the 30% probability level. The crystal is enantiomerically pure; all molecules in the crystal are identical. C1 determined by the X-ray data to have the “R” conformation

**X-Ray Structure Determination of 3.4.** X-ray intensity data from a colorless plate crystal were measured at 100(2) K using a Bruker SMART APEX diffractometer (Mo K $\alpha$  radiation,  $\lambda = 0.71073 \text{ \AA}$ )<sup>44</sup>. The raw area detector data frames were reduced and corrected for absorption effects with the SAINT+ and SADABS programs<sup>45</sup>. Final unit cell parameters were determined by least-squares refinement of 6635 reflections from the data set. Direct

methods structure solution, difference Fourier calculations and full-matrix least-squares refinement against  $F^2$  were performed with SHELXS/L<sup>45</sup> as implemented in OLEX2.<sup>46</sup>

The compound crystallizes in the triclinic crystal system. The space group P1 (No. 1) was eventually confirmed by obtaining a stable and sensible solution and refinement of the structure. The absolute structure (Flack) parameter refined to 0.02(8), indicating the correct crystal handedness and the absence of inversion twinning. A solution in space group P-1 (No. 2) showed that adjacent tri(phenyl)silicon groupings are actually consistent with the inversion symmetry in P-1, but that the  $-C_{10}H_{17}$  substituents are not, as the inversion operation imposes two-fold disorder on this part of the molecule. The structure is therefore partly but not entirely consistent with P-1 and is pseudosymmetric. The asymmetric unit in the correct space group P1 (No. 1) consists of two independent, chemically identical but conformationally distinct molecules. Non-hydrogen atoms were refined with anisotropic displacement parameters. Hydrogen atoms were placed in geometrically idealized positions and included as riding atoms.

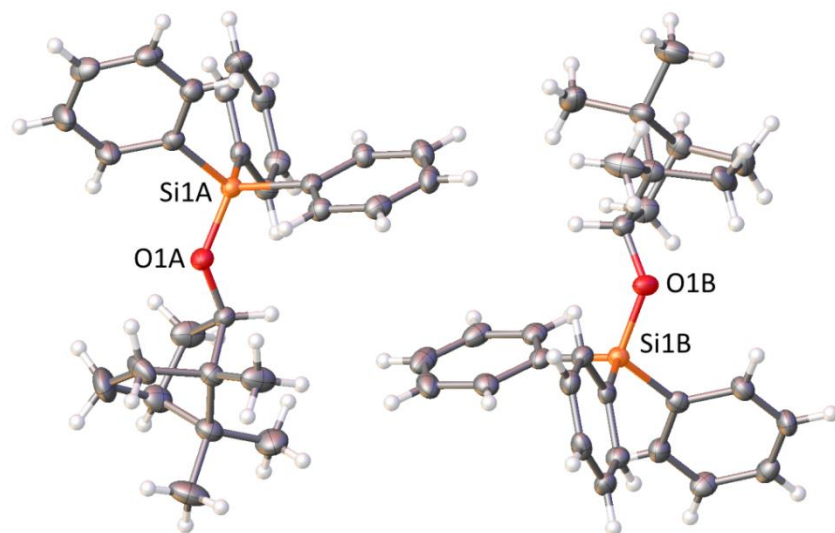


**Figure 3.10** Asymmetric unit of the crystal. Two independent, chemically identical but conformationally distinct molecules, labeled “A” and “B”.

**Table 3.5** Crystal Data and Structure Refinement for (*S*)-**3.2**

Identification code	PJSI19
Empirical formula	$C_{27}H_{24}O_2Si$
Formula weight	408.55
Temperature/K	296(2)
Crystal system	monoclinic
Space group	P21
$a/\text{\AA}$	10.9603(11)
$b/\text{\AA}$	7.6260(8)
$c/\text{\AA}$	13.2439(14)
$\alpha/^\circ$	90.00
$\beta/^\circ$	92.830(3)
$\gamma/^\circ$	90.00
Volume/ $\text{\AA}^3$	1105.6(2)

Z	2
$\rho_{\text{calc}}/\text{mm}^3$	1.227
m/mm 1	0.127
F (000)	432.0
Crystal size/mm <sup>3</sup>	0.38 × 0.34 × 0.12
2 $\Theta$ range for data collection	3.08 to 50.02°
Index ranges	-12 ≤ h ≤ 13, -9 ≤ k ≤ 9, -15 ≤ l ≤ 15
Reflections collected	12988
Independent reflections	3883[R(int) = 0.0597]
Data/restraints/parameters	3883/1/271
Goodness-of-fit on F <sup>2</sup>	0.860
Final R indexes [ $I \geq 2\sigma(I)$ ]	R1 = 0.0421, wR2 = 0.0658
Final R indexes [all data]	R1 = 0.0634, wR2 = 0.0721
Largest diff. peak/hole / e Å <sup>-3</sup>	0.24/-0.16
Flack parameter	0.04(11)

**Table 3.6.** Crystal Data and Structure Refinement for (*R*)-3.2

Identification code	mmm119am
Empirical formula	C <sub>27</sub> H <sub>24</sub> O <sub>2</sub> Si
Formula weight	408.55
Temperature/K	200(2)
Crystal system	monoclinic
Space group	P21
a/Å	11.0421(6)
b/Å	7.5831(4)
c/Å	12.9825(7)
α/°	90.00
β/°	92.9590(10)
γ/°	90.00
Volume/Å <sup>3</sup>	1085.62(10)
Z	2
ρ <sub>calc</sub> /mm <sup>3</sup>	1.250
m/mm 1	0.129
F (000)	432.0
Crystal size/mm <sup>3</sup>	0.32 × 0.28 × 0.12
2θ range for data collection	3.14 to 52.74°
Index ranges	-13 ≤ h ≤ 13, -9 ≤ k ≤ 9, -16 ≤ l ≤ 16
Reflections collected	15452
Independent reflections	4452[R(int) = 0.0422]

Data/restraints/parameters	4452/1/271
Goodness-of-fit on F2	0.955
Final R indexes [ $I \geq 2\sigma(I)$ ]	R1 = 0.0376, wR2 = 0.0740
Final R indexes [all data]	R1 = 0.0458, wR2 = 0.0772
Largest diff. peak/hole / e Å <sup>-3</sup>	0.20/-0.17
Flack parameter	0.03(9)

**Table 3.7.** Crystal Data and Structure Refinement for **3.4**.

Identification code	CIS-497
Empirical formula	C <sub>28</sub> H <sub>32</sub> OSi
Formula weight	412.63
Temperature/K	100(2)
Crystal system	triclinic
Space group	P1 (No. 1)
a/Å	10.4387(6)
b/Å	11.1375(6)
c/Å	11.3286(6)
$\alpha$ /°	91.3171(12)
$\beta$ /°	113.6586(10)
$\gamma$ /°	104.2860(11)
Volume/Å <sup>3</sup>	1157.97(11)
Z	2

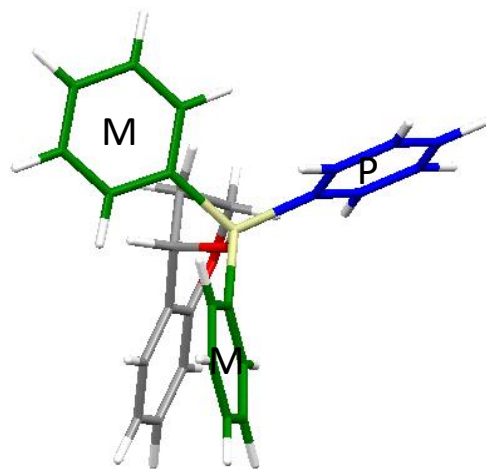
$\rho_{\text{calc}}/\text{mm}^3$	1.183
m/mm <sup>1</sup>	0.118
F (000)	444.0
Crystal size/mm <sup>3</sup>	0.54 × 0.36 × 0.06
2 $\Theta$ range for data collection	3.8 to 52.78°
Index ranges	-13 ≤ h ≤ 13, -13 ≤ k ≤ 13, -14 ≤ l ≤ 14
Reflections collected	17804
Independent reflections	9341[R(int) = 0.0259]
Data/restraints/parameters	9341/3/547
Goodness-of-fit on F <sup>2</sup>	1.030
Final R indexes [I ≥ 2σ (I)]	R1 = 0.0418, wR2 = 0.0961
Final R indexes [all data]	R1 = 0.0480, wR2 = 0.0999
Largest diff. peak/hole / e Å <sup>-3</sup>	0.45/-0.18
Flack parameter	0.02(8)

### Molecular Modeling Information

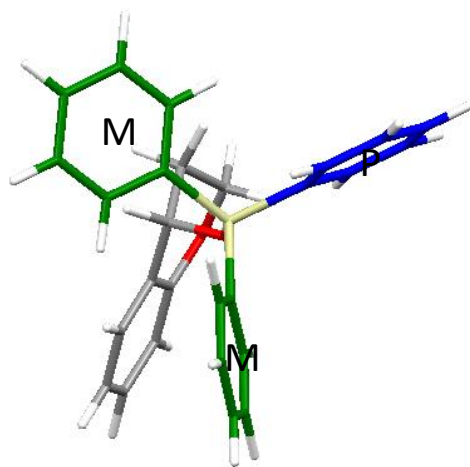
Conformer searches were carried out using the Monte Carlo for Complex Chemical System (MCCCS) Towhee<sup>51</sup> plug-in built into Sciencomics' Materials Processes and Simulations (MAPS) platform<sup>52</sup>. The conformers with energies within 2 kcal/mol relative to the lowest energy conformer were selected and the structures were optimized using DFT (B3LYP) with 6-311++\*\* basis set in Spartan<sup>53</sup>. For all optimized structures, frequency calculations were carried out at the same level of theory to confirm that the conformers were stable. A



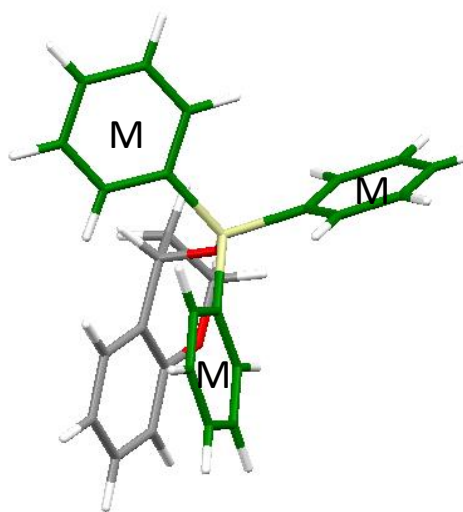
Boltzmann distribution of the selected conformers was calculated on the basis of  $\Delta G$  and  $T = 298 \text{ K}$ .



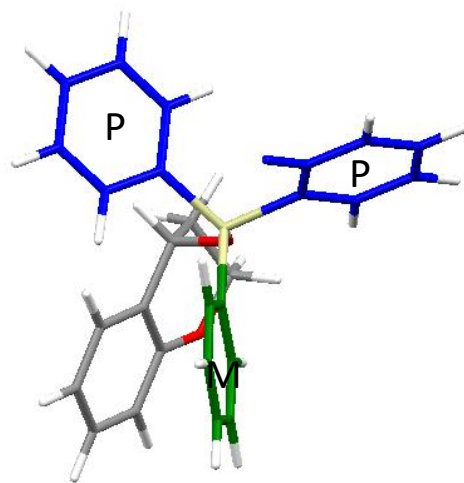
*MPM* table 3.4, entry 1



*MPM* table 3.4, entry 2



*MMM* table 3.4, entry 3



*PMP* table 3.4, entry 4

**Figure 3.11** Calculated conformers of (*S*)-3.2 with the lowest energy

**Table 3.8.** Absolute Energies of the Conformers of (S)-3.2:

<i>MPM 1</i>	-1483.64749 au
<i>MPM 2</i>	-1450.64854 au
<i>MMM</i>	-1450.64632 au
<i>PMP</i>	-1450.64487 au

**Table 3.9.** Cartesian Coordinates of the Conformers of (S)-3.2:

***MPM 1***

	X	Y	Z
Si	-0.079778	0.399407	-0.692982
O	1.008222	-0.509593	0.299019
O	2.933222	-2.649593	2.368019
C	0.618222	-1.777593	0.771019
H	-0.387778	-2.114593	0.431019
C	1.626222	-2.812593	0.267019
H	1.263222	-3.838593	0.499019
H	1.740222	-2.733593	-0.835982
C	2.978222	-2.596593	0.956019
H	3.676223	-3.385593	0.606019
H	3.416222	-1.621593	0.646019
C	1.803222	-2.123593	2.977019
C	1.814222	-2.034593	4.376019
H	2.694222	-2.336593	4.930019

C	0.701222	-1.558593	5.072019
H	0.725222	-1.494593	6.152019
C	-0.444778	-1.170593	4.375019
H	-1.307778	-0.803593	4.915019
C	-0.477778	-1.254593	2.981019
H	-1.371778	-0.943593	2.456019
C	0.636222	-1.735593	2.274019
C	-0.977778	1.637408	0.356019
C	-2.100778	2.311408	-0.150981
H	-2.476778	2.102408	-1.144982
C	-2.758778	3.268408	0.626019
H	-3.625778	3.781408	0.231019
C	-2.296778	3.565408	1.910019
H	-2.806778	4.307408	2.511019
C	-1.169778	2.910408	2.415019
H	-0.807778	3.146408	3.408019
C	-0.505778	1.956408	1.638019
H	0.372222	1.474408	2.048019
C	-1.242778	-0.640593	-1.702982
C	-0.839778	-1.151593	-2.945982
H	0.148222	-0.946593	-3.341982
C	-1.718778	-1.928593	-3.706982
H	-1.408778	-2.308593	-4.671982

C	-2.998778	-2.215593	-3.222982
H	-3.679778	-2.813593	-3.813982
C	-3.395778	-1.733593	-1.972982
H	-4.383778	-1.961593	-1.594982
C	-2.519778	-0.955593	-1.210982
H	-2.848778	-0.600593	-0.242981
C	0.956222	1.429407	-1.836982
C	2.352222	1.470408	-1.695982
H	2.857222	0.897407	-0.927982
C	3.124222	2.257408	-2.555982
H	4.200223	2.283408	-2.444982
C	2.508222	3.012408	-3.557982
H	3.107222	3.621408	-4.221982
C	1.118222	2.979408	-3.700982
H	0.641222	3.565408	-4.475982
C	0.344222	2.192408	-2.843982
H	-0.730778	2.182408	-2.977982

### **MPM 2**

	X	Y	Z
Si	-0.585148	0.513537	0.333389
O	0.104852	-0.363463	-0.988611
O	1.134852	-2.716463	-3.494611

C	0.482852	-1.706463	-0.807611
H	0.462852	-2.061463	0.247389
C	-0.462148	-2.603463	-1.610611
H	-0.295148	-3.668463	-1.336611
H	-1.520148	-2.353463	-1.377611
C	-0.194148	-2.428463	-3.108611
H	-0.870148	-3.110463	-3.665611
H	-0.449148	-1.393463	-3.428611
C	2.132852	-2.283463	-2.634611
C	3.453852	-2.352463	-3.096611
H	3.658852	-2.709463	-4.098611
C	4.518852	-1.955463	-2.283611
H	5.532852	-2.007463	-2.656611
C	4.274852	-1.489463	-0.989611
H	5.099852	-1.178463	-0.362611
C	2.966852	-1.423463	-0.507611
H	2.792852	-1.050463	0.495389
C	1.892852	-1.831463	-1.314611
C	0.668852	1.779537	0.847389
C	0.534852	2.458537	2.068389
H	-0.292148	2.250537	2.736389
C	1.481852	3.412537	2.452389
H	1.379852	3.925537	3.400389

C	2.560852	3.705537	1.614389
H	3.294852	4.443537	1.912389
C	2.690852	3.046537	0.389389
H	3.523852	3.277537	-0.262611
C	1.746852	2.090537	0.003389
H	1.871852	1.598537	-0.953611
C	-1.114148	-0.535463	1.774389
C	-2.398148	-1.100463	1.809389
H	-3.112148	-0.915463	1.016389
C	-2.778148	-1.918463	2.878389
H	-3.771148	-2.347463	2.905389
C	-1.875148	-2.188463	3.910389
H	-2.170148	-2.822463	4.736389
C	-0.588148	-1.647463	3.870389
H	0.115852	-1.865463	4.663389
C	-0.205148	-0.830463	2.802389
H	0.804852	-0.438463	2.787389
C	-2.037148	1.437537	-0.359611
C	-2.379148	1.311537	-1.716611
H	-1.811148	0.677537	-2.385611
C	-3.472148	2.010537	-2.235611
H	-3.730148	1.910537	-3.282611
C	-4.232148	2.839537	-1.405611

H	-5.078148	3.379537	-1.810611
C	-3.899148	2.967537	-0.054611
H	-4.489148	3.608537	0.587389
C	-2.806148	2.269537	0.468389
H	-2.570148	2.382537	1.519389

**MMM**

	X	Y	Z
Si	0.422889	-0.283944	0.686630
O	1.014889	0.592056	-0.683370
O	0.936889	1.784056	-3.930371
C	0.474889	1.846056	-1.024370
H	0.138889	2.428056	-0.136370
C	1.597889	2.648056	-1.687370
H	1.258889	3.688056	-1.888371
H	2.481889	2.703056	-1.014370
C	1.994889	1.980056	-3.013371
H	2.760889	2.615056	-3.505371
H	2.478889	0.999056	-2.816371
C	-0.330111	1.574056	-3.404371
C	-1.362111	1.321056	-4.318371
H	-1.143111	1.248056	-5.376371
C	-2.681111	1.168056	-3.883371

H	-3.468111	0.971056	-4.599371
C	-2.986111	1.284056	-2.527371
H	-4.008111	1.173056	-2.190371
C	-1.971111	1.535056	-1.603371
H	-2.230111	1.611056	-0.557370
C	-0.638111	1.668056	-2.025371
C	-1.107111	-1.207945	0.190630
C	-1.274111	-1.618945	-1.141370
H	-0.530111	-1.388945	-1.895370
C	-2.422111	-2.317945	-1.525370
H	-2.555111	-2.612945	-2.558371
C	-3.397111	-2.636945	-0.576370
H	-4.284111	-3.180945	-0.874370
C	-3.221111	-2.262945	0.757630
H	-3.969111	-2.522945	1.495630
C	-2.078111	-1.555945	1.142630
H	-1.961111	-1.287945	2.185630
C	0.199889	0.719056	2.238630
C	1.187889	0.729056	3.236630
H	2.102889	0.161056	3.127630
C	0.999889	1.466056	4.410630
H	1.758889	1.458056	5.182630
C	-0.169111	2.210056	4.592630



H	-0.316111	2.777056	5.502630
C	-1.150111	2.218056	3.598630
H	-2.057111	2.793056	3.738630
C	-0.966111	1.477056	2.427630
H	-1.751111	1.490056	1.685630
C	1.745889	-1.563945	0.927630
C	3.063889	-1.290945	0.522630
H	3.329889	-0.343944	0.069630
C	4.067889	-2.248945	0.690630
H	5.077889	-2.035945	0.364630
C	3.767889	-3.479945	1.278630
H	4.544889	-4.222945	1.403630
C	2.464889	-3.749945	1.706630
H	2.235889	-4.701945	2.168630
C	1.457889	-2.792945	1.539630
H	0.458889	-3.025945	1.883630

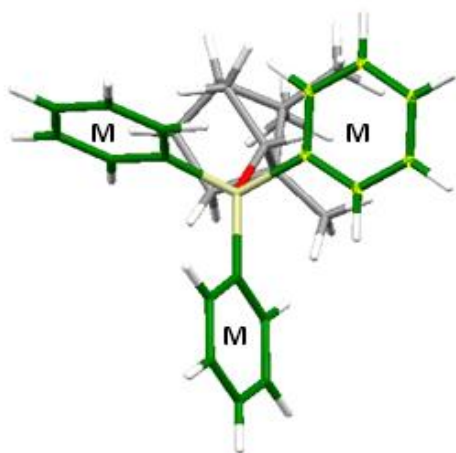
***PMP 1***

	X	Y	Z
Si	-0.484870	-0.276019	-0.582482
O	-1.060870	0.601982	0.797519
O	-0.637870	1.943982	4.058519
C	-0.478870	1.845982	1.114519

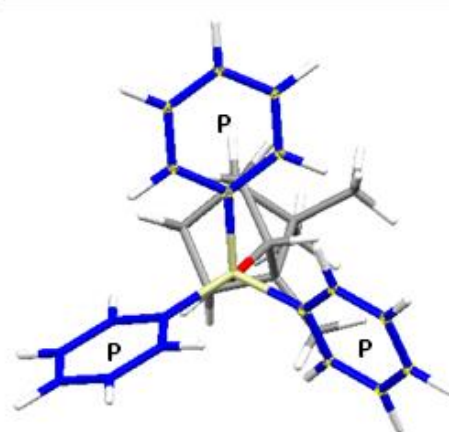
H	-0.209870	2.437982	0.210519
C	-1.533870	2.666982	1.860519
H	-1.179870	3.714982	1.987519
H	-2.481871	2.698982	1.279519
C	-1.785871	2.052982	3.243519
H	-2.523871	2.689982	3.775519
H	-2.249871	1.047982	3.139519
C	0.560130	1.661982	3.418519
C	1.677130	1.438982	4.234519
H	1.573130	1.449982	5.311519
C	2.936130	1.204982	3.675519
H	3.790130	1.030982	4.317519
C	3.095130	1.208982	2.289519
H	4.071130	1.032982	1.855519
C	1.995130	1.439982	1.461519
H	2.142130	1.441982	0.390519
C	0.722130	1.658982	2.011519
C	0.800130	-1.510019	-0.065482
C	1.514130	-2.232019	-1.034482
H	1.336130	-2.076019	-2.091482
C	2.480130	-3.166019	-0.650482
H	3.034130	-3.712019	-1.402482
C	2.732130	-3.394019	0.705519

H	3.483130	-4.115019	1.001519
C	2.007130	-2.699019	1.676519
H	2.196130	-2.882019	2.726519
C	1.035130	-1.769019	1.293519
H	0.480130	-1.255019	2.067519
C	0.022130	0.813982	-2.001482
C	-0.957870	1.524982	-2.711482
H	-2.005871	1.447982	-2.446482
C	-0.595870	2.340982	-3.788482
H	-1.355870	2.878982	-4.339482
C	0.747130	2.460982	-4.156482
H	1.027130	3.089982	-4.991482
C	1.729130	1.768982	-3.443482
H	2.770130	1.863982	-3.725482
C	1.370130	0.951982	-2.367482
H	2.153130	0.429982	-1.835482
C	-1.880870	-1.349019	-1.164482
C	-1.836871	-1.935019	-2.439482
H	-1.008870	-1.750019	-3.111482
C	-2.869871	-2.776019	-2.865482
H	-2.830871	-3.224019	-3.849482
C	-3.949871	-3.042019	-2.019482
H	-4.747871	-3.695019	-2.349482

C	-3.995871	-2.469019	-0.745482
H	-4.830871	-2.680019	-0.089481
C	-2.963871	-1.630019	-0.315482
H	-3.020871	-1.208019	0.679519



*MMM* table 3.4, entry 5



*PPP* table 3.4, entry 6

**Figure 3.12** Calculated conformers of **3.4** in a *MMM* and *PPP* helicity

**Table 3.10.** Absolute Energies of the Conformers of **3.4**

<i>MMM</i>	-1450.68644 au
<i>PPP</i>	-1450.68476 au

**Table 3.11.** Cartesian Coordinates of the Conformers of **3.4**.

**MMM**

	X	Y	Z
Si	0.344742	0.376113	-1.313565
O	-0.456258	0.375113	0.112436
C	-0.205258	-0.328887	1.325436
H	0.776742	-0.321887	1.518436
C	-0.963258	0.314113	2.500436
C	-2.442258	0.389113	2.088436
H	-2.536258	0.759113	1.173436
H	-2.957258	0.955113	2.717436
C	-2.928258	-1.080887	2.143436
H	-3.645258	-1.195887	2.816436
H	-3.261258	-1.380887	1.260436
C	-1.664258	-1.838887	2.544436
H	-1.827258	-2.753887	2.914436
C	-0.723258	-1.796887	1.326436
H	-1.212258	-2.002887	0.490436
H	0.024742	-2.438887	1.429436
C	-0.975258	-0.856887	3.528436
C	-0.369258	1.635113	2.947436
H	0.572742	1.506113	3.184436
H	-0.859258	1.964113	3.730436

H	-0.438258	2.287113	2.220436
C	0.402742	-1.323887	3.991436
H	0.935742	-1.586887	3.213436
H	0.301742	-2.091887	4.592436
H	0.851742	-0.593887	4.465436
C	-1.801258	-0.574887	4.787436
H	-1.349258	0.105113	5.329436
H	-1.893258	-1.399887	5.308436
H	-2.689258	-0.249887	4.529436
C	-0.753258	-0.410887	-2.613565
C	-2.149258	-0.291887	-2.529565
H	-2.539258	0.169113	-1.796565
C	-2.964258	-0.840887	-3.508565
H	-3.906258	-0.743887	-3.445565
C	-2.420258	-1.527887	-4.573565
H	-2.987258	-1.906887	-5.235565
C	-1.052258	-1.664887	-4.675565
H	-0.671258	-2.140887	-5.402565
C	-0.230258	-1.096887	-3.697565
H	0.712742	-1.183887	-3.779565
C	0.743742	2.155113	-1.714565
C	1.151742	3.023113	-0.695565
H	1.175742	2.711113	0.201436

C	1.520742	4.324113	-0.969565
H	1.782742	4.901113	-0.261565
C	1.508742	4.788113	-2.271565
H	1.768742	5.683113	-2.457565
C	1.117742	3.955113	-3.306565
H	1.103742	4.275113	-4.201565
C	0.744742	2.642113	-3.023565
H	0.486742	2.068113	-3.734565
C	1.952742	-0.585887	-1.248565
C	1.961742	-1.951887	-0.957565
H	1.139742	-2.397887	-0.789565
C	3.155742	-2.674887	-0.909565
H	3.142742	-3.603887	-0.710565
C	4.355742	-2.035887	-1.152565
H	5.169742	-2.523887	-1.113565
C	4.373742	-0.689887	-1.449565
H	5.199742	-0.251887	-1.613565
C	3.183742	0.028113	-1.508565
H	3.206742	0.953113	-1.729565

**PPP**

	X	Y	Z
Si	-0.294935	-0.143258	1.341581

O	0.558065	0.131742	-0.022419
C	0.278065	-0.195258	-1.390419
H	-0.702936	-0.346258	-1.511419
C	0.763065	0.916742	-2.351420
C	2.206065	1.249742	-1.955420
H	2.281065	1.407742	-0.981419
H	2.533065	2.049742	-2.439420
C	2.997065	-0.017258	-2.377420
H	3.707065	0.205742	-3.030420
H	3.407065	-0.459258	-1.591419
C	1.924065	-0.905258	-3.011420
H	2.277065	-1.605258	-3.630420
C	1.067065	-1.447258	-1.854419
H	1.635065	-1.804258	-1.126419
H	0.456065	-2.161258	-2.167420
C	0.974065	0.109742	-3.666420
C	-0.164936	2.115742	-2.405420
H	-1.050936	1.829742	-2.710420
H	0.196065	2.779742	-3.030420
H	-0.237936	2.513742	-1.513419
C	-0.292936	-0.516258	-4.251420
H	-0.779936	-0.989258	-3.544420
H	-0.048936	-1.148258	-4.959420



H	-0.862936	0.187742	-4.625420
C	1.624065	0.915742	-4.794420
H	1.024065	1.642742	-5.063420
H	1.790065	0.328742	-5.561420
H	2.472065	1.290742	-4.479420
C	0.775065	0.591742	2.673581
C	2.171065	0.496742	2.615581
H	2.576065	0.050742	1.881581
C	2.977065	1.039742	3.610581
H	3.922065	0.958742	3.555581
C	2.398065	1.695742	4.677581
H	2.948065	2.077742	5.350581
C	1.030065	1.795742	4.769581
H	0.635065	2.236742	5.513581
C	0.232065	1.256742	3.780581
H	-0.711936	1.338742	3.853581
C	-1.953936	0.730742	1.300581
C	-2.015936	2.099742	0.977581
H	-1.212936	2.564742	0.773581
C	-3.216936	2.786742	0.950581
H	-3.235936	3.711742	0.739581
C	-4.390936	2.111742	1.237581
H	-5.220936	2.573742	1.208581

C	-4.366936	0.764742	1.566581
H	-5.173936	0.306742	1.771581
C	-3.149936	0.087742	1.596581
H	-3.135936	-0.835258	1.823581
C	-0.636936	-1.947258	1.693581
C	-1.075936	-2.822258	0.695581
H	-1.138936	-2.512258	-0.200419
C	-1.422936	-4.141258	0.985581
H	-1.707936	-4.722258	0.291581
C	-1.353936	-4.603258	2.298581
H	-1.593936	-5.499258	2.501581
C	-0.934936	-3.752258	3.301581
H	-0.892936	-4.062258	4.197581
C	-0.574936	-2.443258	3.005581
H	-0.278935	-1.874258	3.705581

### 3.8 References

1. Jacobsen, E. N.; Pfaltz, A.; Yamamoto, H., *Comprehensive Asymmetric Catalysis I-III*. Springer-Verlag: New York, 1999; Vol. 1-3.
2. Noyori, R., Asymmetric catalysis: Science and opportunities (Nobel lecture). *Angew. Chem. Int. Ed.* **2002**, *41* (12), 2008-2022.
3. Ooi, T.; Maruoka, K., Recent advances in asymmetric phase-transfer catalysis. *Angew. Chem. Int. Ed.* **2007**, *46* (23), 4222-4266.
4. Wolf, C.; Bentley, K. W., Chirality sensing using stereodynamic probes with distinct electronic circular dichroism output. *Chem. Soc. Rev.* **2013**, *42* (12), 5408-5424.
5. Labuta, J.; Hill, J. P.; Ishihara, S.; Hanyková, L.; Ariga, K., Chiral Sensing by Nonchiral Tetrapyrroles. *Acc. Chem. Res.* **2015**, *48* (3), 521-529.
6. Ściebura, J.; Skowronek, P.; Gawroński, J., Trityl Ethers: Molecular Bevel Gears Reporting Chirality through Circular Dichroism Spectra. *Angew. Chem. Int. Ed.* **2009**, *48* (38), 7069-7072.
7. Katoono, R.; Kawai, H.; Fujiwara, K.; Suzuki, T., Dynamic Molecular Propeller: Supramolecular Chirality Sensing by Enhanced Chiroptical Response through the Transmission of Point Chirality to Mobile Helicity. *J. Am. Chem. Soc.* **2009**, *131* (46), 16896-16904.
8. Ściebura, J.; Gawroński, J., Double Chirality Transmission in Trityl Amines: Sensing Molecular Dynamic Stereochemistry by Circular Dichroism and DFT Calculations. *Chem. – Eur. J.* **2011**, *17* (47), 13138-13141.
9. Katoono, R.; Kawai, H.; Ohkita, M.; Fujiwara, K.; Suzuki, T., A C<sub>3</sub>-symmetric chiroptical molecular propeller based on hexakis(phenylethynyl)benzene with a threefold

terephthalamide: stereospecific propeller generation through the cooperative transmission of point chiralities on the host and guest upon complexation. *Chem. Commun.* **2013**, 49 (88), 10352-10354.

10. Katoono, R.; Fujiwara, K.; Suzuki, T., Complexation-induced inversion of helicity by an organic guest in a dynamic molecular propeller based on a tristerephthalamide host with a two-layer structure. *Chem. Commun.* **2014**, 50 (41), 5438-5440.

11. Prusinowska, N.; Bendzińska-Berus, W.; Jelecki, M.; Rychlewska, U.; Kwit, M., Triphenylacetic Acid Amides: Molecular Propellers with Induced Chirality. *Eur. J. Org. Chem.* **2015**, (4), 738-749.

12. Prusinowska, N.; Bendzińska-Berus, W.; Szymkowiak, J.; Warzajtis, B.; Gajewy, J.; Jelecki, M.; Rychlewska, U.; Kwit, M., Double helicity induction in chiral bis(triphenylacetamides). *Rsc. Adv.* **2015**, 5 (101), 83448-83458.

13. Clark, R. W.; Deaton, T. M.; Zhang, Y.; Moore, M. I.; Wiskur, S. L., Silylation-Based Kinetic Resolution of alpha-Hydroxy Lactones and Lactams. *Org. Lett.* **2013**, 15 (24), 6132-6135.

14. Gust, D.; Mislow, K., Analysis of Isomerization in Compounds Displaying Restricted Rotation of Aryl Groups. *J. Am. Chem. Soc.* **1973**, 95 (5), 1535-1547.

15. Boettche.Rj; Gust, D.; Mislow, K., Dynamic Stereochemistry of Triarylsilanes. *J. Am. Chem. Soc.* **1973**, 95 (21), 7157-7158.

16. Mislow, K., Stereochemical Consequences of Correlated Rotation in Molecular Propellers. *Acc. Chem. Res.* **1976**, 9 (1), 26-33.

17. Hummel, J. P.; Zurbach, E. P.; Dicarolo, E. N.; Mislow, K., Conformational-Analysis of Triarylsilanes. *J. Am. Chem. Soc.* **1976**, 98 (24), 7480-7483.

18. Iwamura, H.; Mislow, K., Stereochemical Consequences of Dynamic Gearing. *Acc. Chem. Res.* **1988**, *21* (4), 175-182.
19. Rappoport, Z.; Biali, S. E., Threshold rotational mechanisms and enantiomerization barriers of polyarylvinyll propellers. *Acc. Chem. Res.* **1997**, *30* (8), 307-314.
20. Lightner, D. A.; Gurst, J. E., *Organic Conformational Analysis and Stereochemistry from Circular Dichroism Spectroscopy*. Wiley-VCH: New York, 2000.
21. Skowronek, P.; Scianowski, J.; Pacula, A. J.; Gawronski, J., Chirality transfer through sulfur or selenium to chiral propellers. *Rsc. Adv.* **2015**, *5* (85), 69441-69444.
22. Wuts, P. G. M.; Greene, T. W., *Protective Groups in Organic Synthesis* 3rd ed.; Wiley-Interscience: New York, 1999.
23. Blackwell, J. M.; Foster, K. L.; Beck, V. H.; Piers, W. E., B(C<sub>6</sub>F<sub>5</sub>)<sub>3</sub>-catalyzed silylation of alcohols: A mild, general method for synthesis of silyl ethers. *J. Org. Chem.* **1999**, *64* (13), 4887-4892.
24. Berova, N.; Nakanishi, K.; Woody, R. W., *Circular Dichroism-Principles and Applications*. 2nd ed.; Wiley-VCH: New York, 2000.
25. Berova, N., Polavarapu, P. L., Nakanishi, K., Woody, R. W., *Comprehensive Chiroptical Spectroscopy: Applications in Stereochemical Analysis of Synthetic Compounds, Natural Products, and Biomolecules*. John Wiley & Sons: 2012; Vol. 2.
26. Sreerama, N.; Woody, R. W., Estimation of protein secondary structure from circular dichroism spectra: Comparison of CONTIN, SELCON, and CDSSTR methods with an expanded reference set. *Anal. Biochem.* **2000**, *287* (2), 252-260.

27. Hall, V.; Sklepari, M.; Rodger, A., Protein Secondary Structure Prediction from Circular Dichroism Spectra Using a Self-Organizing Map with Concentration Correction. *Chirality*. **2014**, *26* (9), 471-482.
28. Woody, R. W., The development and current state of protein circular dichroism. *Biomed. Spectrosc. Ima*. **2015**, *4* (1), 5-34.
29. Berova, N.; Di Bari, L.; Pescitelli, G., Application of electronic circular dichroism in configurational and conformational analysis of organic compounds. *Chem. Soc. Rev.* **2007**, *36* (6), 914-931.
30. Pescitelli, G.; Di Bari, L.; Berova, N., Conformational aspects in the studies of organic compounds by electronic circular dichroism. *Chem. Soc. Rev.* **2011**, *40* (9), 4603-4625.
31. Dinitto, J. M.; Kenney, J. M., Noise Characterization in Circular Dichroism Spectroscopy. *Appl. Spectrosc.* **2012**, *66* (2), 180-187.
32. Savitzky, A.; Golay, M. J. E., Smoothing + Differentiation of Data by Simplified Least Squares Procedures. *Anal. Chem.* **1964**, *36* (8), 1627-&.
33. Crabbe, P., *Optical Rotatory Dispersion and Circular Dichroism In Organic Chemistry*. Holden-Day: San Francisco, 1965.
34. Kalsi, P. S., *Spectroscopy of Organic Compounds*. New Age International: New Delhi, 2007.
35. Cottrell, T. L., *The Strengths of Chemical Bonds*. 2nd ed.; Butterworths: London, 1958.
36. Wikipedia  
[https://en.wikipedia.org/wiki/Monte\\_Carlo\\_molecular\\_modeling](https://en.wikipedia.org/wiki/Monte_Carlo_molecular_modeling).

37. Lee, C.; Yang, W.; Parr, R. G., *Phys. Rev. B* **1988**, *37* 785-789.
38. Becke, A. D., *J. Chem. Phys.* **1993**, *98* 5648-5652
39. *Spartan 10, Program for Calculation of Molecular Properties, Wavefunction Inc.*  
Irvine, CA, USC, 2015
40. Hayase, S.; Onishi, Y.; Suzuki, S.; Wada, M., Photopolymerization of Cyclohexene Oxide by the Use of Photodecomposable Silyl Peroxide - Aluminum Complex Arylsilyl Peroxide Catalyst. *Macromolecules*. **1986**, *19* (4), 968-973.
41. Lage, M. L.; Bader, S. J.; Sa-ei, K.; Montgomery, J., Chemoselective hydrosilylation of hydroxyketones. *Tetrahedron*. **2013**, *69* (27-28), 5609-5613.
42. Alberti, A.; Guerra, M.; Pedulli, G. F., C-13 Hyperfine Splittings and Geometry at the Radical Center in Bicyclo[2.2.1]Hept-2-Yl Radicals. *J. Am. Chem. Soc.* **1981**, *103* (22), 6604-6606.
43. Sheppard, C. I.; Taylor, J. L.; Wiskur, S. L., Silylation-Based Kinetic Resolution of Monofunctional Secondary Alcohols. *Org. Lett.* **2011**, *13* (15), 3794-3797.
44. *SMART Version 5.630, SAINT+ Version 6.45. Bruker Analytical X-ray Systems*,. Madison, Wisconsin, USA., 2003.
45. Sheldrick, G. M., A short history of SHELX. *Acta. Crystallogr. A*. **2008**, *64*, 112-122.
46. Dolomanov, O. V.; Bourhis, L. J.; Gildea, R. J.; Howard, J. A. K.; Puschmann, H., OLEX2: a complete structure solution, refinement and analysis program. *J. Appl. Crystallogr.* **2009**, *42*, 339-341.
47. Lepage, Y., Computer Derivation of the Symmetry Elements Implied in a Structure Description. *J. Appl. Crystallogr.* **1987**, *20*, 264-269.

48. Spek, A. L., Lepage - an Ms-Dos Program for the Determination of the Metrical Symmetry of a Translation Lattice. *J. Appl. Crystallogr.* **1988**, *21*, 578-579.
49. Vandersluis, P.; Spek, A. L., Bypass - an Effective Method for the Refinement of Crystal-Structures Containing Disordered Solvent Regions. *Acta. Crystallogr. A.* **1990**, *46*, 194-201.
50. Spek, A. L., *PLATON, A Multipurpose Crystallographic Tool*. Utrecht University: Utrecht, The Netherlands, 1998.
51. Martin, M. G., MCCCCS Towhee: a tool for Monte Carlo molecular simulation. *Mol. Simulat.* **2013**, *39* (14-15), 1184-1194.
52. *Materials and Processes Simulations (MAPS)*, Copyright Scienomics SARL. Paris, France., 2004-2013.
53. Wavefunction Inc.: Irvine, CA, USA, 2015.



## CHAPTER 4

# MECHANISTIC INVESTIGATION OF Silylation-based KINETIC RESOLUTIONS: STEREOCHEMISTRY STUDIES OF SILICON

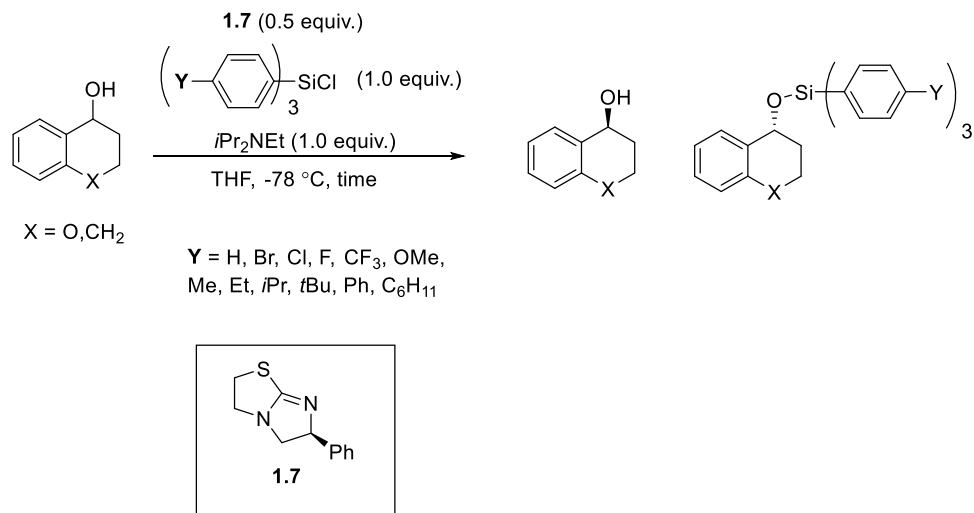
### 4.1 Introduction

In this chapter, the endeavors to understand the mechanism of silylation-based kinetic resolutions will be addressed. The efforts will be focused on investigating the orientation of how everything comes together during nucleophilic displacement on a chiral silicon compound, resulting in either retention or inversion of the silicon chiral center. This can be achieved by studying the stereogenic center at silicon of an enantiopure chiral silane. The goal of the work described herein is to depict a complete mechanistic picture of silylation-based kinetic resolution, along with other approaches currently ongoing in the lab.

In Chapter 3, we showed evidence of chirality transmission from point chirality to helical chirality of a triphenylsilyl group through CD spectroscopy, crystal structures and molecular modeling. This helps us understand the importance of the three phenyl groups at silicon for good selectivity (See Chapter 3 for detailed discussions).

Previously, a linear-free energy relationship study<sup>1</sup> was conducted in the Wiskur group to investigate the electronic and steric effects around the triphenylsilyl chloride in the silylation-based kinetic resolution. This study employed two different benzylic

alcohols, 4-chromanol and  $\alpha$ -tetralol, and a variety of synthetically prepared triphenylsilyl chlorides bearing *para*-electron-withdrawing or *para*-electron-donating groups (Scheme 4.1). The results showed electron-donating groups slow down the reaction rate and improve selectivity, while electron-withdrawing groups increase the reaction rate and decrease selectivity. A weak correlation of selectivity factors to Charton<sup>2-6</sup> values was observed, indicating a small steric effect of the substituents on the *para* position of the triphenylsilyl chloride to the selectivity. The electronic effects, on the other hand, were found to have a much larger impact on selectivity. According to the Hammond postulate, the electron-donating groups result in a late transition state, in which the incoming alcohol is more involved in the rate-determining step. Therefore, the diastereomeric transition states between the two enantiomers have a larger energy difference as compared to electron-withdrawing substituted triphenylsilyl chlorides. The rate data suggests a significant redistribution of charge occurs in the transition state, with an overall decrease in positive charge or increase of negative charge. This also gave us an initial hypothesis that the enantioselective step proceeds through a tetracoordinate intermediate with an S<sub>N</sub>2-like alcohol attack on the catalyst activated silyl chloride.

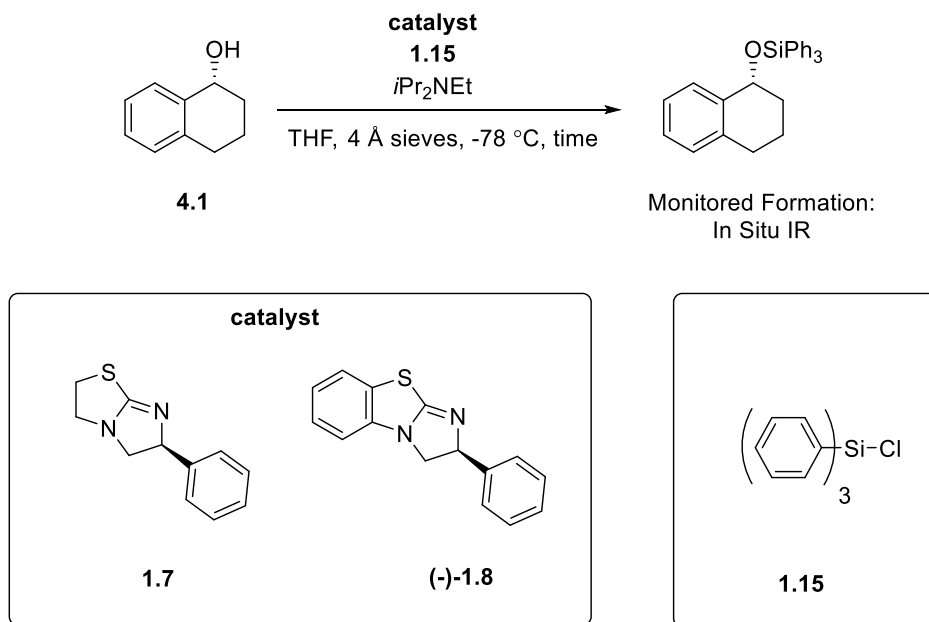


### Scheme 4.1 Linear-Free Energy Relationship Studies of Triarylsilyl Chlorides

With the linear-free energy relationship data in hand, we next turned to investigate the kinetics of this silylation methodology through reaction progress kinetic analysis (RPKA). The RPKA is an efficient method for kinetic analysis developed by Blackmond<sup>7</sup>, and it has been successfully employed to investigate a variety of complex, catalytic reactions.<sup>8-11</sup> The RPKA allows the investigators to gather kinetic data in fewer experiments than classic approaches while running kinetic experiments under conditions similar to actual reaction conditions. This means that one can avoid the use of reagents in ten-fold excess common to classic approaches,<sup>12</sup> which provides data that should be more accurate to the true catalytic cycle.

The fast reacting enantiomer (*R*)-tetralol **4.1** was used in these kinetic experiments with catalysts **1.7** and (-)-**1.8**. Reaction conditions were similar to the previously optimized conditions employing triphenylsilyl chloride **1.15** as the silyl source and *iPr*<sub>2</sub>NEt as the base (Scheme 4.2). These kinetic analyses determined that the reaction was first order in catalyst and alcohol. The base had no effect on reaction rate (zero order), indicating a fast

deprotonation step after the rate determining step. The silyl chloride, however, had a fractional order between one and two, suggesting a complicated mechanism involving two different silicon intermediates. From this kinetic data, a mechanism was proposed involving both a pentacoordinate **4.2** and tetracoordinate **4.3** silicon species (Figure 4.1). The mechanistic cycle starts with an equilibrium between free catalyst (-)-**1.8** and the first equivalent of silyl chloride **1.15** to form the pentacoordinate silicon intermediate **4.2**. This intermediate was then reacted with the second equivalent of **1.15** to form the reactive tetracoordinate silicon intermediate **4.3** along with the pentacoordinate silicon **4.4**. The presumed rate determining step is the alcohol **4.1** attacking the reactive species **4.3** to yield the product. Since the base has a reaction order of zero, the next deprotonation step is considered to be fast and frees the catalyst to participate in the next cycle.



**Scheme 4.2 General Scheme of Kinetic Runs**

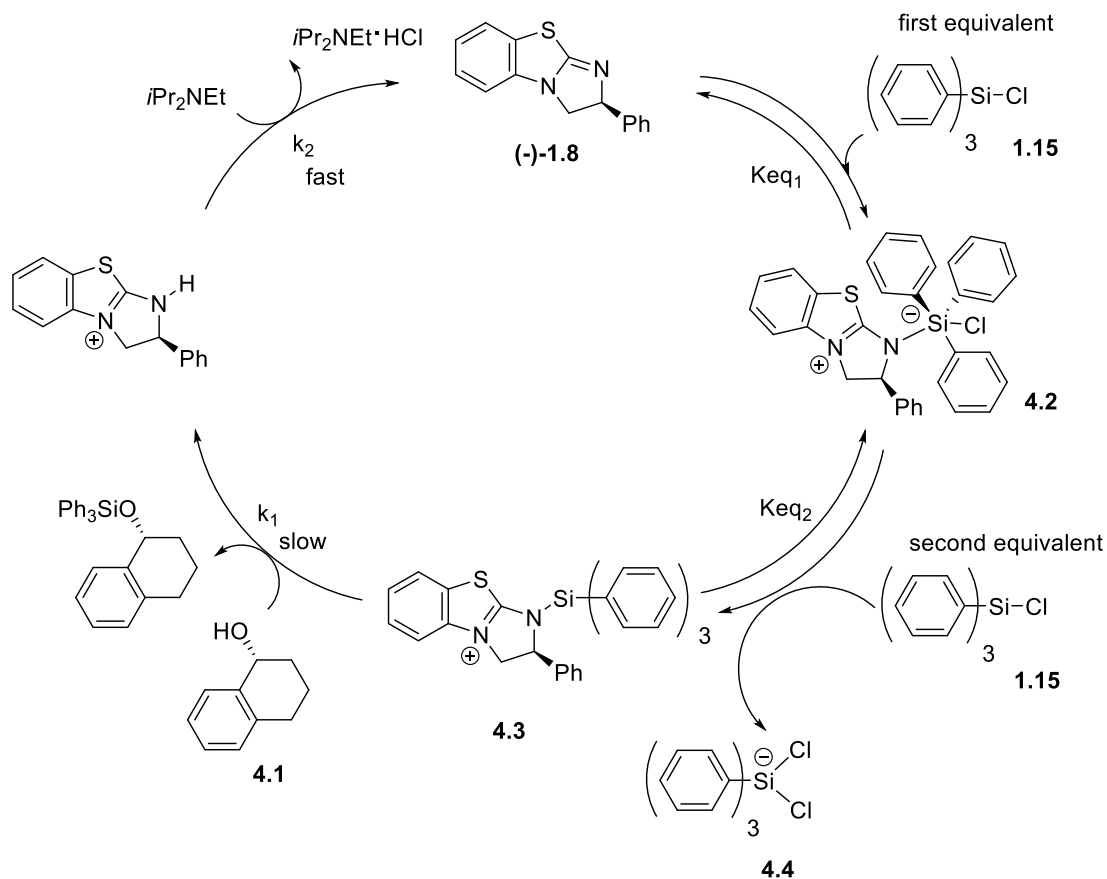


**Figure 4.1 Proposed Mechanistic Cycle of Silylation-Based Kinetic Resolution**

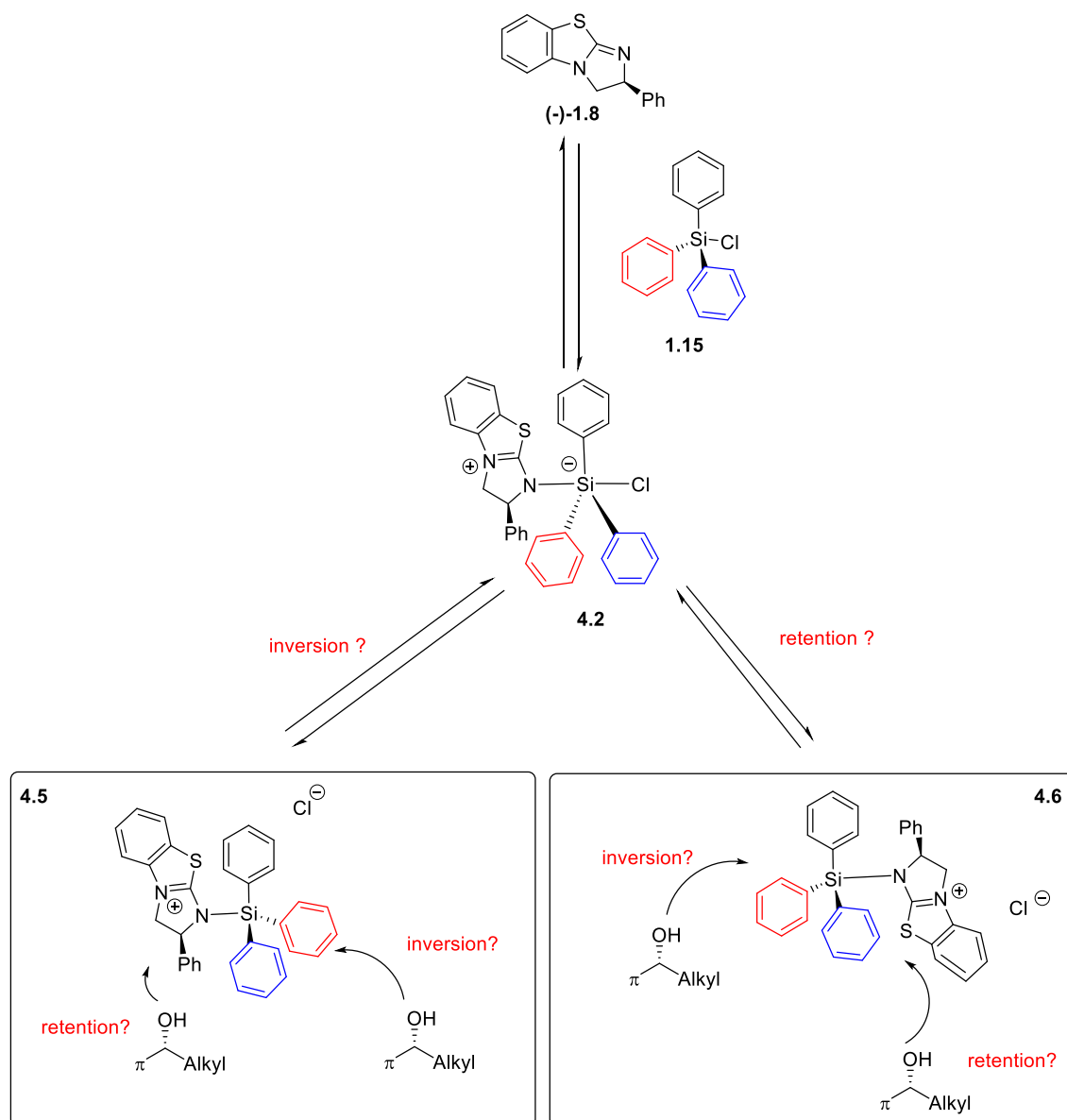
#### 4.2 Our Focus on Stereogenic Center at Silicon

With this kinetic data and proposed mechanistic cycle in hand, we next turned our focus on the investigation of the proposed transition state and intermediate. More specifically, we would like to study the chirality transmission on the stereogenic center at silicon in silylation-based kinetic resolutions. Determining the retention or inversion of nucleophilic displacement at silicon will provide useful information to elucidate the mechanism. pentacoordinate intermediate **4.2** has the possibility to go through a Berry pseudorotation<sup>13</sup> which will lead to a loss of stereochemical information instantaneously. However, if it goes through a fast pentacoordinate intermediate followed by a quick

transformation to tetracoordinate intermediate **4.3**, then this isn't a problem and the same level of stereochemical information should be retained at silicon (Figure 4.1).

As previously discussed, the pentacoordinate intermediate **4.2** will be converted to a reactive tetracoordinate intermediate **4.3** via interacting with the second equivalent of **1.15** (Figure 4.1). In terms of the nucleophilic displacement of chlorine at silicon, this process will undergo either an overall inversion of configuration to yield intermediate **4.5** or an overall retention of configuration to yield intermediate **4.6** (Scheme 4.3). For each of the possible tetracoordinate intermediates, the alcohol can approach from either the back side of the catalyst giving another inversion or from the same side of the catalyst through a retention of configuration pathway (Scheme 4.3).

Previous attempts to isolate or analyze the intermediates via low temperature and ambient temperature NMR have been unsuccessful. Thus, with the plausible outcomes showing in Scheme 4.3, an experiment-based approach to explore this species was designed where an enantiopure chiral silyl chloride could be used as a chiral probe in the kinetic resolution. We were hoping to understand the stereochemistry of the mechanism by investigating the absolute configuration of the silyl ether products derived from chiral silyl chlorides.



**Scheme 4.3 Step-Wise Investigations of Nucleophilic Displacement**

### 4.3 Previous Investigations of Nucleophilic Displacement at Silicon

Stereochemical studies of substitution at silicon by nucleophiles have been carried out decades ago.<sup>14-21</sup> Based on these previous investigations, it is summarized that the nucleophilic displacement reaction at silicon must proceed with either retention or inversion of configuration mainly based on the nature of the leaving group at silicon and

the electronic character of the nucleophile.<sup>18, 20</sup> Generally, the nature of the leaving group plays an important role to determine the configuration of displacement. With the specific focus on the silylation-based kinetic resolution, valuable information was obtained from Corriu's studies that the nucleophilic displacement of Si-H bond normally undergoes retention of configuration at silicon and the Si-Cl bond mainly proceeds with inversion of configuration.<sup>20</sup> This was explained by suggesting the tendency of an Si-X bond to be stretched in the pentacoordinate silicon intermediate under the influence of a nucleophile controls its ability to be cleaved with inversion (Figure 4.2).

In addition to the influence of the leaving group, the electronic character of the nucleophile also has a level of control on the stereochemistry at silicon which could be concluded as hard nucleophiles give predominant retention of configuration while softer nucleophiles normally proceed with inversion of configuration.<sup>20</sup>

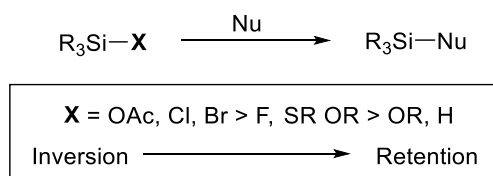


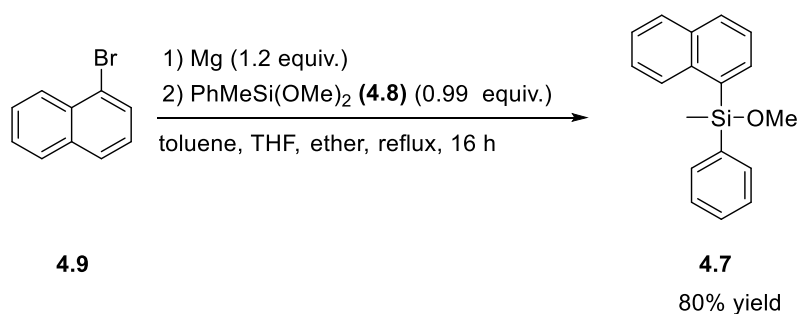
**Figure 4.2 Tendency of Si-X to Be Displaced with Inversion**

The most well studied chiral silane is the methyl(1-naphthyl)phenyl silane and its derivatives.<sup>22</sup> This specific chiral silane has been utilized as a chiral probe for the investigation of mechanisms in a variety of reactions, including reductions<sup>23</sup>, hydrolysis<sup>24</sup>, or other substitutions.<sup>14, 17, 21</sup>



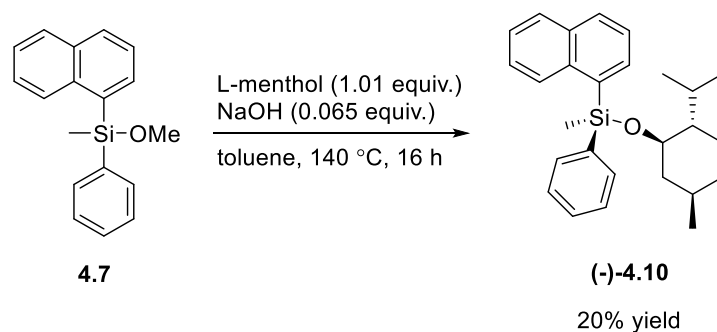
#### 4.4 Synthesis of Enantioenriched Chiral Silanes And Silyl Chlorides

Synthesis of the enantioenriched methyl(1-naphthyl)phenyl silane was prepared in a four-step synthesis according to existing literature procedures.<sup>14, 25</sup> To begin with, the racemic methoxymethylnaphthylphenyl silane **4.7** was prepared in excellent yield via a Grignard reaction, replacing a methoxy group from commercially available dimethoxymethylphenyl silane **4.8** with 1-naphthylmagnesium bromide **4.9** (Scheme 4.4).



**Scheme 4.4 Synthesis of Racemic Methoxymethylnaphthylphenyl Silane**

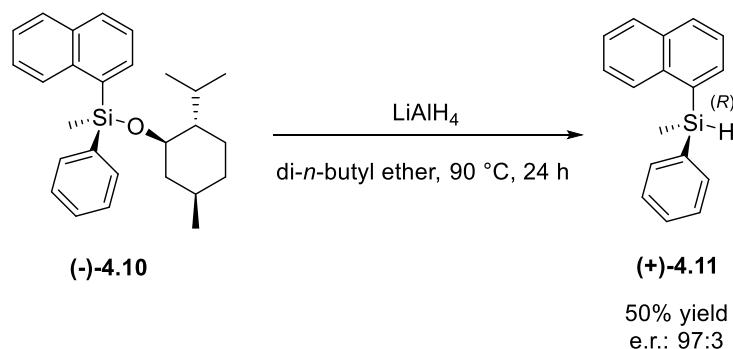
Next, the methoxy group of **4.7** was replaced with an L-menthoxy group using sodium hydroxide as the base and L-menthol (Scheme 4.5). Toluene is used as the solvent to remove methanol in an azeotrope to facilitate the reaction. Then, a silica gel chromatography is required to isolate the products from the mixture of unreacted starting material and products. The mixture of diastereomers in the products is enriched in a classic resolution using pentane at -78 °C. The enantioenriched single diastereomer (-)-**4.10** was crystallized out of solution (Scheme 4.5). Low yield was achieved due to the multiple purification steps.



Silica gel chromatography followed by a  
crystallization of single diastereomer  
from pentane at  $-78\text{ }^\circ\text{C}$

### Scheme 4.5 Synthesis of Enantioenriched L-Menthoxymethylnaphthylphenyl Silane

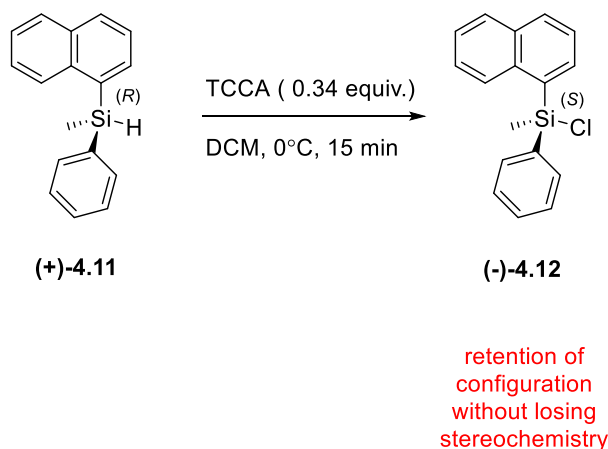
The synthesis of chiral silane (+)-**4.11** was achieved by a stereoretentive lithium aluminum hydride reduction in refluxing di-*n*-butyl ether (Scheme 4.6). Silica gel chromatography is needed for this reaction, yielding 50% of the enantioenriched chiral silane (e.r.: 97:3).



### Scheme 4.6 Synthesis of Enantioenriched Methyl naphthylphenyl Silane

The last step, chlorination of (+)-**4.11**, proved to be challenging. Initial attempts using sulfuryl chloride and chlorine gas showed either no efficiency or the loss of e.r. to chlorinate this chiral silane. The successful chlorination of (+)-**4.11** was achieved by using trichloroisocyanuric acid (TCCA) as the chlorination reagent. TCCA is a powerful chlorine

source for the conversion of Si-H functional silanes and siloxanes to the corresponding Si-Cl functional moieties.<sup>26</sup> For the chlorination of (+)-**4.11**, one third equivalent of the TCCA was used in dichloromethane. The reaction reached full conversion at 0 °C in 15 minutes. It showed a retention of configuration at silicon without losing any stereochemistry. (Scheme 4.7).

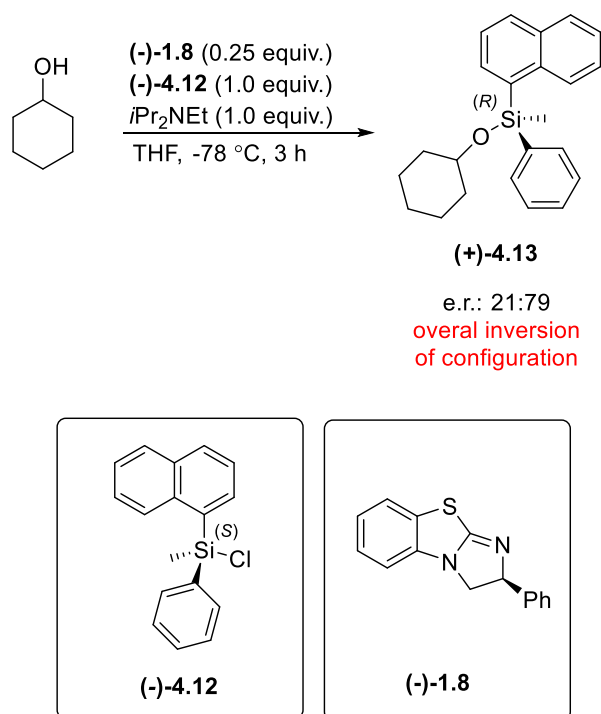


**Scheme 4.7 Synthesis of Enantioenriched Chiral Silyl Chloride**

#### 4.5 Results and Discussions

With the enantioenriched chiral silyl chloride (-)-**4.12** prepared, cyclohexanol and catalyst (-)-**1.8** were used in the silylation under the previously optimized reaction conditions (Scheme 4.8). The use of an achiral alcohol is to avoid the possible influence of a chiral alcohol to the stereochemistry at the silicon. In this experiment, aliquots were taken throughout the reaction to determine the relationship of reaction time. The e.r. of the product was determined by HPLC and compared to reported optical rotation data.<sup>21</sup> The e.r. of the product, however, remained the same for all aliquots at a ratio of 21:79, showing an *R* configuration at silicon. The conversion of these aliquots was difficult to determine

from  $^1\text{H}$  NMR due to the volatility of cyclohexanol. This result indicated an overall inversion of configuration at silicon from silyl chloride (-)-**4.12** to silyl ether (+)-**4.13**. This result could reasonably conclude that the mechanism does not proceed with a true double  $\text{S}_{\text{N}}2$  backside attack type of transformation. It must proceed with one inversion and one retention for silyl chloride to the silyl ether product. Based on our previous proposed mechanism, this could indicate quick transformation from the unreacted silyl chloride (-)-**4.12** through the pentacoordinate intermediate **4.2** to the reactive intermediate, either **4.5** or **4.6** (Scheme 4.3).

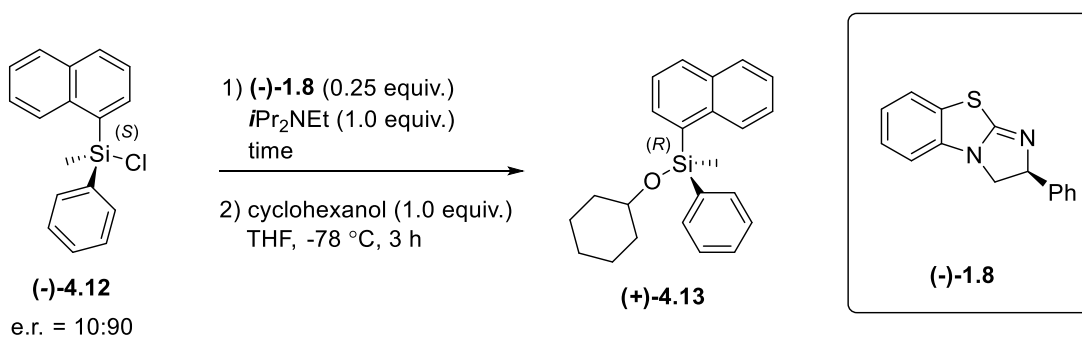


**Scheme 4.8** Silylation of Cyclohexanol Using Enantioenriched Chiral Silyl Chloride

Since the silyl chloride (-)-**4.12** was added last in these experiments, one possible explanation for the observation that all the aliquots have the same e.r. is the fast rate of the cyclohexanol attacking the reactive intermediate. To further support this hypothesis,

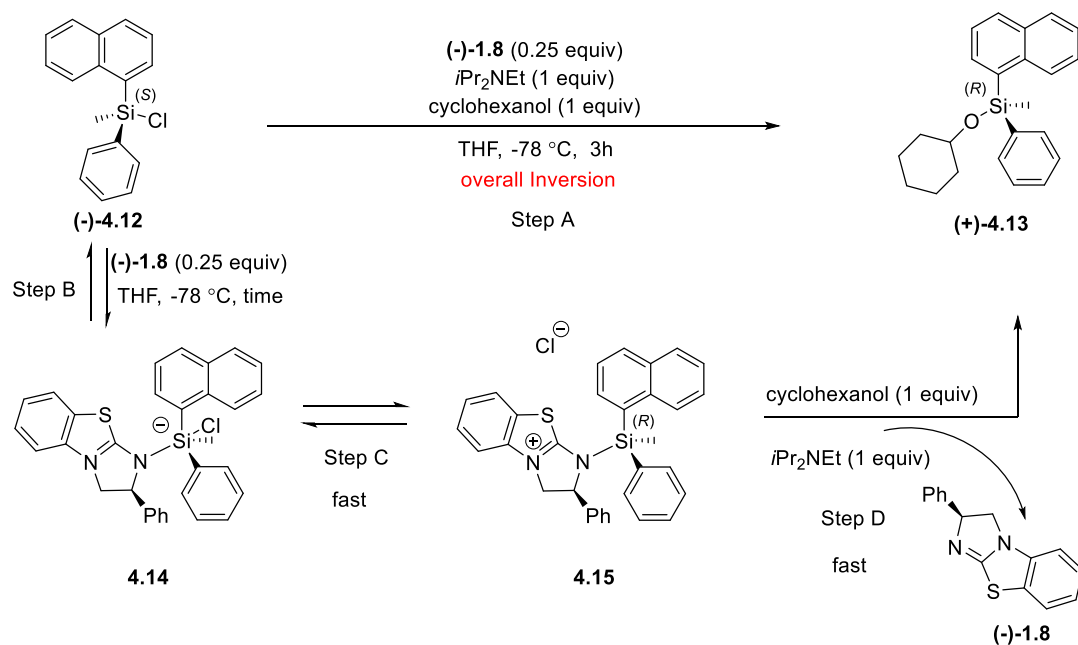
several experiments were designed in which the intermediate was allowed to pre-form for varying amounts of time. The cyclohexanol was then added to the solution and was allowed to stir for 3 hours to reach full conversion. The first run let the intermediate pre-form for 30 seconds before the cyclohexanol was added, the e.r. of the product dropped compared with the silyl chloride being added last, with an overall inversion of configuration (Table 4.1, entry 1). When more time was given to pre-form the intermediate, the e.r. of the product decreased with the same configuration at silicon (Table 4.1, entry 2-3). This could be explained by the potential racemization of the silicon stereocenter during the pre-formation of the intermediate. Due to the structure of the less sterically hindered cyclohexanol, it seems cyclohexanols react with the intermediate at a very fast rate once added to the solution, therefore preventing the racemization shown when the catalyst and silyl chloride are allowed to pre-mix.

**Table 4.1 Investigation of Fast Rate of Cyclohexanol Attacking Intermediate**



Entry	time	configuration of product (e.r.)	overall stereospecificity at silicon
1	30 s	<i>R</i> (36:64)	Inversion
2	10 min	<i>R</i> (43:57)	Inversion
3	20 min	<i>R</i> (42:58)	Inversion

Scheme 4.9 shows the proposed mechanistic steps for the asymmetric silylation of cyclohexanols. As mentioned previously the overall change in stereochemistry at silicon is inversion of configuration (Scheme 4.9, Step A). Based on the previously proposed mechanism (Figure 4.1), Step A can be split into three steps (Step B, Step C and Step D in Scheme 4.9). We observed a potential racemization in Step B (Table 4.1, entry 1-3), which could be explained by the possible racemization through a Berry pseudorotation<sup>13</sup> in the pre-formation of pentacoordinate intermediate **4.14**. Step C is the transformation of the pentacoordinate intermediate **4.14** to the reactive tetracoordinate intermediate **4.15**. Step D is the cyclohexanol attack of the reactive intermediate **4.15**. The overall inversion of configuration at silicon indicated a fast transformation from **4.14** to **4.15** in Step C which minimized racemization as well as a fast nucleophilic attack of the cyclohexanol to **4.15** in Step D (Scheme 4.9). We want to understand the directionality of attack at each step and to investigate the formation of intermediates **4.14** and **4.15**. Thus, a detailed investigation of the nucleophilic displacement at silicon in Step B and Step C would be necessary to start with.



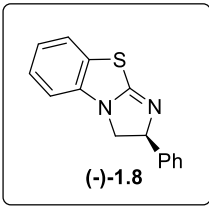
#### Scheme 4.9 Proposed Mechanistic Paths of Silylation for Cyclohexanol

Due to the difficulties in isolating and quantifying the formation of these intermediates, the investigation of Step B and Step C in Scheme 4.9 was designed to allow  $(-)\text{-4.12}$  and  $(-)\text{-1.8}$  to react for varying amounts of time before a lithium aluminum hydride ( $\text{LiAlH}_4$ ) reduction of the mixture was conducted. The reduced silane was purified via silica gel chromatography and the e.r. of the silane was determined by HPLC. The stereochemistry of the silicon was determined by comparing optical rotation with reported data.<sup>14</sup>

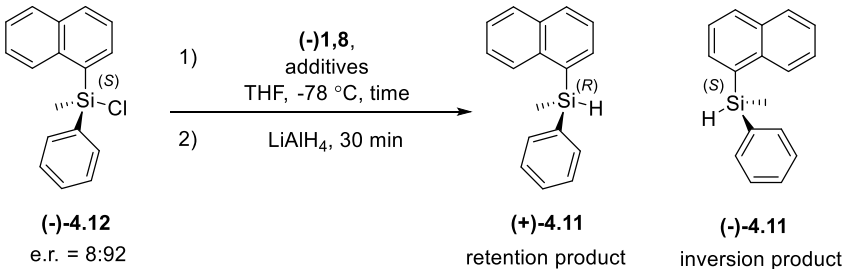
Overall inversion of configuration with a loss of e.r. was observed by reducing the mixture quickly after the silyl chloride  $(-)\text{-4.12}$  interacted with catalyst  $(-)\text{-1.8}$  (Table 4.2, entry 1). Due to the trend discussed previously, when chlorine is used as a leaving group, an inversion of configuration is normally observed at silicon (Figure 4.2).<sup>20</sup> Thus, the reasonable configurational assignment from pentacoordinate intermediate **4.14** to form the

tetracoordinate intermediate **4.15** should be the inversion of configuration at silicon (Scheme 4.10, Step C). For the  $\text{LiAlH}_4$  reduction of intermediate **(-)-4.12** and **4.15**, it is reasonable to assign the inversion of configuration at silicon for Step E and Step F based on similar studies reported in the literature (Scheme 4.10).<sup>20</sup> Thus, the observation of an overall inversion as well as a loss of e.r. (Table 4.2, entry 1) could be explained that more **(-)-4.11** was obtained as the reduced product than **(+)-4.11** within a short reaction time, indicating only a small percentage of starting material **(-)-4.12** was involved in the formation of intermediates (Scheme 4.10). The observed loss of e.r. in entry 1 could be explained by the possible formation of a pentacoordinate silicon species **4.14**, leading to a quick racemization process through Berry pseudorotation (Scheme 4.10, Step B).

**Table 4.2 Investigation of Stereochemistry at Silicon**



**(-)-1.8**



**(-)-4.12**  
e.r. = 8:92

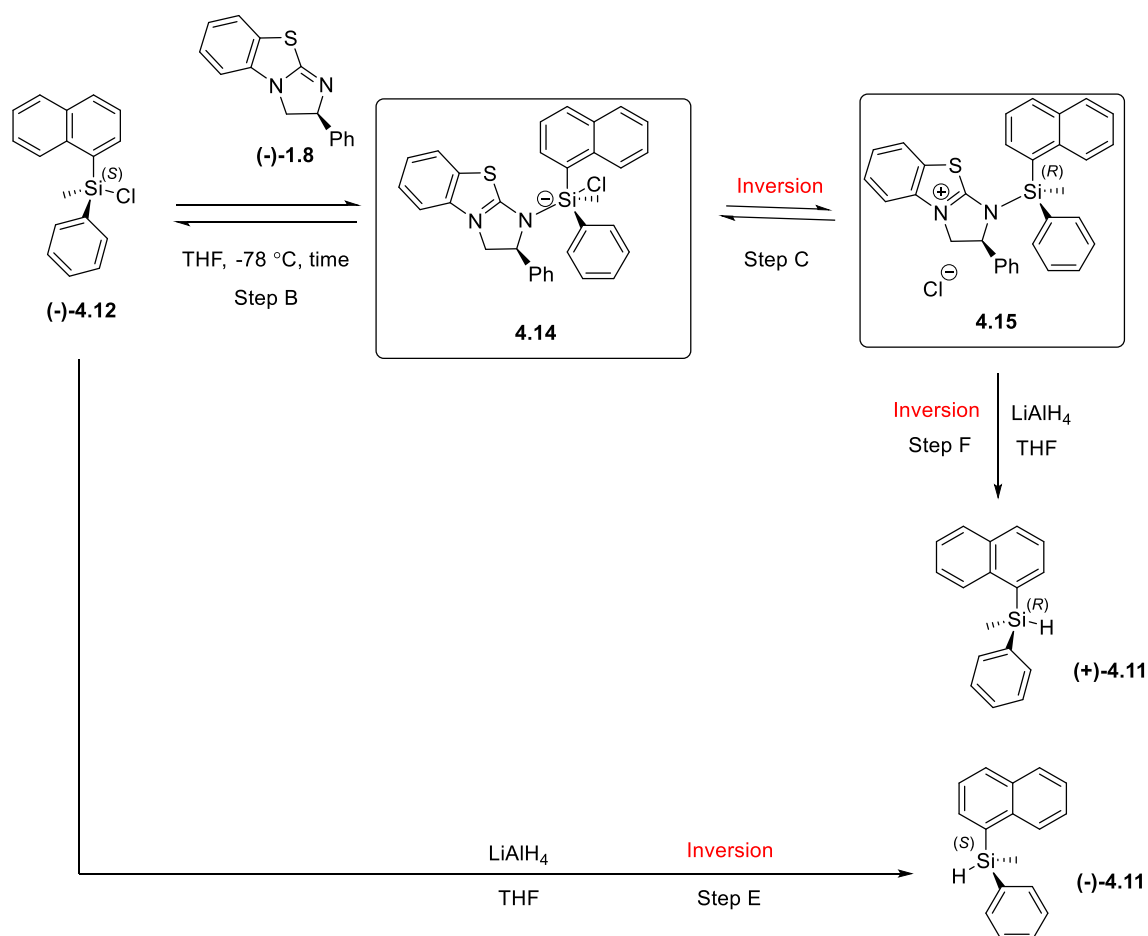
**(+)-4.11**  
retention product

**(-)-4.11**  
inversion product

Entry	(-)-1.8 loading	time	additives	configuration of Si (e.r.)	overall stereochemistry
1	1	30 s	—	<b>S</b> (43:57)	Inversion
2	1	10 min	—	<b>R</b> (53:47)	Retention
3	1	20 min	—	<b>R</b> (74:26)	Retention
4	0.25	30 s	—	<b>S</b> (24:76)	Inversion
5	0.25	10 min	—	<b>S</b> (46:54)	Inversion
6	0.25	20 min	—	<b>R</b> (60:40)	Retention



When the reaction time was increased, a change of stereochemistry from *S* to *R* at silicon was observed as well as an increase of e.r. (Table 4.2, entry 2-3). This could be explained that by extending the reaction time, more intermediate **4.15** was formed through a transformation of **4.14** (Scheme 4.10, Step B and Path C), thus there will be more (+)-**4.11** observed as the product than (-)-**4.11** after the reduction.

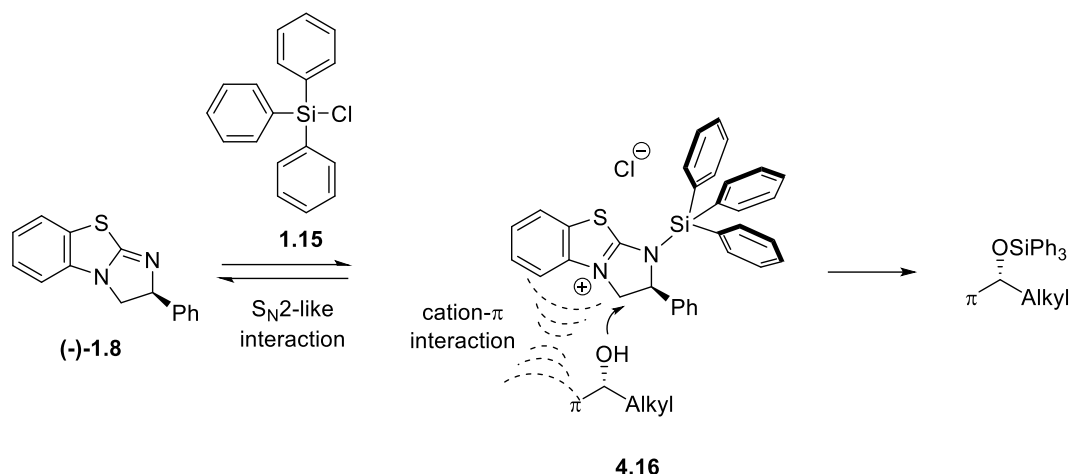


**Scheme 4.10 Stepwise Investigation of Stereochemistry at Silicon**

Further investigations on lowering the loading of catalyst (-)-**1.8** to a quarter equivalent, which is similar to the reaction conditions in our silylation-based kinetic resolution, limited the formation of intermediate **4.15**. This was observed as the e.r. was

changing slowly over a period of time compared to runs with one equivalent of catalyst loading (Table 4.2, entry 4-6 versus entry 1-3 respectively).

With all the data collected to date from this chiral silyl chloride investigation, a reasonable conclusion can be made that the first interaction of catalyst (-)-**1.8** with silyl chloride (-)-**4.12** results in a pentacoordinate intermediate **4.14** with possible Berry pseudorotation. This is quickly transformed into a tetracoordinate intermediate **4.15** with an inversion of configuration at silicon regarding (-)-**4.12**. Considering the overall stereochemical outcome at silicon of this simulated silylation-based kinetic resolution of cyclohexanol is inversion of configuration (Scheme 4.9, Step A), we can draw the conclusion that the cyclohexanol attacks the reactive intermediate with retention of configuration at silicon (Scheme 4.9, Step D). The retention of configuration in Step D in Scheme 4.9 gave us a hint that the alcohol may approach the intermediate from the catalyst side **4.16** in the general silylation-based kinetic resolution (Scheme 4.11). Interestingly, this type of approach would be consistent with the transition states proposed by Birman indicating that a cation- $\pi$  interaction is important between the catalyst and the substrate.<sup>27-</sup>  
<sup>28</sup> In our silylation-based kinetic resolution, the helical twist formation of the triphenyl group on silicon enhances the chiral environment of the intermediate, forcing the alcohol to approach from a very specific direction (discussion of helical twist formation of triphenyl group is in Chapter 3). The possible cation- $\pi$  interaction also explains the importance of incorporation of a  $\pi$  system on one side of an alcohol substrate employed in order to obtain good selectivity, by stabilizing and directing the alcohol in its approach when reacting with the reactive intermediate.



**Scheme 4.11 Proposed Mechanism of Alcohol Approaches from Catalyst Side**

#### 4.6 Conclusions and Outlook

In conclusion, the mechanistic investigations have been carried out looking at the stereochemistry at silicon by employing the synthesized chiral silyl chloride (-)-**4.12**. Based on the result to date as well as similar studies reported,<sup>20</sup> we proposed a pentacoordinate intermediate **4.14** was formed and quickly transformed to a tetracoordinate intermediate **4.15** via an overall inversion of configuration at silicon regarding silyl chloride (-)-**4.12**. There is a possible Berry pseudorotation of **4.14**, which may cause the quick racemization at the silicon stereogenic center. The alcohol approaches the reactive intermediate **4.15** on the same side of the catalyst giving retention of configuration at silicon. The possible cation- $\pi$  interaction between the intermediate and the alcohol may explain the importance of having a  $\pi$  system on one side of the alcohol.

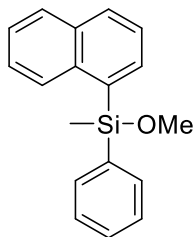
These chiral silyl chloride studies, the liner-free energy relationship investigations,<sup>1</sup> as well as the still ongoing kinetic studies in the Wiskur group, are the approaches toward a full understanding of the mechanism of silylation-based kinetic resolution. Additionally, <sup>29</sup>Si NMR studies of the intermediate or transition state is

important in having a thorough understanding of the mechanism. Computational studies similar to the acylation-based reactions should also be pursued.

## 4.7 Experimental

### General Information

All the reactions were carried out under a nitrogen atmosphere using oven-dried glassware. Molecular sieves and Celite were activated in an oven at 170 °C before use. Tetrahydrofuran (THF), Toluene and diethyl ether were dried by passing through a column of activated alumina before use and stored over molecular sieves. Dibutyl ether and trichloroisocyanuric acid (TCCA) were obtained from major commercial sources and used without further purifications. NMR spectra were recorded with a 300 MHz or 400 MHz instrument for  $^1\text{H}$  and a 101 MHz instrument for  $^{13}\text{C}$  with complete proton decoupling. Chemical shifts were reported in ppm with TMS or chloroform as an internal standard (TMS 0.00 ppm or  $\text{CHCl}_3$  7.26 ppm for  $^1\text{H}$  and 77.16 for  $^{13}\text{C}$ ). Optical rotations were obtained utilizing a polarimeter. Enantiomeric ratios were determined via HPLC using an Agilent 1200 series. The chiral stationary phases were Daicel Chiralcel OD-H column, and the enantiomers were measured by a diode array detector in comparison with the racemic materials.

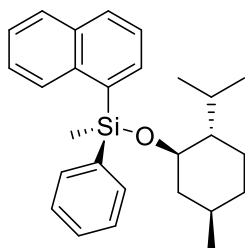


#### 4.7

methoxy(methyl)(naphthalen-1-yl)(phenyl)silane

Procedure was adapted from reported literature.<sup>14</sup> A 250 mL Schlenk flask was equipped with stir bar and charged with 2.08g of Mg turnings. The flask was then flame dried and equipped with flame dried reflux condenser and fitted with septa. The apparatus was then purged with argon and fitted with an argon balloon. The turnings were then suspended in dry ether (5 mL), toluene (10 mL) and THF (5 mL). The mixture was warmed to 60 °C and a few drops of 2-bromonaphthelene was added and allowed to stir for 5 min. The remainder of 2-bromonaphthelene was added slowly (10 min in total) and the mixture was allowed to reflux for 1 hour. The mixture was then cooled to room temperature. A solution of dimethoxymethylphenylsilane was prepared (13.1 mL in 10 mL of THF) under argon. The solution was added slowly to the Grignard solution producing an exothermic reaction and gentle reflux for 16 hours. The mixture was removed from heat and allowed to cool to room temperature. The reaction was quenched with 20 mL of saturated NH<sub>4</sub>Cl, 20 mL of water and 20 mL of diethyl ether. The organic was extracted three times with diethyl ether and concentrated by Rotary Evaporator. The residue was purified through a silica gel chromatography with straight hexanes to yield a yellow oil, 15.8 g, 80%. <sup>1</sup>H NMR (400 MHz, CDCl<sub>3</sub>) δ ppm 8.17 (dd, *J* = 7.6, 1.8 Hz, 1H), 7.99 – 7.72 (m, 4H), 7.69 – 7.32 (m, 7H), 3.58 (s, 3H), 0.80 (s, 1H). <sup>13</sup>C NMR (101 MHz, CDCl<sub>3</sub>) δ ppm 138.6,

137.6, 136.7, 136.3, 135.9, 135.7, 133.1, 132.2, 131.2, 130.8, 130.3, 128.5, 127.9, 127.4, 53.6, 2.9.

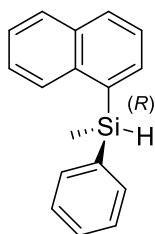


**(-)-4.10**

(S)-(L-menthoxy)(methyl)(naphthalen-1-yl)(phenyl)silane

Procedure was adapted from reported literature.<sup>14</sup> A 100 mL round bottom flask fitted with stir bar was added 15.8 g of previously synthesized **4.7**. Next, 8.95 g of L-menthol was added followed by 148 mg of solid NaOH. The mixture was then dissolved in 20 mL of dry toluene. The round bottom was then fitted with a 20 cm vigreux distillation apparatus with a 100-mL collection flask. The mixture was then heated to 140 °C for 13 hours as 2.6 ml of MeOH-toluene azeotrope was collected. The resulting brown solution was then allowed to cool to room temperature and the mixture was treated with a pad of silica gel chromatography using ether. The residue was purified via silica gel chromatography using straight hexanes to yield a yellow oil. The <sup>1</sup>H NMR indicated the oil is a mixture of the diastereomers. The oil was then diluted with twice its volume with pentane in a 250-mL round bottom flask and cooled to -78 °C for three days. The crystal formed was washed with cold pentane to yield a white solid, 4.5 g, 20 %. <sup>1</sup>H NMR (400 MHz, CDCl<sub>3</sub>) δ ppm 8.06 (d, *J* = 8.4 Hz, 1H), 7.99 – 7.78 (m, 4H), 7.65 – 7.28 (m, 7H), 3.53 (td, *J* = 10.1, 4.4 Hz, 1H), 2.24 (td, *J* = 7.0, 2.5 Hz, 1H), 1.84 (ddd, *J* = 11.6, 4.6, 2.1 Hz, 1H), 1.58 (dt, *J* = 6.4, 2.7 Hz, 2H), 1.37 – 1.00 (m, 3H), 0.84 – 0.80 (m, 6H), 0.81 (dd,

$J = 7.9, 2.2$  Hz, 3H), 0.48 (d,  $J = 6.9$  Hz, 3H).  $^{13}\text{C}$  NMR (101 MHz,  $\text{CDCl}_3$ )  $\delta$  ppm 135.7, 134.9, 131.2, 130.2, 129.7, 129.3, 128.8, 128.5, 127.2, 126.6, 126.5, 126.3, 126.0, 125.6, 74.3, 50.9, 46.0, 35.1, 32.3, 25.8, 23.3, 22.9, 22.0, 16.2.

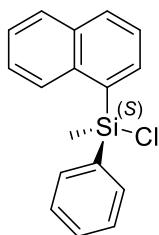


**(+)-4.11**

(*R*)-methyl(naphthalen-1-yl)(phenyl)silane

Procedure was adapted from reported literature.<sup>14</sup> Into a 100 mL Schlenk flask equipped with stir bar, was added 692 mg of  $\text{LiAlH}_4$ . The flask was purged with nitrogen and sealed with septum. The  $\text{LiAlH}_4$  was then suspended with stirring in 8 mL diethyl ether. The previously synthesized (-)-4.10, 5.92 g, was dissolved in 8 mL of dibutyl ether with heating. This solution was added to the  $\text{LiAlH}_4$  slurring via syringe. The remaining silane was washed with another 8 mL of dibutyl ether and added to the flask. The flask was then fitted with a reflux condenser and heated to 90 °C for 18 hours. Full conversion was monitored by  $^1\text{H}$  NMR and the mixture was then allowed to cool to room temperature. Excess  $\text{LiAlH}_4$  was quenched with acetone slowly and then by 1N HCl. The organic layer was extracted with diethyl ether and concentrated by Rotary Evaporator. The product was purified via silica gel chromatography with straight hexanes to yield white solid, 1.8 g, 50%.  $^1\text{H}$  NMR (400 MHz,  $\text{CDCl}_3$ )  $\delta$  ppm 8.14 – 8.03 (m, 1H), 7.96 – 7.73 (m, 3H), 7.65 – 7.30 (m, 8H), 5.38 (q,  $J = 3.9$  Hz, 1H), 0.78 (d,  $J = 3.9$  Hz, 3H)  $^{13}\text{C}$  NMR (101 MHz,

CDCl<sub>3</sub>)  $\delta$  ppm 139.3, 137.7, 136.9, 136.8, 136.2, 135.8, 133.5, 133.4, 132.9, 130.9, 129.4, 129.1, 19.8

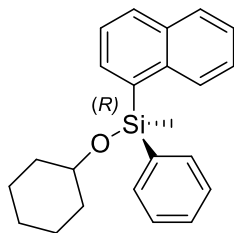


**(-)-4.12**

(S)-chloro(methyl)(naphthalen-1-yl)(phenyl)silane

To a 4-dram vial was equipped with stir bar and septum. In the vial under argon, 112 mg (0.45 mmol) of synthesized (*R*)-methylnaphthylphenylsilane (+)-**4.11** was added. The starting materials were dissolved in 2 mL of dry THF at 0 °C for 5 min. Then 36 mg (0.153) of trichloroisocyanuric acid (TCCA) was grounded and added via spatula to the mixture. The reaction was allowed to react for 10 min and the conversion was monitored by <sup>1</sup>H NMR. Once it reacted the full conversion, the mixture was filtered through a pad of Celite and concentrated by Rotary Evaporator. The solvent was removed completely in vacuum to yield a white solid, 125 mg, 96%. The level of enantioenrichment and configuration was determined from comparison of optical rotation to the literature, [ $\alpha$ ]<sub>D</sub><sup>25</sup>: -6.4 c = 0.94 pentane, [ $\alpha$ ]<sub>D</sub><sup>25</sup>: -6.3 c = 4.0 pentane (97% ee, (*S*)-configuration).<sup>29</sup> **<sup>1</sup>H NMR** (400 MHz, CDCl<sub>3</sub>)  $\delta$  ppm 8.05 (d, *J* = 8.3 Hz, 1 H), 7.98 (d, *J* = 8.3 Hz, 1 H), 7.90-7.86 (m, 2 H), 7.67-7.64 (m, 2 H), 7.53-7.37 (m, 6 H), 1.09 (s, 3 H). **<sup>13</sup>C NMR** (101 MHz, CDCl<sub>3</sub>)  $\delta$  ppm 136.1, 135.5, 135.2, 134.0, 133.4, 131.8, 131.4, 130.5, 129.0, 128.2, 128.1, 126.3, 125.8, 125.0, 2.44. **HRMS** (EI) Calculated for (M<sup>+</sup>) (C<sub>17</sub>H<sub>15</sub>ClSi<sup>+</sup>): 282.0626 Observed: 282.0631. **IR** (neat, cm<sup>-1</sup>) 1589, 1459, 1428, 1257, 1111, 997.





**(+)-4.13**

(*R*)-(cyclohexyloxy)(methyl)(naphthalen1-yl)(phenyl)silane

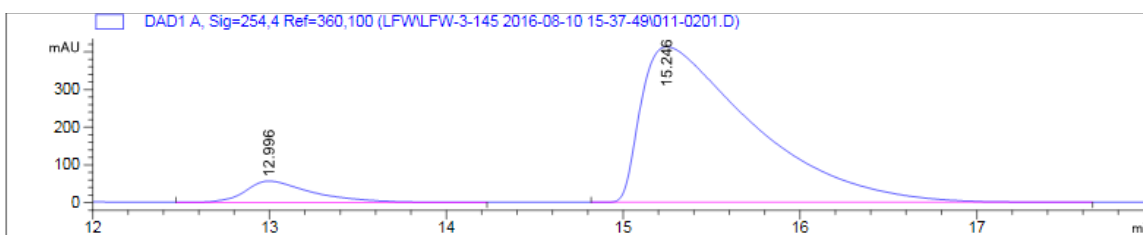
To a 1-dram vial with an oven dried Teflon coated stir bar and activated 4Å molecular sieves, the cyclohexanol (0.06 mmol), catalyst (-)-**1.8** (0.015 mmol) and *N,N*-diisopropylethylamine (0.06 mmol) was added. The mixture was dissolved in 0.8 mL THF and was then purged with argon and sealed with a septum. A stock solution of (-)-**4.12** in THF was prepared (0.06 mmol (-)-**4.12** dissolved in 0.2 mL THF) and was added to the vial via syringe. The reaction was allowed to react for three hours and the mixture was concentrated. The product was isolated as a colorless oil after silica gel chromatography purification (5% EtOAc in hexanes), 18 mg, 86%. <sup>1</sup>H NMR (400 MHz, CDCl<sub>3</sub>) δ ppm 8.21 (d, *J* = 8.2 Hz, 1 H), 7.89 (d, *J* = 8.2 Hz, 1 H), 7.83-7.80 (m, 2 H), 7.62-7.60 (m, 2 H), 7.47-7.37 (m, 7 H), 3.82-2.75 (m, 1 H), 1.82-1.86 (m, 4 H), 1.50-1.13 (m, 6 H), 0.78 (s, 3 H). <sup>13</sup>C NMR (101 MHz, CDCl<sub>3</sub>) δ ppm .137.6, 137.0, 134.9, 134.8, 134.2, 133.3, 130.5, 129.5, 129.0, 128.6, 127.8, 125.7, 125.4, 124.9, 71.7, 35.7, 25.6, 24.0, -1.1. Optical rotation: [α]<sub>D</sub><sup>25</sup>: +3.4 *c* = 2.6 CHCl<sub>3</sub>; [α]<sub>D</sub><sup>25</sup>lit: +6.7 *c* = 1.2 CHCl<sub>3</sub>.<sup>21</sup> Configuration is (*R*) at silicon. This conforms to the e.r. as determined by HPLC on OD-H column, 0.4 mL flow rate, λ = 254 nm.

## General Procedure of Chiral Silyl Chloride Investigations

### Control Study

To a 1-dram vial with an oven dried Teflon coated stir bar and activated 4Å molecular sieves, 0.8 mL dried THF was added. The vial was then purged with argon and sealed with a septum. A stock solution of (-)-**4.12** in THF was prepared (0.36 mmol (-)-**4.12** dissolved in 1 mL THF) and 0.2 mL of the solution was added to the vial via syringe. The reaction was quenched with 0.1 mL 1M LiAlH<sub>4</sub>/THF solution right after the (-)-**4.12** was added. The mixture was allowed to react for another 30 minutes and the excess LiAlH<sub>4</sub> was quenched with 0.5 mL water. Organic layer was extracted with diethyl ether three times and concentrated via Rotary Evaporator. The product was purified via silica gel chromatography with straight hexanes. The e.r. was determined by HPLC.

HPLC using OD-H column 1mL/min flow rate at 254 nm. t<sub>R</sub> 12.9 min for (*R*)-enantiomer (minor) and 15.2 min for (*S*)-enantiomer (major). (er = 8:92). Indicating the silyl chloride (-)-**4.12** was enantiomerical enriched to start with.



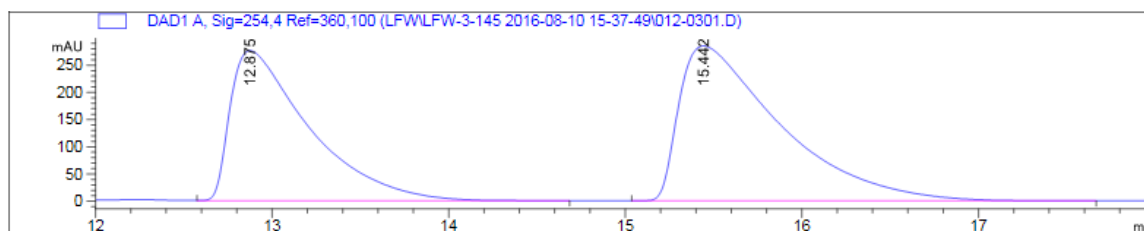
Peak #	RetTime [min]	Type	Width [min]	Area [mAU*s]	Height [mAU]	Area %
1	12.996	VB	0.3882	1504.78857	56.59629	7.6548
2	15.246	BB	0.6405	1.81532e4	413.21356	92.3452

### 1 equivalent of catalyst (-)-1.8

To a 1-dram vial with an oven dried Teflon coated stir bar and activated 4Å molecular sieves, the catalyst (-)-1.8 (15.12 mg, 0.06 mmol) was added with 0.8 mL dried THF. The vial was then purged with argon and sealed with a septum. A stock solution of (-)-4.12 in THF was prepared (0.36 mmol (-)-4.12 dissolved in 1 mL THF) and 0.2 mL of the solution was added to the vial via syringe. The reaction was allowed to run for varying amounts of time and quenched with 0.1 mL 1M LiAlH<sub>4</sub>/THF solution. The mixture was allowed to reaction for another 30 minutes and the excess LiAlH<sub>4</sub> was quenched with 0.5 mL water. Organic layer was extracted with diethyl ether three times and concentrated via Rotary Evaporator. The product was purified via silica gel chromatography with straight hexanes. The e.r. was determined by HPLC.

#### Table 4.2, Entry 1

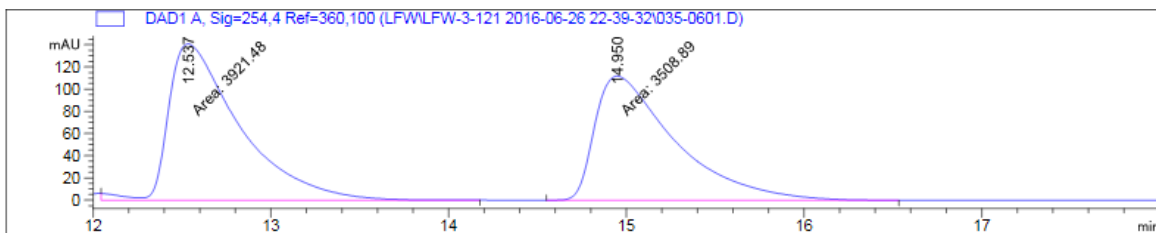
HPLC using OD-H column 1mL/min flow rate at 254 nm. *t<sub>R</sub>* 12.9 min for (*R*)-enantiomer (minor) and 15.4 min for (*S*)-enantiomer (major). (er = 43:56).



Peak #	RetTime [min]	Type	Width [min]	Area [mAU*s]	Height [mAU]	Area %
1	12.875	VB	0.4530	8596.36230	276.28915	43.1912
2	15.442	BB	0.5810	1.13067e4	284.92899	56.8088

**Table 4.2, Entry 2**

**HPLC** using OD-H column 1mL/min flow rate at 254 nm.  $t_R$  12.5 min for (*R*)-enantiomer (major) and 15.0 min for (*S*)-enantiomer (minor). (er = 53:47).



Peak #	RetTime [min]	Type	Width [min]	Area [mAU*s]	Height [mAU]	Area %
1	12.537	MM	0.4636	3921.48462	140.96721	52.7764
2	14.950	MM	0.5220	3508.89282	112.03629	47.2236

**Table 4.2, Entry 3**

**HPLC** using OD-H column 1mL/min flow rate at 254 nm.  $t_R$  13.8 min for (*R*)-enantiomer (major) and 16.5 min for (*S*)-enantiomer (minor). (er = 74:26).



Peak #	RetTime [min]	Type	Width [min]	Area [mAU*s]	Height [mAU]	Area %
1	13.825	MM	0.4086	332.86768	13.57697	73.6231
2	16.541	MM	0.4326	119.25638	4.59480	26.3769

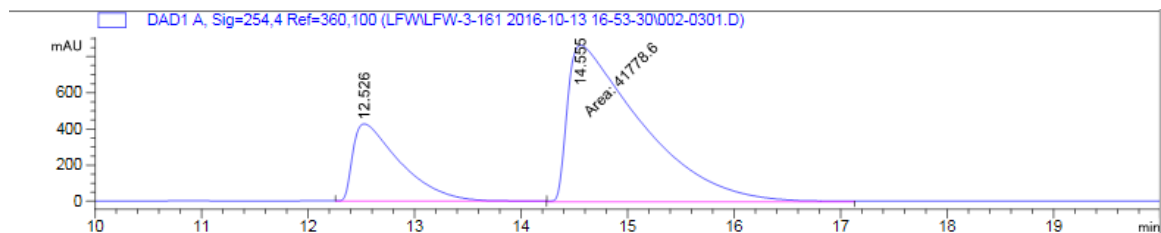
### 0.25 equivalent of catalyst (-)-1.8

To a 1-dram vial with an oven dried Teflon coated stir bar and activated 4Å molecular sieves, the catalyst (-)-1.8 (3.78 mg, 0.015 mmol) was added with 0.8 mL dried

THF. The vial was then purged with argon and sealed with a septum. A stock solution of (-)-**4.12** in THF was prepared (0.36 mmol (-)-**4.12** dissolved in 1 mL THF) and 0.2 mL of the solution was added to the vial via syringe. The reaction was allowed to run for varying amounts of time and quenched with 0.1 mL 1M LiAlH<sub>4</sub>/THF solution. The mixture was allowed to react for another 30 minutes and the excess LiAlH<sub>4</sub> was quenched with 0.5 mL water. Organic layer was extracted with diethyl ether three times and concentrated via Rotary Evaporator. The product was purified via silica gel chromatography with straight hexanes. The e.r. was determined by HPLC.

#### Table 4.2, Entry 4

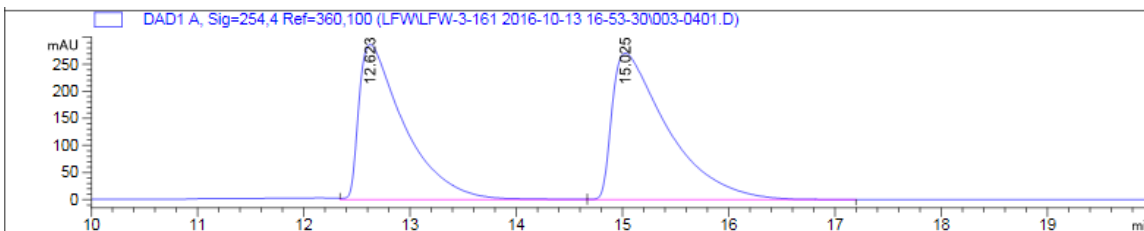
HPLC using OD-H column 1mL/min flow rate at 254 nm. t<sub>R</sub> 12.5 min for (*R*)-enantiomer (minor) and 14.6 min for (*S*)-enantiomer (major). (er = 24:76).



Peak #	RetTime [min]	Type	Width [min]	Area [mAU*s]	Height [mAU]	Area %
1	12.526	VV	0.4522	1.32100e4	427.81363	24.0232
2	14.555	MM	0.8043	4.17786e4	865.68567	75.9768

### Table 4.2, Entry 5

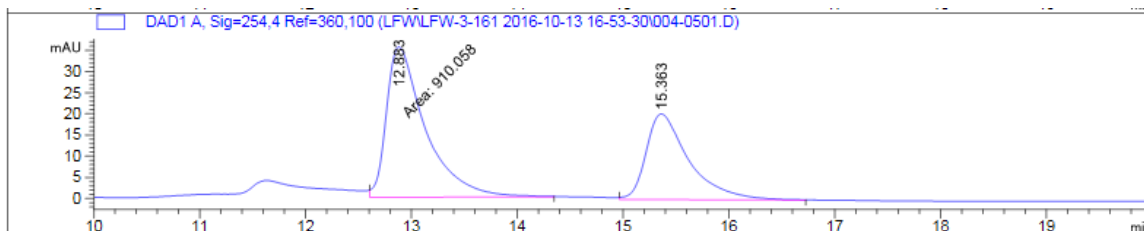
HPLC using OD-H column 1mL/min flow rate at 254 nm.  $t_R$  12.6 min for (*R*)-enantiomer (minor) and 15.0 min for (*S*)-enantiomer (major). (er = 46:54).



Peak #	RetTime [min]	Type	Width [min]	Area [mAU*s]	Height [mAU]	Area %
1	12.623	VV	0.4302	8498.81152	286.41321	46.4011
2	15.025	VB	0.5292	9817.15918	270.65710	53.5989

### Table 4.2, Entry 6

HPLC using OD-H column 1mL/min flow rate at 254 nm.  $t_R$  12.9 min for (*R*)-enantiomer (major) and 15.4 min for (*S*)-enantiomer (minor). (er = 61:39).



Peak #	RetTime [min]	Type	Width [min]	Area [mAU*s]	Height [mAU]	Area %
1	12.883	MM	0.4268	910.05780	35.54211	61.4544
2	15.363	BB	0.4132	570.80969	20.23151	38.5456

#### 4.8 References

1. Akhani, R. K.; Moore, M. I.; Pribyl, J. G.; Wiskur, S. L., Linear Free-Energy Relationship and Rate Study on a Silylation-Based Kinetic Resolution: Mechanistic Insights. *J. Org. Chem.* **2014**, *79* (6), 2384-2396.
2. Charton, M.; Charton, B., Steric Effects .5. Barriers to Internal-Rotation. *J. Am. Chem. Soc.* **1975**, *97* (22), 6472-6473.
3. Charton, M., Steric Effects .4. E1 and E2 Eliminations. *J. Am. Chem. Soc.* **1975**, *97* (21), 6159-6161.
4. Charton, M., Steric Effects .3. Bimolecular Nucleophilic-Substitution. *J. Am. Chem. Soc.* **1975**, *97* (13), 3694-3697.
5. Charton, M., Steric Effects .2. Base-Catalyzed Ester Hydrolysis. *J. Am. Chem. Soc.* **1975**, *97* (13), 3691-3693.
6. Charton, M., Steric Effects .1. Esterification and Acid-Catalyzed Hydrolysis of Esters. *J. Am. Chem. Soc.* **1975**, *97* (6), 1552-1556.
7. Blackmond, D. G., Reaction progress kinetic analysis: A powerful methodology for mechanistic studies of complex catalytic reactions. *Angew. Chem. Int. Ed.* **2005**, *44* (28), 4302-4320.
8. Shekhar, S.; Ryberg, P.; Hartwig, J. F.; Mathew, J. S.; Blackmond, D. G.; Strieter, E. R.; Buchwald, S. L., Reevaluation of the mechanism of the amination of aryl halides catalyzed by BINAP-ligated palladium complexes. *J. Am. Chem. Soc.* **2006**, *128* (11), 3584-3591.

9. Blackmond, D. G.; Ropic, M.; Stefinovic, M., Kinetic studies of the asymmetric transfer hydrogenation of imines with formic acid catalyzed by Rh-diamine catalysts. *Org. Process. Res. Dev.* **2006**, *10* (3), 457-463.
10. Mathew, J. S.; Klussmann, M.; Iwamura, H.; Valera, F.; Futran, A.; Emanuelsson, E. A. C.; Blackmond, D. G., Investigations of Pd-catalyzed ArX coupling reactions informed by reaction progress kinetic analysis. *J. Org. Chem.* **2006**, *71* (13), 4711-4722.
11. Ruiz-Castillo, P.; Blackmond, D. G.; Buchwald, S. L., Rational Ligand Design for the Arylation of Hindered Primary Amines Guided by Reaction Progress Kinetic Analysis. *J. Am. Chem. Soc.* **2015**, *137* (8), 3085-3092.
12. Lineweaver, H.; Burk, D., The determination of enzyme dissociation constants. *J. Am. Chem. Soc.* **1934**, *56*, 658-666.
13. Berry, R. S., Correlation of Rates of Intramolecular Tunneling Processes, with Application to Some Group-V Compounds. *J. Chem. Phys.* **1960**, *32* (3), 933-938.
14. Sommer, L. H.; Michael, K. W.; Frye, C. L.; Parker, G. A., Stereochemistry of Asymmetric Silicon .I. Relative + Absolute Configurations of Optically Active Alpha-Naphthylphenylmethylsilanes. *J. Am. Chem. Soc.* **1964**, *86* (16), 3271-&.
15. Sommer, L. H.; Citron, J. D., Stereochemistry of Asymmetric Silicon .7. Silicon-Nitrogen Bond. *J. Am. Chem. Soc.* **1967**, *89* (23), 5797-&.
16. Citron, J. D., Preparation, Resolution and Dynamic Stereochemistry of 7h-7-Methyl-7-Silabenz[D,E]Anthracene System. *J. Organomet. Chem.* **1975**, *86* (3), 359-367.
17. Kawashima, T.; Kroshefsky, R. D.; Kok, R. A.; Verkade, J. G., Optical Resolution Studies of Cyclophosphamide. *J. Org. Chem.* **1978**, *43* (6), 1111-1114.



18. Corriu, R. J. P.; Guerin, C., Nucleophilic-Substitution at Silicon - Influence of the Attacking Allyllithium and Aryloxide Anion on the Stereochemistry and a Simple Mechanistic Proposal. *J. Organomet. Chem.* **1982**, 225 (1), 141-150.
19. Terunuma, D.; Senda, K.; Sanazawa, M.; Nohira, H., The Configurations of Benzylmethyl(Ortho- or Para-Tolyl)Silylmethylamine and the Stereochemistry of the Reactions of Benzylmethyl-Methoxyphenylsilane with Some Organo-Metallic Agents. *B. Chem. Soc. Jpn.* **1982**, 55 (3), 924-927.
20. Corriu, R. J. P.; Guerin, C., Nucleophilic Displacement at Silicon - Recent Developments and Mechanistic Implications. *Adv. Organomet. Chem.* **1982**, 20, 265-312.
21. Shinke, S. T., Teruhisa; Kawakami, Yusuke, Stereochemistry in Lewis acid-catalyzed silylation of alcohols, silanols, and methoxysilanes with optically active methyl(1-naphthyl)phenylsilane. *Silicon Chemistry* **2007**, 3 (5).
22. Sommer, L. H.; Frye, C. L., Optically Active Organosilicon Compounds Having Reactive Groups Bonded to Asymmetric Silicon - Displacement Reactions at Silicon with Pure Retention and Pure Inversion of Configuration. *J. Am. Chem. Soc.* **1959**, 81 (4), 1013-1013.
23. Sommer, L. H.; Blankman, H. D.; Miller, P. C., Non-Rearrangement Reactions of the Neopentyl-Oxygen Bond - New Syntheses of Neopentyl Halides. *J. Am. Chem. Soc.* **1951**, 73 (7), 3542-3542.
24. Sommer, L. H.; Frye, C. L., Stereochemistry of Chloride Ion Displacement from Silicon - Hydrolysis and Methanolysis of an Optically Active Organochlorosilane. *J. Am. Chem. Soc.* **1960**, 82 (15), 4118-4119.

25. Ojima, Y.; Yamaguchi, K.; Mizuno, N., An Efficient Solvent-Free Route to Silyl Esters and Silyl Ethers. *Adv. Synth. Catal.* **2009**, *351* (9), 1405-1411.
26. Varaprath, S.; Stutts, D. H., Utility of trichloroisocyanuric acid in the efficient chlorination of silicon hydrides. *J. Organomet. Chem.* **2007**, *692* (10), 1892-1897.
27. Birman, V. B.; Li, X. M., Benzotetramisole: A remarkably enantioselective acyl transfer catalyst. *Org. Lett.* **2006**, *8* (7), 1351-1354.
28. Li, X. M.; Liu, P.; Houk, K. N.; Birman, V. B., Origin of enantioselectivity in CF(3)-PIP-catalyzed kinetic resolution of secondary benzylic alcohols. *J. Am. Chem. Soc.* **2008**, *130* (42), 13836-13837.
29. Sommer, L. H.; Ulland, L. A., Chirality and Structure of Organosilicon Radicals. *J. Org. Chem.* **1972**, *37* (24), 3878-&.